

# Metal Catalysed Alkylation of Carbonyl Compounds with Formaldehyde

*Patrizia Lorusso*



University of  
St Andrews

This thesis is submitted in partial fulfilment for the degree of PhD

at the

University of St Andrews

13<sup>th</sup> May 2015

### **Candidate's declarations**

I, Patrizia Lorusso, hereby certify that this thesis, which is approximately 36,800 words in length, has been written by me, and that it is the record of work carried out by me, or principally by myself in collaboration with others as acknowledged, and that it has not been submitted in any previous application for a higher degree.

I was admitted as a research student in November 2010 and as a candidate for the degree of Ph.D. in December 2011; the higher study for which this is a record was carried out in the University of St Andrews between 2010 and 2015.

Date ..... signature of candidate .....

### **Supervisor's declaration**

I hereby certify that the candidate has fulfilled the conditions of the Resolution and Regulations appropriate for the degree of Ph.D. in the University of St Andrews and that the candidate is qualified to submit this thesis in application for that degree.

Date ..... signature of supervisor .....  
(David Cole-Hamilton)

## Permission for publication

In submitting this thesis to the University of St Andrews I understand that I am giving permission for it to be made available for use in accordance with the regulations of the University Library for the time being in force, subject to any copyright vested in the work not being affected thereby. I also understand that the title and the abstract will be published, and that a copy of the work may be made and supplied to any bona fide library or research worker, that my thesis will be electronically accessible for personal or research use unless exempt by award of an embargo as requested below, and that the library has the right to migrate my thesis into new electronic forms as required to ensure continued access to the thesis. I have obtained any third-party copyright permissions that may be required in order to allow such access and migration, or have requested the appropriate embargo below.

The following is an agreed request by candidate and supervisor regarding the publication of this thesis:

Embargo on all print and electronic copy for a period of 2 years on the following grounds:

- Publication would be commercially damaging to the industrial partner
- Publication would preclude future publication

Date ..... signature of candidate .....

signature of supervisor .....

(David Cole-Hamilton)

*To my family*  
*Alla mia famiglia*

“When you have eliminated all which is impossible, then whatever remains, however improbable, must be the truth.”

— **Arthur Conan Doyle**, *The Case-Book of Sherlock Holmes* —

“I have not failed, I’ve just found 10,000 ways that won’t work”

— **Thomas Alva Edison** —

“I think this just might be my masterpiece”

— **Lt. Aldo Raine** from *Inglourious Basterds*, written and directed by Quentin Tarantino —



## ***Acknowledgements***

Finally this experience came to an end and I would like to thank my supervisor Prof. David J. Cole-Hamilton. I remember what you told me on the day of the interview “There is nothing you can’t learn”. When you have the chance of working with such a wonderful person and brilliant scientist you will learn something new every time you knock on his office door or every time he comes around the labs. Have you ever seen a Professor, close to “retirement”, wearing his labcoat and “playing around” the fume hoods? I did. Every student was a new challenge for you so thank you for giving me this opportunity and never giving up on me. Thank you also for opening the doors of your house to all of us, giving us the chance to meet your amazing wife and your children.

I would like to thank Lucite International and Dr Graham R. Eastham for funding my Ph.D. and Dr David Johnson and Mark Waugh for the fruitful discussions.

Special thanks go to Prof. Michael Bühl for helping me with DFT calculations. The first time I met him he asked me “What do you know about Linux or Unix?” but luckily I did not say that the only thing that crossed to my mind was the penguin logo, he would have probably given up on me immediately. Thank you for your time and patience. I would like to thank also Dr Nicolas Sieffert and Dr Herbert Früchtl, they kindly answered all my naive questions.

I am grateful to Prof. Alexandra Slawin and Dr David Cordes for the crystallographic data and Dr Tomas Lebl and Melanja Smith for assistance with NMR studies.

Jacorien, you are the very first person I met in Scotland, thank you for welcoming me. Your help and expertise during my Ph.D. is priceless. You have been a colleague but also a friend. You have been always there for me, whatever the reason was so thank you my dear.

Another special person I had the chance to work with is Peter. Why do you have to consult Wikipedia when you have Peter? Everyone in the labs and in the department loved him because he was always helpful and kind, I never saw him upset, angry or raising his voice. Thank you for sharing your coffee breaks with us and being there every time we needed your help even when you were already retired.

Special thanks go to Jenny, Stuart, Andrey, Brunilde, Seb and Sabrina. Lab days and pub nights were full of joy and fun with you.

Thank you also to James, Mark, Ruben and all former labmates.

I would like to thank my dear friend Roberto, we shared the same pain in two different countries, Flavio, friends I had to leave and people I met along the way.

Thank you Adrián for your endless support. Thank you for being always patient and understanding and for being always so positive and optimistic. “Everything is going to be fine, I know it” even if you did not know of course but this is what makes you so special. In a few words, thank you for being part of my life.

And last but not least, thanks to my family, for your support, for your smiles when I was back home and your tears when I had to fly off again. You have been always proud of me and this is rewarding.

*Papi, croce e delizia. Ale, tempestosamente insostituibile. Mamma, con te non mi sento mai sola, grazie per essere sempre così perfetta. Averi è un privilegio.*



**Table of Contents**

<b>Abbreviations and Acronyms</b>	x
<b>Abstract</b>	xiii
<b>Chapter 1</b>	<b>1</b>
<b>Commercialised processes in the production of MMA</b>	
1.1 General Introduction	2
1.2 The Classical Route: ACH	2
1.3 Competitive routes to the production of MMA: C <sub>2</sub> -C <sub>4</sub> manufacturing routes	4
1.3.1 C <sub>3</sub> manufacturing routes	4
1.3.2 C <sub>4</sub> manufacturing routes	5
1.3.3 C <sub>2</sub> manufacturing routes	6
1.4 Lucite Alpha Process	7
1.5 Conclusions and Prospective Work	8
1.6 References	9
<b>Chapter 2</b>	<b>10</b>
<b>Transition metal-catalysed dehydrogenation of alcohols under homogeneous conditions: a journey from H<sub>2</sub> production to alkylation reactions</b>	
2.1 Introduction	11
2.2 Dehydrogenative oxidation to aldehydes and ketones	12
2.3 Dehydrogenative oxidation to carboxylic acid derivatives	19
2.3.1 Ester or Acid formation	19
2.3.2 Amide formation	26
2.4 Dehydrogenative activation of alcohols for alkylation reactions	29
2.4.1 C-C bond formation	30
2.4.2 C-N bond formation	34
2.5 Conclusions	35
2.6 References	36

---

**Chapter 3** 39

**Upon the  $\alpha$ -methylenation of methyl propanoate via catalytic dehydrogenation of methanol**

3.1 Introduction	40
3.2 Results and Discussion	42
3.3 Conclusions	54
3.4 Experimental Section	55
3.4.1 General materials and methods	55
3.4.2 General instruments	56
3.4.3 General procedure for deuterium labelling experiment (MeP, base and CD <sub>3</sub> OD)	56
3.4.4 Time dependent deuterium labelling study with NaP as base	57
3.4.5 General procedure for base catalysed condensation of MeP and formaldehyde	57
3.4.6 General procedure for catalytic batch reactions	58
3.4.7 Reaction conditions for catalytic batch reactions reported in Table 3.2.1	58
3.4.8 Reaction using <sup>2</sup> H or <sup>13</sup> C labelled methanol	59
3.5 References	63

---

**Chapter 4** 65

**Mechanistic understanding of methanol dehydrogenation catalysed by [RuH<sub>2</sub>(CO)(PPh<sub>3</sub>)<sub>3</sub>]: a blended experimental and theoretical approach**

4.1 Introduction	66
4.2 Results and Discussion	67
4.3 Conclusions and Future Work	81
4.4 Experimental Section	82
4.4.1 General material, methods and instruments	82
4.4.2 Experiment using CH <sub>3</sub> OH and CD <sub>3</sub> OD (1:1) for determining the <sup>1</sup> H/ <sup>2</sup> H KIE	82
4.4.3 Computational details	83
4.4.3.1 Geometry optimisation and thermodynamic corrections	83
4.4.3.2 Energies	84
4.4.4 Tables	85
4.4.4.1 GAS and COSMO Energies for selected isomers	86

4.4.4.2 BSSE corrections at the B97-D/ECP3 level of theory	87
4.4.4.3 Comparisons of different isotopomers at the RI-BP86/ECP1 level of theory	87
4.5 References	88

## **Chapter 5** 90

### **Ru-catalysed decarbonylation of methanol: an insight into the mechanism**

5.1 Introduction	91
5.2 Results and Discussion	92
5.3 Conclusions and Future Work	105
5.4 Experimental Section	106
5.4.1 General materials and methods	106
5.4.2 General instruments	106
5.4.3 Synthetic procedures and mechanistic studies	107
5.4.3.1 $[\text{RuH}_2(\text{CO})(\text{PPh}_3)_3]$ ( <b>5</b> )	107
5.4.3.2 Mixture $[\text{RuHD}(\text{CO})(\text{PPh}_3)_3]$ ( <b>16</b> ) and $[\text{RuH}_2(\text{CO})(\text{PPh}_3)_3]$ ( <b>5</b> )	107
5.4.3.3 Potential $[\text{RuD}_2(\text{CO})(\text{PPh}_3)_3]$ ( <b>19</b> )	108
5.4.3.4 $[\text{RuH}_2(^{13}\text{CO})(\text{PPh}_3)_3]$ ( <b>12</b> ) (experiment used for determining the KIE)	108
5.4.3.5 Mixture of $[\text{RuH}_2(^{13}\text{CO})(\text{PPh}_3)_3]$ ( <b>12</b> ) and $[\text{RuHD}(\text{CO})(\text{PPh}_3)_3]$ ( <b>16</b> ) (KIE)	108
5.4.3.6 Mixture of $[\text{RuH}_2(\text{CO})(\text{PPh}_3)_3]$ ( <b>5</b> ) and $[\text{RuHD}(\text{CO})(\text{PPh}_3)_3]$ ( <b>16</b> ) (KIE)	109
5.4.3.7 Time and temperature dependent NMR studies with $\text{NaOCD}_3$	109
5.4.3.8 Time and temperature dependent NMR studies with $\text{NaOCH}_3$	109
5.4.3.9 Identification of $[\text{RuH}_2(\text{N}_2)(\text{PPh}_3)_3]$ ( <b>20</b> )	109
5.4.3.10 Identification of $[\text{RuH}_2(\text{PPh}_3)_4]$ ( <b>21</b> )	110
5.5 References	110

## **Chapter 6** 111

### **Intermolecular alkylation of carbonyl compounds via coinage metal catalysed C-H bond activation**

6.1 Introduction	112
6.2 Results and Discussion	116
6.3 Conclusions and Future Work	139
6.4 Experimental Section	139

6.4.1 General materials and methods	139
6.4.2 General instruments	140
6.4.3 Synthetic procedures	141
6.4.3.1 1-hydroxy-2-methyl-3-pentanone ( <b>P1</b> )	141
6.4.3.2 [Au(IPr){CH(CH <sub>3</sub> )C(O)CH <sub>2</sub> CH <sub>3</sub> }] ( <b>4</b> )	142
6.4.3.3 [Au(IPr){OC(O)CH <sub>2</sub> CH <sub>3</sub> }] ( <b>5</b> )	142
6.4.3.4 [Au(IPr){CH(CH <sub>3</sub> )C(O)CH <sub>3</sub> }] ( <b>7</b> ) and [Au(IPr){CH <sub>2</sub> C(O)CH <sub>2</sub> CH <sub>3</sub> }] ( <b>8</b> ) (1:1)	143
6.4.3.5 Attempted $\alpha$ -activation of DEK with complexes ( <b>1</b> ) and ( <b>2</b> )	144
6.4.3.6 Attempted $\alpha$ -activation of MeP with complex <b>3</b>	145
6.4.4 Catalytic experiments	145
6.4.4.1 Reaction conditions for catalytic experiments using DEK as substrate	145
6.4.4.2 Reaction procedure for Entry 14 of Table 6.4.4.1	146
6.4.4.3 Catalytic experiments using MEK, acetone, 2,4-dimethyl-3-pentanone	147
6.4.5 Mechanistic studies	147
6.4.5.1 Stoichiometric functionalisation of DEK with alcoform*	147
6.4.5.2 Stoichiometric functionalisation of DEK with <sup>13</sup> C labelled alcoform*	148
6.4.5.3 Blank experiment with ( <b>4</b> ) and methanol	148
6.4.6 DFT calculations	148
6.4.6.1 Computational details	148
6.4.6.2 GAS and PCM Energies	149
6.5 References	150
<b>General Conclusions</b>	153
<b>Appendix 1</b>	156
<b>Appendix 2</b>	177

**Abbreviations and Acronyms**

Å	angstrom
ACH	acetone cyanohydrin
A- <i>i</i> PrPNP	4,5-bis(diisopropylphosphinomethyl)acridine
Ar	aryl
BDTBPMB	1,2-bis(di- <i>tert</i> -butylphosphinomethyl)benzene
bipy	2,2'-bipyridyl
br	broad
BSSE	Basis Set Superposition Error
Bu	butyl
<i>t</i> -Bu (at the beginning)	<i>tert</i> -butyl
<i>t</i> Bu (in the middle)	
<i>t</i> -BuP	<i>tert</i> -butyl propanoate
<i>t</i> Bu-PNN	2-(di- <i>tert</i> -butylphosphinomethyl)-6-(diethylaminomethyl)pyridine
BV	Baeyer-Villiger
BVMO	Baeyer-Villiger Monooxygenase
calcd	calculated
cat.	catalyst
cod	1,5-cyclooctadiene
COE	cyclooctene
conv.	conversion
COSMO	conductor-like screening model
COSY	correlation spectroscopy
Cp*	1,2,3,4,5-pentamethylcyclopentadiene
<i>m</i> CPBA	<i>meta</i> -chloroperoxybenzoic acid
d	doublet
dba	<i>trans,trans</i> -dibenzylideneacetone
DBU	1,8-diazobicyclo[5.4.0]undec-7-ene
DCM	dichloromethane
DEK	diethyl ketone or 3-pentanone
DEPTQ	Distortionless Enhancement by Polarization Transfer with retention of quaternaries
DFT	Density Functional Theory
DHC	dehydrogenative coupling
DMSO	dimethyl sulfoxide
dppf	1,1'-bis(diphenylphosphino)ferrocene
dppp	1,2-bis(diphenylphosphino)propane
ECP	Effective Core Potential
ESI	electronic supporting information
Et	ethyl

g	grams
GBL	$\gamma$ -butyrolactone
GC	Gas Chromatography
GC-FID	Gas Chromatography-Flame Ionization Detector
GC-MS	Gas Chromatography-Mass Spectroscopy
GHMBC	Gradient Heteronuclear Multiple Bond Coherence
GHSQC	Gradient Heteronuclear Single Quantum Coherence
h	hour
HMBC	Heteronuclear Multiple Bond Correlation
HPNP	bis[(2- <i>diisopropylphosphino</i> )ethyl]amine
HPNP <sup>Ph</sup>	HN(CH <sub>2</sub> CH <sub>2</sub> PPh <sub>2</sub> ) <sub>2</sub>
IMes	1,3-bis(2,4,6-trimethylphenyl)imidazol-2-ylidene
int.	intermediate
<i>i</i> Pr	1,3-( <i>diisopropyl</i> )imidazol-2-ylidene
<i>i</i> Pr <sub>2</sub> Me <sub>2</sub>	1,3-bis( <i>isopropyl</i> -4,5-dimethyl)imidazol-2-ylidene
<i>i</i> Pr (L)	1,3-bis(2,6- <i>diisopropylphenyl</i> )imidazol-2-ylidene
<i>i</i> Pr	<i>isopropyl</i>
IS	internal standard
J	coupling constant
KIE	kinetic isotope effect
kJ	kilojoule
L	neutral ligand
$\mu$ L	microliter
LTM	late-transition metal
m	multiplet
M	metal
MAA	methacrylic acid
Me	methyl
MEK	methyl ethyl ketone or 2-butanone
MeP	methyl propanoate
MiBu	methyl isobutyrate (methyl 2-methylpropanoate)
mg	milligrams
MHz	megahertz
min	minutes
mL	milliliters
MMA	methyl methacrylate
mmol	millimoles
mol	moles
MTBE	methyl <i>tert</i> -butyl ether
NaP	sodium propanoate
NMR	Nuclear Magnetic Resonance
NMR	<i>N</i> -heterocyclic carbene
PBE	Perdue Burke Ernzerhof



Ph	phenyl
PNN and PNP	generic tridentate pyridine-based ligand chelating in a pincer-type manner
PNN*	deprotonated PNN
PPh <sub>3</sub>	triphenylphosphine
ppm	parts per million
Py	pyridyl
q	quartet
R	alkyl group
RT	room temperature
s	singlet
SCF	Self-Consistent Field
SDD	Stuttgart Dresden potential
sept	septet
S <sub>N</sub> 2	nucleophilic substitution
t	triplet
t	time
T	temperature
TBA	<i>tert</i> -butanol
TFPAA	trifluoroperoxyacetic acid
THF	tetrahydrofuran
TMEDA	tetramethylethylene diamine
TMS	tetramethylsilane
TOF	turnover frequency
TON	turnover number
tpa	tons per annum
TS	transition state
UDEFT	Uniform Driven Equilibrium Fourier Transform
XRD	X-Ray Diffraction

## ***Abstract***

Formaldehyde is a chemical used widely in the manufacture of building materials. A remarkable example is represented by the Lucite two-step Alpha technology for the large scale production of methyl methacrylate (MMA), the essential building block of all acrylic-based products.

Esters and ketones are important intermediates in the manufacture of acrylate esters therefore  $\alpha$ -hydroxymethylenation of carbonyl compounds using formaldehyde as a one carbon alkylating agent and subsequent dehydration to the corresponding methylenated derivatives has been explored in the current work.

We report a novel catalytic approach for the synthesis of methyl methacrylate (MMA) via one-pot  $\alpha$ -methylenation of methyl propanoate (a chemical intermediate of the ALPHA process) with formaldehyde, generated *in situ* by Ru-catalysed dehydrogenation of methanol. Elucidation of the mechanism involved in the catalytic dehydrogenation of methanol along with the collateral alcohol decarbonylation reaction was gained through a combined experimental and DFT study. The development of an alternative process where anhydrous formaldehyde is produced *in situ* would provide a simplification over the current second step of the ALPHA technology where the formaldehyde is initially produced as formalin, subsequently dehydrated to afford anhydrous formaldehyde in order to ensure high selectivity to MMA.

As an alternative approach, ketones, in particular 3-pentanone and 2-butanone, were targeted as potential substrates in order to overcome some of the problems related to competing reactions that occur at the ester group. Hydroxymethylenation, followed by dehydration and Baeyer-Villiger oxidation, possibly catalysed by enzymes to reverse the normal selectivity, leads to the formation of acrylate esters. The catalytic reaction is enabled by a gold carbene hydroxide complex in such a way that the substrate undergoes C-H activation and the nascent metal alkyl acts as a nucleophile towards the electrophilic formaldehyde, supplied in the form of alcoform\* (solution of paraformaldehyde in methanol).

# *Chapter 1*

## **Commercialised processes in the production of Methyl Methacrylate (MMA)**

Methyl methacrylate is a chemical intermediate used in the large scale production of homo- or copolymers. In this chapter we report the state of the art on the production of MMA from the classical ACH process to more competitive and environmentally benign C<sub>2</sub>-C<sub>4</sub> manufacturing routes with a special attention to Lucite ALPHA technology.

---

**Keywords:** MMA · C<sub>2</sub>-C<sub>4</sub> routes · ALPHA technology

## 1.1 General Introduction

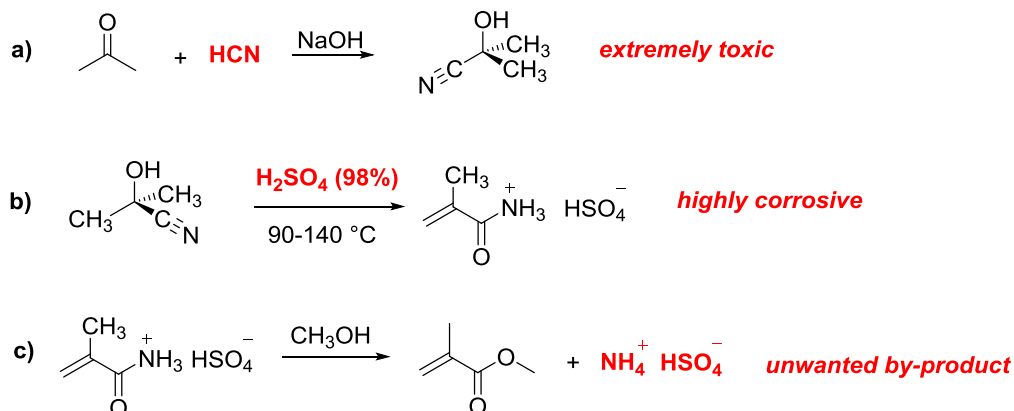
Methyl Methacrylate (MMA) is the essential building block of all acrylic-based products. It is successfully used in the manufacture of Poly(methyl methacrylate) (PMMA), commonly called by the trademarks *Plexiglas* (Rohm and Haas), *Perspex* (ICI) or *Lucite* (DuPont) or simply acrylic, using free radical initiation, or used in the production of other polymers and resins when combined with other monomers.

The methacrylic polymer, due to its exceptional optical clarity, weather and UV light resistance, ability to take colour and biocompatibility is widely used in several commercial fields including construction, signboards, shatterproof and lightweight substitute for glass (mobile phones screens, aquariums, submarine viewing ports), vehicles and lighting equipments, surface coatings, LCD screens, medical device, dental products and bone cements.<sup>[1][2]</sup>

## 1.2 The Classical Route: ACH

MMA was commercialised for the first time in 1937 by **Rohm and Haas Company**, by the acetone cyanohydrin (ACH) process. Although the ACH process involves the dangerous chemical HCN and produces large amounts of ammonium bisulfate waste, it was for a long time the only commercialised process in the manufacture of MMA and it is still adopted by most manufacturers even nowadays.

This process consists of three steps: **a)** formation of cyanohydrin from reaction of acetone with HCN, **b)** conversion of the cyanohydrin of acetone to the amide of methacrylic acid, **c)** conversion of the amide salt to the methyl ester (Scheme 1.2.1).



**Scheme 1.2.1** The classical route to MMA involving acetone cyanohydrin (ACH).

The first step involves the nucleophilic addition of cyanide anion on the carbonyl carbon of acetone affording cyanohydrin in high yield and selectivity (92-99%). This reaction is catalysed by sodium hydroxide and occurs under mild conditions (temperatures below 40 °C). The subsequent conversion of the cyanohydrin of acetone to the amide salt of methacrylic acid requires the presence of sulfuric acid, which plays two roles. It is necessary for conversion of the hydroxyl group of cyanohydrin to the double bond via protonation and water elimination and also for transformation of the cyano group to the amide salt via acid-catalysed hydrolysis. Finally, the generated amide salt is converted to methyl methacrylate by treatment with methanol. In this last step a four-coordinate intermediate is formed by nucleophilic addition of methanol on the carbonyl carbon. Finally, if ammonia is ejected from this intermediate then methyl methacrylate will be formed in good selectivity (77%). However, the Achilles' heel of this protonation is the generation of a large amount of the unwanted ammonium bisulfate byproduct, which together with the use HCN, one of most toxic chemical used in industrial processes, represent the two major drawbacks for this route.<sup>[1c]</sup>

This has provided the motivation for the development of new processes with lower manufacturing costs and greater environmental acceptability. The wide market and ever growing demand of acrylics however, has led in the last decades to the development and commercialisation of new industrial processes with more economic advantages and less environmental impact.

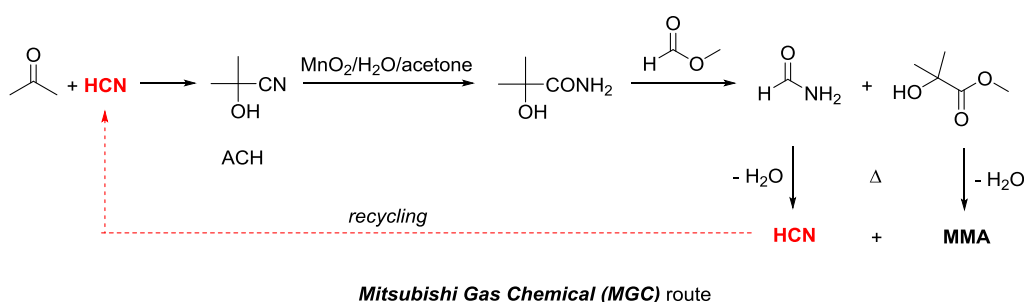
### 1.3 Competitive routes to the production of MMA: C<sub>2</sub>-C<sub>4</sub> manufacturing routes

#### 1.3.1 C<sub>3</sub> manufacturing routes

Although the ACH route was the only commercialised process in the manufacture of MMA for a long time, other research efforts were directed at the possibility of reforming this old process by recycling ammonium bisulfate (ICI process) and HCN (Mitsubishi process).

**ICI (Imperial Chemical Industries)** developed a process for the conversion of the ammonium bisulfate to sulfuric acid, which can be reintroduced into the ACH process. This process proceeds via ammonium bisulfate pyrolysis to afford sulfur trioxide, water and ammonia. The ammonia then undergoes a further oxidation to give nitrogen and water, while addition of water to the previously formed sulfur trioxide, finally generates sulfuric acid.

On the other hand, the aim of the **Mitsubishi Gas Chemicals (MGC)** process is the capture of the nitrogen atom of the cyano group into a new molecule, a formamide, which can breakdown to water and HCN when heated to high temperature. The ACH is in fact hydrated to  $\alpha$ -hydroxyisobutyramide by a manganese oxide catalyst and subsequently esterified to  $\alpha$ -hydroxy isobutyrate by methyl formate which in turn is converted into formamide. Dehydration reactions occurring on both products generate respectively MMA and HCN which is recycled into the ACH process, instead of being discarded as ammonium bisulfate. The advantages of this modified ACH route process are that, the use of sulfuric acid is not required and the transesterification reaction is performed with methyl formate rather than methanol.

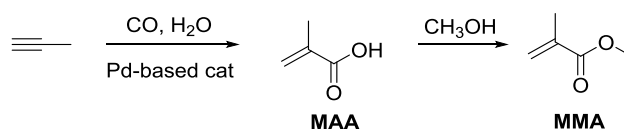


**Scheme 1.3.1** Mitsubishi Gas Chemical route: a reformation of the ACH sulfo process

However, both processes still preserve the step involving acetone and HCN to generate the carbon atoms of MMA and in this way some problems connected to the old process are still

retained: the employment of HCN which requires great safety measures, limiting therefore the industrial scale-up together with the increase of costs.

The **Shell** technology, which was sold to **Ineos Acrylics**, is a one-step process which consists of a Pd-catalysed carbonylation of methyl acetylene<sup>[3]</sup> leading to the formation methacrylic acid, finally converted into MMA by methanol transesterification.<sup>[4]</sup> High catalyst activity (MMA formation rates of 20-50 kmol/h per mol of Pd) and selectivity to MMA (99 %) are achieved using a (diphenyl)phosphine ligand bearing a 2-pyridyl substituent (2-PyPPh<sub>2</sub>)<sup>[5]</sup> and an excess of an acid containing weakly coordinating anions (e.g sulfonates). The twin problems of this technology that limit the industrial scalability, are the availability and feedstock contamination with the isomer allene, which has a similar boiling point of propyne and is responsible for catalyst poisoning.



**Shell** process (currently bought by **Ineos Acrylics**)

**Scheme 1.3.2** The Shell technology sold to Ineos Acrylics

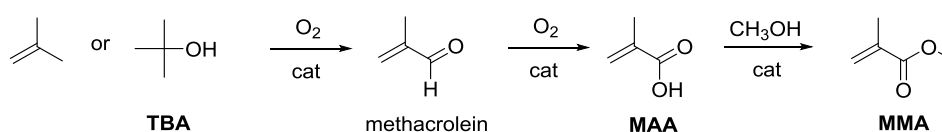
**Evonik industries** disclosed the intent of building the first start-up plant for the large scale production of MMA based on the more eco-friendly AVENEER<sup>®</sup> process, for which a pilot plant has been operating since 2007, for the middle of 2015.<sup>[6]</sup> This technology, like the parent ACH sulfo process, uses acetone, methanol, ammonia and methane but it does not require sulfuric acid. Besides this convenient aspect it has a higher efficiency than the ACH route and allows to reduce the CO<sub>2</sub> emission by almost 50 % in comparison with conventional processes.

### 1.3.2 C<sub>4</sub> manufacturing routes

Alternative C<sub>4</sub> routes, based on isobutene or *tert*-butanol (TBA) have been commercialised by Japanese companies, following the development of high performance oxidation catalysts, and they are responsible of more than 50 % of MMA supply in Japan. Direct oxidation methods consist of a two-step gas-phase oxidation of isobutene or TBA to methacrylic acid and its subsequent esterification, performed by methanol, to afford MMA. The direct oxidation plants

have been commercialised by **Mitsubishi Rayon** (MRC), **Japan Methacrylic Monomer** and **Kyodo Monomer** companies and consist of two catalytic oxidation steps, for which excellent catalysts have been patented.

The **Asahi** Japanese company established and commercialised a two-step process which involves direct oxidative esterification of methacrolein. In fact the methacrolein, produced by oxidation of TBA as reported above, is recovered as a liquid phase with methanol, oxidised with oxygen or air on a Pd/Pb catalyst and simultaneously esterified to MMA with 93 % yield.



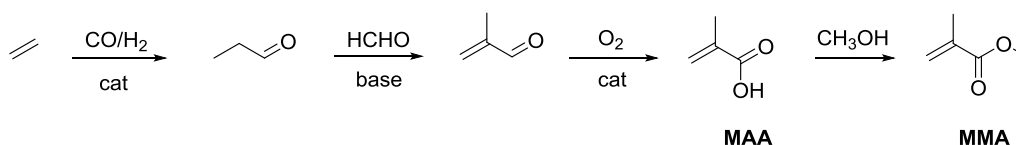
**Isobutene or TBA route**

**Scheme 1.3.3** The C<sub>4</sub>-isobutene or *tert*-butanol route of the Japanese companies Mitsubishi Rayon and Asahi.

### 1.3.3 C<sub>2</sub> manufacturing routes

C<sub>2</sub> routes based on ethene as raw material for the production of MMA via intermediates such as propanal, propanoic acid or methyl propanoate, have been investigated. These C<sub>2</sub> routes are defined by condensation reactions of such intermediates with formaldehyde affording methacrolein, methacrylic acid (MAA) or methyl methacrylate.

Worldwide, the most competitive MMA manufacturing technology is represented by the **BASF** process, which consists of a hydroformylation of ethene to propanal, followed by its condensation with formaldehyde to afford methacrolein which finally undergoes oxidation giving methacrylic acid. The esterification of MAA generates the final MMA.



**BASF process**

**Scheme 1.3.4** The ethene-based process of the German giant chemical company BASF.



Finally, the new ALPHA plant of **Lucite Int.**, a result of 20 years of R&D, has become a highly competitive process for the manufacture of MMA (described in § 1.4).

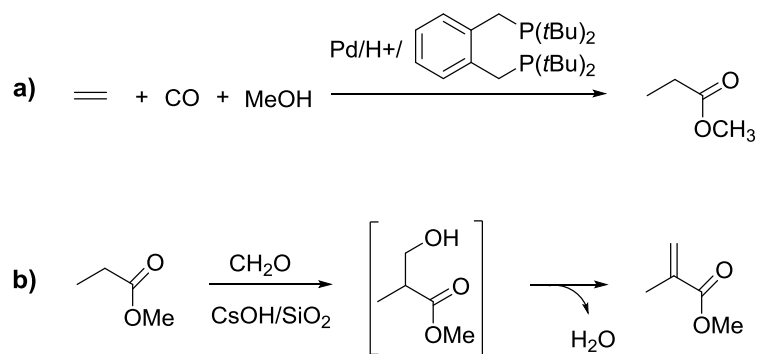
MRC and Lucite have been also working on the development of bio-routes to MMA using renewable feedstocks.

## 1.4 Lucite Alpha Process

Lucite International, a leader in acrylic-based products, developed and commercialised in Singapore, during 2007-8, the first ALPHA technology (Scheme 1.4.1), a two-step patented process to MMA. The ALPHA process (120,000 tpa plant in Singapore and 250,000 tpa in Saudi Arabia), is a high-yield low-cost and much more environmentally benign process.<sup>[1a, 7]</sup>

The first step deals with the methoxycarbonylation of ethene to methyl propanoate (MeP), performed in the presence of a catalyst developed by Lucite Int. The catalyst is based on a zero valent palladium complex of formula  $[L_2Pd(dba)]$  (where  $L_2 = 1,2$ -bis(di-*tert*-butylphosphinomethyl)benzene (BDTBPMB) and  $dba = trans,trans$ -dibenzylideneacetone), afforded by addition of the bidentate phosphine ligand  $L_2$  to  $[Pd_2(dba)_3]$ . When this complex is treated with a sulfonic acid it provides an active species which is able to catalyse the conversion of ethene, CO and MeOH to methyl propanoate. This first step has been optimised with very high selectivity (99.98%) to the desired product and high rates at low catalyst loading (50,000 mol of product per mol of catalyst per hour) and catalyst lifetimes exceed 1M turnovers.<sup>[8]</sup>

The second step furnishes MMA via condensation of MeP with gaseous formaldehyde, at 320 °C and a pressure of 2 bar on a fixed bed of catalyst (caesium oxide on silica). Unlike the previous reaction, this one is a multistep process which only proceeds in low yield (17 % per pass). It requires two parallel MMA reactors for guaranteeing a continuous production of MMA during the alternative, *in situ*, regeneration of reactors (the deposit of a coke on the catalyst bed is responsible for the activity and selectivity decrease). Despite these negative aspects, it has been optimised to a level that allows it to be commercialised.



**Scheme 1.4.1** The two-step ALPHA technology for the production of MMA developed by Lucite Int.

## 1.5 Conclusions and Prospective Work

Among the commercialised processes the Lucite Technology is an innovative process with a greater scalability, lower manufacturing costs and the lowest fixed capital investment according to SRI Consulting. However it is affected by lower per-pass conversions in the second reaction step and higher utilities costs.

Therefore, our research efforts, in collaboration with Lucite Int., were directed at the possibility of exploring alternative routes to the manufacture of methyl methacrylate involving methyl propanoate and in the second place ketones such as 3-pentanone and 2-butanone, which can be oxidised to corresponding esters via a Baeyer-Villiger (BV) reaction. Formaldehyde was always used as a C<sub>1</sub> alkylating agent under homogeneous conditions. However, formaldehyde could be in principle generated *in situ* by catalysed dehydrogenation of methanol or derived from alcoform, a solution of formaldehyde in methanol in the form of different chain length oligomers of methoxymethanol.

The formation of the new C-C bond may occur via a simple base-catalysed condensation of the  $\alpha$ -deprotonated substrate with the nascent formaldehyde, for which the electrophilicity is temporarily enhanced by partial coordination to the metal centre, or through activation of the  $\alpha$ -C-H bond of the substrate upon coordination to a metal centre. These two examples of alkylation processes will be discussed in detail in Chapters 3 and 6 respectively.

The present thesis is organised into 5 chapters besides the current introduction on the MMA manufacture (state of the art):

- *Transition metal-catalysed dehydrogenation of alcohols under homogeneous conditions: a journey from H<sub>2</sub> production to alkylation reactions*
- *Upon the  $\alpha$ -methylenation of methyl propanoate via catalytic dehydrogenation of methanol*
- *Mechanistic understanding of methanol dehydrogenation catalysed by [RuH<sub>2</sub>(CO)(PPh<sub>3</sub>)<sub>3</sub>]: a blended experimental and theoretical approach*
- *Ru-catalysed decarbonylation of methanol: an insight into the mechanism*
- *Intermolecular alkylation of carbonyl compounds via coinage metal catalysed C-H bond activation*

Each chapter consists of a detailed introduction connecting the main research scope with the investigation undertaken, a developed section of results and discussion, conclusions and possible perspectives, experimental section and bibliography, therefore no further details will be provided in this pilot chapter.

## 1.6 References

- [1] a) B. Harris, *Ingenia* **2010**, 19-23; b) K. Nagai, *Appl. Catal., A* **2001**, 221, 367-377; c) M. M. Green, H. A. Wittcoff, in *Organic Chemistry Principles and Industrial Practice*, Wiley-VCH, Weinheim, **2003**, pp. 137-156.
- [2] Special Report "Methyl Methacrylate: A Techno-Commercial Profile" from Chemical Weekly, June 29, 2010.
- [3] a) E. Drent, EP271145, **1988**; b) E. Drent, P. H. M. Budzelaar, EP386834, **1990**; c) E. Drent, P. H. M. Budzelaar, W. W. Jager, J. Stapersma, EP441447, **1991**
- [4] M. J. Doyle, J. Van Gogh, C. J. C. Van Ravenswaay, EP392601, **1990**
- [5] E. Drent, P. Arnoldy, P. H. M. Budzelaar, *J. Organomet. Chem.* **1994**, 475, 57-63.
- [6] from Evonik industries' Press release, September 27, **2012**.
- [7] G. R. Eastham, R. P. Tooze, X. L. Wang, K. Whiston, World Patent 96/19434, **1996**
- [8] W. Clegg, M. R. J. Elsegood, G. R. Eastham, R. P. Tooze, X. L. Wang, K. Whiston, *Chem. Commun. (Cambridge)* **1999**, 1877-1878.

# Chapter 2

## Transition metal-catalysed dehydrogenation of alcohols under homogeneous conditions: a journey from H<sub>2</sub> production to alkylation reactions

The current introduction engages the main achievements in the area of “*transition metal-catalysed dehydrogenation of alcohols under homogeneous conditions*”. Dehydrogenation of alcoholic substrates can be considered as an alternative methodology to generate H<sub>2</sub>, a potential benign fuel, or a strategy to temporarily enhance their reactivity by oxidation to the corresponding carbonyl derivatives which can be used as alkylating agents in the formation of new C-C and C-N bonds, an approach of particular interest in pharmaceutical manufacture.

**Keywords:** transition metals · homogeneous catalysis · alcohol dehydrogenation · H<sub>2</sub> · alkylation

## 2.1 Introduction

*“Prince Charles has spoken about his decision to convert his Aston Martin sports car to run on waste wine”* – from BBC news of 10<sup>th</sup> July 2008.

The idea of converting ethanol into a bio-fuel would probably not cross your mind if you are drinking a glass of wine from an expensive bottle of 1990 Pinot Noir of the French estate *Domaine de la Romanée-Conti*, however the aim of the news is certainly to draw attention to the contribution of inorganic chemistry to industrial research.

The development of new energy systems based on renewable resources in order to face the dangerous climate changes related to the unrestricted use of fossil fuels, of which reserves are in addition progressively depleting, has been for example one of the biggest challenges in this century with alcohols playing a key role in the so called “hydrogen economy” (§ 2.2 and 2.3).

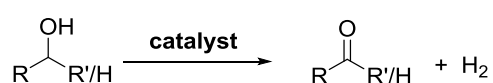
The catalytic dehydrogenative oxidation of alcohols represents also an alternative tool used to convert less reactive substrates, such as alcohols, into alkylating agents to achieve new bond formation, a greener and atom-efficient methodology (§ 2.4).

Despite the fascinating chemistry of alcohols and the number of outstanding publications that have appeared, the present introduction will cover the main achievements in the confined area of *“transition metal-catalysed dehydrogenation of alcohols under homogeneous conditions”* and will be organised into three sections based on the reaction scope with a greater emphasis on the chemistry strictly related to the current thesis:

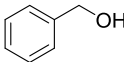
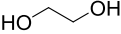
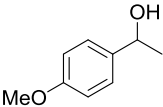
- ♦ Dehydrogenative oxidation to aldehydes and ketones
- ♦ Dehydrogenative oxidation to carboxylic acid derivatives
- ♦ Dehydrogenative activation of alcohols for alkylation reactions: C-C and C-N bond formation

## 2.2 Dehydrogenative oxidation to aldehydes and ketones

The most recent review of H<sub>2</sub> production from alcohols was published by Grützmacher in 2014<sup>[1]</sup> and it summarises the work reported in more than 300 papers proving the growing attention to H<sub>2</sub> as a potential benign fuel when combined with fuel cells.<sup>[2]</sup> H<sub>2</sub> in fact has been targeted as an ideal energy carrier which can be “chemically” stored by incorporation into small organic molecules such as alcohols, overcoming the safety risks related to the conventional storage<sup>[3]</sup> and worldwide transport of large amounts of this chemical without neglecting the significant volume and weight demand of the required equipment.



**Scheme 2.2.1** General representation of catalysed dehydrogenative oxidation of alcohols to generate the corresponding carbonyl compounds with liberation of H<sub>2</sub> gas.

Substrate Chart						
	1-heptanol	cyclooctanol	EtOH	1-propanol	2-propanol	
<b>S1</b>	<b>S2</b>	<b>S3</b>	<b>S4</b>	<b>S5</b>	<b>S6</b>	<b>S7</b>
	1-butanol	1-hexanol	1,4-butanediol	1-pentanol	MeOH	glycerol
<b>S8</b>	<b>S9</b>	<b>S10</b>	<b>S11</b>	<b>S12</b>	<b>S13</b>	<b>S14</b>

**Figure 2.2.1** Representation and numbering codes of the Substrates (S) reported in § 2.2 and 2.3

**Dehydrogenative Oxidation of Alcohols to Aldehydes and Ketones:  
Catalyst (C) Chart with best reported TONs and TOFs for selected Substrates (S)**

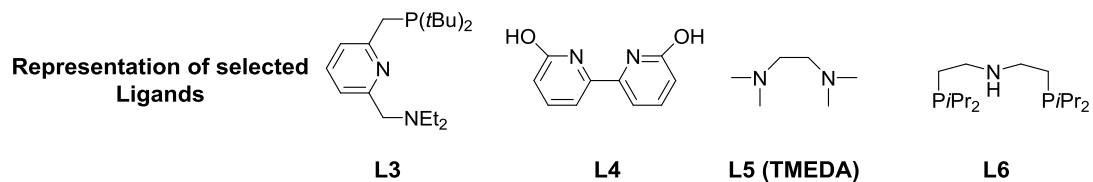
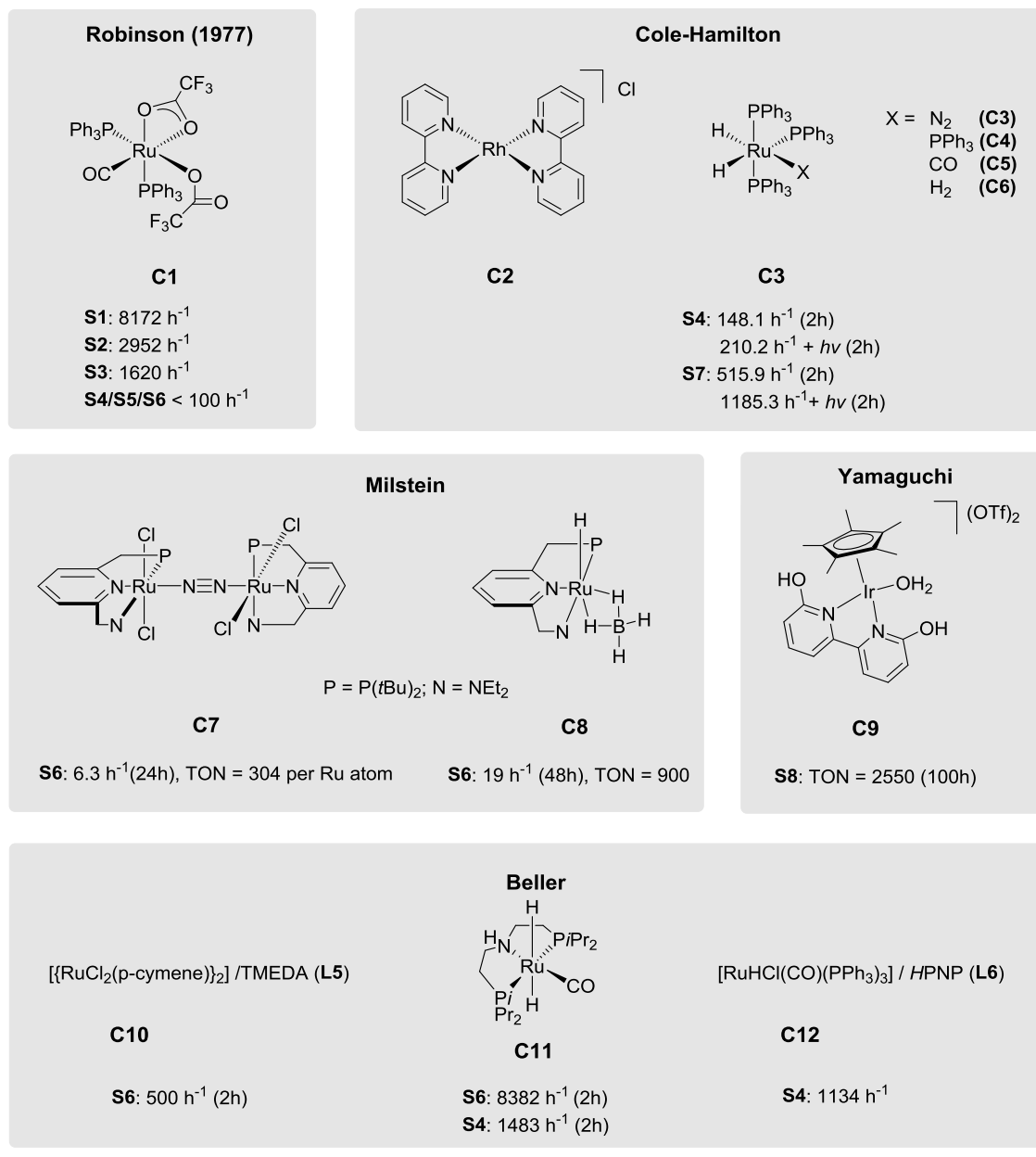
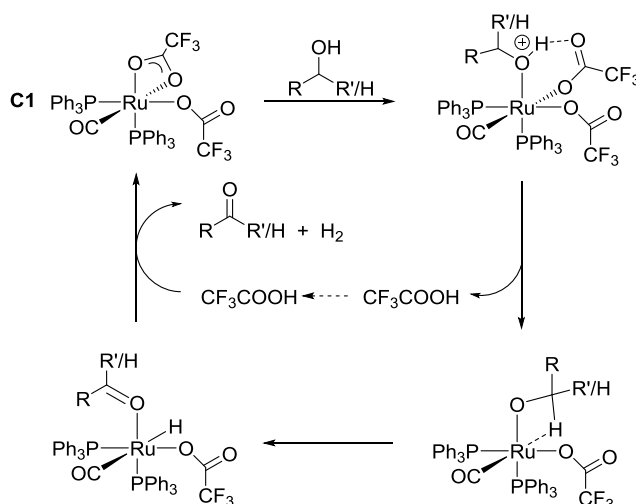


**Figure 2.2.2** Representation of dehydrogenative catalysts (C) used for the production of aldehydes and ketones along with evolution of H<sub>2</sub> and respective best reported TONs and TOFs for selected substrates (S).

One of the earliest examples of acid-promoted dehydrogenation of primary and secondary alcohols to generate H<sub>2</sub> gas along with carbonyl compounds was reported by Dobson and Robinson in 1977.<sup>[4]</sup> The most active catalyst was found to be a Ru(II) complex [Ru(OCOCF<sub>3</sub>)<sub>2</sub>(CO)(PPh<sub>3</sub>)<sub>2</sub>] (**C1**) (cat. loading 0.03 %) bearing a more readily dissociative carboxylate ligand (**L1** = OCOCF<sub>3</sub>) in the presence of an excess of trifluoroacetic acid. The turnover frequencies (TOFs) achieved with catalyst **C1** were of the order of 8172 h<sup>-1</sup> for benzyl alcohol (**S1**), 2952 h<sup>-1</sup> for 1-heptanol (**S2**) and 1620 h<sup>-1</sup> for cyclooctanol (**S3**) while TOFs lower than 100 h<sup>-1</sup> were obtained for EtOH (**S4**), 1-propanol (**S5**) and 2-propanol (**S6**). The proposed mechanism involves an initial coordination of the alcohol which is further deprotonated by the carboxylate ligand leading to the liberation of the free acid and generation of the alkoxide complex, which in turn undergoes β-H abstraction to afford a Ru(II) hydride species and the corresponding carbonyl compound (aldehyde or ketone). The subsequent recoordination of the acid allows the release of H<sub>2</sub> and regeneration of the catalyst.



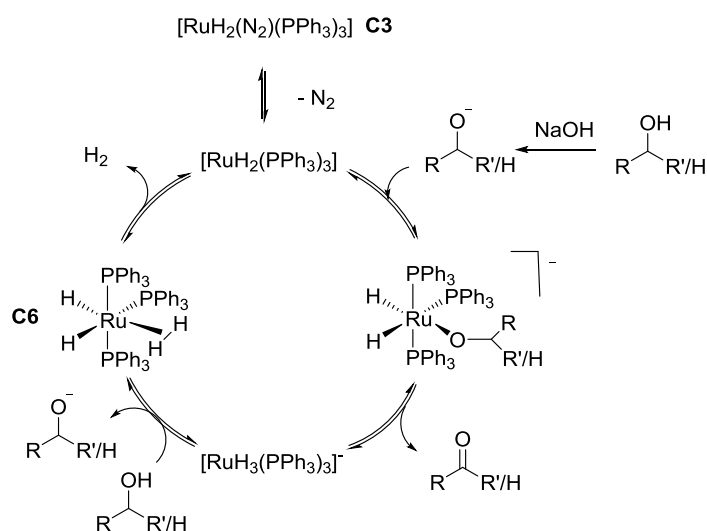
**Scheme 2.2.2** Proposed mechanism for acid-promoted dehydrogenation of primary and secondary alcohols catalysed by **C1** as reported in Wills *et al.* review.<sup>[4-5]</sup>

In the late '80s Cole-Hamilton *et al.* reported for the first time that reasonable rates of H<sub>2</sub> production could be obtained by dehydrogenation of lower molecular weight alcoholic substrates catalysed by ruthenium and rhodium precursors in the presence of an excess of a base.<sup>[6]</sup> In one of their early works using [Rh(bipy)<sub>2</sub>]Cl (**C2**), (**L2** = bipy = 2,2'-bipyridyl), the most efficient of Rh catalysts, they demonstrated that the continuous removal of H<sub>2</sub> at high temperatures (120 °C), in order to prevent the re-hydrogenation of the newly formed carbonyl



products (principle of microscopic reversibility), converts the thermodynamically unfavourable process into a highly favourable one ( $\Delta G = +41.2$  kJ/mol against  $-33.3$  kJ/mol for the production of acetal and H<sub>2</sub> from ethanol).<sup>[6a]</sup> Reasonably high TOFs were achieved with [RuH<sub>2</sub>(N<sub>2</sub>)(PPh<sub>3</sub>)<sub>3</sub>] (**C3**) and [RuH<sub>2</sub>(PPh<sub>3</sub>)<sub>4</sub>] (**C4**) catalysts, moreover both catalyst activity was significantly increased by irradiation with visible light, from 148.1 h<sup>-1</sup> to 210.2 h<sup>-1</sup> when using ethanol as substrate and from 515.9 h<sup>-1</sup> to 1185.3 h<sup>-1</sup> with (CH<sub>2</sub>OH)<sub>2</sub> (**S7**) in the presence of catalyst **C3** after 2 h, as the most remarkable examples.<sup>[6b]</sup> Added base plays a key role in these systems as confirmed by the very minor activity observed in its absence. The base acts as a co-catalyst but at the same time can promote unwanted side reactions like alcohol or aldehyde decarbonylation, aldol and Tishchenko reactions.<sup>[7]</sup> Concerning the mechanism involved in the Ru-catalysed reactions, a preliminary coordination of the alkoxide into a vacant site created by loss of a N<sub>2</sub> or PPh<sub>3</sub> ligand was proposed, followed by  $\beta$ -H transfer with subsequent release of an alkanal and loss of H<sub>2</sub> acting as a good leaving group from a molecular hydrogen complex.<sup>[6b]</sup>

<sup>6c]</sup> All Ru-catalysed reactions were performed at 150 °C.<sup>[6b]</sup>



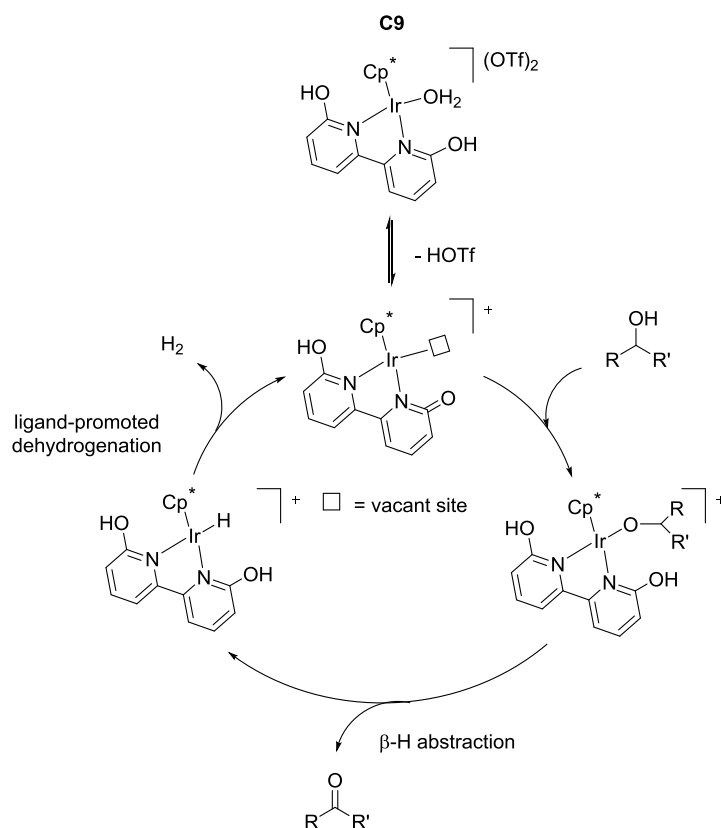
**Scheme 2.2.3** Proposed mechanism for the production of H<sub>2</sub> from alcohols catalysed by **C3**.

As mentioned before, decarbonylation of the new formed alkanals may occur as a side reaction during these catalytic systems resulting in the formation of a stable and inactive carbonyl species in the case of rhodium complexes<sup>[6c]</sup>, while [RuH<sub>2</sub>(X)(PPh<sub>3</sub>)<sub>3</sub>] (where X = H<sub>2</sub>, N<sub>2</sub> or PPh<sub>3</sub>) easily decarbonylates alcohols to give a still active species [RuH<sub>2</sub>(CO)(PPh<sub>3</sub>)<sub>3</sub>] (**C5**).<sup>[6b]</sup> Catalyst **C5** was already reported by Morton and Cole-Hamilton as an active species for alcohol

dehydrogenation (e.g. TOF of 62 h<sup>-1</sup> were achieved for ethanol at 150 °C in the presence of NaOH), but more recently we demonstrated that it could be successfully employed as a dehydrogenative catalyst for the most challenging substrate methanol in a one-pot system for the methylenation of methyl propanoate (see chapter 3). Bühl and co-workers reported a comprehensive computational study on both the dehydrogenation<sup>[8]</sup> and the collateral decarbonylation<sup>[9]</sup> of several alcohols catalysed by the catalyst precursor [RuH<sub>2</sub>(H<sub>2</sub>)(PPh<sub>3</sub>)<sub>3</sub>] (**C6**). The DFT study revealed that methanol dehydrogenation can follow four competitive pathways due to very close activation free energies with rate-determining steps of different natures (β-H transfer, dissociation of H<sub>2</sub> or partial decoordination of the HCHO product) while the investigation of ethanol and 1-propanol showed that the dehydrogenation process is kinetically favoured for higher molecular weight alcohols.<sup>[8]</sup> For the first time a plausible pathway for the dehydrogenation of methanol catalysed by the active species **C5** was proposed (see Chapter 3) based on previously published work<sup>[8, 10]</sup> and computed intermediates (see Chapter 4) following the same protocol used by Sieffert and Bühl in their analogous study.<sup>[8-9, 11]</sup>

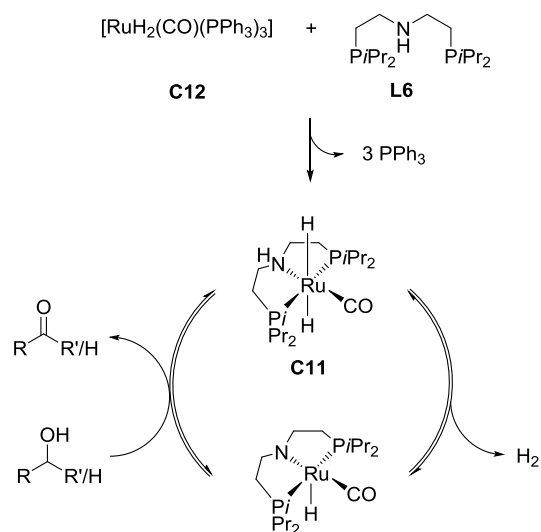
Milstein *et al.* reported a series of electron-rich PNN- and PNP-type Ru(II) catalysts for the dehydrogenation of secondary alcohols to the corresponding ketones. In 2006 they developed a N<sub>2</sub> bridged Ru(II) dinuclear complex [RuCl<sub>2</sub>(*t*Bu-PNN)]<sub>2</sub>(μ-N<sub>2</sub>) (**C7**) (**L3** = *t*Bu-PNN = 2-(di-*tert*-butylphosphinomethyl)-6-(diethylaminomethyl)pyridine) as a promising catalyst for the dehydrogenation of 2-propanol to acetone upon addition of a base (TON = 304 per Ru atom; TOF = 6.3 h<sup>-1</sup> after 24 h).<sup>[12]</sup> Later on, by treatment of complex **C7** with an excess of NaBH<sub>4</sub> they generated a more efficient catalyst, [RuH(BH<sub>4</sub>)(*t*Bu-PNN) (**C8**), even under neutral conditions. The Ru(II) hydrido borohydride complex **C8** exhibited TON of 900 (TOF of 19 h<sup>-1</sup> after 48 h) for the conversion 2-propanol to acetone at 105 °C and also relatively higher catalytic activity in comparison with the PNP-derivative.<sup>[13]</sup>

Yamaguchi *et al.* reported a novel catalytic system (oxidant free) for the oxidation of primary and secondary alcohols performed in an aqueous medium under mild conditions in the presence of a water soluble Cp\*Ir complex (**C9**) bearing 6,6'-dihydroxy-2,2'-bipyridine (**L4**) as a functional ligand. The highest TONs (2550 after 100 h) were accomplished when the reaction was performed using 1-(4-methoxyphenyl)ethanol (**S8**) as substrate and a very small catalyst loading.<sup>[14]</sup>



**Scheme 2.2.4** Plausible mechanism for the dehydrogenative oxidation of alcohols catalysed by **C9** as reported by Yamaguchi *et al.*<sup>[14]</sup>

More recently Beller *et al.* developed more efficient catalytic systems for the dehydrogenation of thermodynamically less favourable aliphatic primary alcohols in which the active species is generated *in situ* from a series of Ru precursors in combination with amine or tridentate, pyridine-based ligands, chelating in a pincer-type manner. They demonstrated that the catalyst activity is clearly influenced by the nature of the coordinated ligands (phosphines < polyamines < PNP). In the presence of  $[\{\text{RuCl}_2(\text{p-cymene})\}_2]$  (**C10**) and an excess of tetramethylethylenediamine (**L5** = TMEDA), H<sub>2</sub> is produced from 2-propanol at 90 °C with TOFs slightly higher than 500 h<sup>-1</sup> after 2 hours reaction time.<sup>[15]</sup> One of the most significant advances so far reported for 2-propanol and ethanol concerns the Ru catalyst  $[\text{RuH}_2(\text{CO})(\text{HPNP})]$  (**C11**) (**L6** = HPNP = bis[(2-diisopropylphosphino)ethyl]amine) obtained from precursor **C5** under neutral and mild conditions (90 °C) for which TOFs of 8382 and 1483 h<sup>-1</sup> respectively were achieved after 2 hours reaction time.<sup>[16]</sup> The catalyst precursor  $[\text{RuHCl}(\text{CO})(\text{PPh}_3)_3]$  (**C12**) combined with the PNP ligand **L6** gave TOF of 1134 h<sup>-1</sup> for the dehydrogenation of ethanol.<sup>[16]</sup>



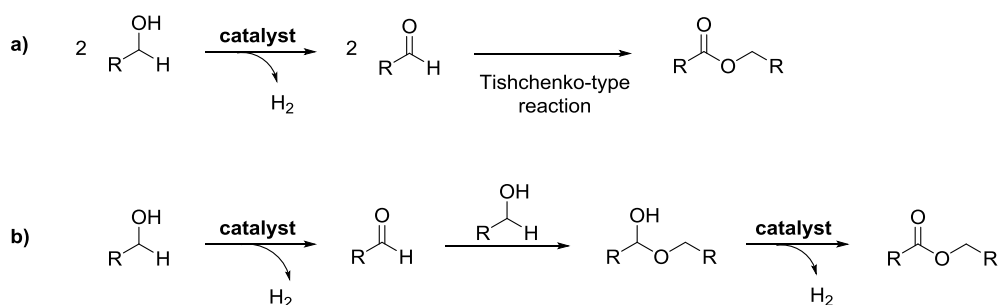
**Scheme 2.2.5** Proposed mechanism for dehydrogenation of alcohols catalysed by the precursor **C12** in the presence of ligand **L6** as reported by Beller *et al.*<sup>[16]</sup>

## 2.3 Dehydrogenative oxidation to carboxylic acid derivatives

Oxidation of alcohols to carboxylic acid derivatives following oxidant-free processes with production of H<sub>2</sub> as the only by-product, represent a more benign, safe and atom-efficient approach than conventional protocols, with the addition that alcohols could be available from biomass.

### 2.3.1 Ester or Acid formation

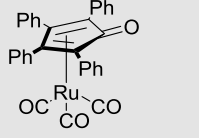
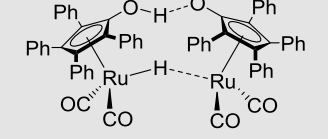
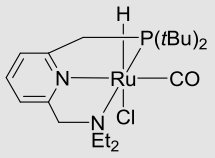
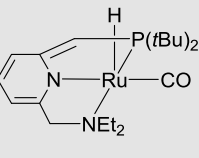
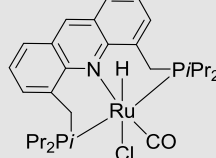
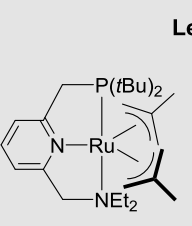
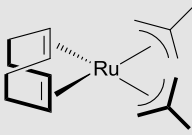
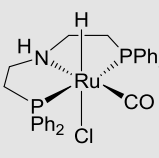
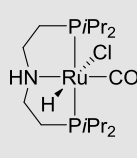
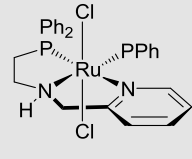
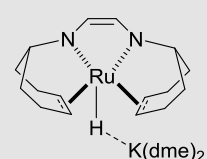
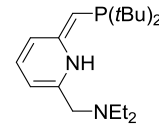
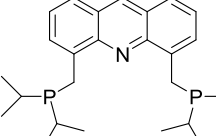
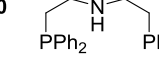
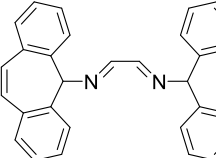
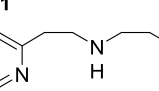
Dehydrogenation of primary alcohols to afford esters proceeds via a preliminary dehydrogenation of the substrate to the corresponding aldehyde followed by a second functionalisation step that may involve: **a)** disproportionation of the aldehyde according to a Tishchenko-type reaction<sup>[7]</sup> or **b)** formation of a hemiacetal by coupling of the unreacted alcohol with the nascent aldehyde, which in turn dehydrogenates to the corresponding ester.



**Scheme 2.3.1** Dehydrogenation of primary alcohols to the corresponding ester via **a)** Tishchenko-type reaction or **b)** further dehydrogenation of the hemiacetal intermediate.

The most popular organic reactions employed for the synthesis of esters and carboxylic acids are the Cannizzaro and the Tishchenko processes. The Cannizzaro reaction is a base-catalysed disproportionation of an aldehyde to a carboxylic acid and a primary alcohol<sup>[17]</sup> while the Tishchenko reaction refers to the metal-catalysed (transition metal complexes, metal alkoxides, lanthanoid complexes) disproportionation of an aldehyde to afford an ester.<sup>[7]</sup>

**Dehydrogenative Oxidation of Alcohols to Esters or Acids:  
Catalyst (C) Chart and best reported TONs and TOFs for selected Substrates (S)**

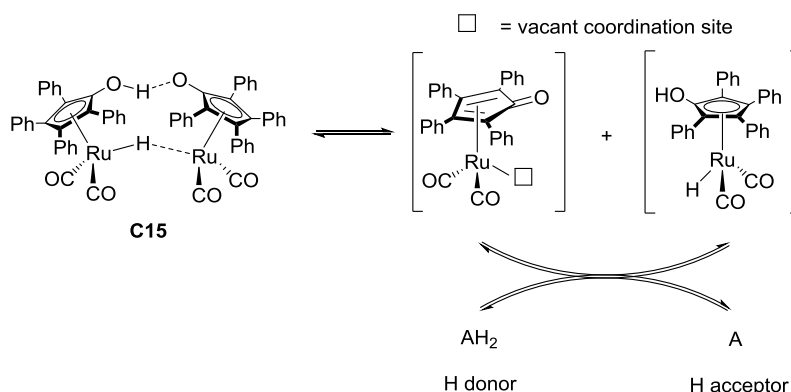
<p><b>Murahashi</b></p> <p>[RuH<sub>2</sub>(PPh<sub>3</sub>)<sub>4</sub>]</p> <p><b>C4</b></p> <p>S9: 48.5 (24h) S10: 49 (24h) S11: 49.5 (3h)</p>	<p><b>Shvo</b></p> <div style="display: flex; justify-content: space-around;"> <div data-bbox="509 367 788 624"> <p>[Ru<sub>3</sub>(CO)<sub>12</sub>]</p> <p><b>C13</b></p> <p>S9: 65 (2h)</p> </div> <div data-bbox="804 367 1003 624">  <p><b>C14</b></p> <p>S1: 405 (1h) S12: 250 (1h)</p> </div> <div data-bbox="1019 367 1347 624">  <p><b>C15 Shvo's catalyst</b></p> </div> </div>	
<p align="center"><b>Milstein</b></p> <div style="display: flex; justify-content: space-around;"> <div data-bbox="245 714 469 1039"> <p><b>C7</b></p>  <p><b>C16</b></p> <p>S1: 1970 (24h) S10: 1926 (24h) S9: 1880 (24h)</p> </div> <div data-bbox="509 714 788 1039">  <p><b>C17</b></p> <p>S1: 911 (4h) S10: 990 (6h) S9: 900 (5h)</p> </div> <div data-bbox="1019 714 1347 1039">  <p><b>C18</b></p> <p>S10: 4115 (80h)</p> </div> </div>		
<p align="center"><b>Leitner</b></p> <div style="display: flex; justify-content: space-around;"> <div data-bbox="245 1128 469 1532">  <p><b>C19</b></p> <p>S10: 4300 (20h)</p> </div> <div data-bbox="469 1128 676 1532">  <p><b>C20</b></p> </div> </div>	<p align="center"><b>Beller</b></p> <div style="display: flex; justify-content: space-around;"> <div data-bbox="692 1128 1003 1532">  <p><b>C21 Ru-MACHO</b></p> <p>S4: 1134 h<sup>-1</sup> (2h) S4: 15 400 (46h) S14 (pure): 11 477 h<sup>-1</sup> (1h)/10 318 h<sup>-1</sup> (2h) S14 (diluted): 18 507 h<sup>-1</sup> (1h)/14 834 h<sup>-1</sup> (2h) S14 (industrial): 30 199 h<sup>-1</sup> (1h)/25 088 h<sup>-1</sup> (2h) S7: 64 459 h<sup>-1</sup> (1h)/59 253 h<sup>-1</sup> (2h)</p> </div> <div data-bbox="1019 1128 1347 1532">  <p><b>C23</b></p> <p>S13: 4734 h<sup>-1</sup> (3h) S13: 350 000 (23d)</p> </div> </div>	
<p align="center"><b>Gusev</b></p>  <p><b>C22</b></p> <p>S4: 17 000 (40h)</p>	<p align="center"><b>Grützmacher</b></p>  <p><b>C24</b></p> <p>S13: 24 000 h<sup>-1</sup></p>	<p align="center"><b>Representation of selected Ligands</b></p> <div style="display: flex; flex-direction: column;"> <div data-bbox="788 1599 1003 1733"> <p><b>L7</b></p>  </div> <div data-bbox="1035 1599 1315 1733"> <p><b>L8</b></p>  </div> <div data-bbox="788 1778 1003 1845"> <p><b>L10</b></p>  </div> <div data-bbox="1035 1778 1315 1935"> <p><b>L11</b></p>  </div> <div data-bbox="788 1890 1003 1980"> <p><b>L12 (Trop<sub>2</sub>dad)</b></p>  </div> </div>

**Figure 2.3.1** Representation of dehydrogenative catalysts (**C**) for the production of esters and acids along with evolution of H<sub>2</sub> and respective best reported TONs and TOFs for selected substrates (**S**).

[RuH<sub>2</sub>(PPh<sub>3</sub>)<sub>4</sub>] (**C4**), which is a well known catalyst for the Tishchenko reaction as reported by Yamamoto *et al.* in 1979,<sup>[18]</sup> has been successfully employed for the oxidative condensation of primary alcohols and diols to the corresponding esters and lactones by Murahashi *et al.*

The best TONs for catalyst **C4** were achieved using 1-butanol (**S9**) and 1-hexanol (**S10**) as substrates for the production of the corresponding esters (respectively 48.5 and 49 TON over 24 h reaction time at 180 °C), and 1,4-butanediol (**S11**) for the production of  $\gamma$ -butyrolactone (GBL) (49.5 TON over 3 h).<sup>[19]</sup>

Shvo *et al.* developed Ru catalysts able to promote the oxidative coupling of primary alcohols to esters via dehydrogenation of alcohols, followed by Tishchenko-type disproportionation of the formed aldehydes to the corresponding ester. Whereas the commercially available [Ru<sub>3</sub>(CO)<sub>12</sub>] (**C13**) operates in the presence of a sacrificial H-acceptor,<sup>[20]</sup> the Ru species [( $\eta^4$ -C<sub>4</sub>Ph<sub>4</sub>CO)Ru(CO)<sub>3</sub>] (**C14**) and the dimeric species denoted as Shvo's catalyst<sup>[21]\*</sup> (**C15**), that could be generated *in situ* from catalyst **13**, act as catalyst precursors for the acceptorless dehydrogenation of alcohols.<sup>[22]</sup> The catalyst **13** provided TON of the order of 65 after 2 hours reaction time for the esterification of 1-butanol (**S9**)<sup>[20]</sup>, while catalysts **C14** and **C15** exhibited higher catalytic activity when isolated and directly used in catalysis with TON of 405 when using benzyl alcohol as substrate and 250 in the case of 1-pentanol (**S12**) (1 h reaction time in both cases) in an open reaction system.<sup>[22a]</sup>

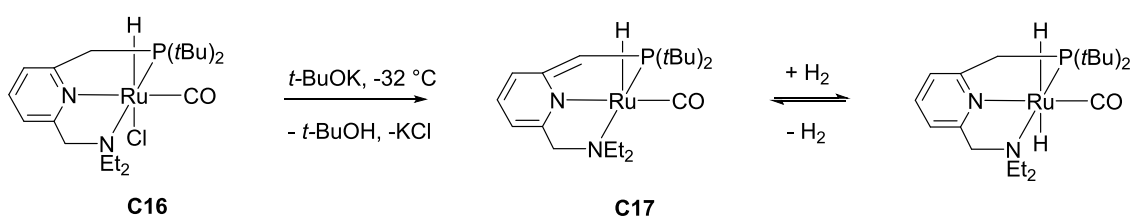


**Scheme 2.3.2** Shvo's catalyst dissociation into an Oxidising and a Reducing species as reported in the corresponding review.<sup>[21]</sup>

\* Shvo's catalyst  $\{[\text{Ph}_4(\eta^5\text{-C}_4\text{CO})]_2\text{H}\}\text{-Ru}_2(\text{CO})_4(\mu\text{-H})$  (**C15**) was initially identified as  $\{[\text{Ph}_4(\eta^4\text{-C}_4\text{CO})](\text{CO})_2\text{Ru}\}_2$  as it was reported in ref **20** (for a comprehensive review on Shvo's catalyst see ref [21]).

Other Ru catalysts able to catalyse the acceptorless dehydrogenative coupling reactions of alcohols (DHC) to afford esters via the formation of an hemiacetal species, with high efficiency under mild conditions have been reported by Milstein *et al.* and they deal with the Ru(II) hydride complexes typically bearing electron-rich PNP and PNN ligands. Complex [RuHCl(PNN)(CO)] (**C16**) (PNN = **L3**), and its dearomatised derivative [RuH(PNN\*)(CO)] (**C17**) (deprotonated PNN\* = **L7**), accomplished TONs over 900 and ester yields over 90 % in relatively short reaction time and under neutral conditions when using catalyst **C17** (Table 2.3.1, Entries 7-9), while longer reaction times and the presence of a base were required in the case of catalyst **C16** (Table 2.3.1, Entries 4-6).<sup>[23]</sup> The dinuclear Ru(II) complex **C7**, already presented in Section 2.2, was successfully employed also for the esterification of alcohols with very high TON under basic conditions (>1000 after 24 h depending on the nature of the substrate)<sup>[12]</sup> (Table 2.3.1, Entries 1-3).

The reaction mechanism proposed for this kind of catalysts involves an aromatisation/dearomatisation process of the *N*-heterocycle occurring during the coordination of the alcohol which generates an aromatic, coordinatively saturated alkoxy hydride complex. The hemilability of the amine group triggers the β-H abstraction process which terminates in the formation of a dihydrido intermediate and release of the aldehyde. The subsequent loss of H<sub>2</sub> enables catalyst regeneration.<sup>[12, 23]</sup>



**Scheme 2.3.3** Dearomatisation/Aromatisation of the *N*-heterocycle of **C16** as reported by Milstein *et al.*<sup>[23]</sup>

In 2009 they reported the acridine-based ruthenium pincer complex RuHCl(CO)(A-*i*PrPNP) (**C18**) (**L8** = A-*i*PrPNP = 4,5-bis-(diisopropylphosphinomethyl)acridine) as a catalyst for the conversion of alcohols to esters in the presence of catalytic amount of a base (1 equivalent relative to Ru) (Table 2.3.1, Entry 10) while under neutral conditions the selective synthesis of acetals occurs.<sup>[24]</sup>



**Table 2.3.1** Dehydrogenation of primary alcohols to esters with evolution of H<sub>2</sub> catalysed by complexes **7**, **16**, **17** and **18** under neutral or basic conditions as reported in the corresponding work of Milstein *et al.*<sup>[12, 23]</sup>

Entry	Cat.	Substrate	Base		T [°C]	t [h]	Conv. [%]	Yield [%]		TON
			[mmol]					ester	by-product <sup>a</sup>	
1	<b>7</b>	Benzyl alcohol	NaOiPr	0.02	100	24	99.5	98.5	0.2	1970
2	<b>7</b>	1-hexanol	NaOiPr	0.02	100	24	99	96.2	0.5	1926
3	<b>7</b>	1-butanol	NaOiPr	0.02	100	24	96	94	0.6	1880
4	<b>16</b>	Benzyl alcohol	KOH	0.01	115	72	100	99.5	0.0	995
5	<b>16</b>	1-hexanol	KOH	0.01	115	24	95	94.5	0.1	945
6	<b>16</b>	1-butanol	KOH	0.01	117	72	92.5	91.5	1.0	915
7	<b>17</b>	Benzyl alcohol	-	-	115	4	93.2	91.1	1.0	911
8	<b>17</b>	1-hexanol	-	-	115	6	99	99	0.0	990
9	<b>17</b>	1-butanol	-	-	117	5	91	90	0.5	900
10	<b>18</b>	1-hexanol	KOH	0.01	157	80	93.4	82.3	6.4	4115

Reaction conditions: cat. **7** (0.005 mmol), cat **16**, **17** and **18** (0.01 mmol), alcohol (10 mmol) except for Entry 10 (50 mmol). <sup>a</sup>The minor species corresponds to an aldehyde in all entries except for entry 10 where it is an acetal.

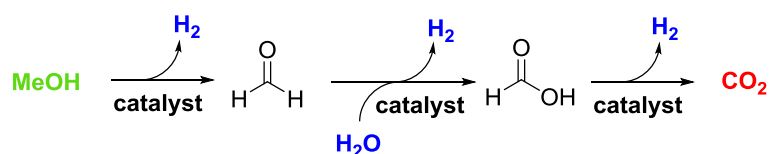
Based on the concept of hemilabile and cooperative ligands novel catalysts have been developed in the last years. In 2012 Leitner *et al.* reported an efficient approach for the conversion of primary alcohols to esters along with the formation of H<sub>2</sub> catalysed by *in situ* formed Ru Milstein-type catalysts. The pre-catalyst [Ru(PNN)(2-methylallyl)<sub>2</sub>] (**C19**) was obtained by treating the Ru precursor [Ru(cod)(2-methylallyl)<sub>2</sub>] (**C20**) (**L9** = cod = 1,5-cyclooctadiene) with the PNN **L3** ligand. Using 1-hexanol as substrate, the pre-catalyst **C19** gave TON of 4300 after 20 hours,<sup>[25]</sup> a remarkable activity when compared with Milstein's catalyst **C17** under similar reaction conditions.

The Milstein's catalyst **C17**, however, exhibited no activity when employing ethanol as substrate to synthesise ethyl acetate, an important industrial intermediate, for which the current manufacturing process relies on petrochemical feedstock. Based on the recent achievements in the field of "hydrogen economy", ethyl acetate was obtained from ethanol by Beller and co-workers using the Takasago catalyst known as Ru-MACHO<sup>®</sup><sup>[26]</sup> (**C21**), [RuHCl(HPNP<sup>Ph</sup>)(CO)] (HPNP<sup>Ph</sup> = **L10** = HN(CH<sub>2</sub>CH<sub>2</sub>PPh<sub>2</sub>)<sub>2</sub>), that showed very high activity. In the presence of 25 ppm of catalyst **21** and 1.3 % of NaOEt, TOF of 1134 h<sup>-1</sup> (2h) were reported. By modulating the catalyst loading and the base concentration they improved the yield of ethyl

acetate (50 ppm of catalyst and 0.3 % of the base) with still very high TON (15 400 after 46h).<sup>[27]</sup>

Gusev and co-workers presented an efficient and versatile air-stable Ru catalyst [RuCl<sub>2</sub>(PPh<sub>3</sub>)(PNN)] (**C22**) (L11 = PNN = PyCH<sub>2</sub>NHC<sub>2</sub>H<sub>4</sub>PPh<sub>2</sub>) for alcohol dehydrogenation, in particular it exhibited TON up to 17 000 in 40 h for the dehydrogenative coupling of ethanol to afford ethyl acetate besides evolution of H<sub>2</sub> gas under reflux.<sup>[28]</sup>

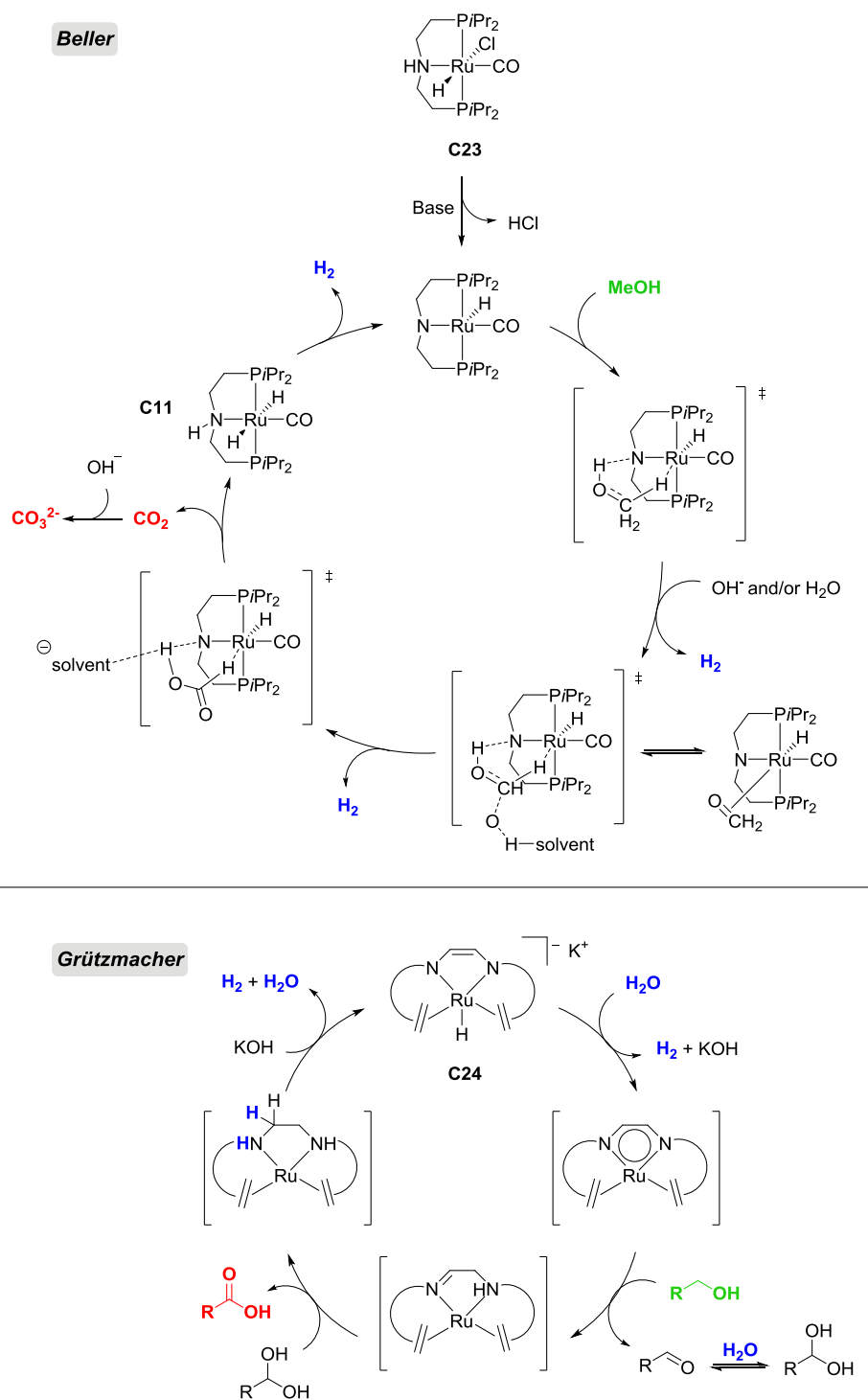
Based on the well known properties of Ru-MACHO (**C21**) on the dehydrogenation of ethanol, Beller *et al.* developed a catalytic cycle for the dehydrogenation of methanol (**S13**) at very low temperature. The reported catalyst [RuHCl(HPNP)(CO)] (**C23**) (HPNP = L6) exhibited TOF of 4734 h<sup>-1</sup> after 3h and TON of 350 000 after 23 days, a period of time after which the catalyst appeared still active. In the proposed mechanism the species **C23** acts as a pre-catalyst activated by the base with loss of HCl. The active species, by interaction with methanol through binding of the OH group of methanol with the amino moiety of the cooperative ligand and the H of the methyl group with the Ru centre, produces H<sub>2</sub> and generates a transient formaldehyde molecule which still remains coordinated to the metal centre. Upon attack of the hydroxide, present in the reaction medium, to the coordinated formaldehyde, the formation of CH<sub>2</sub>(OH)<sub>2</sub> is observed. The latter species undergoes a second outer-sphere dehydrogenation process which terminates into the liberation of a second molecule of H<sub>2</sub> and generation of the formate HCO<sub>2</sub><sup>-</sup>. At this stage the catalyst can release the formate and restart the cycle by reacting with methanol or undergo a third dehydrogenation step leading to CO<sub>2</sub> and H<sub>2</sub> along with the regeneration of the active species.<sup>[29]</sup>



**Scheme 2.3.4** Schematic outline of the catalysed process for methanol reforming occurring via three dehydrogenation steps under homogeneous conditions, as reported by Beller *et al.*<sup>[29]</sup>

Another successful catalyst was presented by Grützmacher *et al.* for the dehydrogenation of aqueous methanol under slightly basic homogeneous conditions. The catalyst [K(dme)<sub>2</sub>][RuH(trop<sub>2</sub>dad)] (**C24**), bearing the cooperative and chemically non-innocent ligand trop<sub>2</sub>dad (**L12**), operates through a sequence of three dehydrogenation steps with liberation of

3 equivalents of H<sub>2</sub>, similarly to complex **C23**. Methanol is firstly dehydrogenated to formaldehyde which reacts with water to form CH<sub>2</sub>(OH)<sub>2</sub>. Di(hydroxy)methane is further dehydrogenated to formic acid which is finally converted to CO<sub>2</sub> and H<sub>2</sub> with TOF of 24 000 h<sup>-1</sup>.<sup>[30]</sup>



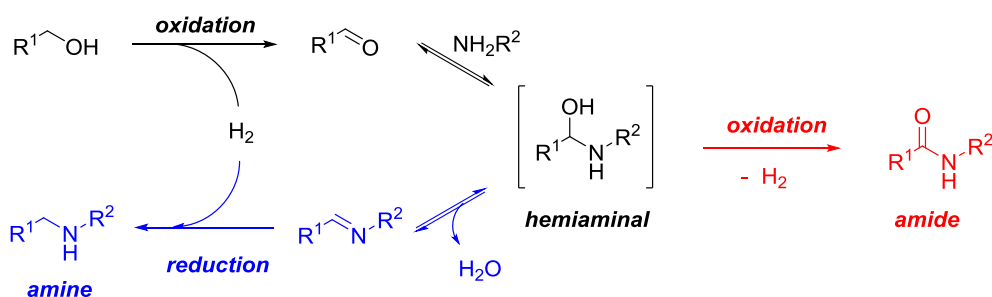
**Scheme 2.3.5** Proposed mechanisms for the aqueous-phase dehydrogenation of methanol catalysed by Beller' and Grützmacher's complexes **C23** and **C24** as reported in Grützmacher *et al.* review.<sup>[1]</sup>

A novel protocol for the production of H<sub>2</sub> has been introduced by Beller *et al.* and concerns the dehydrogenation of polyols which have been considered as a good compromise between simple alcoholic substrates and more complex biomass. Glycerol (**S14**) was firstly undertaken under investigation due to its great availability as by-product on the large scale production of biodiesel. Ru-MACHO provided unprecedented TOFs for H<sub>2</sub> generation along with formic acid and propane-1,2-diol, respectively of the order of 11 477 h<sup>-1</sup> after 1h (10 318 h<sup>-1</sup> after 2h) from pure glycerol, 18 507 h<sup>-1</sup> after 1h (14 834 h<sup>-1</sup> after 2h) from diluted glycerol as a consequence of increased solubility of the base in water and 30 199 h<sup>-1</sup> after 1h (25 088 h<sup>-1</sup> after 2h) from industrial glycerol which has a glycerol content around 86-88 %. Likewise remarkable catalyst activity was achieved for catalyst **C21** (64 459 h<sup>-1</sup> after 1h and 59 253 h<sup>-1</sup> after 2 h) when using ethylene glycol (**S7**) as substrate under the optimised reaction conditions reported for glycerol dehydrogenation (<1 ppm of catalyst in the presence of KOH at 125 °C).<sup>[31]</sup>

### 2.3.2 Amide formation

The amide group is widespread in pharmaceutical and biologically active compounds. Novel chemical approaches for the synthesis of amides have been investigated with the aim of developing new catalytic, waste-free and chemoselective processes.

Amide bond formation through catalysed dehydrogenative coupling of primary alcohols with amines can be conceptually associated to the oxidation of alcohols to esters, which implies dehydrogenation of the primary alcohol to the aldehyde which reacts with the amine to form an hemiaminal intermediate further dehydrogenated to the amide product. However, a competing N-alkylation reaction leading to the formation of amines may occur under certain conditions (the latter case will be discussed later on), that proceeds via dehydration of the hemiaminal.



**Scheme 2.3.2.1** General mechanism for amide formation through catalysed dehydrogenative coupling of alcohols with amines and competing amine formation through N-alkylation reaction (in blue) as depicted in Crabtree's review.<sup>[21]</sup>

Murahashi *et al.* observed the formation of 5- and 6-membered rings when reacting alcohols with amines in the presence of the previously reported Ru catalyst **C4**. In order to favour the formation of lactams rather than cyclic amines addition of water was essential. The role of the added water is probably to inhibit the dehydration of the hemiaminal intermediate to the imine which would be subsequently hydrogenated to the corresponding amine.<sup>[32]</sup>

Milstein's dearomatised Ru-PNN catalyst **C17** was successfully used to synthesise secondary amides by reacting aliphatic primary alcohol with primary amines,<sup>[12]</sup> whereas formation of tertiary amides from secondary amines was catalysed by a novel class of Ru(II)-PNN catalysts (**C25** and **C26**) (**L13** and **L14** = PNN = bipyridine derivatives, Figure 2.3.2.1) (TONs up to 2750 for **C26**).<sup>[33]</sup> As reported in the ester formation paragraph, catalyst **C17** does not require any activation by a base or other additives because the dearomatised PNN ligand acts as a cooperative ligand through an aromatisation/dearomatisation mechanism.

Madsen *et al.* demonstrated that secondary amides could be produced in good yields using a Ru-NHC catalyst formed *in situ* from [Ru(cod)Cl<sub>2</sub>] (**C27**), imidazolium salt and phosphine (**L15** = tricyclopentylphosphine). The reaction however requires longer reaction times and higher catalyst loading (5 %).<sup>[34]</sup>

Other examples of Ru catalysed amidation of amines with alcohols were reported by the research groups of Hong,<sup>[35]</sup> Crabtree<sup>[36]</sup> and Glorius<sup>[10]</sup> (**C28**, **C29** and **C30**). In particular, Glorius *et al.* proposed a biscarbene Ru complex to promote both the base-free synthesis of esters and amides and the *N*-formylation of several amines via dehydrogenation of methanol in the presence of styrene as sacrificial hydrogen acceptor.<sup>[10]</sup>

Grützmacher and co-workers proposed a more advantageous and efficient method (ambient temperature, low catalyst loading, easy workup and chemoselectivity) for the dehydrogenative coupling of several functionalised primary alcohols with amines, methanol or water, catalysed by a Rh species [Rh(trop<sub>2</sub>N)(PPh<sub>3</sub>)] (**C31**) (trop<sub>2</sub>N = **L16**) directly used as catalyst or formed *in situ* from a more stable precursor in the presence of a base (hydroxide or alkoxide). The Rh centre and the amino ligand, which act as a Lewis acid and a Lewis base respectively, are directly involved in the monohydride mechanism. The catalyst is then regenerated by transferring molecular H<sub>2</sub> to an easily hydrogenable substrate like cyclohexanone or MMA.<sup>[37]</sup>

Williams *et al.* established a one-pot system for the synthesis of amides from alcohols through oxime rearrangement, using the Ir catalyst [Ir(Cp\*)Cl]<sub>2</sub> (**C32**). The alcohol is initially oxidized to

the corresponding aldehyde. Upon addition of the hydroxylamine to the mixture containing the aldehyde, the oxime is formed and undergoes rearrangement to provide the final primary amide with moderate to excellent yields.<sup>[38]</sup>

**Dehydrogenative Oxidation of Alcohols to Amides:  
Catalyst Chart**

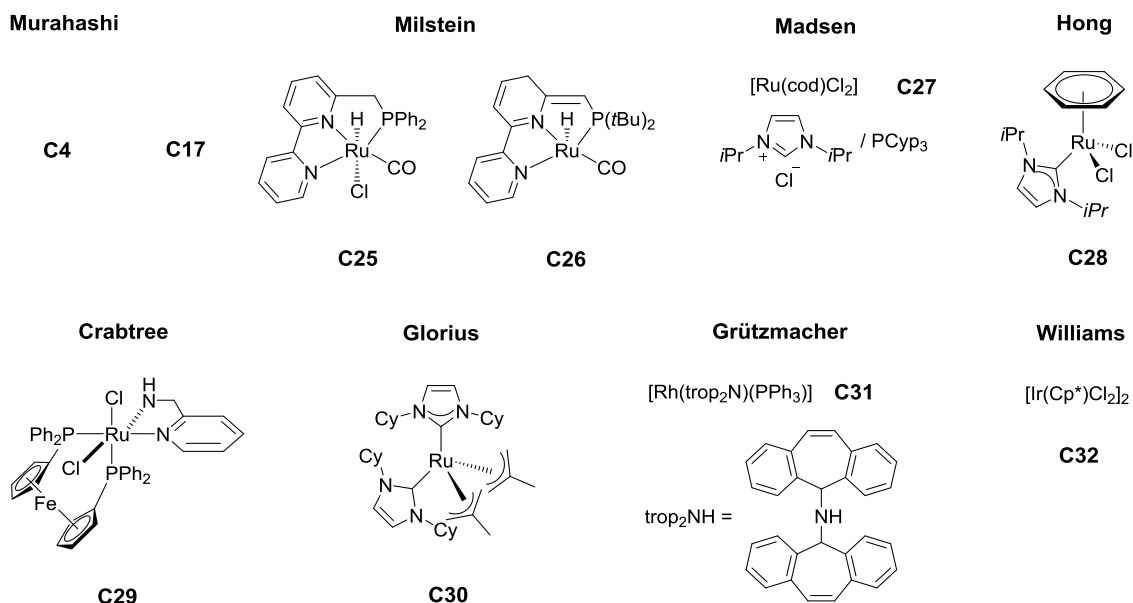


**Figure 2.3.2.1** Representation of dehydrogenative oxidation catalysts used for the amide synthesis.

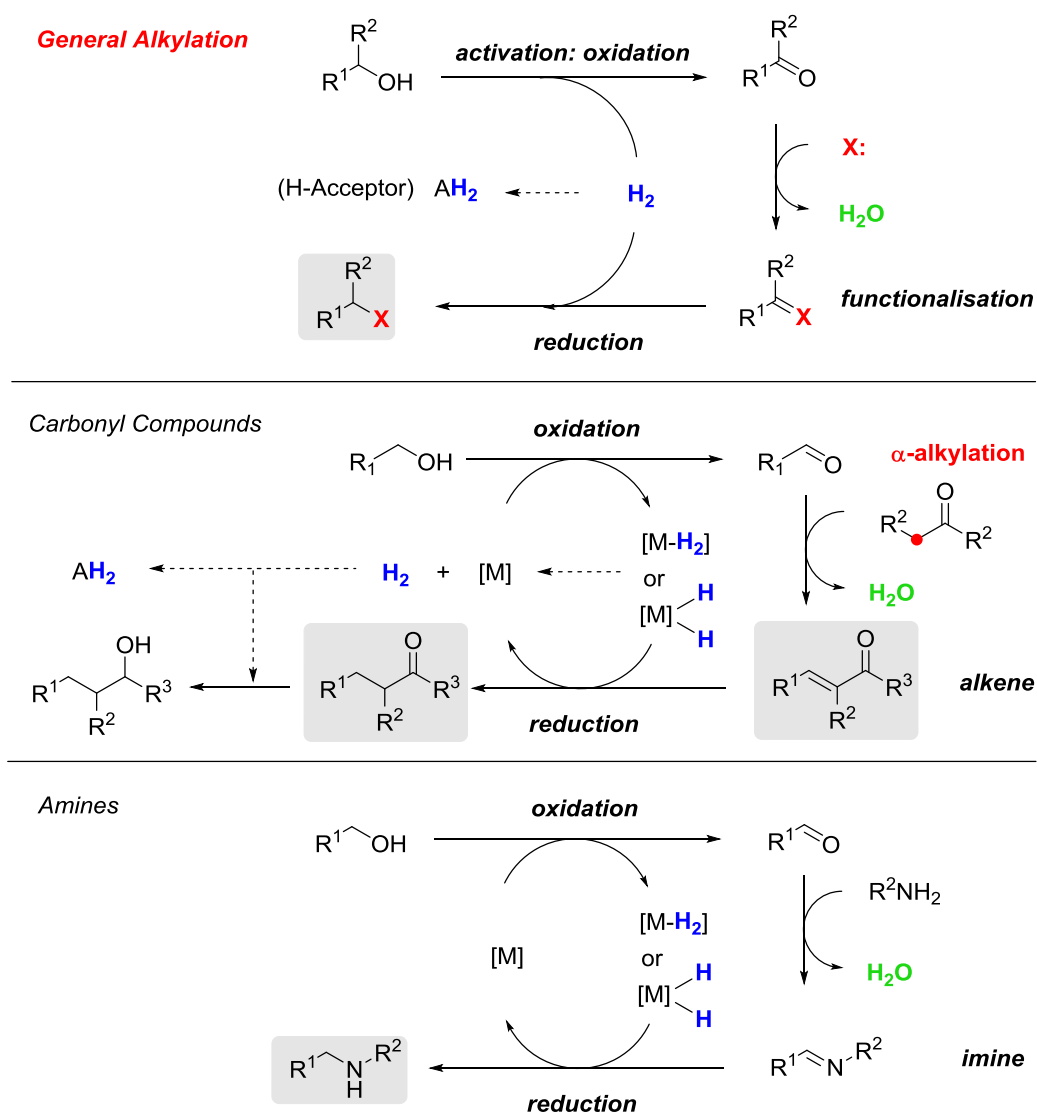
## 2.4 Dehydrogenative activation of alcohols for alkylation reactions through a “borrowing hydrogen strategy”

Alcohols are important starting materials in chemical transformations, in particular in the formation of new C-C<sup>[39]</sup> and C-N<sup>[39b, 39c, 40]</sup> bonds, however their reactivity requires to be temporarily enhanced by conversion into more reactive carbonyl compounds which can act as good electrophiles or good nucleophiles via their corresponding enols or enolates.

Conventional methods convert alcohols into toxic and mutagenic alkylating agents (alkyl halides or other alkylating agent) which can then undergo nucleophilic substitution with nucleophiles on the C or N atoms. The “borrowing hydrogen strategy” represents, therefore, an appealing alternative approach developed in organic synthesis, with a particular interest in pharmaceutical manufacture, to avoid the employment of mutagenic agents. The generation of water as the only by-product in most of the cases, instead of waste salts, makes the so called “hydrogen auto-transfer process” a more environmental benign technology.

The alcohol is oxidised to the corresponding aldehyde through a temporary transfer of H<sub>2</sub> to the catalyst which may proceed via a dihydride intermediate or not, depending on the nature of the catalyst. The C-C bond formation proceeds via the formation of an alkene ( $\alpha,\beta$ -unsaturated intermediate) by an appropriate *in situ* reaction (Aldol condensation, Wittig reaction, etc.) of the nascent aldehyde with the *enolate* derived from *ketones* (arising from dehydrogenation of another alcohol molecule or added as reagent) or *esters*. With returning of the borrowed hydrogen to the alkene, the overall formation of the new C-C bond is observed in the final product. The carbonyl group can be further hydrogenated to afford an alcohol as final species. In the presence of a suitable sacrificial hydrogen acceptor, however, the alkene could be isolated (see Scheme 3.4.1). Several other substrates including nitriles, nitroalkanes, barbituric acids or other active methylene compounds can be alkylated using the borrowing hydrogen strategy.

A similar mechanism occurs when the more reactive aldehyde undergoes condensation with an *amine* to afford the imine which in turn provides the final amine upon returning of the borrowed hydrogen (see Scheme 2.4.1).



**Scheme 2.4.1** Schematic outline for alkylation reactions using alcohols as alkylating agents via the “borrowing hydrogen strategy”: new C-C and C-N bonds formation.

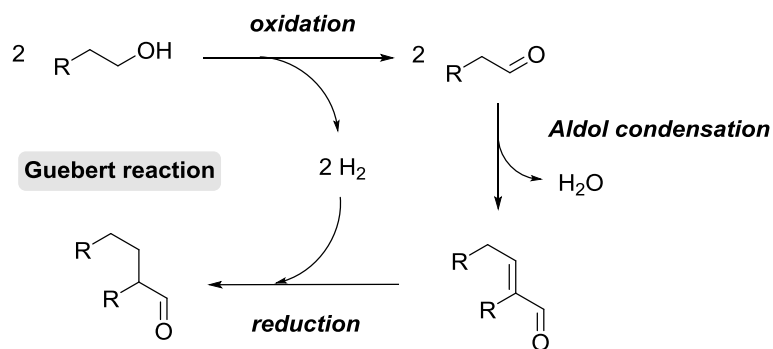
### 2.4.1 C-C bond formation

The carbonyl species that undergoes the α-alkylation process can be either formed *in situ* from another alcohol molecule (crossed Aldol pathway) or added as a carbonyl substrate.

A peculiar case of crossed Aldol pathway is the Guebert reaction in which primary aliphatic alcohols are converted into the corresponding β-alkylated dimer alcohol. The reaction proceeds via three steps: dehydrogenation of the alcohols to the corresponding aldehydes, aldol condensation reaction of the carbonyl intermediates along with elimination of water and



hydrogenation of the  $\alpha$ - $\beta$  unsaturated aldehyde (see Scheme 2.4.1.1). The reaction occurs at high temperatures and requires the presence of metal hydroxides or alkoxides and an hydrogenation catalyst (Ni Raney, Pd).<sup>[41]</sup>



**Scheme 2.4.1.1** General mechanism for the Guebert reaction.

Shim and co-workers reported several examples of C-C bond formation achieved by  $\alpha$ -alkylation of ketones (including acetophenone **S15** and tetralone **S16**) with primary alcohols (good yields were obtained with benzyl alcohol)<sup>[42]</sup> or  $\beta$ -alkylation of secondary alcohols with primary alcohols<sup>[43]</sup> through *in situ* dehydrogenation of the alcoholic substrates promoted by [RuCl<sub>2</sub>(PPh<sub>3</sub>)<sub>3</sub>] (**C33**) in the presence of KOH, using dioxane as H donor. The addition of an excess of 1-dodecene as sacrificial hydrogen acceptor was found to favour the regioselective alkylation reaction to the ketone product whereas in the absence of the alkene the formation of the corresponding alcohol was observed.<sup>[42-43]</sup>

Yus *et al.* employed an alternative Ru catalyst, [RuCl<sub>2</sub>(dmsO)<sub>4</sub>] (**C34**) to promote the  $\alpha$ -alkylation of methyl aryl ketones (**S17**) with primary alcohols under analogous reaction conditions reported by the research group of Shim.<sup>[44]</sup> According to the reaction mechanism the amount of KOH employed could be catalytical, however the product yield appeared negatively affected by lower amounts of the base suggesting that it may have a second role besides the deprotonation of the ketone to afford the enolate. The base in fact can be involved in the deprotonation of the alcohol probably acting as a driving force to the formation of the alkoxy-Ru intermediate.<sup>[44a]</sup>

An alternative route for the synthesis of  $\alpha$ -alkylated ketones with primary alcohols was investigated by Ishii and co-workers by using the Ir catalyst [Ir(cod)Cl]<sub>2</sub> (**C34**) in the presence of PPh<sub>3</sub> and KOH,<sup>[45]</sup> with high regioselectivity in the case of unsymmetrical ketones with *n*-BuOH.

The same catalytic system appeared to be active also in absence of a base, although higher temperatures were required, for the alkylation of ester nitriles like alkyl cyanoacetates (**S18**) with primary alcohols or diols to give the corresponding  $\alpha$ -alkylated products in good yields. This unusual feature of an alcohol activation catalyst may suggest that the hydride ligand of a potential Ir dihydride intermediate, presumably formed *in situ*, catalyses the aldol condensation reaction by acting as an internal base.<sup>[46]</sup>

The research group of Grigg, which reported one of earliest example of homogeneous catalysed  $\alpha$ -alkylation of nitriles,<sup>[47]</sup> published work in 2006 on the selective monoalkylation of aryl acetonitriles (**S19**) with a wide range of alcohols catalysed by [Cp\*IrCl<sub>2</sub>]<sub>2</sub> (**C32**), a green (solvent-free process which produces water as the only by-product) and atom-efficient protocol that can be performed by conventional heating or microwave irradiation. The alcohol is dehydrogenated to the corresponding aldehyde which is then engaged in the hydrogen transfer cascade through a Knoevenagel-type addition with the nitrile.<sup>[48]</sup>

Grigg *et al.* also reported the Ir catalysed (**C34**) alkylation of other activated methylene nucleophiles, including bioactive compounds of great interest in pharmaceutical chemistry like coumarins and quinolones<sup>[49]</sup> (**S20**), barbituric acids<sup>[50]</sup> (**S21**), oxindoles<sup>[51]</sup> (**S22**) and indoles (**S23**). Madsen and co-workers on the other hand reported a Ru-catalysed alkylation of oxindoles with alcohols.<sup>[52]</sup>

Williams *et al.* used the active species [Ru(xantphos)H<sub>2</sub>(CO)(PPh<sub>3</sub>)<sub>2</sub>] (**C35**), formed *in situ* by combination of the Ru precursor **C5** with the bidentate phosphorus ligand (**L17** = xantphos), to achieve the alkylation of the ketonitrile *t*-BuC(O)CH<sub>2</sub>CN (**S24**) with alcohols. The mechanism proposed involves the loss of H<sub>2</sub> from **C35** to allow the coordination of the incoming alcohol via an oxidative addition of the OH group. The subsequent  $\beta$ -hydrogen elimination affords the corresponding aldehyde which undergoes a Knoevenagel-type condensation with the ketonitrile affording a temporary alkene species. The Ru dihydride species acts as a hydrogenating catalyst towards the new formed C=C bond which is  $\pi$ -coordinated to the metal centre, generating the final C-C bond and the Ru active species.<sup>[53]</sup> Addition of a competitive hydrogen acceptor which can intercept the H<sub>2</sub> allows isolation of the  $\alpha,\beta$ -unsaturated intermediate as final product. Crotononitrile was found to be an efficient sacrificial hydrogen acceptor in the [Ru]/xantphos catalytic system,<sup>[54]</sup> including the oxidation of primary alcohols to methyl esters in the presence of methanol.<sup>[55]</sup>

Williams and co-workers used Ru-NHC H-transfer catalysts to promote an oxidation-indirect Wittig reaction-reduction cascade where the transient aldehyde, derived from dehydrogenation of an alcoholic substrate, undergoes nucleophilic addition with a phosphonium ylide to form an adduct that is consequently reduced. By screening a range of Ru-NHC catalysts, the complex [Ru(IMes)H<sub>2</sub>(CO)(PPh<sub>3</sub>)<sub>2</sub>] (**C36** (L18 = IMes = 1,3-bis(2,4,6-trimethylphenyl)imidazol-2-ylidene) allowed the reaction between benzyl alcohols and the phosphonium ylide (**S25**) under milder conditions<sup>[56]</sup> in comparison with the previous attempts reported when using an [Ir(cod)Cl]<sub>2</sub>/dppp/Cs<sub>2</sub>CO<sub>3</sub> (L19 = dppp = 1,2-bis(diphenylphosphino)propane) catalytic system.<sup>[57]</sup> The [Ru(IiPr<sub>2</sub>Me<sub>2</sub>)H<sub>2</sub>(CO)(PPh<sub>3</sub>)<sub>2</sub>] (**C37**) (L20 = 1,3-bis(*isopropyl*-4,5-dimethyl)imidazol-2-ylidene) complex proved to be more active for the synthesis of the nitrile following the pathway described above and at the same time it does not require activation with vinylsilane since spontaneous loss of H<sub>2</sub> occurs.<sup>[58]</sup>

Novel catalytic systems for the nucleophilic addition of dienes (1,3-cyclohexadiene **S26**)<sup>[59]</sup> and 1,3-enynes<sup>[60]</sup> (**S27**) to carbonyl compounds *in situ* generated via dehydrogenation of benzyl alcohols were developed by Krische *et al.*

#### C-C bond formation

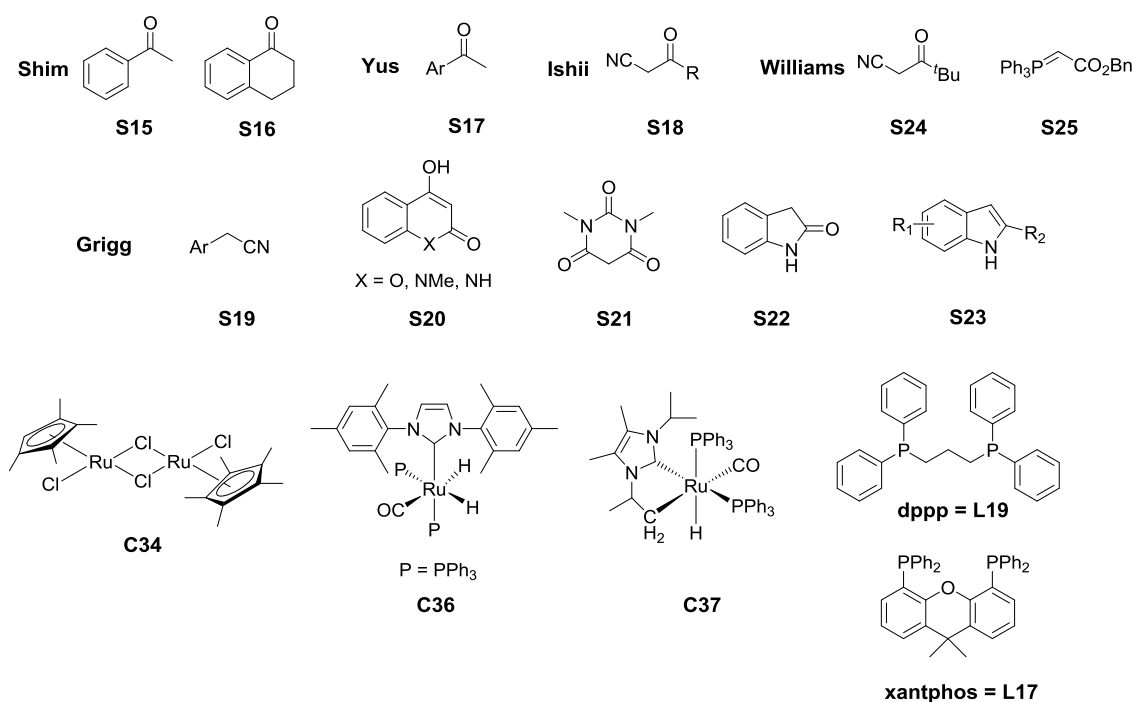


**Figure 2.4.1.1** Selected substrates involved in alkylation reactions with alcohols; representation of selected catalysts and ligands.

## 2.4.2 C-N bond formation

The very first examples of transition metal-catalysed (Ru, Ir and Rh species) *N*-alkylation of amines with alcohols using the borrowing hydrogen strategy were reported by Grigg *et al.*<sup>[61]</sup> and Watanabe *et al.* in 1981<sup>[62]</sup>. These two independent studies have been followed by a large number of publications reporting several catalysts and substrates summarised in Lamb and Williams' review.<sup>[63]</sup>

One of most effective catalytic system for the formation of a new C-N bond was reported by Fujita and Yamaguchi and includes the combination of the Ir catalyst **C32**<sup>[64]</sup> with K<sub>2</sub>CO<sub>3</sub> for the synthesis of amines<sup>[65]</sup> and indoles,<sup>[66]</sup> or with NaHCO<sub>3</sub><sup>[67]</sup>. The second system was also employed to synthesise secondary and tertiary amines through a one-pot multialkylation process of ammonium salts. In particular, the reactions between alcohols and ammonium acetate (**S28**) gave exclusively tertiary amines while those with ammonium tetrafluoroborate (**S29**) afforded selectively secondary amines. In the latter case, when the alcohols involved are diols, 5- and 6-membered cyclic amines were obtained respectively.<sup>[67b]</sup>

Alternative Ir catalysts include the complex **C34** with dppf (**L21** = 1,1'-bis(diphenylphosphino)ferrocene), for the *N*-alkylation of phenethylamine (**S30**) and tryptamine (**S31**),<sup>[68]</sup> substructures of particular interest for their pharmacological activity, or with P,N-ligands for the monoalkylation of (hetero)aromatic amines.<sup>[69]</sup>

Beller and co-workers investigated the combination of the Ru precursor **C13** with several sterically hindered phosphines<sup>[70]</sup> (e.g. **L22** = *N*-phenyl-2-(dicyclohexylphosphanyl)pyrrole) which was found to be the most active system for the *N*-alkylation of secondary alcohols among Ru-based catalysts, with the *in situ* catalyst **C13/L22** exhibiting the highest activity and selectivity.<sup>[71]</sup>

The conversion of primary amines into secondary amines using alcohols as alkylating agents has been achieved by Williams *et al.* with the Ru catalyst precursor **C10** in the presence of bidentate phosphines.<sup>[72]</sup> The catalytic system **C10/L21** was applied to the synthesis of tertiary amines like morpholine (**P1**) and piperidine-containing products (**P2**) which are molecules of pharmaceutical interest, including the synthesis of Piribedil (**P3**), a piperazine dopamine agonist used in the treatment of Parkinson's disease, avoiding therefore the use of harmful alkyl halides.<sup>[73]</sup>

Williams and co-workers demonstrated that N-alkyl anilines could be formed via an indirect aza-Wittig reaction between the newly formed aldehyde and an iminophosphorane (**S35**), a process catalysed by **C34** in combination with bidentate phosphines (e.g. dppf).<sup>[74]</sup>

Madsen and co-workers developed a method for the synthesis of piperazines by cyclocondensation of diols and amines in the presence of the already mentioned catalytic system **C32**/NaHCO<sub>3</sub>.<sup>[75]</sup> Besides the Ir catalysts, examples of Ru-catalysed N-heterocyclisations of diols with amines, diamines or amines containing additional heteroatoms leading to the formation of respectively piperidines,<sup>[76]</sup> piperazines<sup>[76-77]</sup> (**P4**) and morpholines<sup>[76b]</sup> have been reported. The Ru complex **C33** was described as an excellent catalyst for this kind of reactions together with a Ru species bearing tridentate PNP ligands.<sup>[76a]</sup>

Several other heterocycles such as N-substituted pyrroles and pyrrolidines,<sup>[78]</sup> quinolines,<sup>[79]</sup> and indoles<sup>[80]</sup> can be formed by reaction of alcohols with amines *via* an hydrogen transfer mechanism.

## 2.5 Conclusions

The catalysed dehydrogenation of alcohols has been successfully employed to accomplish two important goals. The first one deals with oxidation of alcohols to carbonyl compounds along with generation of H<sub>2</sub> gas which is considered a potential energy carrier. In combination with membrane fuel cells the chemical energy in fact can be converted into electricity, a more environmental friendly technology.

The second scope regards the activation of alcohols to more reactive substrates that can act as alkylating agents for the formation of new C-C and C-N bonds, a synthetic procedure of particular interest in pharmaceutical manufactures since it avoids the formation of toxic and mutagenic reagents, besides the formation of water as the only by-product.

In the current thesis we focused in particular on the dehydrogenation of methanol catalysed by Ru-based catalysts for the production of formaldehyde which was used as a one carbon alkylation agent for the methylenation of MMA in a one-pot catalytic system (see chapter 3).

## 2.6 References

- [1] M. Trincado, D. Banerjee, H. Grutzmacher, *Energy & Environmental Science* **2014**, *7*, 2464-2503.
- [2] For other review on the topic see: a) C. Johnson Tarn, J. Morris David, M. Wills, *Chem Soc Rev* **2010**, *39*, 81-88; b) G. E. Dobereiner, R. H. Crabtree, *Chem. Rev. (Washington, DC, U. S.)* **2010**, *110*, 681-703.
- [3] A. F. Dalebrook, W. Gan, M. Grasemann, S. Moret, G. Laurency, *Chem. Commun. (Cambridge, U. K.)* **2013**, *49*, 8735-8751.
- [4] A. Dobson, S. D. Robinson, *Inorg. Chem.* **1977**, *16*, 137-142.
- [5] C. Johnson Tarn, J. Morris David, M. Wills, *Chem Soc Rev* **2010**, *39*, 81-88.
- [6] a) D. Morton, D. J. Cole-Hamilton, *J. Chem. Soc., Chem. Commun.* **1987**, 248-249; b) D. Morton, D. J. Cole-Hamilton, *J. Chem. Soc., Chem. Commun.* **1988**, 1154-1156; c) D. Morton, D. J. Cole-Hamilton, I. D. Utuk, M. Paneque-Sosa, M. Lopez-Poveda, *J. Chem. Soc., Dalton Trans.* **1989**, 489-495.
- [7] O. P. Tormakangas, A. M. P. Koskinen, *Recent Res. Dev. Org. Chem.* **2001**, *5*, 225-255.
- [8] N. Sieffert, M. Buehl, *J. Am. Chem. Soc.* **2010**, *132*, 8056-8070.
- [9] N. Sieffert, R. Reocreux, P. Lorusso, D. J. Cole-Hamilton, M. Buehl, *Chem. - Eur. J.* **2014**, *20*, 4141-4155.
- [10] N. Ortega, C. Richter, F. Glorius, *Org. Lett.* **2013**, *15*, 1776-1779.
- [11] N. Sieffert, M. Buhl, *Inorg. Chem.* **2009**, *48*, 4622-4624.
- [12] J. Zhang, M. Gandelman, L. J. W. Shimon, D. Milstein, *Dalton Trans.* **2007**, 107-113.
- [13] J. Zhang, E. Balaraman, G. Leitius, D. Milstein, *Organometallics* **2011**, *30*, 5716-5724.
- [14] R. Kawahara, K.-i. Fujita, R. Yamaguchi, *J. Am. Chem. Soc.* **2012**, *134*, 3643-3646.
- [15] H. Junge, B. Loges, M. Beller, *Chem. Commun. (Cambridge, U. K.)* **2007**, 522-524.
- [16] M. Nielsen, A. Kammer, D. Cozzula, H. Junge, S. Gladiali, M. Beller, *Angew. Chem. Int. Ed.* **2011**, *50*, 9593-9597.
- [17] S. Cannizzaro, *Ann. Ch. Pharm., lxxviii*, 129.
- [18] H. Horino, T. Ito, A. Yamamoto, *Chem. Lett.* **1978**, 17-20.
- [19] a) S. Murahashi, K. Ito, T. Naota, Y. Maeda, *Tetrahedron Lett.* **1981**, *22*, 5327-5330; b) S. Murahashi, T. Naota, K. Ito, Y. Maeda, H. Taki, *J. Org. Chem.* **1987**, *52*, 4319-4327.
- [20] Y. Blum, D. Reshef, Y. Shvo, *Tetrahedron Lett.* **1981**, *22*, 1541-1544.
- [21] B. L. Conley, M. K. Pennington-Boggio, E. Boz, T. J. Williams, *Chem. Rev. (Washington, DC, U. S.)* **2010**, *110*, 2294-2312.
- [22] a) Y. Blum, Y. Shvo, *J. Organomet. Chem.* **1985**, *282*, C7-C10; b) Y. Blum, Y. Shvo, *Israel Journal of Chemistry* **1984**, *24*, 144-148.
- [23] J. Zhang, G. Leitius, Y. Ben-David, D. Milstein, *J. Am. Chem. Soc.* **2005**, *127*, 10840-10841.
- [24] C. Gunanathan, L. J. W. Shimon, D. Milstein, *J. Am. Chem. Soc.* **2009**, *131*, 3146-3147.
- [25] M. H. G. Precht, K. Wobser, N. Theyssen, Y. Ben-David, D. Milstein, W. Leitner, *Catal. Sci. Technol.* **2012**, *2*, 2039-2042.
- [26] W. Kuriyama, T. Matsumoto, O. Ogata, Y. Ino, K. Aoki, S. Tanaka, K. Ishida, T. Kobayashi, N. Sayo, T. Saito, *Organic Process Research & Development* **2012**, *16*, 166-171.
- [27] M. Nielsen, H. Junge, A. Kammer, M. Beller, *Angew. Chem. Int. Ed.* **2012**, *51*, 5711-5713, S5711/5711-S5711/5711.
- [28] D. Spasyuk, D. G. Gusev, *Organometallics* **2012**, *31*, 5239-5242.
- [29] M. Nielsen, E. Alberico, W. Baumann, H.-J. Drexler, H. Junge, S. Gladiali, M. Beller, *Nature (London, U. K.)* **2013**, *495*, 85-89.

- [30] R. E. Rodriguez-Lugo, M. Trincado, M. Vogt, F. Tewes, G. Santiso-Quinones, H. Gruetzmacher, *Nat. Chem.* **2013**, *5*, 342-347.
- [31] Y. Li, M. Nielsen, B. Li, P. H. Dixneuf, H. Junge, M. Beller, *Green Chem.* **2015**, *17*, 193-198.
- [32] T. Naota, S. Murahashi, *Synlett* **1991**, 693-694.
- [33] D. Srimani, E. Balaraman, P. Hu, Y. Ben-David, D. Milstein, *Adv. Synth. Catal.* **2013**, *355*, 2525-2530.
- [34] L. U. Nordstrom, H. Vogt, R. Madsen, *J. Am. Chem. Soc.* **2008**, *130*, 17672-17673.
- [35] C. Chen, Y. Zhang, S. H. Hong, *J. Org. Chem.* **2011**, *76*, 10005-10010.
- [36] N. D. Schley, G. E. Dobereiner, R. H. Crabtree, *Organometallics* **2011**, *30*, 4174-4179.
- [37] T. Zweifel, J.-V. Naubron, H. Gruetzmacher, *Angew. Chem. Int. Ed.* **2009**, *48*, 559-563.
- [38] N. A. Owston, A. J. Parker, J. M. J. Williams, *Org. Lett.* **2007**, *9*, 73-75.
- [39] a) G. E. Dobereiner, R. H. Crabtree, *Chem. Rev. (Washington, DC, U. S.)* **2010**, *110*, 681-703; b) T. D. Nixon, M. K. Whittlesey, J. M. J. Williams, *Dalton Trans.* **2009**, 753-762; c) A. J. A. Watson, J. M. J. Williams, *Science (Washington, DC, United States)* **2010**, *329*, 635-636.
- [40] G. Guillena, D. J. Ramon, M. Yus, *Chem. Rev. (Washington, DC, U. S.)* **2010**, *110*, 1611-1641.
- [41] S. Veibel, J. I. Nielsen, *Tetrahedron* **1967**, *23*, 1723-1733.
- [42] C. S. Cho, B. T. Kim, T.-J. Kim, S. C. Shim, *Tetrahedron Lett.* **2002**, *43*, 7987-7989.
- [43] C. S. Cho, B. T. Kim, H.-S. Kim, T.-J. Kim, S. C. Shim, *Organometallics* **2003**, *22*, 3608-3610.
- [44] a) R. Martinez, G. J. Brand, D. J. Ramon, M. Yus, *Tetrahedron Lett.* **2005**, *46*, 3683-3686; b) R. Martinez, D. J. Ramon, M. Yus, *Tetrahedron* **2006**, *62*, 8988-9001; c) R. Martinez, D. J. Ramon, M. Yus, *Tetrahedron* **2006**, *62*, 8982-8987.
- [45] K. Taguchi, H. Nakagawa, T. Hirabayashi, S. Sakaguchi, Y. Ishii, *J. Am. Chem. Soc.* **2004**, *126*, 72-73.
- [46] M. Morita, Y. Obora, Y. Ishii, *Chem. Commun. (Cambridge, U. K.)* **2007**, 2850-2852.
- [47] R. Grigg, T. R. B. Mitchell, S. Sutthivaiyakit, N. Tongpenyai, *Tetrahedron Lett.* **1981**, *22*, 4107-4110.
- [48] C. Lofberg, R. Grigg, A. Whittaker Mark, A. Keep, A. Derrick, *J Org Chem* **2006**, *71*, 8023-8027.
- [49] R. Grigg, S. Whitney, V. Sridharan, A. Keep, A. Derrick, *Tetrahedron* **2009**, *65*, 7468-7473.
- [50] C. Lofberg, R. Grigg, A. Keep, A. Derrick, V. Sridharan, C. Kilner, *Chem Commun (Camb)* **2006**, 5000-5002.
- [51] R. Grigg, S. Whitney, V. Sridharan, A. Keep, A. Derrick, *Tetrahedron* **2009**, *65*, 4375-4383.
- [52] T. Jensen, R. Madsen, *J. Org. Chem.* **2009**, *74*, 3990-3992.
- [53] A. E. W. Ledger, P. A. Slatford, J. P. Lowe, M. F. Mahon, M. K. Whittlesey, J. M. J. Williams, *Dalton Trans.* **2009**, 716-722.
- [54] M. I. Hall, S. J. Pridmore, J. M. J. Williams, *Adv. Synth. Catal.* **2008**, *350*, 1975-1978.
- [55] N. A. Owston, A. J. Parker, J. M. J. Williams, *Chem. Commun. (Cambridge, U. K.)* **2008**, 624-625.
- [56] M. G. Edwards, R. F. R. Jazzar, B. M. Paine, D. J. Shermer, M. K. Whittlesey, J. M. J. Williams, D. D. Edney, *Chem. Commun. (Cambridge, U. K.)* **2004**, 90-91.
- [57] M. G. Edwards, J. M. J. Williams, *Angew. Chem. Int. Ed.* **2002**, *41*, 4740-4743.
- [58] S. Burling, B. M. Paine, D. Nama, V. S. Brown, M. F. Mahon, T. J. Prior, P. S. Pregosin, M. K. Whittlesey, J. M. J. Williams, *J. Am. Chem. Soc.* **2007**, *129*, 1987-1995.

- [59] J. F. Bower, R. L. Patman, M. J. Krische, *Org. Lett.* **2008**, *10*, 1033-1035.
- [60] R. L. Patman, V. M. Williams, J. F. Bower, M. J. Krische, *Angew. Chem. Int. Ed.* **2008**, *47*, 5220-5223.
- [61] R. Grigg, T. R. B. Mitchell, S. Sutthivaiyakit, N. Tongpenyai, *J. Chem. Soc., Chem. Commun.* **1981**, 611-612.
- [62] Y. Watanabe, Y. Tsuji, Y. Ohsugi, *Tetrahedron Lett.* **1981**, *22*, 2667-2670.
- [63] G. W. Lamb, J. M. J. Williams, *Chim. Oggi* **2008**, *26*, 17-19.
- [64] K.-i. Fujita, Y. Enoki, R. Yamaguchi, *Org. Synth.* **2006**, *83*, 217-221.
- [65] a) K.-i. Fujita, R. Yamaguchi, *Synlett* **2005**, 560-571; b) K.-i. Fujita, Z. Li, N. Ozeki, R. Yamaguchi, *Tetrahedron Lett.* **2003**, *44*, 2687-2690.
- [66] K. Fujita, K. Yamamoto, R. Yamaguchi, *Org. Lett.* **2002**, *4*, 2691-2694.
- [67] a) K.-i. Fujita, Y. Enoki, R. Yamaguchi, *Tetrahedron* **2008**, *64*, 1943-1954; b) R. Yamaguchi, S. Kawagoe, C. Asai, K.-i. Fujita, *Org. Lett.* **2008**, *10*, 181-184.
- [68] G. Cami-Kobeci, P. A. Slatford, M. K. Whittlesey, J. M. J. Williams, *Bioorganic & Medicinal Chemistry Letters* **2005**, *15*, 535-537.
- [69] B. Blank, M. Madalska, R. Kempe, *Adv. Synth. Catal.* **2008**, *350*, 749-758.
- [70] A. Tillack, D. Hollmann, D. Michalik, M. Beller, *Tetrahedron Lett.* **2006**, *47*, 8881-8885.
- [71] D. Hollmann, A. Tillack, D. Michalik, R. Jackstell, M. Beller, *Chem. - Asian J.* **2007**, *2*, 403-410.
- [72] M. H. S. A. Hamid, J. M. J. Williams, *Chem. Commun. (Cambridge, U. K.)* **2007**, 725-727.
- [73] M. H. S. A. Hamid, J. M. J. Williams, *Tetrahedron Lett.* **2007**, *48*, 8263-8265.
- [74] G. Cami-Kobeci, J. M. J. Williams, *Chem. Commun. (Cambridge, U. K.)* **2004**, 1072-1073.
- [75] L. U. Nordstrom, R. Madsen, *Chem. Commun. (Cambridge, U. K.)* **2007**, 5034-5036.
- [76] a) R. A. T. M. Abbenhuis, J. Boersma, G. van Koten, *J. Org. Chem.* **1998**, *63*, 4282-4290; b) Y. Tsuji, K. T. Huh, Y. Ohsugi, Y. Watanabe, *J. Org. Chem.* **1985**, *50*, 1365-1370.
- [77] a) K. T. Huh, S. C. Shim, C. H. Doh, *Bull. Korean Chem. Soc.* **1990**, *11*, 45-49; b) J. A. Marsella, *J. Organomet. Chem.* **1991**, *407*, 97-105.
- [78] a) Y. Tsuji, Y. Yokoyama, K. T. Huh, Y. Watanabe, *Bull. Chem. Soc. Jpn.* **1987**, *60*, 3456-3458; b) S. J. Pridmore, P. A. Slatford, A. Daniel, M. K. Whittlesey, J. M. J. Williams, *Tetrahedron Lett.* **2007**, *48*, 5115-5120.
- [79] C. S. Cho, B. T. Kim, H.-J. Choi, T.-J. Kim, S. C. Shim, *Tetrahedron* **2003**, *59*, 7997-8002.
- [80] Y. Tsuji, S. Kotachi, K. T. Huh, Y. Watanabe, *J. Org. Chem.* **1990**, *55*, 580-584.



# Chapter 3

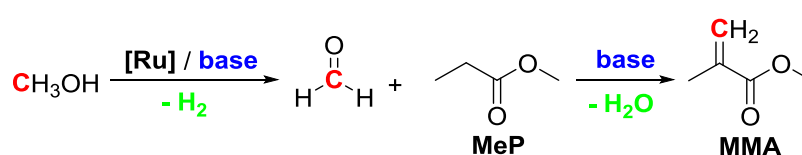
## Upon the $\alpha$ -methylenation of methyl propanoate via catalytic dehydrogenation of methanol

A one-pot system for the conversion of methyl propanoate (MeP) to methyl methacrylate (MMA) has been investigated. In particular, this study is focused on the possibility of performing catalytic dehydrogenation of methanol for the *in situ* production of anhydrous formaldehyde, which is then consumed in a one-pot base-catalysed condensation with MeP to afford methyl 3-hydroxy-2-methylpropanoate, which spontaneously dehydrates to MMA, some of which is subsequently hydrogenated to methyl 2-methylpropanoate (MiBu).

**Keywords:** methyl methacrylate · one-pot conversion · dehydrogenation · methanol · anhydrous formaldehyde · ruthenium

### 3.1 Introduction

Formaldehyde is a chemical used widely in several industrial processes including the manufacture of building materials. A remarkable example in this area is represented by the innovative two-step Alpha technology developed by Lucite for the large scale production of methyl methacrylate (MMA), the essential building block of all acrylic-based products.<sup>[1]</sup> This successful technology involves methoxycarbonylation of ethene to methyl propanoate (MeP), in the presence of a palladium based complex,<sup>[2]</sup> followed by condensation with gaseous formaldehyde on a fixed bed catalyst (caesium oxide on silica), affording MMA as the final product.<sup>[1b, 3]</sup> The formaldehyde involved in this second stage is initially produced as formalin in a separate process and then dehydrated to afford anhydrous formaldehyde, an expensive procedure which is essential for ensuring high selectivity to MMA and preventing excessive catalyst aging. Another drawback of this procedure is represented by the easy polymerisation of paraformaldehyde giving insoluble polyoxymethylenes which can lead to severe fouling of transfer lines.<sup>[3]</sup> The development of an alternative process where anhydrous formaldehyde is produced *in situ* would provide a simplification over the current process. As an alternative second step, the possibility of performing the one-pot  $\alpha$ -methylenation of methyl propanoate has not been investigated so far. In an ideal system, anhydrous formaldehyde would be generated *in situ* by catalytic dehydrogenation of methanol and would subsequently undergo base-catalysed condensation with methyl propanoate to afford methyl 3-hydroxy-2-methylpropanoate as an intermediate, which, in turn, would dehydrate to MMA (Scheme 3.1.1).

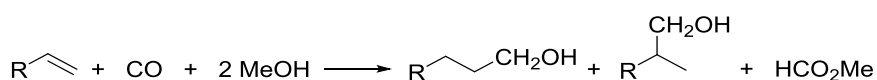


**Scheme 3.1.1** Proposed one-pot formation of methyl methacrylate (MMA) from methyl propanoate (MeP) and methanol.

Alpha methylenation of simple esters can be achieved in low yield using condensation of the ester with formaldehyde catalysed by caesium oxide on silica at high temperature<sup>[3]</sup>, or by a complex series of reactions using Meldrum's acid Eschemoser's iodide salt (dimethylmethylenium iodide).<sup>[4]</sup> We are not aware that it has been achieved using

metal catalysed reactions. However, the reactions involved (Scheme 3.1.1) are very similar to those involved in hydrogen borrowing reactions,<sup>[5]</sup> acceptorless dehydrogenation<sup>[6]</sup> and hydrogen auto-transfer.<sup>[7]</sup> Generally, the hydrogen from the dehydrogenation of the alcohol is transferred back into the product leading to alkylation rather than alkylenation. In addition, the substrates that are alkylated are exclusively ketones rather than esters.

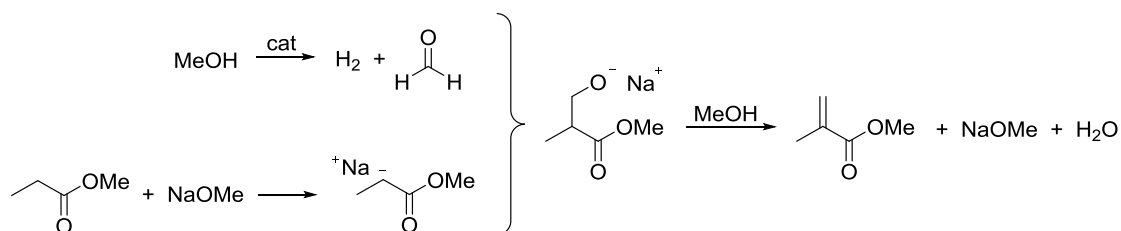
Methanol has only rarely been used as an *in situ* source of formaldehyde. Formaldehyde is presumably formed in the thermal<sup>[8]</sup> or photochemical<sup>[9]</sup> production of hydrogen from methanol, and subsequent reactions of the formed formaldehyde can lead for example to dimethoxymethane,<sup>[9b, 10]</sup> to CO and H<sub>2</sub>,<sup>[9a]</sup> to CO<sub>2</sub> or carbonate in the presence of hydroxide bases,<sup>[8b]</sup> to formylamines on reaction with primary or secondary amines,<sup>[11]</sup> or it can be added to a metal allyl formed from an allene to give 3-hydroxyethyl-1-alkenes in a reaction which is formally the addition of a C-H of methanol across a double bond.<sup>[12]</sup> In early work, some of us showed that, using methanol as the hydrogen source in hydrocarbonylation reactions of 1-hexene to heptanol catalysed by Rh/PET<sub>3</sub> complexes, the formed formaldehyde was converted into methyl formate (Scheme 3.1.2). Interestingly, in these reactions, methanol proved to be a better source of hydrogen than ethanol, 1-butanol or 2-propanol.<sup>[13]</sup>



**Scheme 3.1.2** The use of methanol as a source of hydrogen in the hydrocarbonylation of 1-hexene (R = C<sub>4</sub>H<sub>9</sub>). Methyl heptanoate, methyl 2-methylhexanoate and hexylhexanoate are also significant products. Methyl formate is formed from methanol.<sup>[13]</sup>

### 3.2 Results and Discussion

Minor amounts of MMA were detected after heating MeP together with  $\text{Na}_2\text{CO}_3$  at  $170\text{ }^\circ\text{C}$  in a stainless steel batch autoclave in the absence of any added formaldehyde. In addition to MMA, the GC-MS spectrum of the crude product revealed the presence of the hydrogenated product, methyl 2-methylpropanoate (MiBu) along with 3-pentanone and significant amounts of methanol, suggesting that a carbon alkylating agent and hydrogen source must have been present at some stage during the reaction. Methanol, possibly from hydrolysis of methyl propanoate was believed to be the most likely source of the methylene group in MMA (see Scheme 3.2.1). Based on this observation, the *in situ* generation of anhydrous formaldehyde and hydrogen gas by metal-catalysed dehydrogenation of methanol has been investigated. The role of the base in this system is twofold. It is involved in the deprotonation of methanol affording the alkoxide ion, which is the active species in methanol dehydrogenation, and it is essential for the  $\alpha$ -deprotonation of MeP which can then undergo condensation with the newly formed formaldehyde affording an intermediate species, methyl 3-hydroxy-2-methylpropanoate. The latter provides the desired product, MMA, via spontaneous water elimination (Scheme 3.2.1). Since  $\text{H}_2$  is produced in the reaction system and we wish not to hydrogenate MMA, suitable catalysts should be chemoselective for the dehydrogenation of methanol leading to formaldehyde without promoting the hydrogenation of the C=C bond in MMA to give methyl 2-methylpropanoate (MiBu).



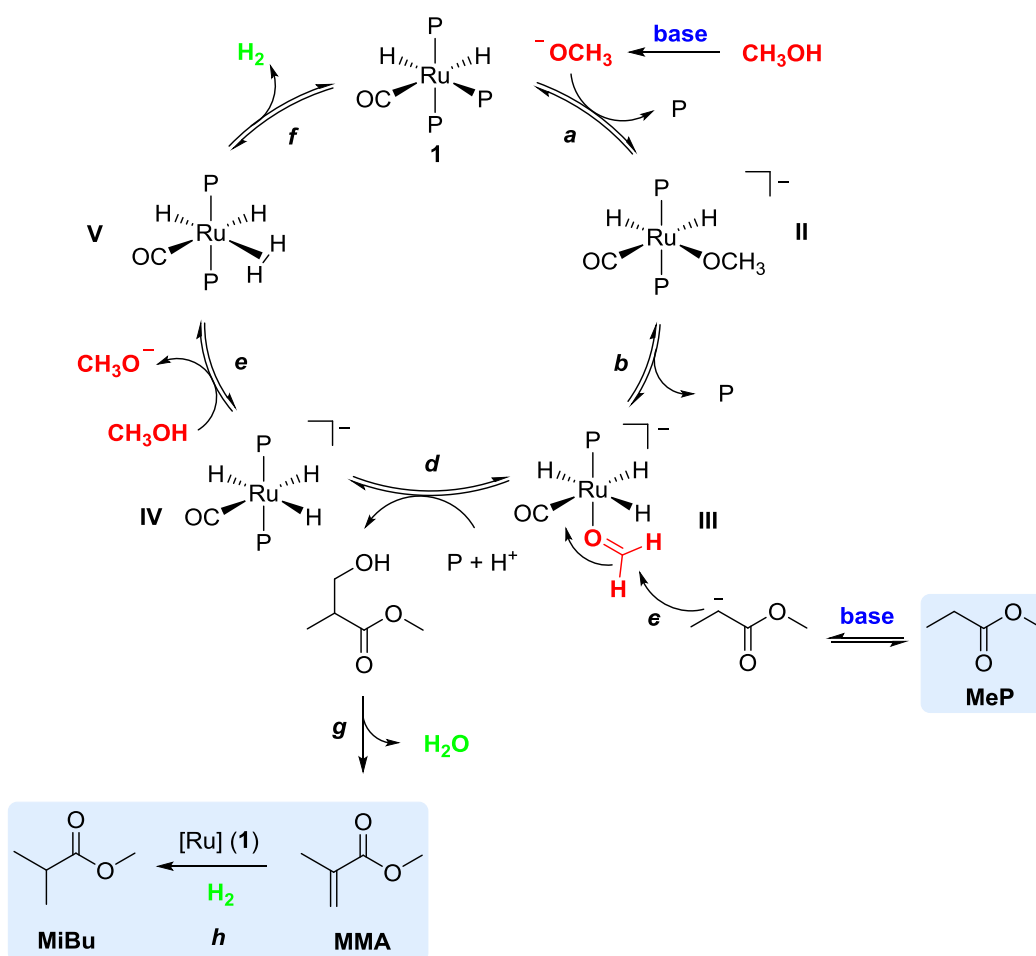
**Scheme 3.2.1** Route to methyl methacrylate involving attack of deprotonated MeP on formaldehyde formed by the *in situ* dehydrogenation of methanol.

Some of us reported in the late 80's that catalytic dehydrogenation of alcohols can be achieved from a wide range of alcoholic substrates using Rh and Ru catalysts.<sup>[14]</sup> Among these catalysts, one of the best was  $[\text{RuH}_2(\text{CO})(\text{PPh}_3)_3]$  (**1**). Similar complexes, such as  $[\text{RuHCl}(\text{CO})(\text{PPh}_3)_3]$  have been reported to give some preference for hydrogenation of C=O over C=C bonds, e. g. in cinnamaldehyde.<sup>[15]</sup> Therefore, based on the principle of microscopic reversibility, it was

examined as a suitable dehydrogenation catalyst in these preliminary studies together with other hydrogenating catalysts. The initial catalyst screening involved four Ru species which exhibited only minor activity, Shvo's catalyst<sup>[16]</sup>(**2**),  $[\text{RuCl}(\text{CO})_2(\eta^5\text{-Ph}_5\text{C}_5)]$ <sup>[17]</sup> (**3**),  $[\text{Ru}(\text{OAc})_2(\text{TriPhos})]$ <sup>[18]</sup>(**4**),  $[\text{RuH}_2(\text{CO})(\text{TriPhos})]$ <sup>[19]</sup>(**5**) and a Rh catalyst  $[\text{RhH}(\text{CO})(\text{PEt}_3)_3]$ <sup>[20]</sup>(**6**) which showed some activity but no selectivity towards MMA (MMA yield 0%; MiBu yield 6 %).

Preliminary studies in which methanol, methyl propanoate and sodium methoxide were heated in the presence of species **1** showed the presence of small amounts of both MMA and MiBu.

Scheme 3.2.2 depicts a plausible mechanism for the formation of MMA based on a published mechanism for the dehydrogenation of methanol, ethanol or propan-2-ol catalysed by related ruthenium complexes.<sup>[21]</sup> In the initial stage a methoxide ion is generated by deprotonation of methanol in the presence of the added base. This species is then believed to enter the cycle by displacing  $\text{PPh}_3$  from  $[\text{RuH}_2(\text{CO})(\text{PPh}_3)_3]$  (**1**), generating an anionic methoxy intermediate **II**; (**b**) loss of  $\text{PPh}_3$  followed by  $\beta$ -hydrogen abstraction allows the formation of coordinated formaldehyde, **III**, onto which (**c**) deprotonated MeP attacks; (**d**) protonation and displacement of methyl 3-hydroxy-2-methylpropanoate by  $\text{PPh}_3$  produces the anionic trihydrido carbonyl complex **IV**; (**e**) the trihydrido complex, by abstracting a proton from a molecule of methanol, could regenerate the methoxide ion and afford molecular hydrogen (which remains associated with the metal complex as a coordinated dihydrogen molecule) **IV**; (**f**) the liberation of molecular hydrogen in the final step regenerates the catalyst **1**; (**g**) the methyl 3-hydroxy-2-methylpropanoate produced in stage **d** spontaneously dehydrates to give MMA as the final product; (**h**) MiBu is then undesirably formed by catalytic hydrogenation of MMA. The nucleophilic attack of deprotonated MeP is shown as occurring to coordinated formaldehyde (**c**) on the basis of a precedent of attack of an amine<sup>[11]</sup> and because coordinated formaldehyde will be a better electrophile. It could also occur onto free formaldehyde.



**Scheme 3.2.2** Proposed mechanism for ruthenium catalyzed dehydrogenation of MeOH leading to the *in situ* production of anhydrous formaldehyde and subsequent condensation with MeP to afford MMA via water elimination and MiBu by hydrogenation of MMA. (P =  $\text{PPh}_3$ ).

The low yields of MMA and MiBu could arise because of poor deprotonation of MeP or low rates of formation of formaldehyde. Hence, a set of deuterium labelling experiments was conducted with the aim of determining the extent to which a variety of bases affect the  $\alpha$ -deprotonation of MeP. Three parallel reactions were performed in the presence of MeP, in methanol- $\text{d}_4$  as solvent and deuterating agent and three different bases,  $\text{K}_2\text{CO}_3$ ,  $\text{NaOH}$  or  $\text{Cs}_2\text{CO}_3$ . Upon heating the mixtures at  $170^\circ\text{C}$  for 2 hours the formation of non-, mono- and bis-deuterated MeP was observed by  $^{13}\text{C}\{^1\text{H}\}$  DEPT analysis of the recovered liquid phases. The methyl group of non deuterated MeP generates a singlet at  $\delta$  9.5 ppm, which results in  $\beta$ -shifted resonances at  $\delta$  9.4 and 9.3 ppm in the mono- and bis-deuterated species respectively. Similarly, the methylene groups give rise to a singlet at  $\delta$  28.1 ( $-\text{CH}_2-$ ), a triplet at  $\delta$  27.8 ( $-\text{CHD}-$ ) and a quintet at  $\delta$  27.5 ppm ( $-\text{CD}_2-$ ). The methyl resonances were used to calculate the ratio of the non-, mono- and bis-deuterated MeP, giving evidence that  $\text{Cs}_2\text{CO}_3$  is the most effective

(fastest) base for the  $\alpha$ -deprotonation with a ratio ( $\text{CH}_2$  :  $\text{CHD}$  :  $\text{CD}_2$ ) of 10 : 41 : 49 %, followed by  $\text{K}_2\text{CO}_3$  with a corresponding ratio of 47 : 42 : 11 %, while  $\text{NaOH}$  was the slowest giving a ratio of 61 : 33 : 6 %. During these experiments, significant amounts of non, mono and bis-deuterated metal propanoate salts were also formed, despite attempts to exclude all water.<sup>[22]</sup> We return to this observation later on.

Based on these results, simple base catalysed condensation experiments of formaldehyde with MeP were conducted to identify the most efficient base, prior to use in the one-pot system. Since none of the attempts with  $\text{K}_2\text{CO}_3$  and  $\text{NaOH}$  was successful, attention was moved to the strong non-nucleophilic organic base, 1,8-diazobicyclo[5.4.0]undec-7-ene (DBU). Even in this case, NMR analysis of the final mixtures revealed the presence of only trace amounts of MMA.<sup>†‡[22]</sup>

Given that none of the previous experiments gave significant quantities of MMA, methanol dehydrogenation to formaldehyde and subsequent condensation with MeP affording MMA was performed in the presence of simple carbonates,  $\text{Cs}_2\text{CO}_3$  and  $\text{Na}_2\text{CO}_3$ . The latter has been reported by Renken and co-workers to catalyse methanol dehydrogenation.<sup>[23]</sup>

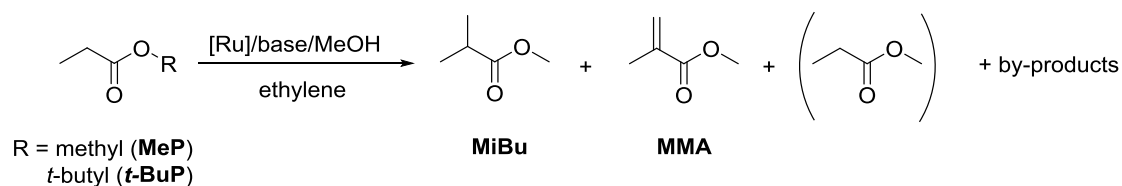
At the end of reactions of MeP with formaldehyde in the presence of  $\text{Cs}_2\text{CO}_3$  or  $\text{Na}_2\text{CO}_3$ , a large amount of solid material was recovered from the batch reactor. This material was again identified as propanoate salts ( $^1\text{H}$  NMR spectroscopy). Our initial conclusion was that these salts might arise from hydrolysis of MeP. The two potential sources of water in this system are the condensation step to form MMA (not observed in this case) and as an impurity in the metal carbonates, which are hygroscopic and usually stored in air. In an attempt to minimise the amount of water and the subsequent ester bond hydrolysis,  $\text{NaOMe}$  (1.46 g, 27 mmol) was employed as the base (MeP: 10 mL, 103.9 mmol). In this case traces of MiBu (0.67 %) and MMA (<0.5 %) were observed, but  $^1\text{H}$  NMR analysis of the solid phase at the end of the reaction showed mainly sodium propanoate. This solid product was isolated (2.53 g, 26 mmol), indicating that all of the sodium methoxide had been converted into sodium propanoate. Similarly, upon heating a mixture of MeP, methanol,  $\text{NaOMe}$  and 0.13% of **1** in toluene, in a

<sup>†</sup> For more details on deuterium labelling and simple base catalysed reaction conditions, see § 3.4

<sup>‡</sup> The deuterium labelling experiments with  $\text{K}_2\text{CO}_3$ ,  $\text{NaOH}$ ,  $\text{Cs}_2\text{CO}_3$  and  $\text{NaP}$  together with the simple base catalysed condensation experiments of formaldehyde with MeP were performed by Dr Jacorien Coetzee during her studies at the University of St Andrews and reported for the first time in the corresponding Ph.D. Thesis. These fundamental experiments are reported in the current work since they are part of a common research project sponsored by the industrial partner Lucite Int. on which the present study was based.

Hastelloy™ autoclave at 170 °C for 3 hours, MMA was produced together with the hydrogenated by-product MiBu, but once again, a substantial amount of methyl propanoate was formed. It is clear from these experiments that the major reaction occurring is the formation of sodium propanoate from MeP and NaOMe.

**Table 3.2.1** shows optimisation of the conditions for MeP and *t*-BuP conversions [%] to MMA and MiBu, employing nucleophilic and non-nucleophilic strong bases at different concentrations.





Entry	Substrate	Cat.	Base	t [h]	MeP	MMA	MiBu	MMA+	Extra MeP
					Conv.	Yield	Yield	MiBu	Conv. <sup>†</sup>
1	MeP	1	NaOMe (25%)	1	25.6	2.7	3.5	6.2	19.4
2	MeP	1	NaOMe (25%)	3	41.1	3.8	5.1	8.9	32.2
3	MeP	1	NaOMe (50%)	3	52.1	1.9	8.8	10.7	41.4
4	MeP	1	NaOMe (100%)	3	96.4	0.3	1.2	1.5	95
5	MeP	1	<i>t</i> -BuONa (26%)	3	35.6	3.5	6.1	9.6	26
6	MeP	1	<i>t</i> -BuONa (26%)	15	42.7	3.6	5.9	9.5	33.2
7	MeP	1	<i>t</i> -BuONa (50%)	3	62.2	3	9.5	12.5	49.7
8	MeP	1 <sup>d</sup>	<i>t</i> -BuONa (50%)	3	47.9	3.3	3.2	6.5	41.4
9	MeP	1	<i>t</i> -BuOK (25%)	3	38.2	2.3	2.7	5	33.2
10	MeP	7	<i>t</i> -BuONa (26%)	3	28	3.9	6.4	10.3	17.7
11	MeP	7	<i>t</i> -BuONa (26%)	15	32.6	2.8	6.3	9.1	23.5
12	MeP	1	NaP (25 %)	15	-	-	-	-	-
13 <sup>§</sup>	MeP	1	NaP (25 %)	15	-	-	-	-	-
14 <sup>§</sup>	MeP	8	NaP (30 %)	15	NQ	DNQ	DNQ	-	-
15	MeP	8	NaOCH <sub>3</sub> (25%)	15	17.7	1.8	4.4	6.2	11.5
16	MeP* <sup>a</sup>	1	<i>t</i> -BuONa (26%)	3	28.5	4.1	7.1	11.2	17.3

Entry	Substrate	Cat.	Base	t [h]	<i>t</i> -BuP	MeP	MMA	MiBu	MMA+MiBu
					Conv.	Yield	yield	Yield	
17	<i>t</i> -BuP	1	NaOMe (25%)	3	98	63	4.4	6.6	11
18	<i>t</i> -BuP	1	<i>t</i> -BuONa (26%)	3	98.5	71	3.3	7.3	10.6
19	<i>t</i> -BuP* <sup>a</sup>	1	<i>t</i> -BuONa (26%)	3	97.2	64.5	4	7.5	11.5
20	<i>t</i> -BuP* <sup>b</sup>	1	<i>t</i> -BuONa (26%)	3	98.3	55.8	3.7	6.4	10
21	<i>t</i> -BuP* <sup>c</sup>	1	<i>t</i> -BuONa (26%)	3	99	78	4.5	7.6	12
22	<i>t</i> -BuP	7	<i>t</i> -BuONa (26%)	3	99.6	58.5	2.7	3	5.7

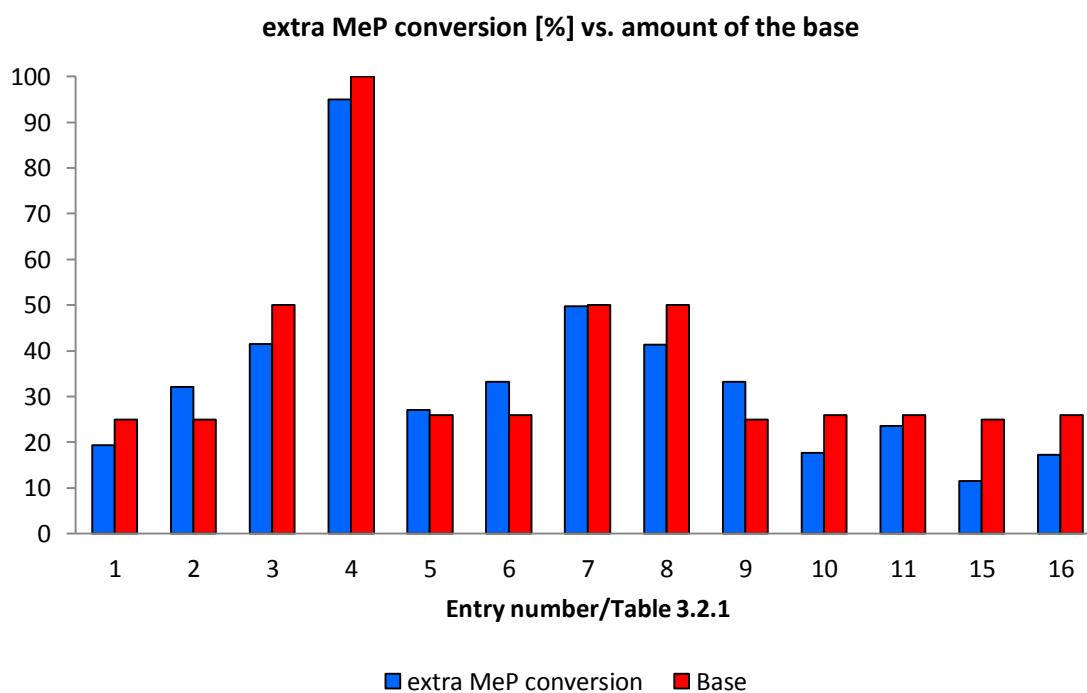
General reaction condition: [RuCl<sub>2</sub>(PPh<sub>3</sub>)<sub>3</sub>] (**7**); [RuH(OCOEt)(CO)(PPh<sub>3</sub>)<sub>2</sub>] (**8**); MeP (10 mL, 103.85 mmol); *t*-BuP (15.65 mL, 103.9 mmol); substrate/MeOH 1:1.8 unless stated otherwise (Entry 14 MeP/MeOH 1:1); catalyst: 0.13 mol % relative to the substrate; solvent: toluene (10 mL); Hastelloy™ autoclave; 170 °C under an atmosphere of ethene (6 bar). § reaction temperature: 200 °C

Conversions [%] were determined by GC-FID analysis using decane as internal standard (IS). NQ (not quantified), DNQ (detected, not quantified).

<sup>†</sup> Mainly NaP.

\*In the presence of *t*-BuOH: <sup>a</sup> MeOH/*t*-BuOH 2:1; <sup>b</sup> MeOH/*t*BuOH 1:1; <sup>c</sup> MeP/MeOH 1:2.7 and MeOH/*t*-BuOH 3:1; the ratios were adjusted by simply adding *t*-BuOH to the standard system.

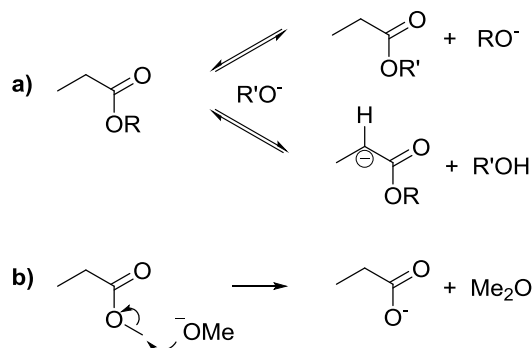
<sup>d</sup> a stoichiometric amount of xantphos was added.<sup>[24]</sup>



**Graph 3.2.1** [MeP conversion – (MMA + MiBu)] compared with the proportion of base employed. [%] Values (relative to MeP) are taken from Table 3.2.1 which summarises the general reaction conditions.

Further confirmation that NaOMe is almost fully consumed in the formation of sodium propanoate comes from an analysis of Table 3.2.1 and Graph 3.2.1, which show the results of a number of experiments carried out under different conditions. In all cases, the total of MMA and MiBu (the major soluble organic products) formed was much less than the conversion of MeP, and substantial amounts of propanoate salts were formed. Comparing the [MeP converted – (MMA+MiBu)] with the amount of base added (Graph 3.2.1), it becomes clear, once again, that the major problem with the reaction is an interaction between the base and MeP, which consumes the base by forming sodium propanoate. This reaction is very surprising as one would expect two possible reactions between a propanoate ester and a sodium alkoxide. The first would be transesterification, which in the case of MeP and NaOMe would not give different products and the second would be the desired  $\alpha$ -deprotonation of MeP (see Scheme 5, reaction mechanism a). Sodium propanoate might be formed by an  $S_N2$  attack of the methoxide ion on the OMe group of MeP to form dimethyl ether with propanoate acting as a leaving group. Although quantitative analysis of Me<sub>2</sub>O is difficult, qualitative GC analysis shows significant quantities of Me<sub>2</sub>O in both the gas and liquid fractions after reactions

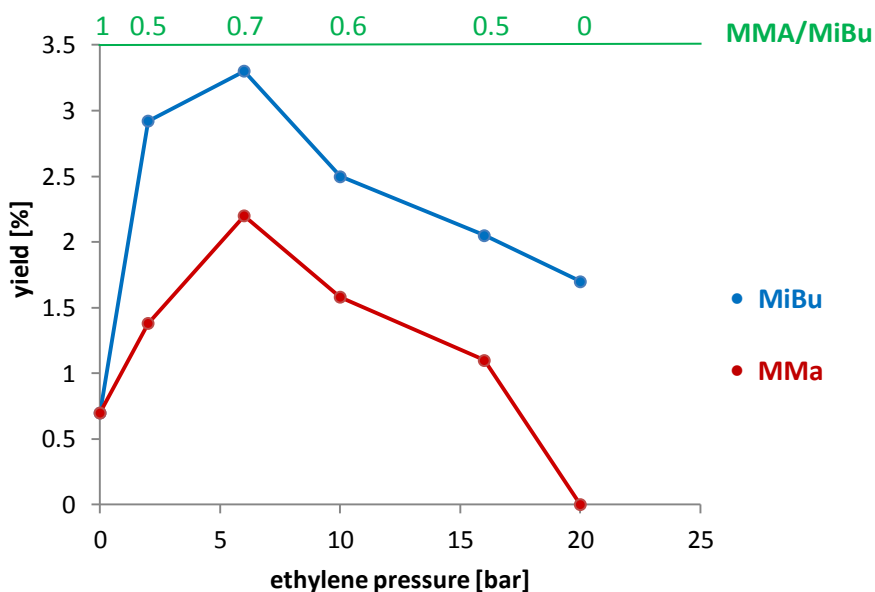
involving MeP and NaOMe with or without methanol (see Scheme 3.2.3, reaction mechanism b).



**Scheme 3.2.3** a) Expected reactions between an alkoxide and a propanoate ester; b) Observed reaction between methyl propanoate and sodium methoxide.

Table 3.2.1 also shows that both MMA and MiBu are formed from systems where methyl propanoate and methanol are reacted with NaOMe in the presence of catalyst **1** (Entries 1-3). Increasing the concentration of base from 26 % relative to MeP to 50 % almost doubles the total conversion to these products, but a higher amount of base reduces the yield of these products dramatically.

MMA is the desired product in these reactions so in order to try to reduce the hydrogenation of MMA to MiBu, we investigated potential sacrificial hydrogen acceptors. Although crotonitrile has been described as a good hydrogen acceptor in ruthenium-catalysed hydrogen transfer reactions,<sup>[24a, 25]</sup> it completely suppressed formation of the desired products when introduced in the one-pot system. Two more attempts were conducted in the presence of benzophenone and methyl acrylate (with the idea of forming more MeP), respectively, but both experiments gave a decrease in terms of MeP conversion. Ethene proved to be a more effective hydrogen acceptor under moderate pressures. Graph 3.2.2 displays optimisation of ethene pressure for the  $\alpha$ -methylenation of MeP, showing an optimum at 6 bar, although MMA was never the major product. All reactions described in Table 3.2.1 were carried out under ethene (6 bar). The high reaction temperature required and the low boiling points of methanol and MeP meant that the reaction could not be carried out in an open system to allow for H<sub>2</sub> venting.



**Graph 3.2.2** Effect of ethene pressure on the yield of MMA and MiBu.

*Reaction conditions:* MeP/MeOH 1:1.2; cat **1**: 0.13 mol % relative to MeP; base: NaOCH<sub>3</sub> (25 % relative to MeP); solvent: toluene (10 ml); Hastelloy™ autoclave, 170 °C, 16 hours. MeP conversions [%] were determined by calibrated GC-FID analysis using toluene as internal standard (IS). Numbers along the top of the Figure are MMA/MiBu ratio.

In order to try to prevent (or slow down) the nucleophilic attack of the methoxide on MeP, we investigated the use of *t*-BuONa in place of methoxide and/or *t*-butyl propanoate (*t*-BuP) in place of MeP. *t*-BuP was chosen since we anticipated that the lower stability of the *t*-BuO<sup>-</sup> ion relative to MeO<sup>-</sup> should reduce the transesterification of *t*-BuP by methanol/methoxide, whilst the steric bulk of the *t*-Bu group should reduce the rate of nucleophilic attack by MeO<sup>-</sup> to produce MeOtBu (MTBE). Using *t*-BuO<sup>-</sup> in place of MeO<sup>-</sup>, we anticipated that the higher basicity and larger steric bulk might favour  $\alpha$ -deprotonation of MeP over nucleophilic attack on the methoxy C atom. In general, using *t*-BuONa allowed a modest increase in MeP conversion to the desired MMA and MiBu (Compare Table 3.2.1, Entries 2 with 5 and 3 with 7). Addition of xantphos (1:1 with Ru), which has been shown to disfavour C=C hydrogenation when used with [RuH<sub>2</sub>(CO)(PPh<sub>3</sub>)<sub>3</sub>],<sup>[24a]</sup> partially inhibited the reaction (Table 3.2.1, Entry 8), while the stronger base *t*-BuOK appeared to be less effective (Table 3.2.1, Entry 9). Very little *t*-BuP or MTBE was produced in these reactions. Changing the catalyst precursor from **1** to [RuCl<sub>2</sub>(PPh<sub>3</sub>)<sub>3</sub>] (**7**), which is expected to react with NaOMe to give **1**,<sup>[26]</sup> had little effect on the formation of the desired products (Table 3.2.1, Entries 10 and 11).

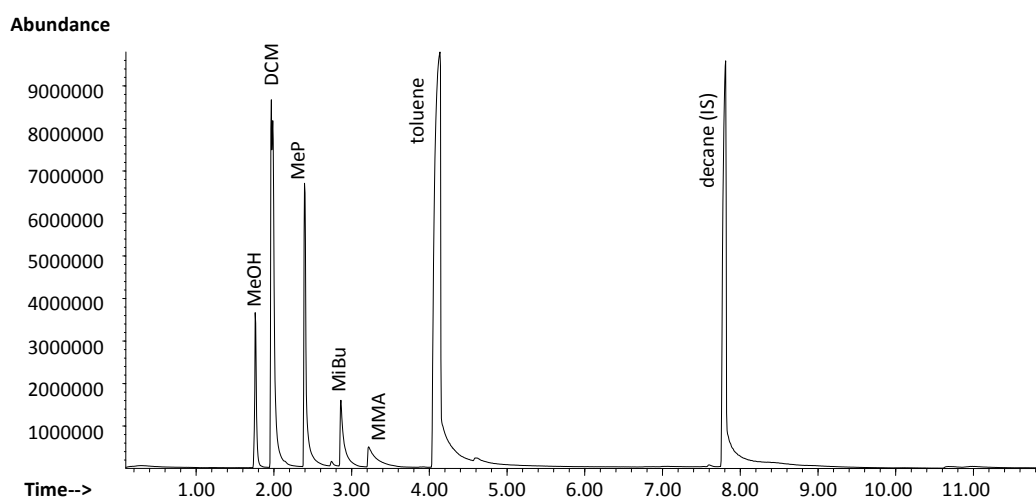


Figure 3.2.1 GC-MS of Entry 10/Table 3.2.1

Minor improvements in the yield of MMA and MiBu were obtained using *t*-BuP in place of MeP (Table 3.2.1, Entries 2 and 17 when using NaOMe as the base; entries 5 and 18 using *t*-BuONa). Species **7** was not as effective under these conditions as  $[\text{RuH}_2(\text{CO})\text{PPh}_3]_3$  (Table 3.2.1, Entry 22). Even in these experiments using *t*-BuP as substrate almost no *t*-BuP was left at the end of the experiments. It had undergone complete transesterification to MeP. *tert*-Butanol (*t*-BuOH) was added to the reaction mixture in an attempt to move the equilibrium back towards *t*-BuP (Table 3.2.1, Entries 19-22) but this had little effect on the yield of MMA and MiBu. It also did not stop the transesterification reaction. Addition of *t*-BuOH to a reaction using MeP and *t*-BuONa did improve the yield somewhat (Table 3.2.1, Entry 16).

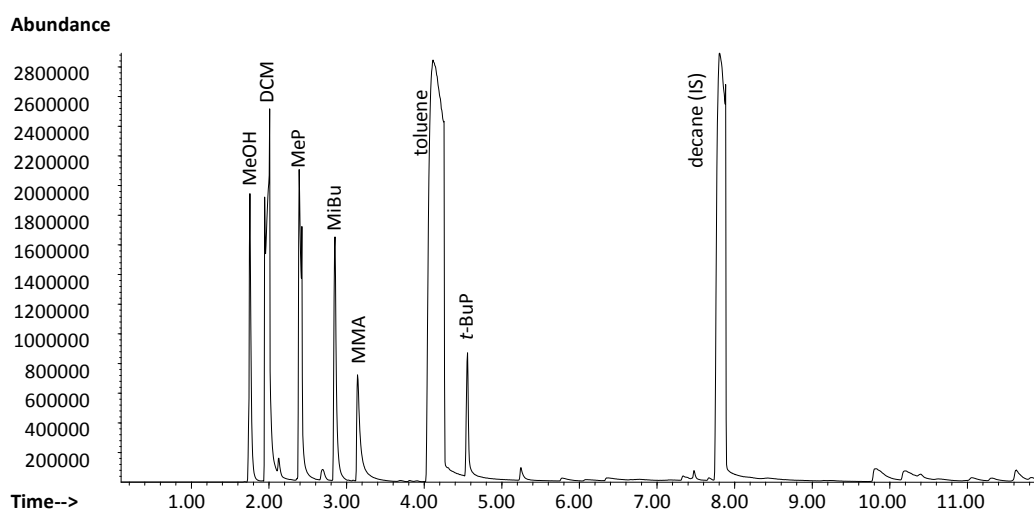
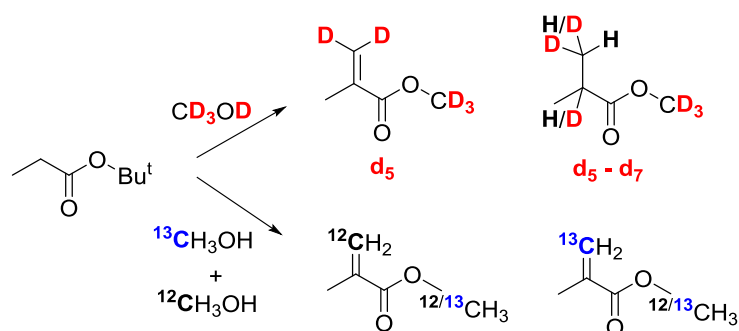


Figure 3.2.2 GC-MS of Entry 17/Table 3.2.1

As indicated above, the major problem with obtaining high yields of methylenation products of MeP is the unexpected  $S_N2$  attack of methoxide ion onto methyl propanoate to give dimethyl ether and propanoate anion. Since methanol is required for the formation of formaldehyde in this system and base is required both for the dehydrogenation of methanol and for the deprotonation of MeP, the only other possibility for preventing the conversion of base to propanoate would be to use sodium propanoate as the base. Initial deuterium labelling studies showed that sodium propanoate is a strong enough base to deprotonate the  $\alpha$ -protons of MeP. Complete H/D exchange with deuteromethanol to the equilibrium position occurred in 5 min upon heating MeP with methanol and NaP at 200°C.<sup>[22]</sup> However, disappointingly, no products were formed when attempting the catalytic reaction using NaP as the base under conditions of Table 3.2.1, Entry 12 and 13. This could be because NaP is not a strong enough base to promote methanol dehydrogenation or because an inactive complex such as [RuH(OCOEt)(CO)(PPh<sub>3</sub>)] (**8**) is formed. To test the latter possibility, we have synthesised complex **8** and shown it to be an active catalyst (Table 1, Entry 15) which even gives a small amount of activity when using NaP as the base (Table 3.2.1, Entry 14).

In order to confirm our assumption that the added methylene (MMA) or methyl group (MiBu) originates from methanol, reactions were carried out using CD<sub>3</sub>OD or <sup>13</sup>CH<sub>3</sub>OH under the conditions of Table 3.2, Entry 18 using *t*-BuP as substrate and *t*-BuONa as base so that the only source of methanol/methoxide was the added methanol (see Scheme 3.2.4). For the <sup>13</sup>C experiment the ratio of <sup>12</sup>CH<sub>3</sub>OH: <sup>13</sup>CH<sub>3</sub>OH used was 8.5:1. Both MMA and MiBu products were shown by GC-MS to contain ca 8-9 % <sup>13</sup>C in the OMe group and in the methylene/methyl group. For the <sup>2</sup>H labelling experiment, CD<sub>3</sub>OD (99%) was used. The MMA mainly contained 5 D atoms, whilst analysis of the [M-OMe]<sup>+</sup> fragment showed that the methylene group contained 2 (68 %) or 1 (20 %) deuterium atoms. The MiBu in this case contained 5, 6 or 7 D atoms in the ratio 29 : 49 : 22 %, whilst the [M-OMe]<sup>+</sup> fragment contained 2, 3 or 4 D atoms in a similar ratio (see Table 3.2.2). These labelling results confirm that, in the predominant pathway for the conversion of MeP to MMA and MiBu in the presence of methanol, the methylene C atom is derived from methanol. However, some H/D exchange occurs possibly with water or with the catalyst. We note that the catalyst undergoes H/D exchange into the *ortho* positions of the phenyl rings as well as into the Ru-H positions.<sup>[27]</sup>



**Scheme 3.2.4** Isotopomers of MeP expected from the methylenation of *t*-BuP in the presence of *t*-BuONa when using labelled methanol if methanol is the source of the methylene group.

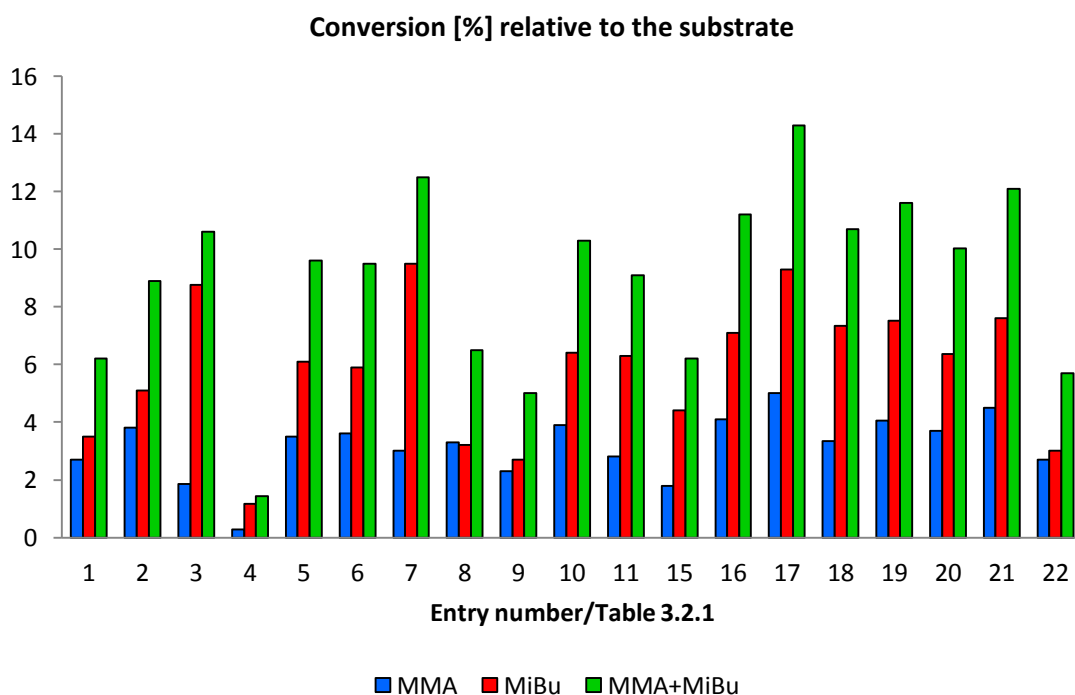
**Table 3.2.2** Intensities of isotopomers of the  $[M-OMe]^+$  signal in the mass spectra of MMA and MiBu when using  $CD_3OD$  or  $^{13}CH_3OH$  for the methylenation of *t*-BuP in the presence of *t*-BuONa.

		Isotopic mass						
		69	70	71	72	73	74	75
<b>MMA</b>	$CH_3OH$	147	7					
	$^{13}CH_3OH/CH_3OH^a$	147	20					
	Assignment	$^{12}C$ 92 %	$^{13}C$ 8 %					
	$CD_3OD$		43	152	28			
	Assignment		$d_1$ 20 %	$d_2$ 68 %	$d_3$ 12 % <sup>b</sup>			
<b>MiBu</b>	$CH_3OH$			88	4			
	$^{13}CH_3OH/CH_3OH^a$			88	12			
	Assignment			$^{12}C$ 92 %	$^{13}C$ 8 %			
	$CD_3OD$					48	83	40
	Assignment					$d_2$ 29 %	$d_3$ 49 %	$d_4$ 22 %

<sup>a</sup> $^{13}CH_3OH/CH_3OH$  is 1:8.5; <sup>b</sup> some  $d_3$ - $[M-OMe]^+$  is observed, suggesting some incorporation of D into the methyl group.

### 3.3 Conclusions

In this study a novel approach for the  $\alpha$ -methylenation of methyl propanoate has been reported involving a one-pot system where four main reactions occur: *methanol dehydrogenation*, providing *in situ* production of anhydrous formaldehyde, *MeP deprotonation* and *condensation* with the new formed formaldehyde and partial *hydrogenation* of the MMA to MiBu. Overall the yields of the two desired products, MMA and MiBu are modest (see Graph 3.3.1), but not very much lower than that obtained in a commercial high temperature condensation of anhydrous formaldehyde with MeP (17 % per pass). The main problem with the reaction is the formation of dimethyl ether and sodium propanoate apparently from the nucleophilic attack of methoxide on MeP with the propanoate anion acting as a leaving group. Attempts to inhibit this kind of reaction using *t*-BuP and *t*-BuONa improved the yield of the desired products but were frustrated by transesterification of the ester with methanol, inevitably present for the formation of formaldehyde. Labelling studies showed that the added methylene (MMA) or methyl group (MiBu) arose predominantly from methanol.



**Graph 3.3.1** Yields of MMA and MiBu for the reactions shown in Table 3.2.1 (Entries 12-14 are not displayed).



## 3.4 Experimental Section

### 3.4.1 General materials and methods

All manipulations and reactions were carried out under N<sub>2</sub> gas (dried through a Cr(II)/silica packed glass column) using different techniques including a standard Schlenk, vacuum line and a glove box. Simple base catalysed experiments and deuterium labelling studies reported in § 3.4.3-3.4.5 were performed under aerobic conditions. Solvents were dried and degassed prior to use unless otherwise stated.

[RuH<sub>2</sub>(CO)(PPh<sub>3</sub>)<sub>3</sub>] (**1**), Shvo's catalyst (**2**), [RuCl(CO)<sub>2</sub>( $\eta^5$ -Ph<sub>5</sub>C<sub>5</sub>)] (**3**), NaOMe, *t*-OBuNa, *t*-OBuK, Cs<sub>2</sub>CO<sub>3</sub>, DBU, sodium propionate, paraformaldehyde, decane (internal standard), methanol, methanol-d<sub>4</sub>, <sup>13</sup>CH<sub>3</sub>OH, methyl methacrylate, methyl isobutyrate, *tert*-butyl propanoate, 3-pentanone and propanoic acid were purchased from Sigma-Aldrich. RuCl<sub>3</sub>·3H<sub>2</sub>O and *tert*-butanol were purchased from Alfa Aesar.

Methyl propanoate (supplied by Lucite Int.) was dried, purified and degassed prior to use, following this standard procedure: pre-treatment with Na<sub>2</sub>CO<sub>3</sub>, stirring over P<sub>2</sub>O<sub>5</sub>, degassing by three freeze-pump-thaw cycles and final collection by trap-to-trap distillation. *tert*-Butyl propanoate and propanoic acid were dried over Na<sub>2</sub>SO<sub>4</sub> and distilled under dinitrogen.

P<sub>2</sub>O<sub>5</sub> and CaCl<sub>2</sub> were purchased from Fluka. Na<sub>2</sub>CO<sub>3</sub> (anhydrous), Na<sub>2</sub>SO<sub>4</sub> (anhydrous) and NaOH (pellets) were purchased from Fisher Scientific.

Toluene was dried using a Braun Solvent Purification System. Methanol was dried and degassed by distillation from magnesium under dinitrogen. All gases were purchased from BOC gases.

Unless otherwise mentioned, all other reagents were used without further purification.<sup>[28]</sup>

[RuCl<sub>2</sub>(PPh<sub>3</sub>)<sub>3</sub>]<sup>[29]</sup> (**7**), RuH(CO)(OCOEt)(PPh<sub>3</sub>)<sub>2</sub><sup>[30]</sup> (**8**), [Ru(OAc)<sub>2</sub>(TriPhos)] (**4**) (triphos = MeC(CH<sub>2</sub>PPh<sub>2</sub>)<sub>3</sub>)<sup>[18]</sup>, [RuH<sub>2</sub>(CO)(TriPhos)]<sup>[19a, 19b]</sup> (**5**) and [RhH(CO)(PEt<sub>3</sub>)<sub>3</sub>]<sup>[31]</sup> (**6**) were prepared by published procedures and all observations and NMR data were in accordance with those reported in the literature.

### 3.4.2 General instruments

NMR spectra were recorded on a Bruker Avance II 400 and 300 MHz Spectrometer ( $^1\text{H}$  NMR at 400 MHz and  $^{13}\text{C}$  NMR at 100 MHz and  $^1\text{H}$  NMR at 300 MHz and  $^{13}\text{C}$  NMR at 75 MHz respectively) at room temperature.  $^1\text{H}$  and  $^{13}\text{C}\{^1\text{H}\}$  spectra are referenced to TMS and the residual proton signal of the solvent was used as internal standard. When needed, NMR assignments were performed with the help of 2D ( $^1\text{H}, ^1\text{H}$ ) COSY experiments.

GC-MS analyses were performed using a Hewlett Packard 6890 series GC system equipped with an Agilent J&W HP-1 column capillary (30.0 m x 248  $\mu\text{m}$  x 0.25  $\mu\text{m}$  nominal). Method: flow rate 0.8 mL  $\text{min}^{-1}$  (He carrier gas), split ratio 100:1, starting temperature 50  $^\circ\text{C}$  (4 min) ramp rate 20  $^\circ\text{C min}^{-1}$  to 130  $^\circ\text{C}$  (2 min), ramp rate 20  $^\circ\text{C min}^{-1}$  to 280  $^\circ\text{C}$  (15.50 min). Quantitative analyses, using decane or toluene as an internal standard were performed using a flame ionization detector (GC-FID) and qualitative analyses using an HP5973 mass selective detector (GC-MS).

GC-FID integration method details: Initial Area Reject 0; Initial Peak Width 0.038; Shoulder Detection OFF; Initial Threshold 19.

Experiments reported in § 3.4.3, 3.4.4 and 3.4.5 were performed by Dr Jacorien Coetzee during her studies at the University of St Andrews and reported for the time in the corresponding Ph.D. Thesis<sup>[22]</sup> as are part of a common project sponsored by the industrial partner Lucite Int.

### 3.4.3 General procedure for deuterium labelling experiment with MeP, base and methanol- $\text{d}_4$

An autoclave was charged with MeP, a base ( $\text{K}_2\text{CO}_3$ , NaOH or  $\text{Cs}_2\text{CO}_3$ , Table 3.4.3.1) and methanol- $\text{d}_4$  and heated at 170  $^\circ\text{C}$  with stirring for 2 hours. The autoclave was then cooled to room temperature, vented to the atmosphere and the obtained product mixture analysed by NMR spectroscopy.

**Table 3.4.3.1** Conditions for deuterium exchange between methanol-d<sub>4</sub> and MeP

Experiment	MeP	Base	Methanol-d <sub>4</sub>
a	0.96 mL, 10.0 mmol	K <sub>2</sub> CO <sub>3</sub> (0.35 g, 2.53 mmol)	3 mL
b	0.96 mL, 10.0 mmol	NaOH (0.12 g, 2.90 mmol)	3 mL
c	0.96 mL, 10.0 mmol	Cs <sub>2</sub> CO <sub>3</sub> (0.82 g, 2.53 mmol)	3 mL

#### 3.4.4 Time dependent deuterium labelling study with NaP as base

Sodium propanoate (5.48 g, 57.05 mmol) was added to a stainless steel autoclave (**A**) fitted with a magnetic stirring bar. The autoclave was then sealed, purged and connected to a second autoclave (**B**), previously purged and sealed, via the gas inlet ports by Swagelock tubing. The two autoclaves were isolated from each other by means of valves. Methyl propanoate (10 mL, 103.85 mmol) and methanol-d<sub>4</sub> (28.97 mL, 713.26 ml) were added to autoclave **A** via the injection port. The resulting mixture was heated to 200 °C with stirring and a sample was taken at t = 0 min (at the time the autoclave reached the set temperature), by briefly opening the valves between the autoclaves and allowing a fraction of the vapour phase to condense into autoclave **B** which was immersed in cold water. Similar experiments were carried out with samples being taken at t = 5 min, 10 min and 60 min by the same method. At the end of each experiment the two autoclaves were disconnected, vented to the atmosphere, opened and the two colourless solutions were analysed by NMR spectroscopy. <sup>13</sup>C{<sup>1</sup>H} NMR spectra were used to quantify deuterium incorporation.<sup>[32]</sup>

#### 3.4.5 General procedure for base catalysed condensation of MeP and formaldehyde

An autoclave charged with MeP, used as received, (0.96 mL, 10 mmol), a base (K<sub>2</sub>CO<sub>3</sub>, NaOH or DBU), paraformaldehyde as formaldehyde source and a solvent (toluene or 2-ethylhexanol) was heated to 170 °C for 1-2 hours with stirring (Table 3.4.5.1). The autoclave was cooled to room temperature, vented to the atmosphere and the reaction mixture analysed by GC and NMR techniques.

Entry	Base	Solvent	Formaldehyde	MMA Yield [%]
1	K <sub>2</sub> CO <sub>3</sub> (2.53mmol)	toluene (10.0 mL)	9.7 mmol	< 1
2	K <sub>2</sub> CO <sub>3</sub> (2.53 mmol)	2-ethylhexanol (11.72mL)	15.0 mmol	0
3	K <sub>2</sub> CO <sub>3</sub> 2.53 mmol	2-ethylhexanol (4.69 mL)	15.0 mmol	0
4	DBU 2.53 mmol	toluene (5.0 mL)	15.0 mmol	< 1
5	DBU 2.53 mmol	2-ethylhexanol (4.69 mL)	15.0 mmol	< 1
6	NaOH 3.0 mmol	2-ethylhexanol (4.69 mL)	15.0 mmol	0

**Table 3.4.5.1** Attempted base catalysed formation of MMA from MeP and formaldehyde

### 3.4.6 General procedure for catalytic batch reactions

Catalytic reactions were carried out in a Hastelloy™ autoclave. In a typical experiment the desired amount of the catalyst and all solid compounds were weighed into the autoclave under an inert atmosphere of dinitrogen (glovebox). The autoclave was then sealed and purged with three vacuum/N<sub>2</sub> cycles. At this point all solvents and solutions were added through the injection port. After these operations the autoclave was pressurized with the desired gas or simply resealed. The reactor was then heated to the desired temperature and the reaction mixture was stirred using a magnetic stirrer. After the set reaction time the autoclave was cooled to room temperature, observing a pressure drop, and fully vented prior to opening the autoclave, giving evidence of two phases, solid and liquid. At this stage decane (internal standard) was added and the reaction mixture vigorously stirred prior to separation of the two phases by filtration. NMR spectroscopy, qualitative GC-MS and quantitative GC-FID spectroscopy were employed to analyse the recovered phases.

### 3.4.7 Reaction conditions for catalytic batch reactions reported in Table 3.2.1

A Hastelloy™ autoclave was fitted with a magnetic stirrer and charged under a dinitrogen atmosphere with the desired catalyst (**1**) (0.124 g, 0.135 mmol), (**7**) (1.129 g, 0.135 mmol) or (**8**) and a base. Toluene (10 mL), MeP (10 mL, 103.85 mmol) or *t*-BuP (15.64 mL, 103.9 mmol) were added together with methanol (7.6 mL, 187.02 mmol) and 2,4-dimethyl-6-tert-butylphenol (Topanol A, 0.01 mL) in order to prevent MMA polymerization. The autoclave was sealed, pressurised with ethene (6 bar) and heated to 170 °C or 200 °C (Entries 13 and 14) for 1-15 hours. Full details and amounts are given in Table 3.2.1

**Table 3.4.7.1** Conditions for methylenation of MeP. The results are presented in Table 3.2.1

Entry	Substrate	[Ru]	Base	<i>t</i> -BuOH	t [h]
1	MeP	1	NaOMe (1.42 g, 26.3 mmol)	-	1
2	MeP	1	NaOMe (1.42 g, 26.3 mmol)	-	3
3	MeP	1	NaOMe (2.8 g, 51.9 mmol)	-	3
4	MeP	1	NaOMe (5.6 g, 103.85 mmol)	-	3
5	MeP	1	<i>t</i> -BuONa (2.6 g, 27.0 mmol)	-	3
6	MeP	1	<i>t</i> -BuONa (2.6 g, 27.0 mmol)	-	15
7	MeP	1	<i>t</i> -BuONa (4.99 g, 51.9 mmol)	-	3
8	MeP	1 <sup>a</sup>	<i>t</i> -BuONa (4.99 g, 51.9 mmol)	-	3
9	MeP	1	<i>t</i> -BuOK (2.95 g, 26.3 mmol)	-	3
10	MeP	7	<i>t</i> -BuONa (2.6 g, 27.0 mmol)	-	3
11	MeP	7	<i>t</i> -BuONa (2.6 g, 27.0 mmol)	-	15
12	MeP	1	NaP (2.5 g, 26.3 mmol)	-	15
13 <sup>c</sup>	MeP	1	NaP (2.5 g, 26.3 mmol)	-	15
14 <sup>b,c</sup>	MeP	8	NaP (2.09 g, 21.8 mmol)	-	15
15	MeP	8	NaOMe (1.42 g, 26.3 mmol)	-	15
16	MeP	1	<i>t</i> -BuONa (2.6 g, 27.0 mmol)	8.9 mL, 93.5 mmol	3
17	<i>t</i> -BuP	1	NaOMe (1.42 g, 26.3 mmol)	-	3
18	<i>t</i> -BuP	1	<i>t</i> -BuONa (2.6 g, 27.0 mmol)	-	3
19	<i>t</i> -BuP	1	<i>t</i> -BuONa (2.6 g, 27.0 mmol)	8.9 mL, 93.5 mmol	3
20	<i>t</i> -BuP	1	<i>t</i> -BuONa (2.6 g, 27.0 mmol)	17.9 mL, 187.02 mmol	3
21	<i>t</i> -BuP	1	<i>t</i> -BuONa (2.6 g, 27.0 mmol)	8.9 mL, 93.5 mmol	3
				(MeOH: 11.36 mL, 280.5 mmol)	
22	<i>t</i> -BuP	7	<i>t</i> -BuONa (2.6 g, 27.0 mmol)	-	3

<sup>a</sup> a stoichiometric amount of xantphos was added; <sup>b</sup> Entry 14: MeP (7 mL, 72.7 mmol), MeOH (2.9 mL, 72.7 mmol) cat. (0.07 g, 0.094 mmol); <sup>c</sup> T = 200 °C

### 3.4.8 Reaction using <sup>2</sup>H or <sup>13</sup>C labelled methanol

The reactions were carried out as described in **Table 3.4.7.1 Entry 18** using CD<sub>3</sub>OD in place of methanol or using a mixture of CH<sub>3</sub>OH (3.38 mL, 83.64 mmol) and <sup>13</sup>CH<sub>3</sub>OH (0.4 mL, 9.87 mmol). In the latter case the reaction was scaled-down to 50 %. After the reaction, the crude solutions were analysed by GC-MS. The relative intensities of the signals from the isotopomers from the parent ion and from [M-OMe]<sup>+</sup> integrated over the whole area of the GC peak were used to determine the relative amounts of different isotopomers present. The products

expected if methanol is the source of the methylene group are shown in Scheme 3.2.4 and the actual mass spectra are shown in Figure 3.4.8.1-3 The observed peak intensities and assignments are in Table 3.2.2.

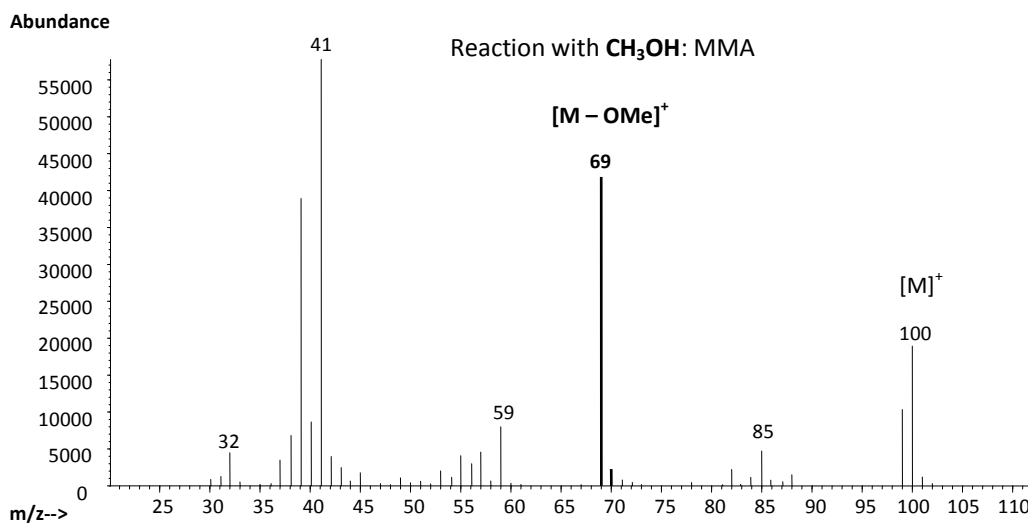
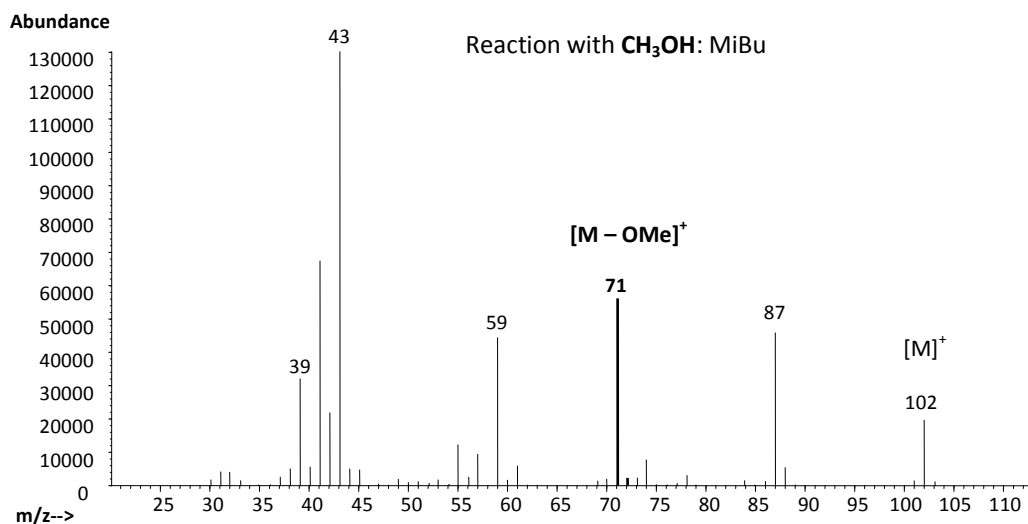
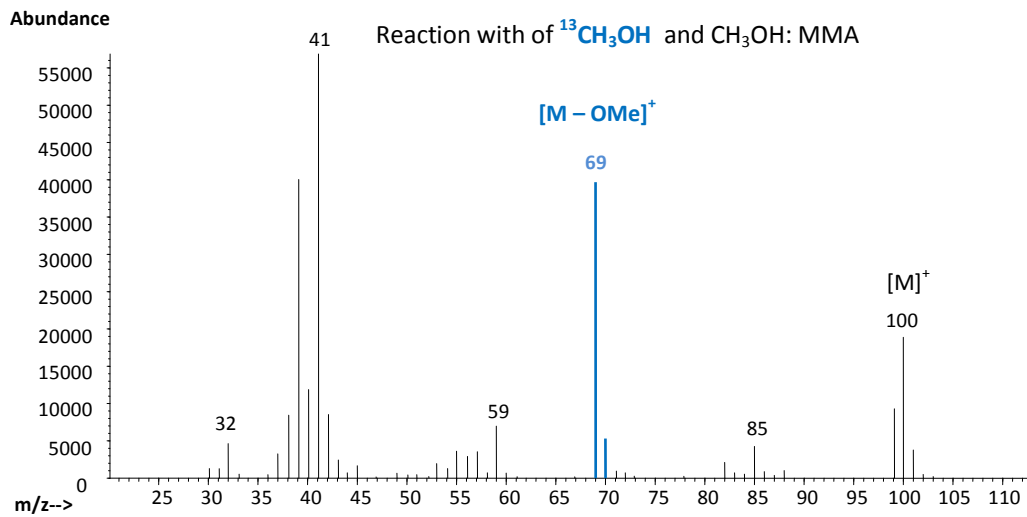
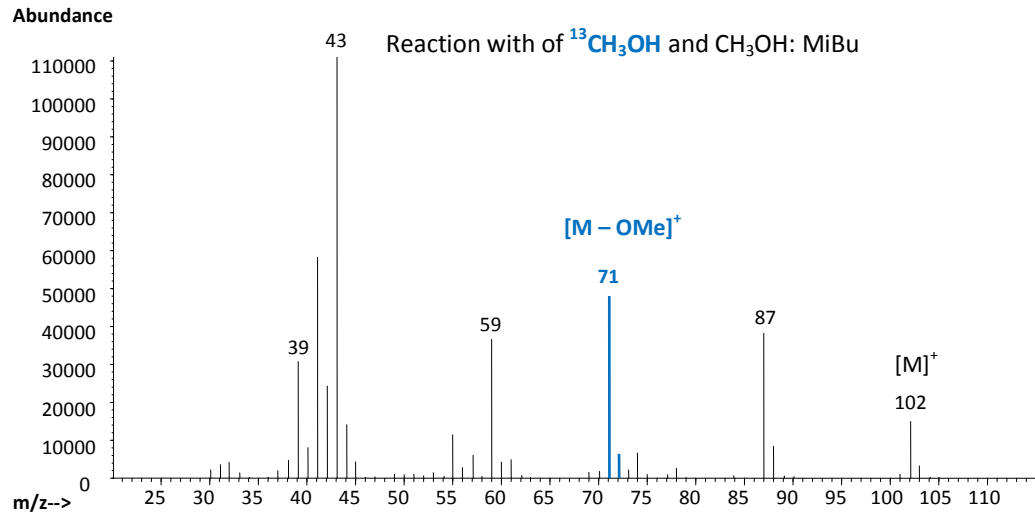


Figure 3.4.8.1 Fragmentation patterns of MiBu and MMA when using only  $\text{CH}_3\text{OH}$ .



**Figure 3.4.8.2** Fragmentation patterns of MiBu and MMA when using  $^{13}\text{CH}_3\text{OH}$  and  $\text{CH}_3\text{OH}$  in a 1:8.5 ratio

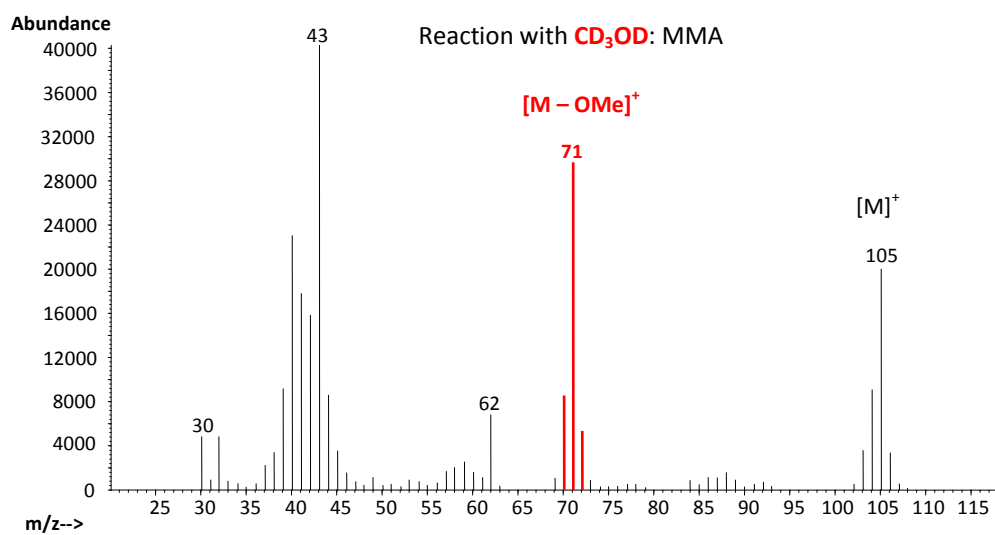
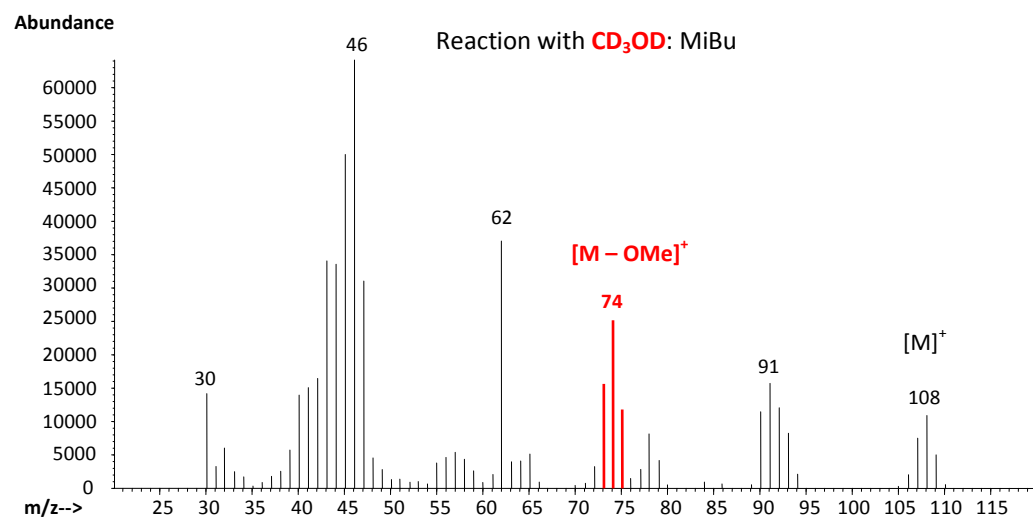


Figure 3.4.8.3 Fragmentation patterns of MiBu and MMA when using only  $\text{CD}_3\text{OD}$ .



### 3.5 References

- [1] a) M. M. Green, H. A. Wittcoff, in *Organic Chemistry Principles and Industrial Practice*, Wiley-VCH, Weinheim, **2003**, pp. 137-156; b) G. R. Eastham, R. P. Tooze, X. L. Wang, K. Whiston, World Patent 96/19434, **1996**; c) K. Nagai, *Appl. Catal., A* **2001**, *221*, 367-377.
- [2] W. Clegg, M. R. J. Elsegood, G. R. Eastham, R. P. Tooze, X. L. Wang, K. Whiston, *Chem. Commun. (Cambridge)* **1999**, 1877-1878.
- [3] B. Harris, *Ingenia* **2010**, December, 18-23.
- [4] B. Hin, P. Majer, T. Tsukamoto, *J. Org. Chem.* **2002**, *67*, 7365-7368.
- [5] M. Hamid, P. A. Slatford, J. M. J. Williams, *Adv. Synth. Catal.* **2007**, *349*, 1555-1575.
- [6] C. Gunanathan, Y. Ben-David, D. Milstein, *Science* **2007**, *317*, 790-792.
- [7] G. Guillena, D. J. Ramon, M. Yus, *Angew. Chem. Int. Ed.* **2007**, *46*, 2358-2364.
- [8] a) D. Morton, D. J. Cole-Hamilton, *J. Chem. Soc.-Chem. Commun.* **1987**, 248-249; b) M. Nielsen, E. Alberico, W. Baumann, H.-J. Drexler, H. Junge, S. Gladiali, M. Beller, *Nature* **2013**, *495*, 85-89.
- [9] a) E. Delgado Lieta, M. A. Luke, R. F. Jones, D. J. Cole-Hamilton, *Polyhedron* **1982**, *1*, 839-840; b) T. Takahashi, S. Shinoda, Y. Saito, *J. Mol. Catal.* **1985**, *31*, 301-309.
- [10] H. Yamamoto, S. Shinoda, Y. Saito, *J. Mol. Catal.* **1985**, *30*, 259-266.
- [11] N. Ortega, C. Richter, F. Glorius, *Org. Lett.* **2013**, *15*, 1776-1779.
- [12] J. Moran, A. Preetz, R. A. Mesch, M. J. Krische, *Nat. Chem.* **2011**, *3*, 287-290.
- [13] J. K. MacDougall, D. J. Cole-Hamilton, *Polyhedron* **1990**, *9*, 1235-1236.
- [14] a) D. Morton, D. J. Cole-Hamilton, *J. Chem. Soc., Chem. Commun.* **1987**, 248-249; b) D. Morton, D. J. Cole-Hamilton, *J. Chem. Soc., Chem. Commun.* **1988**, 1154-1156; c) D. Morton, D. J. Cole-Hamilton, I. D. Utuk, M. Paneque-Sosa, M. Lopez-Poveda, *J. Chem. Soc., Dalton Trans.* **1989**, 489-495.
- [15] a) R. A. Sanchez-Delgado, A. Andriollo, N. Valencia, *J. Mol. Catal.* **1984**, *24*, 217-220; b) R. A. Sanchez-Delgado, M. Medina, F. Lopez-Linares, A. Fuentes, *J. Mol. Catal. A Chem.* **1997**, *116*, 167-177.
- [16] a) B. L. Conley, M. K. Pennington-Boggio, E. Boz, T. J. Williams, *Chem. Rev. (Washington, DC, U. S.)* **2010**, *110*, 2294-2312; b) K. Takahashi, M. Yamashita, T. Ichihara, K. Nakano, K. Nozaki, *Angew. Chem., Int. Ed.* **2010**, *49*, 4488-4490, S4488/4481-S4488/4412.
- [17] a) B. Martin-Matute, M. Edin, K. Bogar, F. B. Kaynak, J.-E. Baeckvall, *J. Am. Chem. Soc.* **2005**, *127*, 8817-8825; b) B. Martin-Matute, J. B. Aberg, M. Edin, J.-E. Baeckvall, *Chem. Eur. J.* **2007**, *13*, 6063-6072, S6063/6061-S6063/6015.
- [18] J. Coetzee, D. L. Dodds, J. Klankermayer, S. Brosinski, W. Leitner, A. M. Z. Slawin, D. J. Cole-Hamilton, *Chem. - Eur. J.* **2013**, *19*, 11039-11050.
- [19] a) F. M. A. Geilen, B. Engendahl, M. Holscher, J. Klankermayer, W. Leitner, *J. Am. Chem. Soc.* **2011**, *133*, 14349-14358; b) M. A. Wood, S. P. Crabtree, D. V. Tyers, WO, 2005051875, **2005**; c) M. Kilner, D. V. Tyers, S. P. Crabtree, M. A. Wood, WO, 2003093208, **2003**
- [20] J. K. MacDougall, M. C. Simpson, M. J. Green, D. J. Cole-Hamilton, *J. Chem. Soc., Dalton Trans.* **1996**, 1161-1172.
- [21] N. Sieffert, M. Buehl, *J. Am. Chem. Soc.* **2010**, *132*, 8056-8070.
- [22] J. Coetzee, Ph.D Thesis "Towards new catalytic systems for the formation of methyl methacrylate from methyl propanoate", University of St Andrews (St Andrews, UK) **2011**.
- [23] a) S. Su, M. R. Prairie, A. Renken, *Appl. Catal., A* **1992**, *91*, 131-142; b) S. Su, M. R. Prairie, A. Renken, *Appl. Catal., A* **1993**, *95*, 131-142.

- [24] a) M. I. Hall, S. J. Pridmore, J. M. J. Williams, *Adv. Synth. Catal.* **2008**, *350*, 1975-1978; b) N. J. Wise, J. M. J. Williams, *Tetrahedron Lett.* **2007**, *48*, 3639-3641; c) M. Kranenburg, Y. E. M. Vanderburgt, P. C. J. Kamer, P. W. N. M. van Leeuwen, K. Goubitz, J. Fraanje, *Organometallics* **1995**, *14*, 3081-3089.
- [25] M. I. Hall, S. J. Pridmore, J. M. J. Williams, *Adv. Synth. Catal.* **2008**, *350*, 1975-1978.
- [26] B. N. Chaudret, D. J. Cole-Hamilton, R. S. Nohr, G. Wilkinson, *J. Chem. Soc. Dal. Trans.* **1977**, 1546-1557.
- [27] P. Lorusso, D. J. Cole-Hamilton, To be published.
- [28] W. L. F. Armarego, C. Chai, *Purification of Laboratory Chemicals*, 5th ed., **2003**.
- [29] P. S. Hallman, T. A. Stephenson, G. Wilkinson, *Inorg. Synth.* **1970**, *12*, 237-240.
- [30] a) R. A. Sanchez-Delgado, *Simp. Quim. Inorg. "Met. Transicion"*, 1st **1985**, 47-54; b) R. A. Sanchez-Delgado, U. Thewalt, N. Valencia, A. Andriollo, R. L. Marquez-Silva, J. Puga, H. Schoellhorn, H. P. Klein, B. Fontal, *Inorg. Chem.* **1986**, *25*, 1097-1106.
- [31] J. K. MacDougall, M. C. Simpson, M. J. Green, D. J. Cole-Hamilton, *J. Chem. Soc., Dalton Trans.* **1996**, 1161-1172.
- [32] J. K. MacDougall, M. C. Simpson, D. J. Cole-Hamilton, *J. Chem. Soc., Dalton Trans.* **1994**, 3061-3065.

# Chapter 4

## **Mechanistic understanding of methanol dehydrogenation catalysed by $[\text{RuH}_2(\text{CO})(\text{PPh}_3)_3]$ : a blended experimental and theoretical approach**

A density functional study (DFT) was undertaken to elucidate the mechanism involved in methanol dehydrogenation catalysed by  $[\text{RuH}_2(\text{CO})(\text{PPh}_3)_3]$ . The investigated channels exhibited a relatively high activation barrier and the rate-determining step was found to be the partial decoordination of the formaldehyde product. The small experimental KIE (1.3) was in good agreement with the computed value (1.6), confirming that the C-H bond under study does not undergo cleavage in the rate-determining step.

---

**Keywords:** ruthenium · methanol · dehydrogenation · KIEs · experimental and DFT study

## 4.1 Introduction

Sieffert and Bühl reported in 2010 an extensive density functional theory (DFT) study<sup>[1]</sup> on the mechanism of alcohol dehydrogenation catalysed by the well-defined  $[\text{RuH}_2(\text{H}_2)(\text{PPh}_3)_3]$ <sup>[2]</sup> complex (**13**), which was believed to be a key active species. The undertaken study arises from the classical Morton and Cole-Hamilton system concerning catalytic hydrogen production, together with the formation of aldehydes, from a wide range of alcoholic substrates using the  $[\text{RuH}_2(\text{X})(\text{PPh}_3)_3]$  catalyst (where  $\text{X} = \text{N}_2, \text{PPh}_3$  or  $\text{H}_2$ )<sup>[3]</sup> and consists of four plausible reaction channels. Two pathways were designed to involve intermediates retaining in all steps the three coordinated  $\text{PPh}_3$  ligands, whilst the dissociation of one phosphine ligand, which can then re-coordinate in each catalytic cycle or remain uncoordinated, occurs in the other pathways. The DFT study disclosed four competitive pathways due to very close activation free energies and sometimes also cross-linked channels.<sup>[1]</sup> The in-depth understanding of these kind of systems is however complicated by the presence of side reactions, in particular alcohol decarbonylation,<sup>[4]</sup> which leads to the formation of the  $[\text{RuH}_2(\text{CO})(\text{PPh}_3)_3]$  and (**1**) complex, already reported by Morton and Cole-Hamilton as an active catalyst for ethanol and other alcohols dehydrogenation in the presence of  $\text{NaOH}$  at  $150\text{ }^\circ\text{C}$ .<sup>[3, 5]</sup> The catalysts **13** and  $[\text{RuH}_2(\text{N}_2)(\text{PPh}_3)_3]$  (**14**) exhibited a similar activity when using  $\text{NaOH}$ ,<sup>[3]</sup> however all compounds  $[\text{RuH}_2(\text{X})(\text{PPh}_3)_3]$  give the carbonyl species **1**, therefore it is not truly possible to know the real rates for any complex rather than **1**. The decarbonylation reaction has been already studied computationally disclosing three alternative routes when using methanol as substrate.<sup>[6]</sup>

In the work reported in Chapter 3 on the production of MMA via  $\alpha$ -methylenation of MeP, we proposed a system involving catalytic dehydrogenation of methanol for the *in situ* production of anhydrous formaldehyde which was then used as one carbon alkylating agent. Among the screened catalysts, **1** was found to be one of the most active species for which a plausible mechanism was proposed based on published work<sup>[1, 7]</sup> (see Chapter 3, Figure 3.2.2). In the current study, following one of the anionic pathways reported by Sieffert and Bühl, which was closer to our hypothetical mechanism (pathway C of the cited paper whereas denoted C\* in the current chapter), we computed two additional channels in which all designed intermediates retain the carbonyl ligand. Experimentally measured and computationally predicted kinetic isotope effects (KIEs) were used for gaining understanding of the dehydrogenation mechanism (the decarbonylation path will be discussed in Chapter 5).

## 4.2 Results and Discussion

A potential and detailed mechanism for the catalysed dehydrogenation of methanol by complex  $[\text{RuH}_2(\text{CO})(\text{PPh}_3)_3]$  (**1**) has been calculated following a computational protocol<sup>[8]</sup> recently developed by Sieffert and Bühl and widely used for investigating multiple reaction channels for alcohol dehydrogenation<sup>[1]</sup> and decarbonylation<sup>[6]</sup> using the  $[\text{RuH}_2(\text{H}_2)(\text{PPh}_3)_3]$  (**13**) catalyst.

The above mentioned protocol will be briefly illustrated in this paragraph to allow full comprehension of data therein reported .

The protocol is based on three computational levels of theory, denoted ECP1, ECP2 and ECP3 (see Experimental Section for a detailed description of methods employed to calculate geometry optimization, thermodynamic corrections and energies).

Geometries of complexes 1-12 were fully optimised at the RI-BP86/ECP1 level of theory together with estimation of thermodynamic corrections. The corresponding thermal corrections to Gibbs Free Energy (denoted  $\delta E_G$ ) for a given step are gathered in Table 4.2.1.

Refined energies were obtained from single-point calculations on the RI-BP86/ECP1 geometries including the B97-D functional (B97-D/ECP2), a method successfully employed to describe bulky transition-metal complexes.<sup>[8-9]</sup> The counterpoise method was used to gain corrected energies for the basis set superposition error (BSSE).<sup>[10]</sup> Correction terms for BSSE energies, denoted  $\delta E_{\text{BSSE}}$ , are reported in Table 4.2.1. Estimation of solvation effects was calculated using the conductor-like screening model (COSMO)<sup>[11]</sup> including a dielectric constant  $\epsilon = 32.63$  to simulate the employment of methanol as solvent in experimental reactions. The solvation effect, noted as  $\delta E_{\text{solv}}$ , was defined as the difference between the reaction energy in the continuum ( $\Delta E_{\text{COSMO}}$ ) and the one in the gas phase ( $\Delta E_{\text{GAS}}$ ), ( $\delta E_{\text{solv}}$ ,  $\Delta E_{\text{COSMO}}$  and  $\Delta E_{\text{GAS}}$  are reported in Table 4.2.1). The final  $\Delta G$  for a given step is calculated as the sum of all correction terms added to the gas-phase reaction energies and gathered in Table 4.2.1.

$$\Delta G = \Delta E_{\text{GAS}} + \delta E_{\text{solv}} + \delta E_{\text{BSSE}} + \delta E_G \quad \text{or simply} \quad \Delta G = \Delta E_{\text{COSMO}} + \delta E_{\text{BSSE}} + \delta E_G$$

$\Delta E_{\text{GAS}}$ ,  $\delta E_{\text{solv}}$  and  $\delta E_{\text{BSSE}}$  were computed at the B97-D/ECP2 level of theory while  $\delta E_G$  at the RI-BP86/ECP1 level.

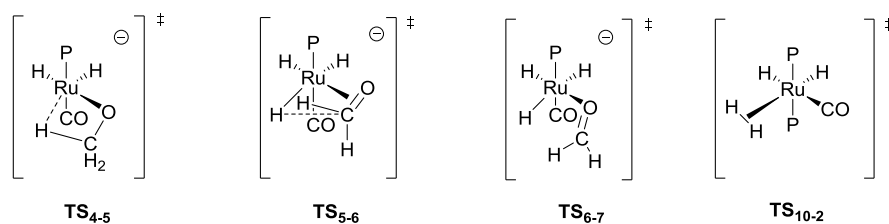
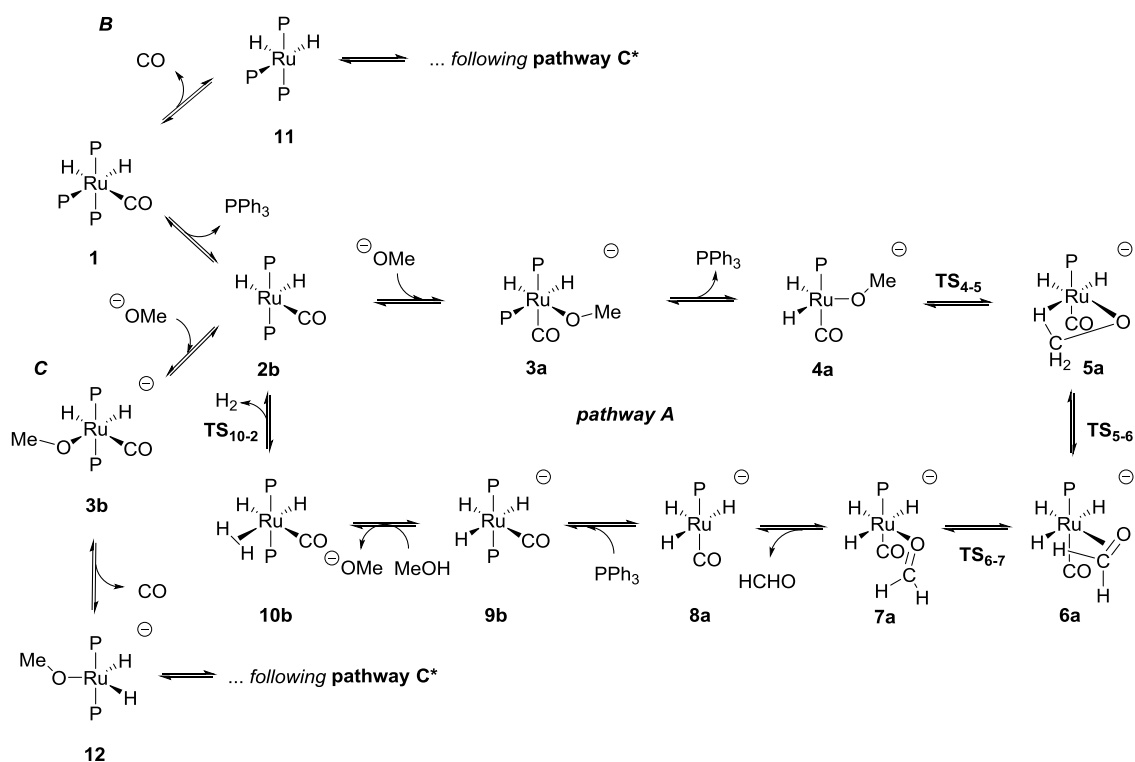
Based on the anionic reaction pathway C\* previously reported by Sieffert and Bühl,<sup>[1]</sup> we investigated an analogous path, denoted **A** (Figure 4.2.1), for the dehydrogenation of methanol catalysed by complex **1**, in which all intermediates retain the carbonyl ligand. Pathway C\* departs from the catalyst precursor **13** that affords the active species [RuH<sub>2</sub>(PPh<sub>3</sub>)<sub>3</sub>] (**14**) by releasing H<sub>2</sub> in the reaction medium. Once formed, the active species is then involved in the dehydrogenation reaction according to the mechanism depicted in Figure 4.2.1.

Similarly, in our proposed reaction path **A** the active species **2b** can arise from **1**, which acts as a catalyst precursor, by dissociation of one of the phosphine ligands. This initiation step involving the PPh<sub>3</sub> decoordination was found to be unfavorable thermodynamically (by 62.0 kJ/mol), suggesting that intermediate **2b** may be present to a small extent in the catalytic system. Since the dehydrogenation reaction occurs under basic conditions (the twofold role of the base in our system has been elucidated in chapter 3), complex **2b** can coordinate the MeO<sup>-</sup> to afford the anionic methoxy intermediate **3a**. The coordination step of MeO<sup>-</sup> appears more favoured ( $\Delta G = 20.9$  kJ/mol). The subsequent step may involve the decoordination of another phosphine ligand from **3a** in order to create a vacant site that would significantly ease the following H-transfer. The phosphine dissociation has been estimated on the order of 7.4 kJ/mol for the phosphine *trans* to the hydride ligand (**3a** → **4a**) and 18.8 kJ/mol for the mutually *trans* phosphine (**3b** → **4a**). The resulting 5-coordinated species **4a** then undergoes  $\beta$ -H abstraction, a reaction that takes place in two steps. In the first step we observe the formation of the first agostic intermediate **5a** by interaction of one hydrogen of the MeO<sup>-</sup> ligand with Ru ( $\Delta G = 29.2$  kJ/mol and  $\Delta G^\ddagger = 32.1$  kJ/mol). In the subsequent step the breaking of the C-H bond followed by full coordination of the H atom to the metal centre ( $\Delta G = -40.2$  kJ/mol and  $\Delta G^\ddagger = -1.6$  kJ/mol)\* affords intermediate **6a** where the HCHO product is  $\pi$ -coordinated to the metal. Because of the reasonably low energy of the latter species, the following decoordination of the formaldehyde product to generate **8a** is therefore very demanding kinetically and thermodynamically (overall  $\Delta G_{6a \rightarrow 8a} = 42.1$  kJ/mol) and proceeds via the  $\eta^2$ - $\eta^1$  slippage of the coordinated HCHO. The formation of intermediate **7a** where the HCHO ligand becomes  $\eta^1$ -coordinated is clearly the rate-determining step ( $\Delta G = 71.2$  kJ/mol and  $\Delta G^\ddagger = 87.6$  kJ/mol). The subsequent recoordination of the PPh<sub>3</sub> ligand can proceed via two intermediates, **9a** or **9b**. The formation of **9b** is thermodynamically favourable ( $\Delta G = -47.1$

\* For clarity:  $\Delta G^\ddagger$  could be negative because the barrier on the potential energy surface ( $\Delta E$ ) disappears at the final  $\Delta G$  level since  $\Delta G = \Delta E_{\text{GAS}} + \delta E_{\text{SOLV}} + \delta E_{\text{BSSE}} + \delta E_{\text{G}}$  (for the correction terms *vide supra*)

kJ/mol) and implies a molecular rearrangement to allow the bulky phosphine to be arranged in the axial position while the carbonyl ligand is shifted on the equatorial plane. The further protonation of **9b** leading to the formation of **10b**, unlike others reported in the literature,<sup>[3, 12]</sup> does not proceed downhill ( $\Delta G = 22.7$  kJ/mol). The H<sub>2</sub> ligand is weakly bonded to the metal centre (3.6 kJ/mol) thus the final dissociation of H<sub>2</sub> from **10b** to afford **2b** is possible and exhibits a small free energy barrier ( $\Delta G^\ddagger = 25.6$  kJ/mol). Whether the phosphine occupies the available vacant site, formation of intermediate **9a** is observed ( $\Delta G = -31.8$ ). The subsequent protonation to afford **10b** is more favoured compared to **9b** ( $\Delta G = 16.4$  kJ/mol) while the next dissociation of H<sub>2</sub> appears to be thermodynamically more demanding ( $\Delta G = 9.8$  kJ/mol and  $\Delta G^\ddagger = 35.3$  kJ/mol). Due to the lower energy of the intermediates bearing the mutually *trans* phosphines and the smaller activation barrier for the dissociation of H<sub>2</sub>, the partial path **9b** → **2b** appears more likely.

A competitive mechanism involving the dissociation of the carbonyl ligand rather than the phosphine ligand in the initiation step or from intermediate **3b** has been investigated. The resulting species, **11** or **12** respectively, once formed would then enter into the well defined pathway C\*. However, the CO dissociation from the starting species **1** or from intermediate **3b** was found to be extremely unfavourable thermodynamically ( $\Delta G = 145.6$  and  $129.6$  kJ/mol respectively).



**Scheme 4.2.1** Reaction *pathway A*: catalytic cycle and representation of the transition states (TS); partial paths *B* and *C* involving CO dissociation from catalyst **1** (*path B*) or intermediate **3b** (*path C*) and subsequent interpolation with pathway C-anionic of the corresponding paper.<sup>[1]</sup>



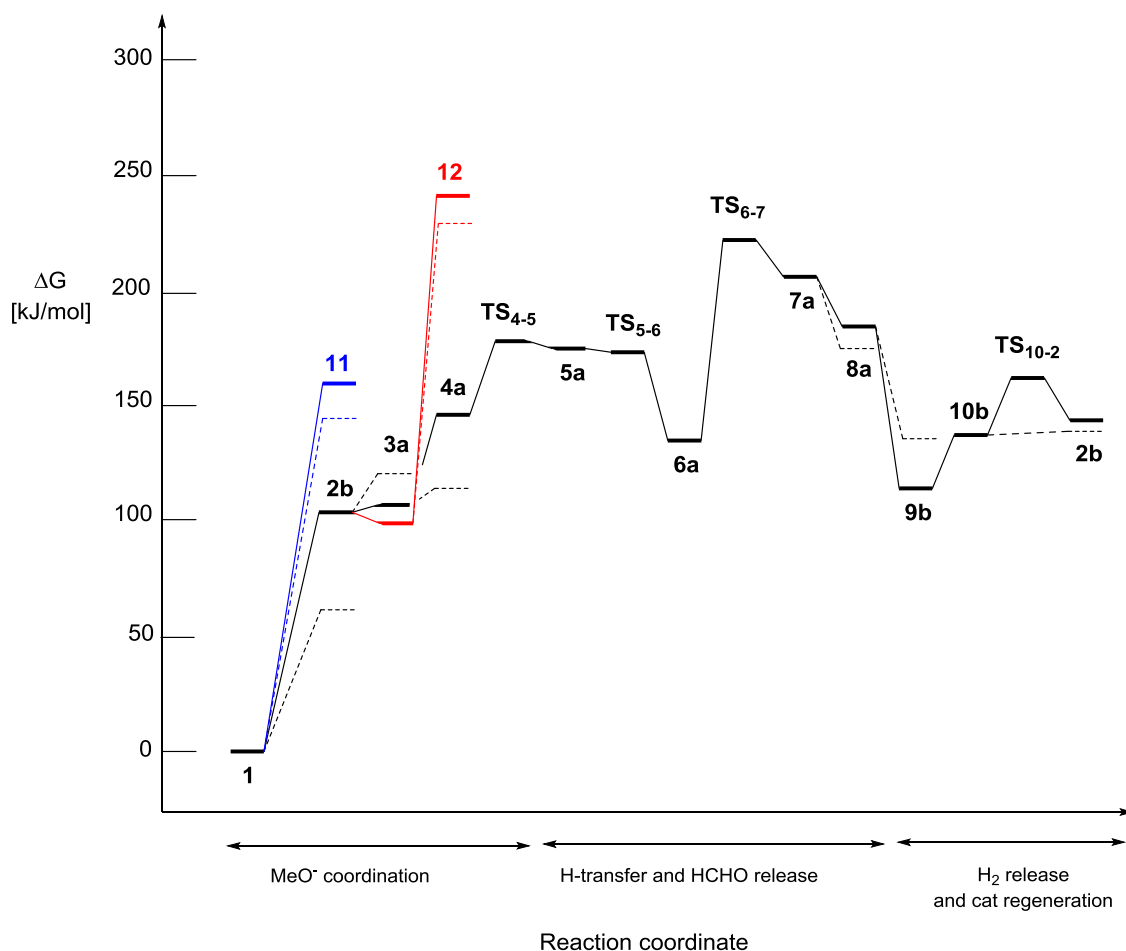
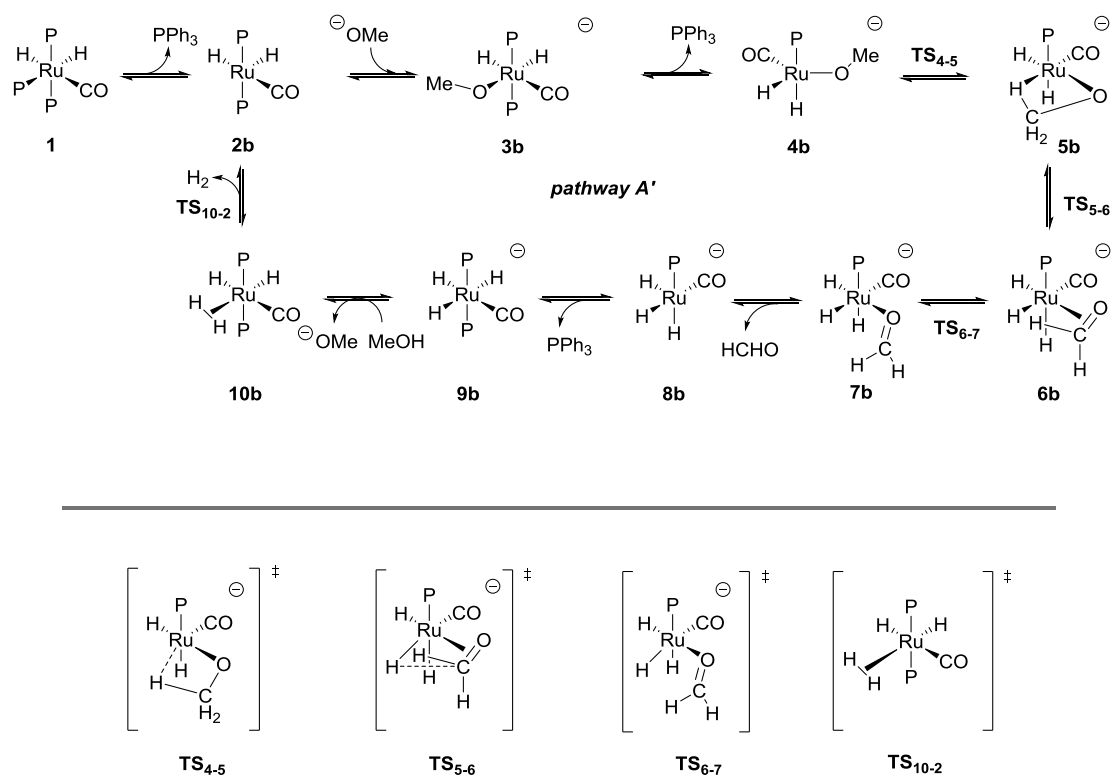


**Figure 4.2.1** Free Energy profile (kJ/mol) with calculations performed at the B97-D/ECP2 level of theory using MeOH as model solvent. The dashed lines refer to BSSE corrected energy. The black graph corresponds to the reaction pathway **A**, the blue graph to the partial path **B** (CO dissociation from **1**) and the red graph to the partial path **C** (CO dissociation from **3b**) (see Scheme 4.2.1 for more reaction pathways details).

An alternative pathway arising from intermediate **2b**, denoted **A'** (see Scheme 4.2.2), where one phosphine ligand and the carbonyl ligand remain mutually *cis* in all intermediates, has been investigated. The coordination of the methoxide to **2b** to afford the  $d^8$  complex **3b** is thermodynamically more favourable in comparison with pathway **A** ( $\Delta G = 16.6$  vs  $20.9$  kJ/mol). The subsequent dissociation of the phosphine ligand leading to intermediate **4b** easily occurs in this specific catalytic cycle ( $\Delta G = -7.4$  kJ/mol). As mentioned before, the resulting 5-coordinated species **5b** undergoes  $\beta$ -H abstraction. The formation of the first agostic intermediate **5b** appears thermodynamically more demanding compared to the corresponding step in pathway **A** ( $\Delta G = 37.0$  kJ/mol and  $\Delta G^\ddagger = 47.8$  kJ/mol) while the following breaking of the C-H bond to afford intermediate **6b** where the HCHO product results  $\pi$ -coordinated to the

metal is less favoured ( $\Delta G = 5.3$  kJ/mol and  $\Delta G^\ddagger = 18.1$  kJ/mol). Because of the higher barrier required in this path for the rotation of the methoxide ligand to gain full equatorial orientation, the decoordination of the formaldehyde product to generate **8b** is therefore considerably eased (overall  $\Delta G_{6b \rightarrow 8b} = -3.6$  kJ/mol). The formation of intermediate **7b** where the HCHO ligand is  $\eta^1$ -coordinated to the metal centre is always the rate-determining step ( $\Delta G = 23.7$  kJ/mol and  $\Delta G^\ddagger = 38.3$  kJ/mol). As reported for pathway **A**, the formation of **9b** is thermodynamically favourable ( $\Delta G = -28.8$  kJ/mol) with the rearrangement of the phosphine in the axial position and the hydride ligand on the equatorial plane. The next steps (from **9b** to **2b**) have been already discussed (*vide supra*).



**Scheme 4.2.2** Reaction pathway **A'**: catalytic cycle and representation of the transition states (TS).

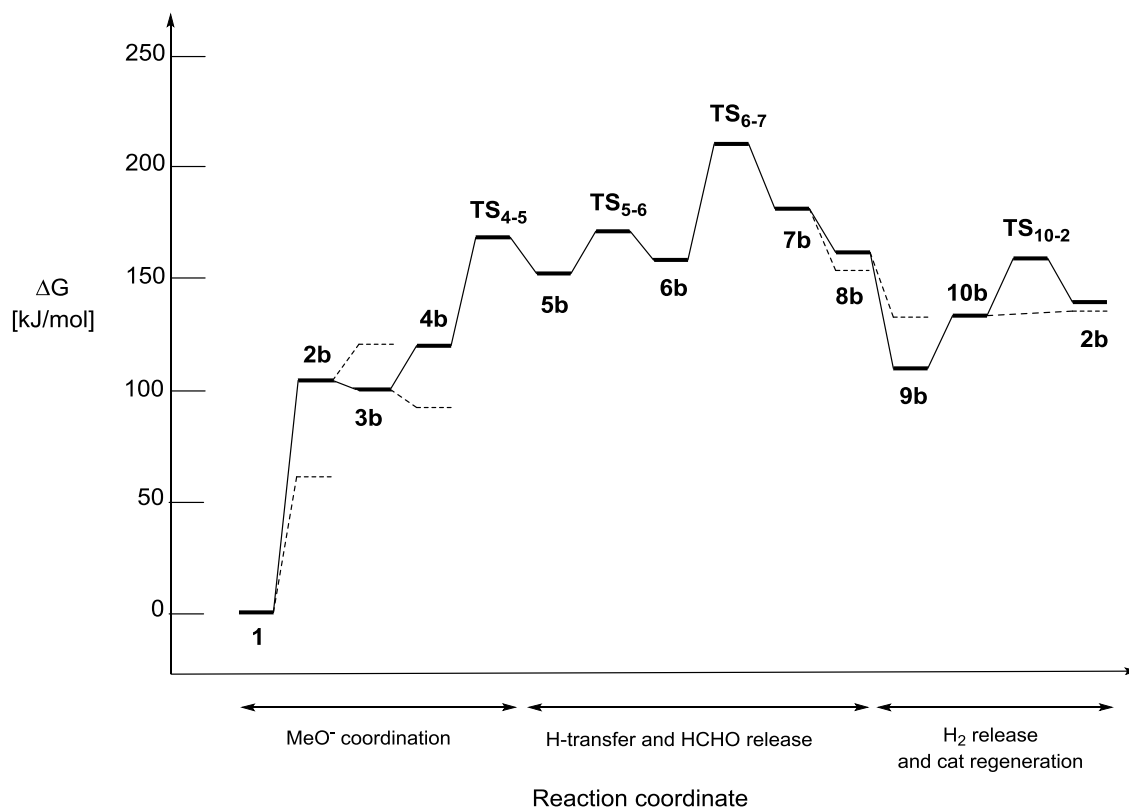


**Figure 4.2.2** Free Energy profile (kJ/mol) with calculations performed at the B97-D/ECP2 level of theory using MeOH as model solvent for pathway **A'**. The dashed lines refer to BSSE corrected energy.

step	$\Delta E_{\text{COSMO}}$	$\Delta E_{\text{GAS}}$	$\delta E_{\text{BSSE}}$	$\delta E_{\text{solv}}$	$\delta E_{\text{G}}$	$\Delta G_1$	$\Delta G_2$
<b>Pathway A</b>							
<b>1</b> $\rightarrow$ <b>2b</b> + PPh <sub>3</sub>	183.8	204.5	-42.6	-20.8	-79.1	104.6	62.0
<b>2b</b> + MeO <sup>-</sup> $\rightarrow$ <b>3a</b>	-56.9	-215.4	18.4	158.4	59.5	2.5	20.9
<b>3a</b> $\rightarrow$ <b>4a</b> + PPh <sub>3</sub>	105.9	156.4	-32	-50.5	-66.5	39.4	7.4
<b>4a</b> $\rightarrow$ <b>5a</b>	26.1	32.7	0.0	-6.6	3.0	29.2	29.2
<b>5a</b> $\rightarrow$ <b>6a</b>	-37.5	-39.4	0.0	1.9	-2.7	-40.2	-40.2
<b>6a</b> $\rightarrow$ <b>7a</b>	83.6	94.7	0.0	-11.1	-12.4	71.2	71.2
<b>7a</b> $\rightarrow$ <b>8a</b> + HCHO	35.3	60.7	-6.7	-25.3	-57.8	-22.4	-29.1
<b>8a</b> + PPh <sub>3</sub> $\rightarrow$ <b>9b</b>	-142.0	-196.7	22.6	54.7	72.2	-69.7	-47.1
<b>9b</b> + MeOH $\rightarrow$ <b>10b</b> + MeO <sup>-</sup>	33.5	148.6	0.0	-115.1	-10.8	22.7	22.7
<b>10b</b> $\rightarrow$ <b>2b</b> + H <sub>2</sub>	54.4	58.9	-3.2	-4.5	-47.6	6.8	3.6
<b>4a</b> $\rightarrow$ TS <sub>4-5</sub> ( <b>a</b> )	32.7	36.9	0.0	-4.2	-0.6	32.1	32.1
<b>5a</b> $\rightarrow$ TS <sub>5-6</sub> ( <b>a</b> )	6.8	4.6	0.0	2.2	-8.4	-1.6	-1.6
<b>6a</b> $\rightarrow$ TS <sub>6-7</sub> ( <b>a</b> )	101.3	114.4	0.0	-13.1	-13.7	87.6	87.6
<b>10b</b> $\rightarrow$ TS <sub>10-2</sub> ( <b>b</b> )	49.1	50.5	0.0	-1.3	-23.5	25.6	25.6
<hr/>							
<b>8a</b> + PPh <sub>3</sub> $\rightarrow$ <b>9a</b>	-134.0	-187.6	25.6	53.6	76.6	-57.4	-31.8
<b>9a</b> + MeOH $\rightarrow$ <b>10a</b> + MeO <sup>-</sup>	23.9	138.9	0.0	-115.0	-7.4	16.4	16.4
<b>10a</b> $\rightarrow$ <b>2a</b> + H <sub>2</sub>	61.4	65.7	-2.7	-4.3	-48.8	12.5	9.8
<b>10a</b> $\rightarrow$ TS <sub>10-2</sub> ( <b>a</b> )	57.9	57.7	0.0	0.2	-22.6	35.3	35.3
<b>Pathway A'</b>							
<b>2b</b> + MeO <sup>-</sup> $\rightarrow$ <b>3b</b>	-68.4	-208.3	20.6	139.9	64.4	-4.0	16.6
<b>3b</b> $\rightarrow$ <b>4b</b> + PPh <sub>3</sub>	87.6	117.9	-27.1	-30.3	-67.9	19.7	-7.4
<b>4b</b> $\rightarrow$ <b>5b</b>	36.5	49.3	0.0	-12.8	0.6	37.0	37.0
<b>5b</b> $\rightarrow$ <b>6b</b>	10.7	-1.0	0.0	11.8	-5.4	5.3	5.3
<b>6b</b> $\rightarrow$ <b>7b</b>	34.4	57.9	0.0	-23.5	-10.6	23.7	23.7
<b>7b</b> $\rightarrow$ <b>8b</b> + HCHO	32.3	45.4	-6.9	-13.1	-52.7	-20.4	-27.3
<b>8b</b> + PPh <sub>3</sub> $\rightarrow$ <b>9b</b>	-118.5	-168.3	22.6	49.7	67.1	-51.4	-28.8
<b>4b</b> $\rightarrow$ TS <sub>4-5</sub> ( <b>b</b> )	52.9	62.4	0.0	-9.4	-5.2	47.8	47.8
<b>5b</b> $\rightarrow$ TS <sub>5-6</sub> ( <b>b</b> )	23.6	15.4	0.0	8.1	-5.5	18.1	18.1
<b>6b</b> $\rightarrow$ TS <sub>6-7</sub> ( <b>b</b> )	47.0	70.7	0.0	-23.7	-8.7	38.3	38.3
<b>Pathway B</b>							
<b>1</b> $\rightarrow$ <b>11</b> + CO	218.5	211.6	-14.6	6.8	-58.3	160.2	145.6
<b>Pathway C</b>							
<b>3b</b> $\rightarrow$ <b>12</b> + CO	201.2	194.3	-11	6.9	-60.6	140.6	129.6

**Table 4.2.1** Reaction Energies in the continuum ( $\Delta E_{\text{COSMO}}$ )<sup>a</sup> and in the gas phase ( $\Delta E_{\text{GAS}}$ )<sup>a</sup>; Correction Terms for BSSE ( $\delta E_{\text{BSSE}}$ )<sup>a</sup>, Solvation ( $\delta E_{\text{solv}}$ )<sup>a,c</sup> and Thermochemistry ( $\delta E_{\text{G}}$ )<sup>b</sup>; Final Free Energies ( $\Delta G$ ) in kJ/mol.  $\delta E_{\text{solv}} = (\Delta E_{\text{COSMO}} - \Delta E_{\text{GAS}})$ ;  $\Delta G_1 = (\Delta E_{\text{COSMO}} + \delta E_{\text{G}})$ ;  $\Delta G_2 = (\Delta E_{\text{COSMO}} + \delta E_{\text{G}} + \delta E_{\text{BSSE}})$ .

<sup>a</sup> B97-ECP2 energies; <sup>b</sup> RI-BP86/ECP1 energies; <sup>c</sup> model solvent MeOH.

Consistently with the previous dehydrogenation<sup>[1]</sup> and decarbonylation<sup>[6]</sup> work, in order to compare the kinetics of the investigated pathways (**A**, **B** and **C**), the initiation steps and overall activation barriers have been recomputed on the ECP3 level of theory. The BSSE corrections (noted  $\delta E'_{\text{BSSE}}$ ) were recalculated using a more accurate approach in regard of the coordination/decoordination of more than one ligand during the overall reaction.  $\Delta E_{\text{GAS}}^{\text{ECP3}}$ ,  $\delta E_{\text{solv}}^{\text{ECP3}}$  and  $\delta E'_{\text{BSSE}}^{\text{ECP3}}$  are reported in Table 4.2.2.

The proposed dehydrogenation of MeOH catalysed by complex **1** appears entropically favoured at high temperatures (negative  $\delta E_{\text{G}}$ ) but whereas pathway **A** is more demanding kinetically and thermodynamically when compared to the dehydrogenation pathway **C\*** proposed for catalyst **13**, opposite is the case of pathway **A'**. The computed overall activation energy at the B97-D/ECP3 level of theory for pathway **A** was found to be 141 kJ/mol (see Table 4.2.2) against the 131.0 kJ/mol for the analogous path **C\*** (value reported in the corresponding papers)<sup>[1, 6]</sup> and the 120.6 kJ/mol for pathway **A'** (see Table 4.2.2), showing therefore the existence of three competitive pathways. Different is the case of the proposed pathways **B** and **C** involving the dissociation of the CO ligand either in the initiation step (from species **1**, path **B**) or from intermediate **3b** (path **C**). Both reactions in fact still appear entropically favoured at high temperatures (negative  $\delta E_{\text{G}}$ ) but the high overall free energy barrier ( $\Delta G = 248.6$  kJ/mol) suggest that we are in the presence of two unfeasible channels failing therefore in the attempt to link the active species **1** with pathway **C\*** under our reaction conditions.

		$\Delta E_{\text{COSMO}}$	$\Delta E_{\text{GAS}}$	$\delta E'_{\text{BSSE}}$	$\delta E_{\text{solv}}$	$\delta E_{\text{G}}$	$\Delta G$
<b>Initiation Free Energies</b>							
<b>A/A'; C</b>	<b>1</b> → <b>2b</b> + PPh <sub>3</sub>	164.6	185.8	-33.1	-21.2	-79.1	52.3
<b>B</b>	<b>1</b> → <b>11</b> + CO	197.9	194.7	-12.3	3.2	-58.3	127.3
<b>Overall Free Energy Barriers</b>							
<b>A</b>	<b>1</b> + MeO <sup>-</sup> → <b>TS<sub>6-7</sub> (a)</b> + 2 PPh <sub>3</sub>	279.6	205.7	-39.2	73.9	-99.5	141
<b>A'</b>	<b>1</b> + MeO <sup>-</sup> → <b>TS<sub>6-7</sub> (b)</b> + 2 PPh <sub>3</sub>	256.5	187.1	-39.6	69.3	-96.2	120.6
<b>B ; C</b>	<b>1</b> + MeO <sup>-</sup> → <b>TS<sub>13-14</sub></b> <sup>a</sup> + PPh <sub>3</sub> + CO	367.0	243.3	-31.9	123.7	-86.5	248.6

**Table 4.2.2** Refined Free Energies (in kJ/mol at the B97-D/ECP3 level) for initiation steps and overall activation barriers of pathways A-C.

<sup>a</sup>The numbering code for the TS refers to the corresponding papers in which it was reported<sup>[1, 6]</sup>; the  $E_{\text{GAS}}^{\text{ECP3}}$ ,  $\delta E_{\text{solv}}^{\text{ECP3}}$ , and  $\delta E_{\text{G}}^{\text{ECP2}}$  values for the **TS<sub>13-14</sub>** were provided by Dr. Sieffert while the  $E_{\text{intra-BSSE}}^{\text{ECP3}}$  could be found in the corresponding ESI.<sup>[1]</sup>

The illustrated pathway **A** and **A'** (see Schemes 4.2.1 and 4.2.2 respectively) would now be revisited from a structural point of view in order to visualise structural rearrangements of the ligands along the dehydrogenation process.

The decoordination of the equatorial PPh<sub>3</sub> from complex **1** significantly effects the P<sub>ax2</sub>-Ru1-P<sub>ax3</sub> angle as a consequence of the loss of such a bulky ligand (from 144.2° in complex **1** to 161.7° in complex **2b**) and the resulting 5-coordinated species **2b** adopts an octahedral geometry with a vacant site (consistently with the optimised geometries reported in pathway C\*)<sup>[1]</sup>. In pathway **A**, the subsequent coordination step of MeO<sup>-</sup> to provide intermediate **3a** implies a potential rearrangement in the coordination sphere of the metal centre. The carbonyl ligand in fact occupies the axial position while one of the phosphine ligands drifts into the equatorial position in order to benefit from the trans effect of the hydride ligand. The O and H atoms of the methoxide ligand bend out of the equatorial plane, due to the high coordination number of the current intermediate **3a**, with the C-O bond of the MeO<sup>-</sup> assuming an almost parallel orientation to the carbonyl ligand (forming a 19.4° C<sub>methoxide</sub>-O<sub>methoxide</sub>-Ru-C<sub>carbonyl</sub> dihedral angle). After decoordination of the equatorial PPh<sub>3</sub> the resulting intermediate **4a** adopts a trigonal-bipyramidal geometry, with the methyl group pointing away from the metal centre and assuming again a parallel orientation to the carbonyl ligand (forming a -0.1° C<sub>methoxide</sub>-O<sub>methoxide</sub>-Ru-C<sub>carbonyl</sub> dihedral angle with P, Ru, O<sub>methoxide</sub> and C<sub>methoxide</sub> atoms lying in the same plane). Similarly, the same geometry was found to lower significantly the energy of intermediate **12**, if the reaction proceeds via CO dissociation (path **C**). The next H-transfer step requires the rotation of the methoxide ligand to gain full equatorial orientation in intermediate **5a**, a process that increases the potential energy of the complex. The full process takes place through the **TS<sub>4,5</sub> (a)** where the O, C and the closest H atoms of the methoxide form a planar 4-membered ring with Ru. During the formation of this transition state the Ru-H distance appears significantly reduced (2.59 vs 3.14 Å of complex **4a**) while the Ru-O distance is slightly elongated (2.17 vs 2.06 Å of complex **4a**). In the intermediate **5a**, as mentioned in the energy discussion, we observe the formation of an agostic interaction between the H of the methoxide and Ru with a shorter Ru-H distance (1.9 Å) and therefore an elongated C-H distance by 0.09 Å. The reaction proceeds with the H-transfer via the **TS<sub>5,6</sub> (a)** as confirmed by the shortening of the Ru-H distance (1.72 Å) and the lengthening of the C-H distance (1.5 Å). The formation of the carbonyl bond in **TS<sub>5,6</sub> (a)** concludes with the formation of the HCHO product in the intermediate **6a** which remains π-coordinated to the metal centre. The newly formed C=O bond is, however, longer than the typical value observed in free formaldehyde

(1.34 vs 1.22 Å)<sup>†[13]</sup>. The dissociation of the HCHO ligand is defined by the increase in the Ru-C distance (from 2.16 Å in complex **6a**, to 3.15 Å in **7a**) and the slippage of the coordinated formaldehyde from a side-on orientation relative to Ru to a parallel end-on orientation relative to the carbonyl ligand. Similarly to intermediate **4a**, the P, Ru, O and C atoms of the HCHO lay on the same plane with a 3.19° C<sub>formyl</sub>-O<sub>formyl</sub>-Ru-C<sub>carbonyl</sub> dihedral angle. The C=O distance (1.25 Å) in both **TS<sub>6-7</sub>(a)** and **7a** is comparable with the one calculated for the free formaldehyde, as a consequence of the slippage from η<sup>2</sup>→η<sup>1</sup> coordination. With regard to the final geometry of complex **8a** after dissociation of HCHO, the same geometry of the 5-coordinated d<sup>6</sup> complex **2b** was observed. The incoming PPh<sub>3</sub> can be accommodated in the vacant octahedral site and afford the most stable intermediate **9b** through a ligand rearrangement (the bulky phosphines are mutually *trans*). The latter species can be protonated leading to the formation of H<sub>2</sub> which remains associated to the metal centre as a coordinated dihydrogen molecule (complex **10b**). The H<sub>2</sub> product is weakly bonded to Ru, therefore it can be released in the catalytic system at high temperature through **TS<sub>10-2</sub>(b)** in which H<sub>2</sub> is already fully decoordinated (Ru-H<sub>H<sub>2</sub></sub> distance is ca 3.5 Å against 1.8 Å in complex **10b**). All atomic distances of intermediates and TSs are in good agreement with those reported for pathway C\*.<sup>[1]</sup>

Concerning pathway **A'**, we will report the different angles and atoms distances that take place during the reaction mechanism. The methyl group of the methoxide ligand of intermediate **3b** bends out of the equatorial plane pointing in the opposite direction of the carbonyl ligand. After decooordination of another phosphine ligand intermediate **4b** adopts a trigonal-bipyramidal geometry forming a -7.6° H<sub>hydride-ax</sub>-Ru-O<sub>methoxide</sub>-C<sub>methoxide</sub> dihedral angle. Formation of intermediate **5b** always occurs through a significant shortening of the Ru-H<sub>methoxide</sub> distance (2.44 vs 3.6 Å of complex **4b**) and slight elongation of Ru-O<sub>methoxide</sub> distance (2.16 vs 2.04 Å of complex **4b**) observed in the corresponding **TS<sub>4-5</sub>(b)**. In intermediate **5b**, when the formation of a 4-membered ring on the equatorial place reached completion, the Ru-H distance appears further reduced (1.88 Å) while the Ru-O distance further increased (2.23 Å). In good accordance with the data reported above (path **A**), the C=O distance in the π-coordinated formaldehyde product shown in complex **6b** is of the order of 1.3 Å. The subsequent dissociation of the HCHO ligand is defined by the increase in the Ru-C distance (from 2.2 Å in complex **6b**, to 3.13 Å in **7b**) and the slippage of the coordinated formaldehyde from a side-on orientation relative to Ru to an almost parallel end-on orientation relative to the carbonyl

<sup>†</sup> The C-O distance in the free formaldehyde is of the order of 1.2 Å (experimental value, see reference associated) and 1.22 Å (computed value).

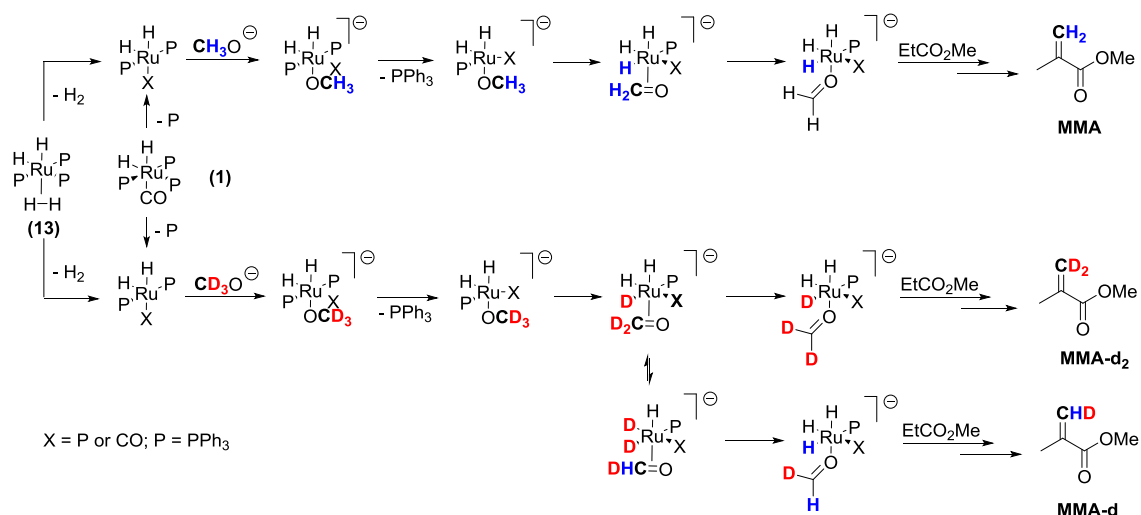
ligand with a  $-11.4^\circ$   $C_{\text{formyl}}-O_{\text{formyl}}-\text{Ru}-C_{\text{carbonyl}}$  dihedral angle. The C=O distance in **TS<sub>6,7</sub> (a)** and **7a** is 1.3 and 1.24 Å respectively, successfully comparable with the free formaldehyde (*vide supra*). Complex **8b** displays the same geometry of the 5-coordinated  $d^6$  complex **2b**. The incoming  $\text{PPh}_3$  can be accommodated in the vacant octahedral site to afford intermediate **9b** through a molecular rearrangement in the coordination sphere of the metal, in fact by shifting the small hydride ligand on the equatorial plane it occupies the position mutually *trans* to the other phosphine ligand.

In the investigated dehydrogenation mechanisms **A** and **A'** catalysed by complex **1**, the highest transition state involves the partial decooordination of the HCHO product (**TS<sub>6,7</sub>**) for which a small  $^1\text{H}/^2\text{H}$  kinetic isotope effect (KIE) was predicted (pathway **A**), respectively 1.6 obtained from free energies and 1.9 from enthalpies. (values displayed in Table 4.2.3).

The corresponding experimental  $^1\text{H}/^2\text{H}$  KIE could be estimated by following the destiny of the formaldehyde product, bearing in mind the one-pot catalytic system we have proposed in chapter 3. The formaldehyde obtained as a product of methanol dehydrogenation can undergo condensation with the  $\alpha$ -deprotonated ester to afford MMA. A similar scenario should be observed when starting from complex **13**, since we have shown that both species, **1** and **13**, act as catalyst precursors generating *in situ* the active 5-coordinated species **2b** or **14** respectively, subsequently involved in the mechanism previously investigated (see Scheme 4.2.1).

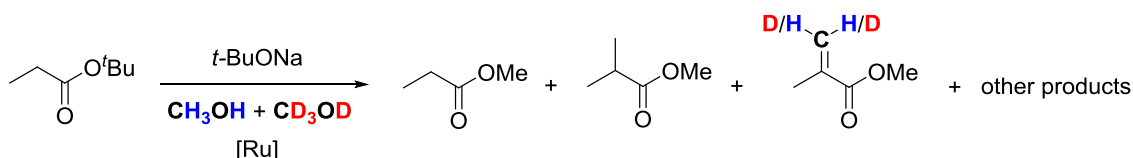
When the reaction is performed using equal amounts of  $\text{CH}_3\text{OH}$  and  $\text{CD}_3\text{OD}$ , we should observe the formation of non-deuterated and bis-deuterated formaldehyde. The latter compound, in turn, can undergo intramolecular H/D exchange to generate the mono-deuterated derivative. The three isotopomers,  $\text{CH}_2\text{O}$ ,  $\text{CHDO}$  and  $\text{CD}_2\text{O}$ , once involved in the subsequent condensation step will afford the non-, mono- and bis-deuterated MMA (MMA, MMA-d and MMA- $d_2$ ). The ratio of  $[\text{MMA} : (\text{MMA-d} + \text{MMA-}d_2)]$  could be directly related to the  $^1\text{H}/^2\text{H}$  KIE.





**Scheme 4.2.3** Overview of the reaction intermediates involved in the formation of MMA, MMA-d and MMA-d<sub>2</sub> when starting from catalyst **1** or **13**.

To determine the deuterium isotope effect the reaction was carried out using *t*-BuP as substrate and *t*-BuONa as base (so that the only source of methanol/methoxide was the added methanol) and equal amounts of CH<sub>3</sub>OH and CD<sub>3</sub>OD (see Scheme 4.2.4 for detailed reaction conditions) and the crude product analysed via GC-MS spectroscopy.



**Scheme 4.2.4** General reaction conditions for the one-pot system depicted above: cat. **1** (0.124 g, 0.135 mmol), *t*-BuP (15.64 mL, 103.9 mmol), *t*-BuONa (2.6 g, 27.0 mmol), toluene (10 mL), methanol (3.8 mL, 93.5 mmol), methanol-d<sub>4</sub> (3.8 mL, 93.5 mmol), 2,4-dimethyl-6-tert-butylphenol (Topanol A, 0.01 mL). Hastelloy™ autoclave; 170 °C under an atmosphere of ethene (6 bar) for 3 h.

The analysis of the [M-OMe]<sup>+</sup> fragment of MMA (peaks at 69, 70 and 71 m/z respectively depicted in Figure 4.2.3), showed that the methylene group contained 0 (56.3 %), 1 (23.0 %) or 2 (20.7 %) deuterium atoms. By assuming that the contribute of the non-deuterated species to the peak at 70 m/z is negligible, these percentages could be used to determine the ratio of [MMA : (MMA-d + MMA-d<sub>2</sub>)] that directly equates to a kinetic isotope effect ( $k_H/k_D$ ) of 1.3 for the dehydrogenation pathway under study, in a good agreement with the values computed

from free energies, 1.6 for pathway A and 1.87 for pathway C\*<sup>[6]</sup> (see Table 4.2.3). Very small H/D KIEs like our experimental value, typically arises from isotopic substitution at a bond that does not undergo cleavage during the rate-determining step (secondary kinetic isotope effect),<sup>[14]</sup> in good accordance with our results where the highest barrier corresponds to the partial decoordination of the formaldehyde product, while much larger values on the order of 6 or more denote the breaking or formation of C-H bonds in the rate-determining step.

	Rate-determining step	Computed <sup>a</sup> <sup>1</sup> H/ <sup>2</sup> H KIE	Experimental <sup>1</sup> H/ <sup>2</sup> H KIE
<b>A</b>	$\eta^2 \rightarrow \eta^1$ slippage of HCHO <b>1</b> + MeO <sup>-</sup> → TS <sub>6-7</sub> ( <b>a</b> ) + 2 PPh <sub>3</sub>	1.6 (1.9)	1.3
<b>C*<sup>[6]</sup></b>	$\eta^2 \rightarrow \eta^1$ slippage of HCHO <b>13</b> + MeO <sup>-</sup> → TS <sub>13-14</sub> <sup>b</sup> + H <sub>2</sub> + PPh <sub>3</sub>	1.87 (4.39)	-

**Table 4.2.3** <sup>1</sup>H/<sup>2</sup>H KIEs determined computationally and experimentally; <sup>a</sup>KIE computed at the RI-BP86/ECP1 level of theory at T = 423 K and p = 1354 atm by substituting all hydrogens, except phenyl hydrogens, with deuterium. Values computed from free energies (values computed from enthalpies are in parenthesis).

<sup>b</sup> The numbering code for the TS refers to the corresponding papers in which it was reported<sup>[1, 6]</sup>

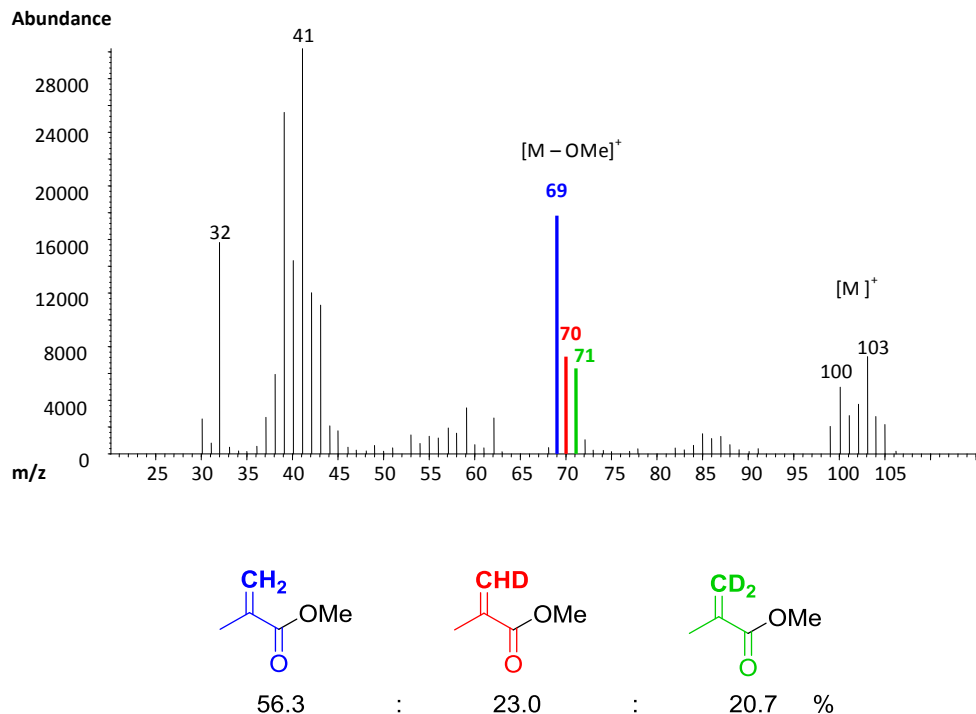


**Figure 4.2.3** Fragmentation pattern of MMA highlighting the fragment [M-OMe]<sup>+</sup>. The peaks at 69, 70 and 71 m/z correspond to the non-, mono- and bis-deuterated MMA in the ratio of 56.7 : 23.3 : 20 % respectively.

### 4.3 Conclusions and Future Work

The present work was focused on the understanding of the mechanism involved in the methanol dehydrogenation catalysed by  $[\text{RuH}_2(\text{CO})(\text{PPh}_3)_3]$ , an attractive reaction largely studied in our laboratories to afford anhydrous formaldehyde which was in turn employed as a one-carbon alkylating agent for the production of MMA. A density functional study (DFT) was undertaken following a protocol recently developed by Sieffert and Bühl and successfully used to elucidate similar alcohol dehydrogenation and decarbonylation reactions catalysed by  $[\text{RuH}_2(\text{H}_2)(\text{PPh}_3)_3]$ . Two plausible reaction channels were designed by retracing one specific pathway of the cited dehydrogenation study and by substituting a phosphine ligand with a carbonyl. Similarly, the rate-determining step was found to be the partial decoordination of the formaldehyde product, in particular the slippage of HCHO from  $\eta^2$  to  $\eta^1$ -coordination to Ru. In order to gain more information about the nature of the transition state involved in the rate-determining step, the  $^1\text{H}/^2\text{H}$  kinetic isotope effect was determined experimentally and computationally. The experimental value of 1.3 was in good agreement with the computed 1.6, confirming that the C-H bond under study does not undergo cleavage in the rate-determining step. The overall reaction, however, exhibited a relatively high activation barrier thus is possible only at high temperature. Potential alternative initiations for the methanol dehydrogenation that would interconnect with the main reaction at a later stage, have been evaluated. The plausible dissociation of the carbonyl ligand rather than a direct loss of  $\text{PPh}_3$  has been already investigated resulting in a thermodynamically very demanding process. The loss of  $\text{H}_2$  from catalyst  $[\text{RuH}_2(\text{CO})(\text{PPh}_3)_3]$  is also a very well known photocatalytic reaction.<sup>[15]</sup> Bearing in mind that a base is required in these catalytic systems, an initiation step involving the nucleophilic attack of the added  $\text{OH}^-$  onto the coordinated CO to produce  $\text{CO}_2$  would be therefore computed. The latter option is rationalised by evidences of  $\text{CO}_2$  and  $\text{CH}_4$  production from ethanol along with  $\text{H}_2$ , reported by Morton and Cole-Hamilton in their pioneering work on alcohol dehydrogenation catalysed by ruthenium precursors.<sup>[5]</sup>

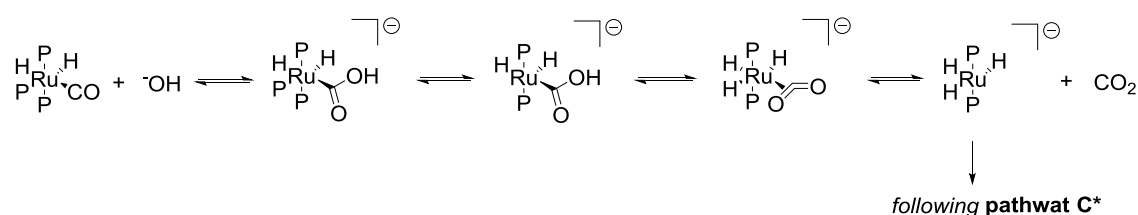


**Figure 4.3.1** Plausible alternative initiation process for the dehydrogenation reaction when using  $\text{OH}^-$  as a base, leading to the production of  $\text{CO}_2$  and the  $[\text{RuH}_3(\text{PPh}_3)_2]^-$  intermediate

## 4.4 Experimental Section

### 4.4.1 General material, methods and instruments

All manipulations and reactions were carried out under N<sub>2</sub> gas (dried through a Cr(II)/silica packed glass column) using different techniques including a standard Schlenk, vacuum line and a glove box. Solvents were dried and degassed prior to use.

[RuH<sub>2</sub>(CO)(PPh<sub>3</sub>)<sub>3</sub>](**1**), *t*-OBuNa, methanol, methanol-d<sub>4</sub> and *tert*-butyl propanoate were purchased from Sigma-Aldrich.

*tert*-Butyl propanoate was dried over Na<sub>2</sub>SO<sub>4</sub> and distilled under dinitrogen. Na<sub>2</sub>CO<sub>3</sub> (anhydrous) was purchased from Fisher Scientific.

Toluene was dried using a Braun Solvent Purification System. Methanol was dried and degassed by distillation from magnesium under dinitrogen. All gases were purchased from BOC gases.

GC-MS analyses were performed using a Hewlett Packard 6890 series GC system equipped with an Agilent J&W HP-1 column capillary (30.0 m x 248 μm x 0.25 μm nominal). Method: flow rate 0.8 mL min<sup>-1</sup> (He carrier gas), split ratio 100:1, starting temperature 50 °C (4 min) ramp rate 20 °C min<sup>-1</sup> to 130 °C (2 min), ramp rate 20 °C min<sup>-1</sup> to 280 °C (15.50 min). Qualitative analyses were performed using an HP5973 mass selective detector (GC-MS).

### 4.4.2 Experiment using equal amounts of CH<sub>3</sub>OH and CD<sub>3</sub>OD for determining the <sup>1</sup>H/<sup>2</sup>H KIE

A Hastelloy™ autoclave was fitted with a magnetic stirrer and charged under a dinitrogen atmosphere with catalyst **1** (0.124 g, 0.135 mmol) and *t*-BuONa (2.6 g, 27.0 mmol). Toluene (10 mL) and *t*-BuP (15.64 mL, 103.9 mmol) were added through the injection port together with methanol (3.8 mL, 93.5 mmol), methanol-d<sub>4</sub> (3.8 mL, 93.5 mmol) and 2,4-dimethyl-6-*tert*-butylphenol (Topanol A, 0.01 mL, in order to prevent MMA polymerisation). The autoclave was sealed, pressurised with ethene (6 bar) and heated to 170 °C for 3 hours. The autoclave was then cooled to room temperature, vented to the atmosphere and the obtained product mixture analysed by GC-MS spectroscopy.

MMA	Isotopic mass		
<b>[M -OMe]<sup>+</sup></b>	<b>69</b>	<b>70</b>	<b>71</b>
<b>Assignment</b>	d <sub>0</sub> 56.3 %	d <sub>1</sub> 23.0 %	d <sub>2</sub> 20.7 %

**Table 4.4.2.1** Intensities of isotopomers of the [M-OMe]<sup>+</sup> signal in the mass spectra of MMA when using equal amounts of CH<sub>3</sub>OH and CD<sub>3</sub>OD or for the methylenation of *t*-BuP catalysed by [RuH<sub>2</sub>(CO)(PPh<sub>3</sub>)<sub>3</sub>] in the presence of *t*-BuONa.

#### 4.4.3 Computational details

We followed a protocol<sup>[8]</sup> recently developed by Sieffert and Bühl:

##### 4.4.3.1 Geometry optimisation and thermodynamic corrections

The same methods and basis sets as in the previous computational studies were employed and quoted in this section from references [1] and [6]:

“Geometry optimizations of complexes 1-12 and thermodynamic corrections were obtained at the RI-BP86/ECP1 level of theory by employing the exchange and correlation functional of Becke<sup>[16]</sup> and Perdew<sup>[17]</sup>, respectively, in conjunction with the SDD basis on Ru, which involves the small-core Stuttgart-Dresden relativistic effective core potential (ECP) together with its valence basis set,<sup>[18]</sup> the standard 6-31G(d,p) basis set for all other elements, except for the C and H atoms of the phenyl rings where the smaller 3-21G basis set was used and suitable auxiliary basis sets for the fitting of the Coulomb potential. Harmonic frequencies were computed analytically and used without scaling to obtain enthalpic and entropic corrections at the experimentally used temperature of 150 °C.<sup>[3]</sup> The corresponding correction terms ( $\delta E_G$ ) were estimated at the RI-BP86/ECP1 level of theory and were obtained as the difference in the energy of a given step ( $\Delta E_{\text{RI-BP86/ECP1}}$ ) and the corresponding free energy ( $\Delta G_{\text{RI-BP86/ECP1}}$ ).

$$\delta E_G = \Delta G_{\text{RI-BP86/ECP1}} - \Delta E_{\text{RI-BP86/ECP1}}$$

The entropic contributions were evaluated at a pressure of 1354 atm to model the changes in entropy for a condensed phase.<sup>[19]</sup> The corresponding correction terms ( $\delta E_G$ ) for each step of the catalytic cycle are gathered in Table 4.2.1 along with other correction terms (see below).

The transition states (denoted **TS<sub>x-y</sub>**) were characterized by a single imaginary frequency and a simple visual analysis of the corresponding vibrational mode was used in this work to ensure that the two desired **x** and **y** minima were connected.”

IRC<sup>[20]</sup> (intrinsic reaction coordinate) calculations would be performed to follow the path from the TS<sub>x-y</sub> in both x and y directions in order to be consistent with the previous studies.

The optimized geometries of the complexes reported in the anionic pathway C\* of the reference paper<sup>[1]</sup> were used to derive the initial structures of complexes **1** and **4-10**. In particular, the starting catalyst **1** was obtained by adding a carbonyl ligand to the previously studied intermediate [RuH<sub>2</sub>(PPh<sub>3</sub>)<sub>3</sub>] (**14**) while intermediates **4-10** were drawn from the analogous complexes by substituting a PPh<sub>3</sub> ligand with CO. Complexes **2** and **3** were constructed by hand starting from the optimised structure of the previous step. Among the potential isomers, only two selected isomers have been investigated for each complex, respectively one species bearing mutually *trans* PPh<sub>3</sub> and CO ligands and one mutually *cis* (GAS and COSMO Energies in kJ/mol for the selected isomers are reported in Table 4.4.4.1).

*BP86/ECP1 coordinates in Å (xyz format) of optimised complexes including total SCF Energy in a.u. are reported in Appendix 1.*

#### 4.4.3.2 Energies

“Single-point calculations were performed on the RI-BP86/ECP1 geometries using 6-31G(d,p) basis on the C and H of the phenyl rings, a larger basis set on all other elements, 6-311+G(d,p) (noted ECP2) and always SDD ECP on Ru<sup>[18]</sup>. Refined energies were therefore obtained from this ECP2 level where the B97-D functional was used (B97-D/ECP2)<sup>[21]</sup> where the suffix D denotes an empirical dispersion correction required for the bulky systems.<sup>[8-9]</sup>

Counterpoise<sup>[10]</sup> and COSMO<sup>[11a]</sup> corrections were also calculated at this level. The counterpoise method was used to gain corrected energies for the basis set superposition error (BSSE) (correction terms for BSSE energies, denoted  $\delta E_{\text{BSSE}}$ , are reported in Table 4.2.1) while estimation of solvation effects was calculated using the conductor-like screening model (COSMO) including a dielectric constant  $\epsilon = 32.63$  to simulate the employment of methanol as solvent in experimental reactions. The solvation effect noted as  $\delta E_{\text{solv}}$  was defined as the difference between the reaction energy in the continuum ( $\Delta E_{\text{COSMO}}$ ) and the one in the gas phase ( $\Delta E_{\text{GAS}}$ ). The final  $\Delta G$  is calculated as the sum of all correction terms added to the gas-phase reaction energies.

$$\Delta G = \Delta E_{\text{GAS}} + \delta E_{\text{solv}} + \delta E_{\text{BSSE}} + \delta E_{\text{G}} \quad \text{or simply} \quad \Delta G = \Delta E_{\text{COSMO}} + \delta E_{\text{BSSE}} + \delta E_{\text{G}}$$

$\Delta E_{\text{GAS}}$ ,  $\delta E_{\text{solv}}$  and  $\delta E_{\text{BSSE}}$  were computed at the B97-D/ECP2 level of theory while  $\delta E_{\text{G}}$  at the RI-BP86/ECP1 level.

The  $^1\text{H}/^2\text{H}$  kinetic isotope effects (KIE) were computed at the RI-BP86/ECP1 level of theory at  $T = 423 \text{ K}$  and  $p = 1354 \text{ atm}$  by substituting all hydrogens, except phenyl hydrogens, by deuterium.

In order to compare the kinetics of the investigated pathway with the previously reported paths,<sup>[1, 6]</sup> the initiation steps and overall activation barriers have been recomputed using a larger basis set, denoted ECP3, where all P, O, C and H atoms are described by the 6-311+G(d,p) basis set and the same SDD ECP on Ru and the same B97-D functional (gas phase and continuum).

The BSSE correction was recalculated using a more accurate approach due to the coordination/decoordination of more than one ligand during the overall reaction, by considering the difference in the intramolecular BSSE between the intermediates and TS.

All RI-BP86/ECP1 calculations were performed with the Gaussian 03 software,<sup>[22]</sup> while B97-D/ECP2 and B97-D/ECP3 (gas phase and COSMO) calculations were performed using the Turbomole package.<sup>‡[23]</sup>

Additional details can be found in the reference published works.<sup>[1, 6]</sup>

#### 4.4.4 Tables

##### 4.4.4.1 GAS and COSMO Energies for selected isomers

---

‡ TURBOMOLE is a quantum chemical program package initially developed at the University Karlsruhe and at the Forschungszentrum Karlsruhe; in 2007, the TURBOMOLE GmbH (Ltd) was founded and is available from <http://www.turbomole.com>

<b>2</b>	<b>a</b>	<b>b</b>	<b>TS<sub>6-7</sub></b>	<b>a</b>	<b>b</b>
	6.2 (5.3)	0.0 (0.0)		20.1 (25.5)	0.0
<b>3</b>	<b>a</b>	<b>b</b>	<b>7</b>	<b>a</b>	<b>b</b>
	0.0 (0.0)	7.0 (-11.4)		13.2 (20.4)	0.0 (0.0)
<b>4</b>	<b>a</b>	<b>b</b>	<b>8</b>	<b>a</b>	<b>b</b>
	31.4 (29.7)	0.0 (0.0)		28.5 (23.5)	0.0 (0.0)
<b>TS<sub>4-5</sub></b>	<b>a</b>	<b>b</b>	<b>9</b>	<b>a</b>	<b>b</b>
	5.9 (9.5)	0.0		9.1 (7.9)	0.0 (0.0)
<b>5</b>	<b>a</b>	<b>b</b>	<b>10</b>	<b>a</b>	<b>b</b>
	14.8 (19.4)	0.0 (0.0)		0.0 (0.0)	0.6 (1.6)
<b>TS<sub>5-6</sub></b>	<b>a</b>	<b>b</b>	<b>TS<sub>10-2</sub></b>	<b>a</b>	<b>b</b>
	3.9 (2.6)	0.0 (0.0)		6.6 (7.1)	0.0 (0.0)
<b>6</b>	<b>a</b>	<b>b</b>			
	0.0 (0.0)	23.6 (28.8)			

**Table 4.4.4.1.1** Relative GAS phase Energies (and COSMO Energies in parenthesis) in kJ/mol (B97-D/ECP2) with that of the lowest stereoisomer set to 0.0 in each case.



#### 4.4.4.2 BSSE corrections at the B97-D/ECP3 level of theory

The intermolecular BSSE for a given step ( $\delta E'_{\text{BSSE}}$ ) is calculated following a method reported in the dehydrogenation work (Energies paragraph)<sup>[1]</sup> and quoted in this paragraph from reference [1].

“It is estimated as the difference of the intramolecular BSSEs ( $E_{\text{intra-BSSE}}$ ) of the intermediates and transition states respectively involved. The  $E_{\text{intra-BSSE}}$  of a given step is in turn calculated as the sum of counterpoise corrections associated to the dissociation of each ligand separately (with the exception of the hydride ligand for which the counterpoise correction is postulated to be 0).”

$$\mathbf{1} + \text{MeO}^- \rightarrow \text{TS}_{6-7} \text{ (a/b)} + 2 \text{PPh}_3$$

$$\delta E'_{\text{BSSE}} = E_{\text{intra-BSSE}}(\text{TS}_{6-7}) - E_{\text{intra-BSSE}}(\mathbf{1})$$

$E_{\text{intra-BSSE}} \mathbf{1}$		$E_{\text{intra-BSSE}} \text{TS}_{6-7} \text{ (a)}$		$E_{\text{intra-BSSE}} \text{TS}_{6-7} \text{ (b)}$	
H	0.0	H	0.0	H	0.0
H	0.0	H	0.0	H	0.0
CO	6.6	H	0.0	H	0.0
P <sub>eq</sub>	17.5	CO	3.7	CO	3.9
P <sub>ax-1</sub>	14.1	HCHO	3.8	HCHO	3.5
P <sub>ax-2</sub>	13.9	P	5.3	P	5.2
<b>Total</b>	<b>52.2</b>	<b>Total</b>	<b>12.9</b>	<b>Total</b>	<b>12.5</b>

**Table 4.4.4.2.1** BSSE corrections for complex **1** and **TS<sub>6-7</sub> (a/b)** calculated at the B97-D/ECP3 level of theory considering the dissociation of each ligand separately; P = PPh<sub>3</sub>

#### 4.4.4.3 Comparisons of different isotopomers at the RI-BP86/ECP1 level of theory

**Table 4.4.4.3.1** Correcting Terms for Free energies of activation ( $\delta E_G$ )<sup>a</sup> and Enthalpies ( $\delta E_H$ )<sup>b</sup> in kJ/mol for the rate-determining steps of pathway **A**.

		<sup>1</sup> H		<sup>2</sup> H	
<i>Overall Reaction</i>		$\delta E_G$	$\delta E_H$	$\delta E_G$	$\delta E_H$
<b>A</b>	<b>1 + MeO<sup>-</sup> → TS<sub>6-7</sub> (a) + 2 PPh<sub>3</sub></b>	-109.5	-16.1	-107.7	-13.8

<sup>a</sup> $\delta E_G = \Delta G - \Delta E$ ; <sup>b</sup> $\delta E_H = \Delta H - \Delta E$  (see Table 4.4.4.4 for the values of  $\Delta G$  and  $\Delta H$ ).

**Table 4.4.4.3.1** Free Energies of activation ( $\Delta G$ ) and Enthalpies ( $\Delta H$ ) in kJ/mol for the rate-determining steps of pathway **A**.

		<sup>1</sup> H			<sup>2</sup> H	
<i>Overall Reaction</i>		$\Delta E$	$\Delta G$	$\Delta H$	$\Delta G$	$\Delta H$
<b>A</b>	<b>1 + MeO<sup>-</sup> → TS<sub>6-7</sub> (a) + 2 PPh<sub>3</sub></b>	14.9	-94.6	-1.2	-92.8	1.1

## 4.5 References

- [1] N. Sieffert, M. Buehl, *J. Am. Chem. Soc.* **2010**, *132*, 8056-8070.
- [2] a) D. G. Gusev, A. B. Vymenits, V. I. Bakhmutov, *Inorg. Chim. Acta* **1991**, *179*, 195-201; b) R. H. Crabtree, D. G. Hamilton, *J. Am. Chem. Soc.* **1986**, *108*, 3124-3125.
- [3] D. Morton, D. J. Cole-Hamilton, *J. Chem. Soc., Chem. Commun.* **1988**, 1154-1156.
- [4] B. N. Chaudret, D. J. Cole-Hamilton, R. S. Nohr, G. Wilkinson, *J. Chem. Soc., Dalton Trans.* **1977**, 1546-1557.
- [5] D. Morton, D. J. Cole-Hamilton, I. D. Utuk, M. Paneque-Sosa, M. Lopez-Poveda, *J. Chem. Soc., Dalton Trans.* **1989**, 489-495.
- [6] N. Sieffert, R. Reocreux, P. Lorusso, D. J. Cole-Hamilton, M. Buehl, *Chem. Eur. J.* **2014**, *20*, 4141-4155.
- [7] N. Ortega, C. Richter, F. Glorius, *Org. Lett.* **2013**, *15*, 1776-1779.
- [8] N. Sieffert, M. Buhl, *Inorg. Chem.* **2009**, *48*, 4622-4624.
- [9] Y. Minenkov, A. Singstad, G. Occhipinti, V. R. Jensen, *Dalton Trans.* **2012**, *41*, 5526-5541.
- [10] S. F. Boys, F. Bernardi, *Molecular Physics* **1970**, *19*, 553-566.
- [11] a) A. Klamt, G. Schueuermann, *J. Chem. Soc., Perkin Trans. 2* **1993**, 799-805; b) Y. Takano, K. N. Houk, *J. Chem. Theory Comput.* **2005**, *1*, 71-78.
- [12] a) D. E. Linn, Jr., J. Halpern, *J. Am. Chem. Soc.* **1987**, *109*, 2969-2974; b) J. Halpern, *Pure Appl. Chem.* **1987**, *59*, 173-180.
- [13] a) T. Oka, *J. Phys. Soc. Jpn.* **1960**, *15*, 2274-2279; b) L. V. Gurvich, I. V. Veyts, C. B. Alcock, V. S. Iorish, Editors, *Thermodynamic Properties of Individual Substances; 4th Edition, Vol. 2: Elements Carbon, Silicon, Germanium, Tin, Lead, and Their Compounds, Pt. 2: Tables*, **1991**.
- [14] M. Gomez-Gallego, M. A. Sierra, *Chem. Rev. (Washington, DC, U. S.)* **2011**, *111*, 4857-4963.
- [15] G. L. Geoffroy, *Prog. Inorg. Chem.* **1980**, *27*, 123-151.
- [16] A. D. Becke, *Phys. Rev. A Gen. Phys.* **1988**, *38*, 3098-3100.
- [17] J. P. Perdew, *Phys. Rev. B* **1986**, *33*, 8822-8824.
- [18] D. Andrae, U. Haeussermann, M. Dolg, H. Stoll, H. Preuss, *Theor. Chim. Acta* **1990**, *77*, 123-141.
- [19] R. L. Martin, P. J. Hay, L. R. Pratt, *J. Phys. Chem. A* **1998**, *102*, 3565-3573.
- [20] a) C. Gonzalez, H. B. Schlegel, *J. Chem. Phys.* **1989**, *90*, 2154-2161; b) C. Gonzalez, H. B. Schlegel, *J. Phys. Chem.* **1990**, *94*, 5523-5527.
- [21] a) S. Grimme, *J. Comput. Chem.* **2004**, *25*, 1463-1473; b) S. Grimme, *J. Comput. Chem.* **2006**, *27*, 1787-1799.
- [22] Gaussian 03, Revision C.02, M. J. Frisch, G. W. Trucks, H. B. Schlegel, G. E. Scuseria, M. A. Robb, J. R. Cheeseman, J. A. Montgomery, Jr., T. Vreven, K. N. Kudin, J. C. Burant, J. M. Millam, S. S. Iyengar, J. Tomasi, V. Barone, B. Mennucci, M. Cossi, G. Scalmani, N. Rega, G. A. Petersson, H. Nakatsuji, M. Hada, M. Ehara, K. Toyota, R. Fukuda, J. Hasegawa, M. Ishida, T. Nakajima, Y. Honda, O. Kitao, H. Nakai, M. Klene, X. Li, J. E. Knox, H. P. Hratchian, J. B. Cross, V. Bakken, C. Adamo, J. Jaramillo, R. Gomperts, R. E. Stratmann, O. Yazyev, A. J. Austin, R. Cammi, C. Pomelli, J. W. Ochterski, P. Y. Ayala, K. Morokuma, G. A. Voth, P. Salvador, J. J. Dannenberg, V. G. Zakrzewski, S. Dapprich, A. D. Daniels, M. C. Strain, O. Farkas, D. K. Malick, A. D. Rabuck, K. Raghavachari, J. B. Foresman, J. V. Ortiz, Q. Cui, A. G. Baboul, S. Clifford, J. Cioslowski, B. B. Stefanov, G. Liu, A. Liashenko, P. Piskorz, I. Komaromi, R. L. Martin, D. J. Fox, T. Keith, M. A. Al-

- Laham, C. Y. Peng, A. Nanayakkara, M. Challacombe, P. M. W. Gill, B. Johnson, W. Chen, M. W. Wong, C. Gonzalez, and J. A. Pople, Gaussian, Inc., Wallingford CT, 2004.
- [23] F. Furche, R. Ahlrichs, C. Haettig, W. Klopper, M. Sierka, F. Weigend, *Wiley Interdiscip. Rev. Comput. Mol. Sci.* **2014**, 4, 91-100.

# Chapter 5

## Ru-catalysed decarbonylation of methanol: an insight into the mechanism

The decarbonylation reaction occurring as side reaction during the dehydrogenation of methanol was investigated computationally and experimentally. The good agreement between computed and experimental KIEs (observed  $k_H/k_D=4$ ), predicted for one specific decarbonylation path designed to proceed via  $[\text{RuH}(\text{OCH}_3)(\text{PPh}_3)_3]$ , confirmed the formation of the first agostic intermediate in the rate-determining step. Additional studies led to the design of new plausible reaction channels involving also an intramolecular exchange of  $^2\text{H}$  and *ortho* C-H deuteration of the phenyl rings of phosphine ligands.

---

**Keywords:** ruthenium · methanol decarbonylation · reaction intermediates · KIEs · *ortho*-deuteration.

The part concerning the combined computational and experimental mechanistic study on methanol decarbonylation catalysed by  $[\text{RuH}_2(\text{H}_2)(\text{PPh}_3)_3]$  is adapted from “*On the Importance of Decarbonylation as Side Reaction in the Ruthenium-Catalyzed Dehydrogenation of Alcohols: a Combined Experimental and Density Functional Study*”, N. Sieffert, R. Reocreux, P. Lorusso, D. J. Cole-Hamilton, M. Bühl, *Chem. Eur. J.* **2014**, *20*, 4141. The computational work was conducted by Sieffert, Reocreux and Bühl.

## 5.1 Introduction

The oxidation of alcohols to carbonyl compounds promoted by dehydrogenating catalysts resulting therefore in the formation of molecular hydrogen is a topic that attracted increasing interest in the last decades since the first very active system developed by Morton and Cole-Hamilton’s using the  $[\text{RuH}_2(\text{X})(\text{PPh}_3)_3]$  catalyst (where X =  $\text{N}_2$ ,  $\text{PPh}_3$  or  $\text{H}_2$ ) in the presence of a base.<sup>[1]</sup> This kind of homogeneous catalytic system for the production of  $\text{H}_2$  are affected by a twofold complexity: on one hand there is the limited understanding of the reaction mechanism due to the multiple steps involved and difficult characterisation of the reaction intermediates, on the other hand we observe the occurrence of side reactions besides  $\text{H}_2$  production that limit their practical use, in fact the produced aldehydes can undergo aldol and Tishchenko<sup>[2]</sup> reactions but can react at the same time with the Ru catalyst generating carbonyl complexes such as  $[\text{RuH}_2(\text{CO})(\text{PPh}_3)_3]$  (**5**) that can still act as a dehydrogenating catalyst<sup>[1a]</sup> (as reported in Chapter 3).

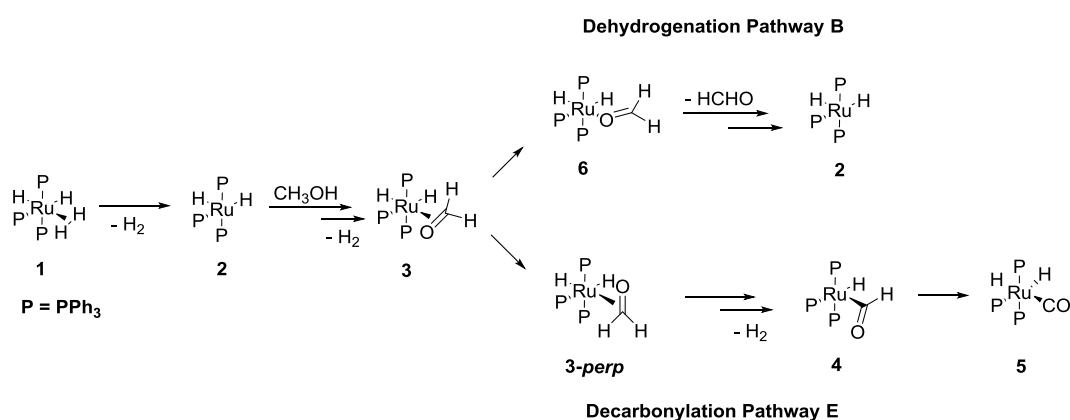
Recently we reported a combined experimental and computational study concerning the mechanism of methanol decarbonylation that occurs as a side reaction during the dehydrogenation process catalysed by  $[\text{RuH}_2(\text{H}_2)(\text{PPh}_3)_3]$  (**1**).<sup>[3]</sup> A Density Functional Study showed that the system can follow multiple reaction pathways with very close activation energies. Kinetic isotope effects (KIEs) were computed for all pathways and determined experimentally for one specific pathway which was designed to start from  $[\text{RuHCl}(\text{PPh}_3)_3]$  (**7**) to provide the final species **5** by reacting with NaOMe in methanol/toluene, via a series of intermediates, believed to be  $[\text{RuH}(\text{OMe})(\text{PPh}_3)_3]$  (**8**),  $[\text{RuH}_2(\text{CH}_2=\text{O})(\text{PPh}_3)_3]$  (**3**) and  $[\text{RuH}(\text{CHO})(\text{PPh}_3)_3]$  (**4**)<sup>[4]</sup>, which unfortunately have never been isolated, although **3** and **4** have been proposed on the basis of IR studies.<sup>[4]</sup>

In this chapter we report isotopic labelling studies, which were designed to measure isotope effects, but which also provide some interesting mechanistic data. The present study will be organised for clarity starting from the discussion of the method used to experimentally

determine the deuterium isotope effect and backwards to the preliminary experiments which revealed some interesting outcomes from a mechanistic point of view.

## 5.2 Results and Discussion

As anticipated in the introduction, the experimental KIE was determined only for the neutral *pathway E* described in our previous work and shown in Figure 5.2.1 which starts from complex **1** involved in the dehydrogenation *pathway B*.<sup>[3]</sup> After the first dehydrogenation and formation of formaldehyde which remains associated side-on to the metal (complex **3**), the formaldehyde ligand rather than dissociating and closing the dehydrogenation cycle, can undergo further dehydrogenation to afford H<sub>2</sub> and the carbonyl complex **5**. A plausible mechanism may involve a preliminary β-hydrogen abstraction from the formaldehyde to afford the formyl complex **4** followed by dissociation of H<sub>2</sub> which creates a vacant site that in turn can accept a second hydrogen atom providing the final carbonyl species **5** by α-hydrogen abstraction.

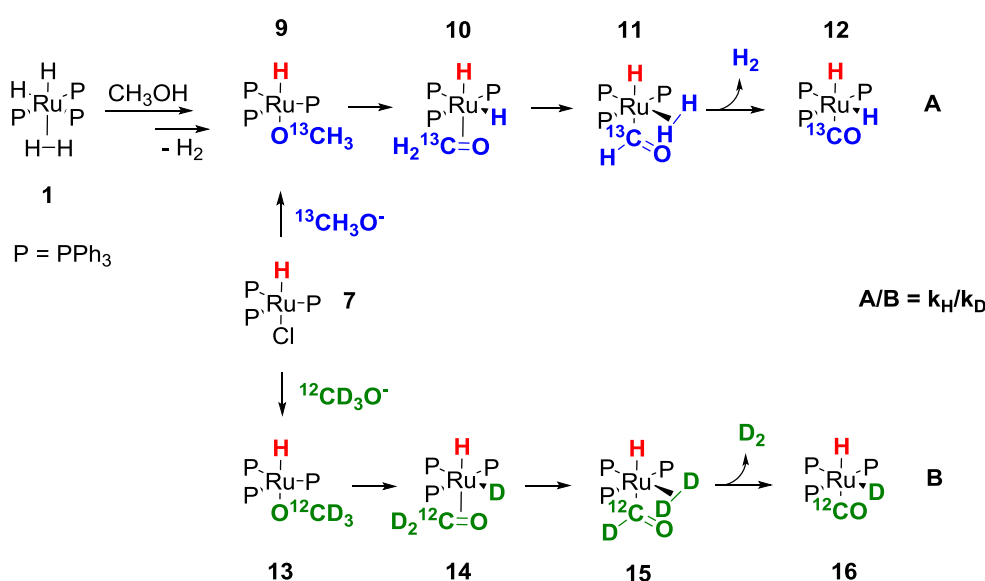


**Scheme 5.2.1** General outline of the dehydrogenation *pathway B* and the decarbonylation *pathway E* starting from complex **1** as reported by Sieffert and co-workers.<sup>[3]</sup>

In the experimental work, to study the decarbonylation pathway in isolation, the pivotal intermediate **3** was obtained by reacting complex [RuHCl(PPh<sub>3</sub>)<sub>3</sub>] (**7**) with NaOMe in methanol/toluene, via the methoxide intermediate [RuH(OMe)(PPh<sub>3</sub>)<sub>3</sub>] (**8**) rather than starting from complex **1** which appeared to be quite unstable due to its tendency to spontaneously dissociate

H<sub>2</sub>

\*[3] (Scheme 5.2.2). To determine the deuterium isotope effect the reaction was carried out using equal amounts of  $^{13}\text{CH}_3\text{OH}$  and  $\text{CD}_3\text{OD}$  each containing dissolved sodium to form the methoxide. This reaction should give  $[\text{RuH}_2(^{13}\text{CO})(\text{PPh}_3)_3]$  (**12**) from  $^{13}\text{CH}_3\text{OH}$  and  $[\text{RuHD}(^{12}\text{CO})(\text{PPh}_3)_3]$  (**16**) from  $^{12}\text{CD}_3\text{OD}$ . Possible subsequent H/D exchange notwithstanding (post-reaction exchange or D exchange into the *ortho* C-H of aromatic rings, the latter one will be discussed in detail later on), the ratio of  $^{13}\text{CO}:^{12}\text{CO}$  relates directly to the kinetic isotope effect  $k_{\text{H}}/k_{\text{D}}$  since the  $^{13}\text{C}$  in the product comes only through H abstraction reactions, whilst the  $^{12}\text{CO}$  comes only from D abstraction reactions.

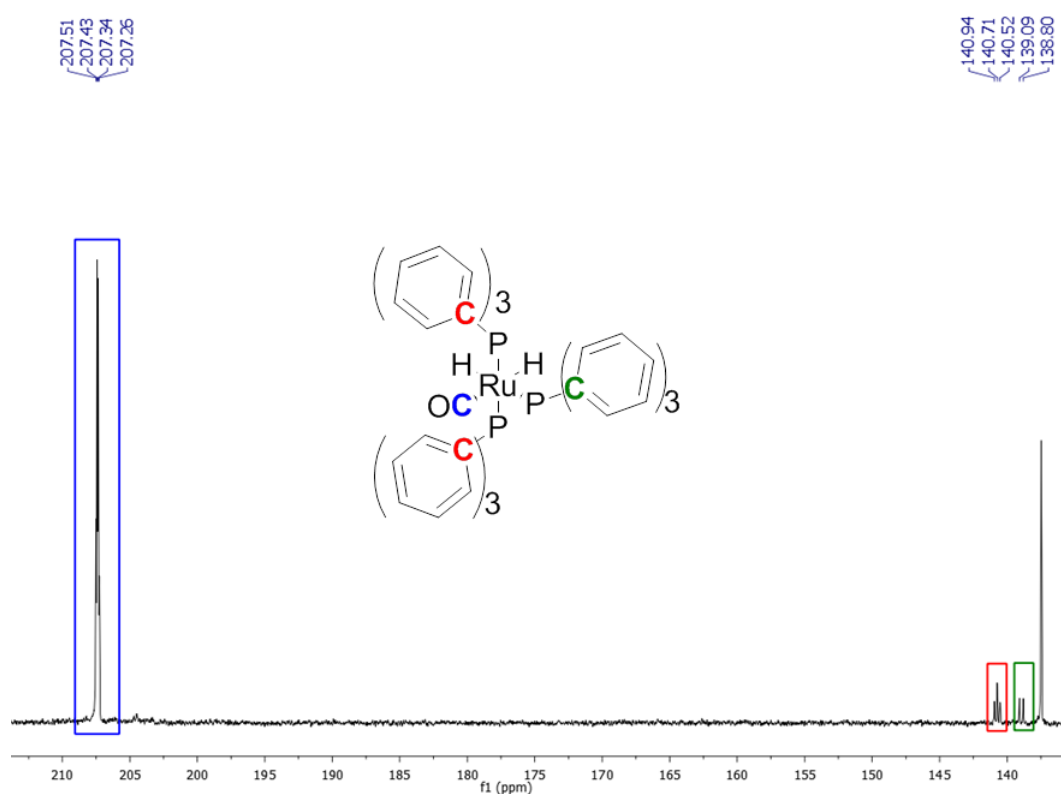


**Scheme 5.2.2** Representation of key intermediates in the synthesis of complexes **12** and **16** by reaction of **7** with  $^{12}\text{CD}_3\text{OD}$  or  $^{13}\text{CH}_3\text{OH}$ .

We have used  $^{13}\text{C}$  NMR to determine the  $^{13}\text{CO}:^{12}\text{CO}$  ratio.  $^{13}\text{C}\{^1\text{H}\}$  NMR spectra of  $[\text{RuH}(\text{H}/\text{D})(^{12/13}\text{CO})(\text{PPh}_3)_3]$  obtained when using  $^{13}\text{CH}_3\text{OH}$ , a mixture of  $^{13}\text{CH}_3\text{OH}$  and  $\text{CD}_3\text{OD}$  and a mixture of  $\text{CH}_3\text{OH}$  and  $\text{CD}_3\text{OD}$  were run on the same spectrometer under identical conditions. Figure 5.2.1 shows part of the  $^{13}\text{C}\{^1\text{H}\}$  spectrum of **12**. The resonance at  $\delta = 207.4$  ppm arises from the carbonyl ( $^{13}\text{CO}$  labelled). Whilst the resonances at  $\delta = 140.7$  ppm (virtual triplet, CPP' spin system, 6C) and  $\delta = 138.9$  ppm (d, 3C) are from the *ipso* carbon atoms of the phenyl groups on the mutually *trans* phosphines and the *cis* phosphine respectively. We used the resonance at  $\delta = 140.7$  ppm as an "internal standard". Integration of the  $^{13}\text{CO}$  signal and the signal at  $\delta = 140.7$  ppm gives a ratio of 100 : 6.34 for **12**. In a sample obtained when using

\* Experimental evidence

CH<sub>3</sub>OH and CD<sub>3</sub>OD (no <sup>13</sup>CO), the resonance at 207.4 ppm is essentially absent with a maximum integral of 1.7 (should be 1 in the basis of 1 % natural abundance of CO) when the integral of the signal at 140.7 ppm is set at 6.34. Integration of these two signals for the complex obtained from the mixture of <sup>13</sup>CH<sub>3</sub>OH and CD<sub>3</sub>OD gives a ratio of 80 : 6.34. The 20 % of naturally abundant CO would contribute 0.2-0.3 to this signal, so this contribution can be ignored. This means that there is 80 % of <sup>13</sup>CO in the mixture of complexes obtained when using <sup>13</sup>CH<sub>3</sub>OH and CD<sub>3</sub>OD (1 : 1) and 20 % of <sup>12</sup>CO. This equates to a kinetic isotope effect ( $k_H/k_D$ ) of 4.



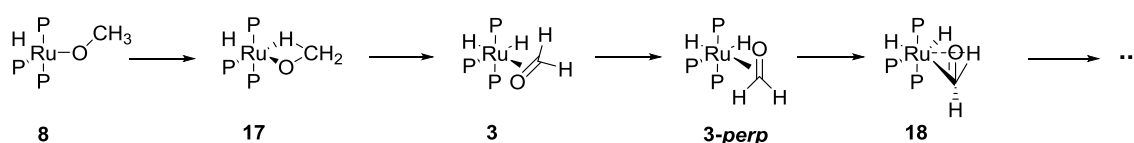
Mixture	Integrals ratio
	$\delta$ 207.4 : 140.7
<sup>13</sup> CH <sub>3</sub> OH	100 : 6.34*
CH <sub>3</sub> OH/CD <sub>3</sub> OD	1.7 : 6.34
<sup>13</sup> CH <sub>3</sub> OH/ <sup>12</sup> CD <sub>3</sub> OD	80 : 6.34

\*Integration is obtained using TopSpin 3.2 while the image is processed with MestReNova

**Figure 5.2.1** Part of the <sup>13</sup>C{<sup>1</sup>H} NMR spectrum of [RuH<sub>2</sub>(<sup>13</sup>CO)(PPh<sub>3</sub>)<sub>3</sub>] (**12**) obtained from the reaction of [RuHCl(PPh<sub>3</sub>)<sub>3</sub>] (**7**) with <sup>13</sup>CH<sub>3</sub>OH containing sodium in toluene.



When comparing this result to the computed ones reported in *Table 5* of the corresponding paper we should consider that the computed values arise from intermediates occurring during the catalytic dehydrogenation process, whereas the former result derives from another precursor, presumably **8**, which is an intermediate in the dehydrogenation *pathway B*<sup>[5]</sup> (not depicted in Scheme 5.2.1), from which the decarbonylation *pathway E* departs at a later point (after intermediate **3**, see Scheme 5.2.1). For the correct interpretation of our experimental result is therefore necessary to create a similar scenario by introducing a "partial" *path E* starting from **8** (Scheme 5.2.3).



**Scheme 5.2.3** Section of decarbonylation *pathway E* starting from methoxide complex **8** of dehydrogenation *pathway B*.

The deuterium KIE computed for this section of the decarbonylation *pathway E* is ca. 3 (see **7** → **TS**<sub>9perp-19</sub> entry in *Table 5* of the corresponding paper; **8** → **TS**<sub>3perp-18</sub> in Scheme 5.2.3), in very good qualitative agreement with the experimental value suggesting that the formation of the first agostic intermediate is the rate-limiting step on this possible decarbonylation pathway. The initial formation of the methoxide complex **8**, however, should not affect the observed KIE, because it is expected to be in rapid exchange with the alcohol in the solution once formed (via [Ru]-OR + HOR' → [Ru]-OR' + HOR), an essential condition to ensure proper scrambling of the labelled alkyl moiety <sup>13</sup>CH<sub>3</sub> and <sup>12</sup>CD<sub>3</sub> prior to decarbonylation. Such exchange processes of metal alkoxides are indeed well known.<sup>[6]</sup>

In the early stage of this study, before concluding that the KIE  $k_{\text{H}}/k_{\text{D}}$  for the investigated decarbonylation pathway could be determined using the <sup>13</sup>C NMR resonances (<sup>13</sup>CO:<sup>12</sup>CO ratio) rather than <sup>1</sup>H resonances due to potential H/D exchange as described before, an accurate analysis of the hydride region of experiments conducted in the presence of different mixtures of CH<sub>3</sub>OH, CD<sub>3</sub>OD and <sup>13</sup>CH<sub>3</sub>OH, gave some interesting mechanistic evidence and so were further investigated.

The figure 5.2.2 shows the hydride region of the Ru final species arising by reaction of **7** (in toluene) with labelled or unlabelled NaOMe when using CH<sub>3</sub>OH, CD<sub>3</sub>OD, <sup>13</sup>CH<sub>3</sub>OH or a 1:1

mixture of CH<sub>3</sub>OH/CD<sub>3</sub>OD (the <sup>1</sup>H NMR spectrum corresponding to the product when using a 1:1 mixture of <sup>13</sup>CH<sub>3</sub>OH/CD<sub>3</sub>OD, which was discussed in the section on <sup>13</sup>C NMR, is omitted due to the complexity of the two hydride resonances which therefore will not provide any additional information to this part of the study).

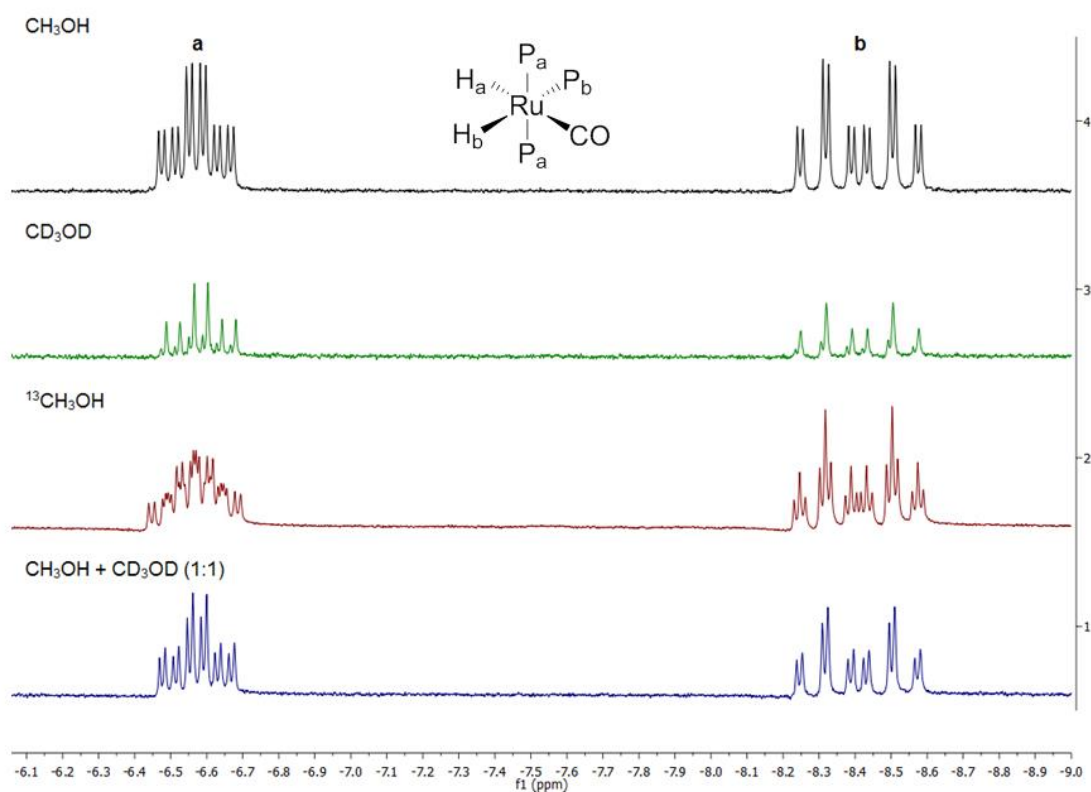


**Figure 5.2.2** Part of the <sup>1</sup>H NMR spectrum (hydride region) of the Ru final species arising by reaction at 100 °C of **7** (in toluene) in CH<sub>3</sub>OH, CD<sub>3</sub>OD, <sup>13</sup>CH<sub>3</sub>OH or a 1:1 mixture of CH<sub>3</sub>OH/CD<sub>3</sub>OD each containing dissolved sodium to form the methoxide.

[RuH<sub>2</sub>(CO)(PPh<sub>3</sub>)<sub>3</sub>] (**5**) was reported for the first time by Hallman, McGarvey and Wilkinson in 1968 and appeared to be one of the most important and widely used homogeneous catalysts. Recently Grushin and Samouei developed a new and simpler synthetic procedure for complex **5** with greater scalability, reporting spectroscopic (NMR) and crystallographic data.<sup>[7]</sup> Despite the readily availability of NMR data of complex **5**, in this paragraph we will briefly summarise <sup>1</sup>H and <sup>31</sup>P{<sup>1</sup>H} NMR resonances in toluene-d<sub>8</sub> prior to discussion of the corresponding <sup>2</sup>H and <sup>13</sup>C labelled compounds.

The hydride *trans* to the carbonyl ligand (H<sub>a</sub>) generates a tdd at -6.5 ppm ( $J_{H_a-P_a} = 30.8$  Hz, *cis*;  $J_{H_a-P_b} = 15.2$  Hz, *cis*;  $J_{H_a-H_b} = 6.4$  Hz), while the hydride *trans* to the phosphine ligand (H<sub>b</sub>) gives

rise to a dtd at -8.4 ppm ( $J_{Hb-Pb} = 74.2$  Hz, *trans*;  $J_{Hb-Pa} = 28.6$  Hz, *cis*;  $J_{Ha-Hb} = 6.4$  Hz) (see Figure 5.2.2, spectrum 4). In the  $^{31}\text{P}\{^1\text{H}\}$  NMR spectrum the two  $P_a$  give rise to a d at 57.4 ppm, while the  $P_b$  generates a t at 45.3 ppm ( $J_{P-P} = 17.7$  Hz).

When the reaction is performed using only  $\text{CD}_3\text{OD}$ , the monohydride species **16** arising from decarbonylation of  $\text{CD}_3\text{OD}$  can exist as two potential isomers, one with Ru-H *trans* to CO and one *trans* to  $\text{PPh}_3$  ligand, which respectively generate a td at -6.5 ppm and a dt at -8.4 ppm (figure 5.2.2, spectrum 3; we will return on this spectrum later on). The td and the dt enhance one of the two peaks of each doublet of the hydride resonances depicted in spectrum 1 (Figure 5.2.2).

When using a 1:1 mixture of  $\text{CH}_3\text{OH}/\text{CD}_3\text{OD}$  (Figure 5.2.2, spectrum 1), we can observe that the hydride resonances do not exhibit any changes in terms of multiplicity but only in terms of intensity. The formation of two isomers of **16** along with **5** is responsible for the asymmetrical intensity of both signals since the monohydride species will contribute only with a td and a dt to both hydride resonances since it lacks the H-H coupling.

The pattern of resonances in the second spectrum (only  $^{13}\text{CH}_3\text{OH}$ ) is affected by the additional coupling of the hydrides with  $^{13}\text{C}(\text{O})$  arising from decarbonylation of  $^{13}\text{CH}_3\text{OH}$  which results in a tddd at -6.5 ppm ( $J_{Ha-C} = 18.7$  Hz), and a dtt at -8.4 ppm (every peak in spectrum 4 should be split in a d due to the extra coupling with the enriched  $^{13}\text{C}$ ). Since  $J_{Hb-C} = J_{H-H}$  the different resonances in the multiplet all appear as triplets (Figure 5.2.2, spectrum 2).

An interesting outcome was observed in the second spectrum corresponding to the reaction with only  $\text{CD}_3\text{OD}$ . The relevant spectrum shows the hydride resonances of the two isomers of **16**, as major species but exhibited also the presence of minor amounts of the corresponding dihydrido carbonyl species **5** (it can be easily compared with the spectrum above) which was not expected to be formed when only deuterated methanol was employed. Further studies were therefore conducted in order to establish according to which mechanism the dihydride species was formed under these reaction conditions.

A similar experiment was performed always using  $\text{NaOCD}_3$  (obtained by reacting sodium metal with  $\text{CD}_3\text{OD}$ ) in toluene at RT and stopped as soon as the mixture turned from purple to orange (8 min) in an attempt to visualise any intermediates and in particular to observe at which stage and under which conditions the monohydride and dihydride species are formed. Surprisingly the collected  $^1\text{H}$  NMR spectrum in  $\text{THF-d}_8$  did not exhibit any signals corresponding to **5** or **16**

in the hydride region while the  $^{31}\text{P}\{^1\text{H}\}$  NMR resonances at 57.4 and 44.8 ppm were comparable with those reported for the mixture of **16** and **5** presumably suggesting the formation in the early stage of a carbonyl bis-deuterated species  $[\text{RuD}_2(\text{CO})(\text{PPh}_3)_3]$  (**19**) which is rapidly converted into species **16** and **5**. The four  $^{31}\text{P}\{^1\text{H}\}$  NMR spectra depicted below (Figure 5.2.3) clearly give evidence of similar resonances corresponding to the species **5** (*spectrum 4*), a mixture of **16** and **5** (*spectrum 3*) obtained using a 1:1 mixture of  $\text{CH}_3\text{OH}/\text{CD}_3\text{OD}$ , a mixture of **16** and **5** (only minor amounts) (*spectrum 2*) obtained using only  $\text{CD}_3\text{OD}$  and the potential species **19** (*spectrum 1*) obtained under different reaction conditions compared with the previous experiments (RT for 8 min) (The  $^{31}\text{P}\{^1\text{H}\}$  NMR spectrum corresponding to the reaction conducted at RT was recorded in  $\text{THF-d}_8$ , while the other NMR spectra corresponding to the experiments conducted at 100 °C respectively were recorded in toluene- $\text{d}_8$ ).

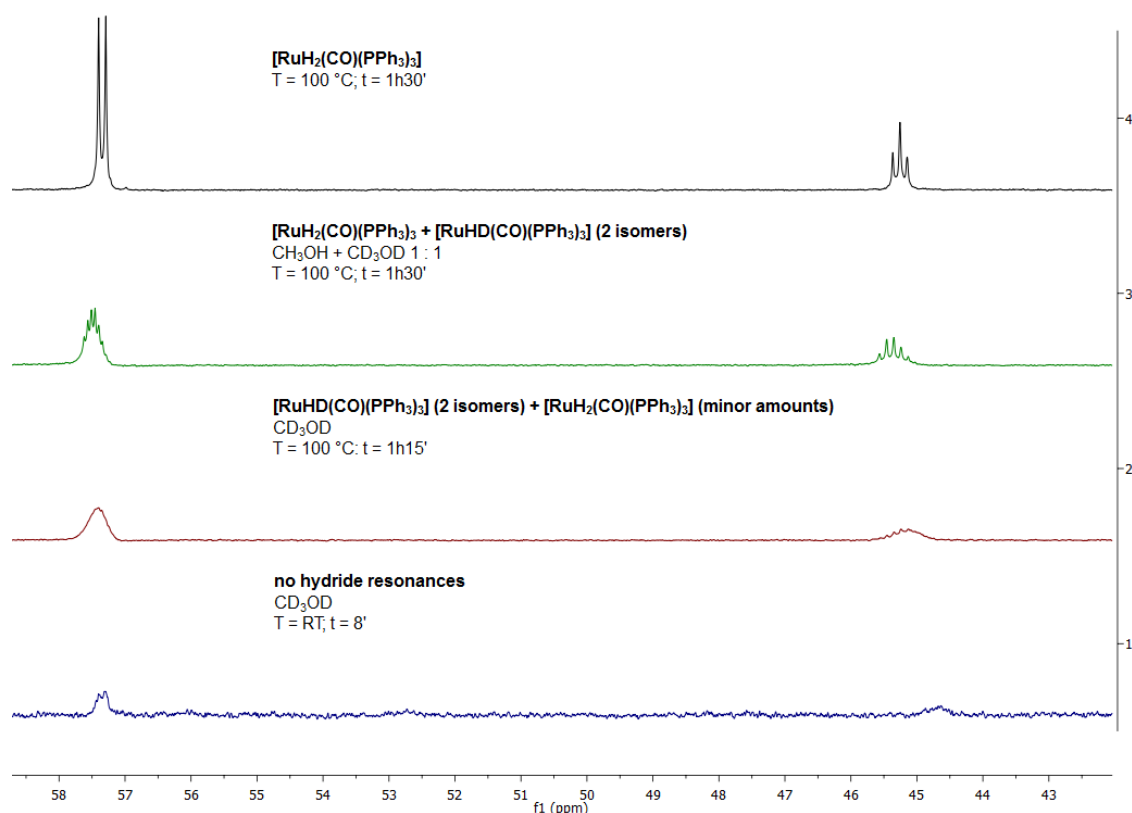


**Figure 5.2.3** Section of  $^{31}\text{P}\{^1\text{H}\}$  NMR spectra probably attributable to  $[\text{RuD}_2(\text{CO})(\text{PPh}_3)_3]$  (**19**) (*spectrum 1*,  $\text{THF-d}_8$ ),  $[\text{RuHD}(\text{CO})(\text{PPh}_3)_3]$  (**16**) and  $[\text{RuH}_2(\text{CO})(\text{PPh}_3)_3]$  (**5**) (*spectrum 2 and 3*, toluene- $\text{d}_8$ ) and species **5** (*spectrum 4*, toluene- $\text{d}_8$ ), obtained under different reaction conditions.

Since decarbonylation of CD<sub>3</sub>OD with quantitative conversion of **7** only occurs at high temperature (100 °C), a further experiment was conducted by using a ramping temperature (20 min at RT, heated to 55 °C for 40 min and subsequently to 100 °C for 30 min) in order to observe the formation of these temperature dependent species. The reaction was performed in toluene-d<sub>8</sub> to allow continuously sampling at each ramping temperature step with immediate cooling to room temperature and collection of the NMR spectrum.

The spectra corresponding to the reaction mixtures analysed after 20 min and 1h (respectively RT and 55 °C) showed the presence of three potential intermediates (Figure 5.2.4, spectra 2 and 3).

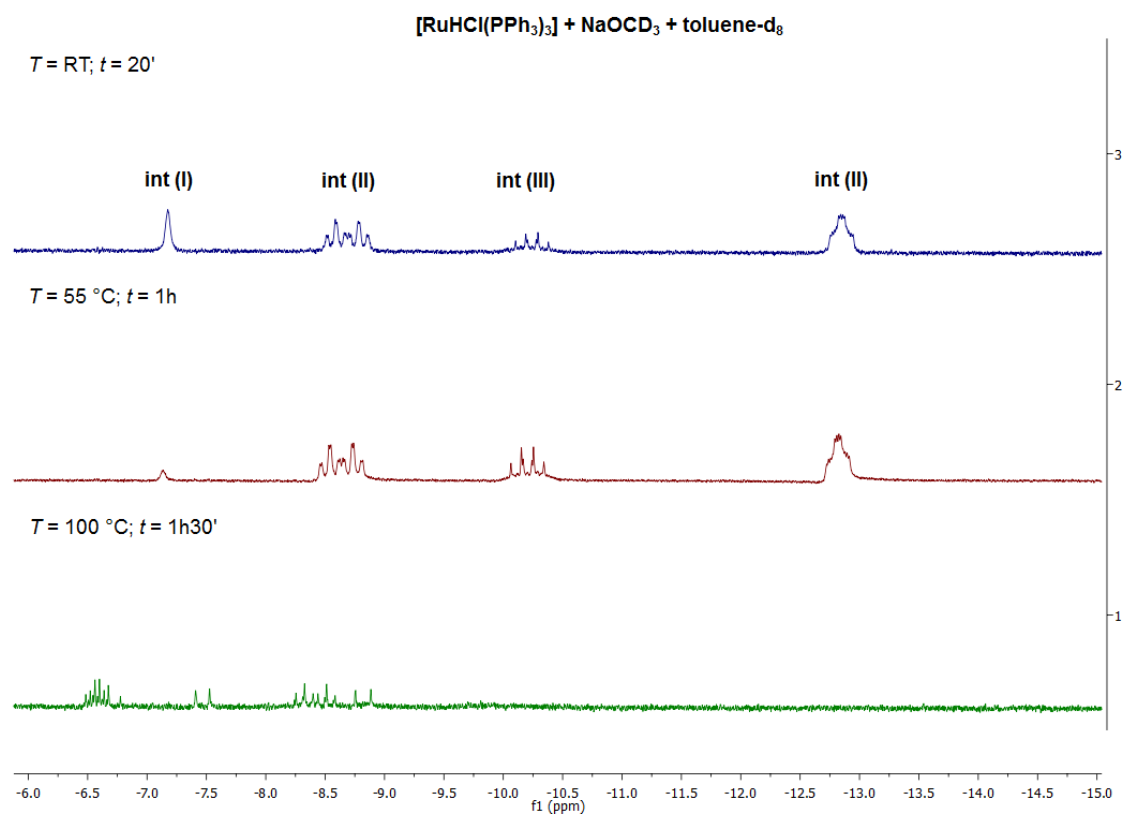


**Figure 5.2.4** Time and temperature dependent <sup>1</sup>H NMR study with NaOCD<sub>3</sub>: hydride region of the reaction mixture.

A similar experiment (15 min at RT, heated to 55 °C for 30 min, and to 100 °C for 30 min) was conducted in the presence of NaOCH<sub>3</sub> (obtained by reaction of sodium metal with CH<sub>3</sub>OH), with the only difference being that the first two ramping temperature steps were shortened in an attempt to observe the formation of similar intermediates (Figure 5.2.5), based on the

evidence that formation of complex **5** already occurs at RT in the presence of a non-deuterated reagent. Surprisingly, the first two spectra collected after 15 min (RT) and 45 min (55 °C) exhibited the same resonances observed when using CD<sub>3</sub>OD along with those corresponding to the complex **5**, as anticipated before. Based on the intensity of the intermediates signal, it is evident that the decarbonylation reaction is much faster when no <sup>2</sup>H is involved.

The further investigation comprises the identification of the three potential intermediates observed in both sets of experiments and elucidation of a plausible mechanism involved.

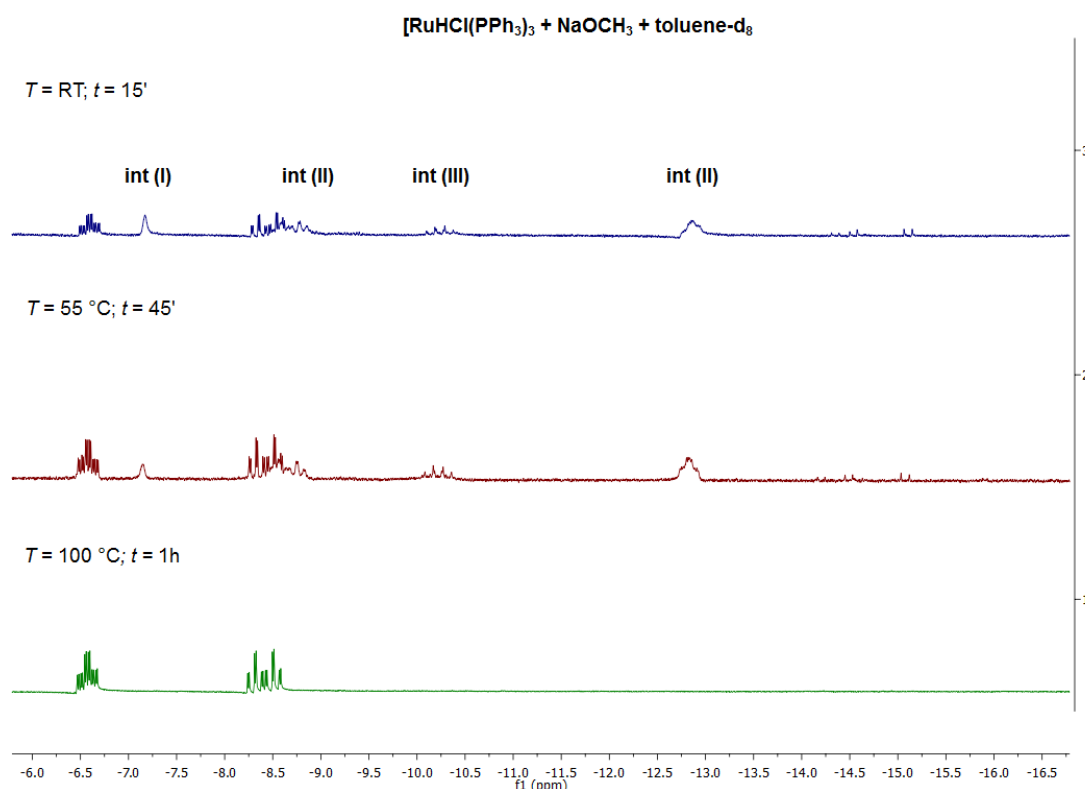
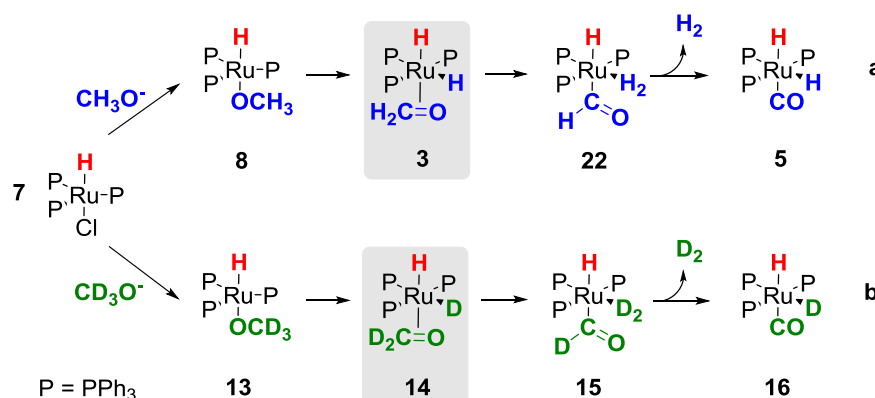


**Figure 5.2.5** Time and temperature dependent <sup>1</sup>H NMR study with NaOCH<sub>3</sub>: hydride region of the reaction mixture.

The signals at -8.6 and -12.8 ppm (**int. II** in Figures 5.2.4 and 5.2.5) are in good agreement with those reported in the literature for the dinitrogen derivative [RuH<sub>2</sub>(N<sub>2</sub>)(PPh<sub>3</sub>)<sub>3</sub>] (**20**), arising from working under a dinitrogen atmosphere.<sup>[8]</sup> To confirm that those resonances belong to **20** a similar experiment was performed this time under argon. In the absence of dinitrogen those signals disappeared giving evidence that the depicted intermediate **II** is the well known complex **20**.

The broad signal at -7.1 ppm (**int. I** in Figures 5.2.4 and 5.2.5) corresponds to another well defined complex,  $[\text{RuH}_2(\text{H}_2)(\text{PPh}_3)_3]$  (**1**).<sup>[9]</sup> Based on the evidence that one of the intermediates is the tetrahydride species **1**, the intermediate **III** at -10.2 ppm was proposed to be the precursor  $[\text{RuH}_2(\text{PPh}_3)_4]$  (**21**). Since **21** is not well characterised in the literature (no  $^1\text{H}$  NMR available), it was synthesised according to a literature procedure and analysed through  $^1\text{H}$  and  $^{31}\text{P}\{^1\text{H}\}$  NMR spectroscopy.<sup>[10]</sup> As disclosed above, the intermediate **III** corresponded to complex **21**. As further confirmation, reaction with  $\text{H}_2$ , slowly bubbled through the mixture containing **21** in an NMR tube, provided complex **1** as the final species.<sup>[10]</sup> It is surprising that the tetrakisphosphine complex forms when there are only three phosphines in the starting material, but the additional resonances displayed in Figure 5.2.4 and 5.2.5, that do not belong to the identified species, may be attributable to mono or bis-phosphine species.

Once the three intermediates were identified we proceeded with the investigation of the mechanism involved by considering the two experiments ( $\text{CH}_3\text{OH}$  and  $\text{CD}_3\text{OD}$ ) separately (Scheme 5.2.4).



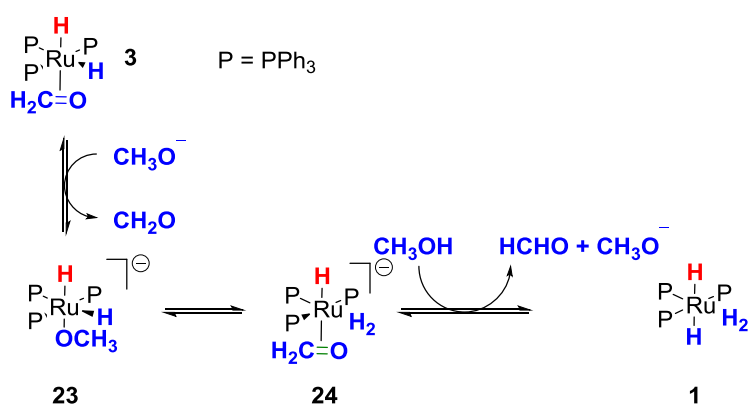
**Scheme 5.2.4** A plausible reaction mechanism for the formation of complex **5** and **16** starting from **7** by decarbonylation of  $\text{CH}_3\text{OH}$  (**a**) or  $\text{CD}_3\text{OD}$  (**b**).

A plausible reaction mechanism for the formation of complex **5** starting from **7** by decarbonylation of  $\text{CH}_3\text{OH}$  is depicted in Scheme 5.2.4 (a) and it involves two subsequent H abstractions with final release of  $\text{H}_2$  into the reaction medium.

In the reaction involving  $\text{CH}_3\text{OH}$  at lower temperature we observed almost a simultaneously formation of complex **5** and the three intermediates that have been identified as the species **1**,

**20** and **21**. Unlike the experiment with CD<sub>3</sub>OD, complex **5** was always present even when the reaction was performed at lower temperature and for short reaction time (8 min), therefore we can hypothesise that intermediates **20** and **21** arise from intermediate **1** which may undergo loss of H<sub>2</sub> followed by rapid coordination of N<sub>2</sub> (when present) or PPh<sub>3</sub>. Intermediate [RuH<sub>2</sub>(PPh<sub>3</sub>)<sub>3</sub>] (**2**), however, was never observed, probably because of its tendency to disproportionate to **21** and a generic [RuH<sub>2</sub>(L)<sub>2</sub>(PPh<sub>3</sub>)<sub>2</sub>], as reported by Halpern et al.<sup>[8]</sup>

The tetrahydride species may be formed from the intermediate **3** according to a hypothetical mechanism summarised below.



**Scheme 5.2.5** Proposed mechanism for the formation of [RuH<sub>2</sub>(H<sub>2</sub>)(PPh<sub>3</sub>)<sub>3</sub>] (**2**) by reaction of **7** with NaOCH<sub>3</sub>. Between compound **24** and **1** there are several steps.

While it was easier to justify the presence of the three intermediates when using only CH<sub>3</sub>OH, it became more challenging when only deuterated solvents (CD<sub>3</sub>OD and toluene-d<sub>8</sub>) were employed because both **1** and **21** appear to contain hydrides and not deuterides.

The extra hydrides (2 to 4) present in the reaction with CD<sub>3</sub>OD may be attributable to an intramolecular exchange of <sup>2</sup>H and *ortho*-deuteration of the phenyl rings of the PPh<sub>3</sub> ligands. Linn and Halpern, in a paper concerning the coordination chemistry of ruthenium polyhydrides in catalytic hydrogenation of ketones and arenes and related kinetic studies, described that, when a solution of [RuH<sub>2</sub>D<sub>2</sub>(PPh<sub>3</sub>)<sub>3</sub>] in THF (prepared by reaction of [RuH<sub>2</sub>(N<sub>2</sub>)(PPh<sub>3</sub>)<sub>3</sub>] with D<sub>2</sub>) was heated to 30 °C, intramolecular exchange with the *ortho* phenyl hydrogens was observed by <sup>2</sup>H NMR studies.<sup>[8]</sup> In a complementary work, Gusev et al. reported that complex **1** in toluene-d<sub>8</sub> under a D<sub>2</sub> atmosphere undergoes isotopic substitution of the hydride ligands and incorporation of deuterium into the *ortho* positions of the phenyl rings of the PPh<sub>3</sub> ligands (<sup>1</sup>H



NMR evidence).<sup>[9a]</sup> These two studies allowed us to strengthen our hypothesis concerning the formation of **5** as minor species, besides the formation of the two different isomers of **16** as final species, in the presence of only deuterated solvents and reagents. In the reported reaction, evidence of *ortho*-deuteration was observed in the corresponding  $^2\text{H}\{^1\text{H}\}$  NMR spectrum in  $\text{CH}_2\text{Cl}_2$  (Figure 5.2.6). The resonances at 7.72, 7.30 and 7.24 ppm may be attributable to  $^2\text{H}$  in the *ortho* positions of the phenyl rings of the phosphine ligands respectively in the three different complexes.<sup>[8]</sup>

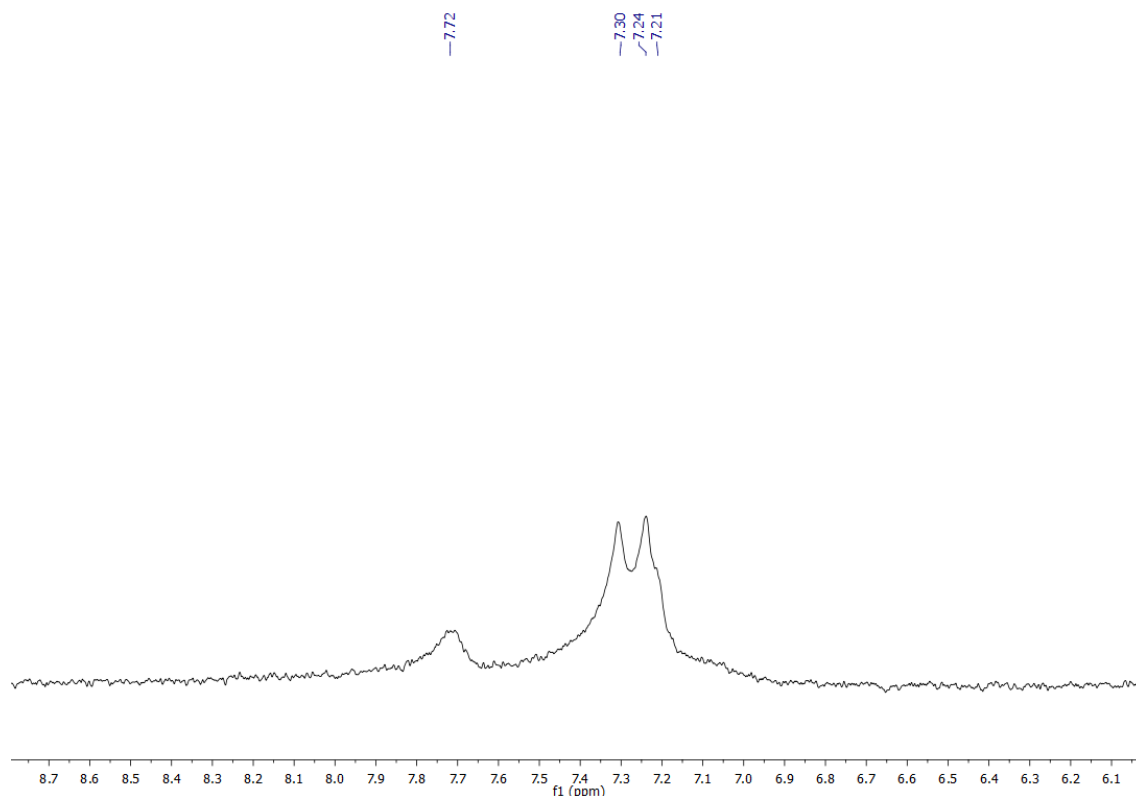
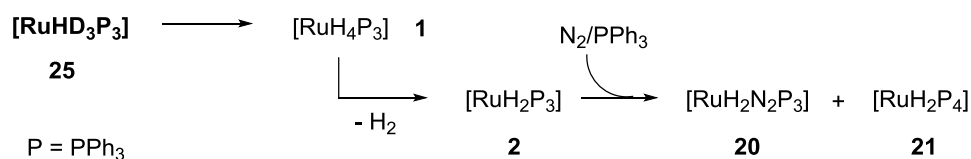


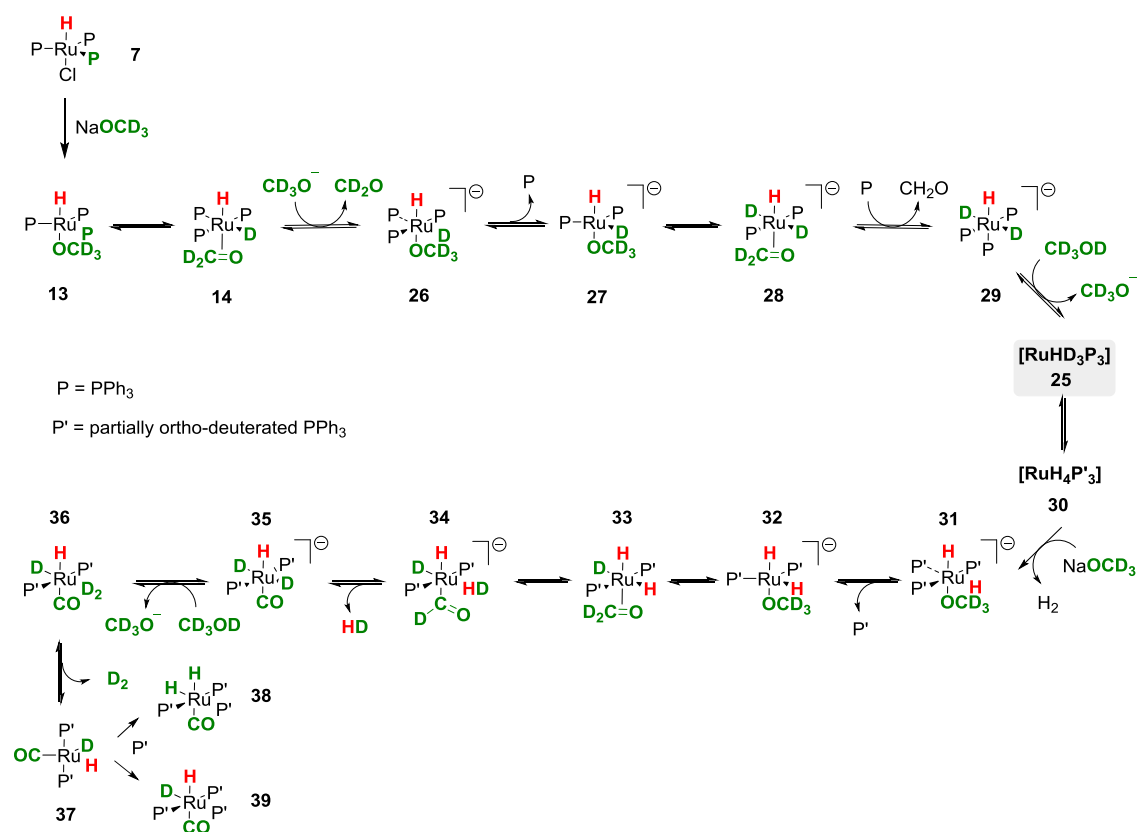
**Figure 5.2.6** Part of the  $^2\text{H}\{^1\text{H}\}$  NMR spectrum ( $\text{CH}_2\text{Cl}_2$ ) showing the resonances potentially attributable to  $^2\text{H}$  in the *ortho* positions of the phenyl rings of the phosphine ligands of complex **16** (two isomers) and **5**.

The tetrahydride species **1** observed prior to formation of complex **5** can arise from a  $[\text{RuHD}_3\text{P}_3]$  intermediate **25** by rapid exchange of  $^2\text{H}$  with the *ortho* hydrogens of the phenyl ring, as previously reported. Once formed, complex **1** can generate intermediates **20** and **21** with a mechanism similar to the one involved when using non-deuterated solvents (Scheme 5.2.6). These two complexes, however, have been reported always by Halpern and co-workers to arise from **1** by rapid substitution of  $\text{N}_2$  or  $\text{PPh}_3$ , probably by dissociation of  $\text{H}_2$ .



**Scheme 5.2.6** Plausible steps involved in the formation of complexes **1**, **20** and **21** prior formation of **5** when employing only deuterated solvents.

The missing link at this stage concerns the formation of this potential intermediate **25** for which we report therefore a plausible mechanism starting from a methoxide derivative along with an alternative pathway for the synthesis of complex **39** which proceeds via bis-phosphine intermediates starting from the formaldehyde complex **33**. The proposed path from **33** is designed following the key intermediates of the anionic reaction *pathway G* investigated in the corresponding paper (Scheme 5.2.7).<sup>[3]</sup>



**Scheme 5.2.7** Proposed mechanism for the formation of the key intermediate **25** along with an alternative pathway for the synthesis of complex **39** via bisphosphine intermediates.

### 5.3 Conclusions and Future Work

In this chapter we presented part of a combined computational and experimental mechanistic study concerning methanol decarbonylation, an important side-reaction that occurs during the alcohol dehydrogenation process catalysed by a classic homogeneous ruthenium catalyst  $[\text{RuH}_2(\text{H}_2)(\text{PPh}_3)_3]$ . H/D and  $^{12}\text{C}/^{13}\text{C}$  KIEs are a useful tool for detecting the rate-limiting step in these multiple pathways reaction mechanisms. The work previously published comprises the full characterization of three distinct decarbonylation pathways, neutral or anionic. Kinetic isotope effects (KIEs) were computed for all pathways and predicted experimentally for one specific decarbonylation path designed to proceed via  $[\text{RuH}(\text{OCH}_3)(\text{PPh}_3)_3]$ . The good agreement between computed and experimental KIEs (observed  $k_{\text{H}}/k_{\text{D}} = 4$ ) disclosed that the rate-limiting step for methanol decarbonylation is the formation of the first agostic intermediate from a transient formaldehyde complex.

Unexpected reaction intermediates have come to light from additional experiments leading to the design of new reaction channels. An interesting outcome was observed in the synthesis of  $[\text{RuHD}(\text{CO})(\text{PPh}_3)_3]$  when using only  $\text{CD}_3\text{OD}$ . The desired species was present as two different isomers along with minor amounts of the corresponding dihydrido carbonyl species which was ascribed to an intramolecular exchange of  $^2\text{H}$  and *ortho* C-H deuteration of the phenyl rings of phosphine ligands.  $[\text{RuH}_2(\text{PPh}_3)_4]$  and  $[\text{RuH}_2(\text{H}_2)(\text{PPh}_3)_3]$  were also observed during the synthesis of  $[\text{RuHD}(\text{CO})(\text{PPh}_3)_3]$  and  $[\text{RuH}_2(\text{CO})(\text{PPh}_3)_3]$  when using respectively  $\text{CD}_3\text{OD}$  and  $\text{CH}_3\text{OH}$ . Although a detailed mechanism was proposed for both cases, the complicated nature of these kind of systems due to multiple and sometimes cross-linked reaction channels, requires a more detailed investigation from a computational and experimental point of view.

## 5.4 Experimental Section

### 5.4.1 General materials and methods

All manipulations and reactions were carried out under Ar or N<sub>2</sub> gas when not specified (dried through a Cr(II)/silica packed glass column) using different techniques including a standard Schlenk, vacuum line and a glove box. Solvents were degassed prior to use and dried when required.

RuCl<sub>3</sub>·3H<sub>2</sub>O was purchased from Alfa Aesar. All solvents were purchased from Sigma-Aldrich.

Toluene was dried using a Braun Solvent Purification System. Methanol was dried and degassed by distillation from magnesium under dinitrogen.

[RuCl<sub>2</sub>(PPh<sub>3</sub>)<sub>3</sub>]<sup>[11]</sup> (**40**), [RuHCl(PPh<sub>3</sub>)<sub>3</sub>]<sup>[12]</sup> (**7**), [RuH<sub>2</sub>(H<sub>2</sub>)(PPh<sub>3</sub>)<sub>3</sub>]<sup>[9a,10]</sup> (**1**) and [RuH<sub>2</sub>(PPh<sub>3</sub>)<sub>4</sub>]<sup>[10]</sup> (**21**) were prepared by published procedures and all observations and NMR data were in accordance with those reported in the literature, except for complex **21** where no NMR data were available. [RuH<sub>2</sub>(CO)(PPh<sub>3</sub>)<sub>3</sub>] (**5**) was prepared by an adaptation of a literature method.<sup>[4]</sup> Sodium methoxide was prepared by reacting sodium metal (supplied by Lancaster Synthesis in mineral oil; the small pieces were washed with hexane) with degassed CH<sub>3</sub>OH, CD<sub>3</sub>OD or <sup>13</sup>CH<sub>3</sub>OH. Triethylamine was purchased from Fischer Scientific and degassed before use. Toluene and diethyl ether were dried using a Braun Solvent Purification System. Methanol was dried and degassed by distillation from magnesium methoxide under dinitrogen. Unless otherwise stated all chemicals were purchased from Aldrich. All gases were purchased from BOC gases. All solvents and deuterated solvents, which were not previously dried, were only degassed prior to use.

### 5.4.2 General instruments

NMR spectra were recorded on a Bruker Avance II 400 and 500 MHz Spectrometer (<sup>1</sup>H NMR at 400 MHz and <sup>13</sup>C NMR at 100 MHz and <sup>1</sup>H NMR at 500 MHz and <sup>13</sup>C NMR at 125 MHz respectively) at room temperature. <sup>1</sup>H and <sup>13</sup>C{<sup>1</sup>H} NMR spectra are referenced to TMS and the residual proton signal of the solvent was used as internal standard. When necessary <sup>2</sup>H{<sup>1</sup>H} NMR spectra were recorded on a 500 MHz Spectrometer.

$^1\text{H}$  NMR solvent residual signals:  $\text{CD}_2\text{Cl}_2$  set at 5.32 ppm; toluene- $\text{d}_8$  at 2.08 ppm; THF- $\text{d}_8$  at 1.72 ppm.  $^{13}\text{C}\{^1\text{H}\}$  NMR solvent signals:  $\text{CD}_2\text{Cl}_2$  set at 53.84 ppm, toluene- $\text{d}_8$  at 20.43 ppm; THF- $\text{d}_8$  at 25.31 ppm.<sup>[13]</sup>

### 5.4.3 Synthetic procedures and mechanistic studies

#### 5.4.3.1 $[\text{RuH}_2(\text{CO})(\text{PPh}_3)_3]$ (**5**) Carbonyldihydridotris(triphenylphosphine)ruthenium(II)

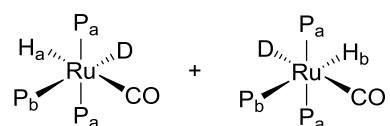
It was prepared by an adaptation of a literature method<sup>[4]</sup>. Sodium methoxide was prepared by reacting sodium metal with  $\text{CH}_3\text{OH}$ , under an inert atmosphere of dinitrogen and the formed solution was subsequently added to a suspension of **7** (0.015 g, 0.016 mmol) in toluene (3 mL). After refluxing the reaction mixture for 1 h at 100 °C, the resulting orange solution was cooled to RT and evaporated to dryness. The recovered solid was washed once with dry and degassed methanol, in order to remove the methoxide, and dried *in vacuo*. The collected yellow solid was finally analysed via NMR spectrometry (toluene- $\text{d}_8$ ).

The  $^1\text{H}$  and  $^{31}\text{P}\{^1\text{H}\}$  spectral data are identical to those described in the literature.<sup>[7]</sup>

#### 5.4.3.2 Mixture $[\text{RuHD}(\text{CO})(\text{PPh}_3)_3]$ (**16**) (major species) and $[\text{RuH}_2(\text{CO})(\text{PPh}_3)_3]$ (**5**) (minor)

As above for **5** except that the methoxide was obtained by reacting sodium (0.01 g, 0.43 mmol) with  $\text{CD}_3\text{OD}$  (0.2 mL, 4.94 mmol). The recovered yellow solid was washed once with dry and degassed  $\text{CD}_3\text{OD}$ , in order to remove the methoxide, filtered and dried *in vacuo* and finally analysed via NMR spectrometry (toluene- $\text{d}_8$ ).

#### Complex (**16**): two isomers



$^1\text{H}$  NMR (400 MHz; toluene- $\text{d}_8$ ):  $\delta = -6.58$  (td, 1H,  $J_{\text{H-P}_b} = 15.11$  and  $J_{\text{H-P}_a} = 30.9$  Hz, H *trans* to CO),  $-8.41$  (dt, 1H,  $J_{\text{H-P}_b} = 28.78$  and  $J_{\text{H-P}_a} = 73.9$  Hz, H *cis* to CO) ppm.

$^{31}\text{P}\{^1\text{H}\}$  NMR (400 MHz, toluene- $\text{d}_8$ ):  $\delta = 57.1$  (br, 4P, mutually *trans* P),  $44.8$  (br, 2P, unique P) ppm.

$^2\text{H}\{^1\text{H}\}$  NMR (500 MHz;  $\text{CH}_2\text{Cl}_2$ ):  $\delta = 7.7, 7.30, 7.2$  ( $^2\text{H}$ , *ortho* position in the *phenyl* rings) ppm.

#### 5.4.3.3 Potential $[\text{RuD}_2(\text{CO})(\text{PPh}_3)_3]$ (19)

For amount refer to § 5.4.3.2. The experiment was performed at RT for 8 min. The reaction was stopped as soon as the mixture turned from purple to orange. The mixture was then reduced to dryness affording a brown solid which was subsequently washed with  $\text{CD}_3\text{OD}$ , filtered using a canula filtration and dried again under vacuum. The collected yellow solid was analysed via NMR spectroscopy.

$^1\text{H}$  NMR (400 MHz;  $\text{THF-d}_8$ ): no signals in the hydride region.

$^{31}\text{P}\{^1\text{H}\}$  (400 MHz;  $\text{THF-d}_8$ ): 57.4 (br, 2P, mutually *trans* P), 44.9 (br, 1P, unique P).

#### 5.4.3.4 $[\text{RuH}_2(^{13}\text{CO})(\text{PPh}_3)_3]$ (12) (experiment used for determining the KIE)

As above for **5** except that the methoxide was obtained by reacting sodium (0.01 g, 0.43 mmol) with  $^{13}\text{CH}_3\text{OH}$  (0.2 mL, 4.94 mmol).

$^1\text{H}$  NMR (400 MHz; toluene- $\text{d}_8$ ):  $\delta = -6.5$  ppm (tddd,  $^2J_{\text{H}\alpha\text{-C}} = 18.7$  Hz,  $\text{H}_\alpha$  *trans* to CO),  $-8.4$  (dt,  $J_{\text{Hb-C}} = J_{\text{H-H}} = 6.4$  Hz,  $\text{H}_\text{b}$  *cis* to CO) ppm.

$^{31}\text{P}\{^1\text{H}\}$  (400 MHz; toluene- $\text{d}_8$ ):  $\delta = 57.4$  (dd, 2P,  $J_{\text{P-P}} = 17.5$  and  $J_{\text{P-C}} = 7.46$  Hz, mutually *trans* P) 45.3 (td, 1P,  $J_{\text{P-P}} = 17.5$  and  $J_{\text{P-C}} = 9.3$  Hz, unique P) ppm.

$^{13}\text{C}\{^1\text{H}\}$  NMR (400 MHz; toluene- $\text{d}_8$ ):  $\delta = 207.4$  (q,  $J_{\text{C-P}} = 8.3$  Hz, CO), 140.7 (vt,  $J_{\text{C-P+CP'}} = 40.8$  Hz,  $\text{C}_{\text{ipso}}$ , mutually *trans* phosphines), 138.9 (d,  $J_{\text{C-P}} = 28.4$  Hz,  $\text{C}_{\text{ipso}}$  unique phosphine).

#### 5.4.3.5 Mixture of $[\text{RuH}_2(^{13}\text{CO})(\text{PPh}_3)_3]$ (12) and $[\text{RuHD}(\text{CO})(\text{PPh}_3)_3]$ (16) (experiment used for determining the KIE)

As above for **5** except that the methoxide was obtained by reacting equal amounts of  $^{13}\text{CH}_3\text{OH}$  (0.2 mL, 4.94 mmol) and  $\text{CD}_3\text{OD}$  (0.2 mL, 4.94 mmol), each containing sodium metal (0.01 g, 0.43 mmol).

#### 5.4.3.6 Mixture of $[\text{RuH}_2(\text{CO})(\text{PPh}_3)_3]$ (**5**) and $[\text{RuHD}(\text{CO})(\text{PPh}_3)_3]$ (**16**) (experiment used for determining the KIE)

As above for **5** except that the methoxide was obtained by reacting equal amounts of  $\text{CH}_3\text{OH}$  (0.2 mL, 4.94 mmol) and  $\text{CD}_3\text{OD}$  (0.2 mL, 4.94 mmol), each containing sodium metal (0.01 g, 0.43 mmol) to form the methoxide.

#### 5.4.3.7 Time and temperature dependent NMR studies with $\text{NaOCD}_3$

A solution of  $\text{CD}_3\text{OD}$  (0.4 mL, 9.8 mmol) containing sodium metal (0.02 g, 0.87 mmol) to form the methoxide, was added to a suspension of **7** (0.06 g, 0.065 mmol) in toluene- $d_8$  (3 mL). The experiment was performed using a ramping temperature (20 min at RT, heated under reflux to 55 °C for 40 min and subsequently to 100 °C for 30 min) with continuously sampling at each ramping temperature step with immediate cooling to room temperature and collection of the NMR spectrum.

Three intermediates were identified via  $^1\text{H}$  NMR: **int. I**  $[\text{RuH}_2(\text{H}_2)(\text{PPh}_3)_3]$  (**1**), **int. II**  $[\text{RuH}_2(\text{N}_2)(\text{PPh}_3)_3]$  (**20**) and **int. III**  $[\text{RuH}_2(\text{PPh}_3)_4]$  (**21**). The  $^1\text{H}$  spectral data of **1**<sup>[9a]</sup> and **20**<sup>[8]</sup> are identical to those described in the literature. Spectral data of **21** are described later on.

#### 5.4.3.8 Time and temperature dependent NMR studies with $\text{NaOCH}_3$

A solution of  $\text{CH}_3\text{OH}$  (0.4 mL, 9.8 mmol) containing sodium metal (0.02 g, 0.87 mmol) to form the methoxide, was added to a suspension of **7** (0.06 g, 0.065 mmol) in toluene- $d_8$  (3 mL). The experiment was performed using a ramping temperature (15 min at RT, heated under reflux to 55 °C for 45 min and subsequently to 100 °C for 30 min) with continuously sampling at each ramping temperature step with immediate cooling to room temperature and collection of the NMR spectrum.

#### 5.4.3.9 Identification of $[\text{RuH}_2(\text{N}_2)(\text{PPh}_3)_3]$ (**20**)

Complex **7** (0.03 g, 0.032 mmol) was suspended in toluene (2 mL) and reacted with  $\text{NaOCD}_3$ , obtained by reaction of sodium metal (0.01 g, 0.43 mmol) with  $\text{CD}_3\text{OD}$  (0.2 mL, 4.9 mmol), at RT for 5 min under Ar. The reaction was stopped as soon as the mixture turned from purple to

red/orange and the flask placed in a cold bath (dry ice/acetone). The mixture was then reduced to dryness affording an orange solid which was subsequently washed with CD<sub>3</sub>OD, filtered using a canula filtration and dried again under vacuum. The collected solid was analysed via NMR spectroscopy and <sup>1</sup>H spectral data were in agreement with those reported in the literature.<sup>[8]</sup>

#### 5.4.3.10 Identification of [RuH<sub>2</sub>(PPh<sub>3</sub>)<sub>4</sub>] (**21**)

Complex **21** was synthesised under argon according to literature procedure.<sup>[10]</sup>

<sup>1</sup>H NMR (400 MHz; toluene-d<sub>8</sub>): δ = -10.2 ppm (m, 2H, AA'MM'X<sub>2</sub>, J<sub>H-P cis</sub> = 34.5 Hz, J<sub>H-P trans</sub> = 70.3 Hz) ppm.

<sup>31</sup>P{<sup>1</sup>H} NMR (400 MHz; toluene-d<sub>8</sub>): δ = 49.1 (t, 2P, J<sub>P-P</sub> = 14.0 Hz), 41 (t, 2P, J<sub>P-P</sub> = 12.4 Hz) ppm.

## 5.5 References

- [1] a) D. Morton, D. J. Cole-Hamilton, *J. Chem. Soc., Chem. Commun.* **1988**, 1154-1156; b) D. Morton, D. J. Cole-Hamilton, I. D. Utuk, M. Paneque-Sosa, M. Lopez-Poveda, *J. Chem. Soc., Dalton Trans.* **1989**, 489-495.
- [2] O. P. Tormakangas, A. M. P. Koskinen, *Recent Res. Dev. Org. Chem.* **2001**, 5, 225-255.
- [3] N. Sieffert, R. Reocreux, P. Lorusso, D. J. Cole-Hamilton, M. Buehl, *Chem. Eur. J.* **2014**, 20, 4141-4155.
- [4] B. N. Chaudret, D. J. Cole-Hamilton, R. S. Nohr, G. Wilkinson, *J. Chem. Soc., Dalton Trans.* **1977**, 1546-1557.
- [5] N. Sieffert, M. Buehl, *J. Am. Chem. Soc.* **2010**, 132, 8056-8070.
- [6] W. Baratta, M. Ballico, A. Del Zotto, E. Herdtweck, S. Magnolia, R. Peloso, K. Siega, M. Toniutti, E. Zangrando, P. Rigo, *Organometallics* **2009**, 28, 4421-4430.
- [7] H. Samouei, V. V. Grushin, *Organometallics* **2013**, 32, 4440-4443.
- [8] D. E. Linn, Jr., J. Halpern, *J. Am. Chem. Soc.* **1987**, 109, 2969-2974.
- [9] a) D. G. Gusev, A. B. Vymenits, V. I. Bakmutov, *Inorg. Chim. Acta* **1991**, 179, 195-201; b) R. H. Crabtree, D. G. Hamilton, *J. Am. Chem. Soc.* **1986**, 108, 3124-3125.
- [10] R. O. Harris, N. K. Hota, L. Sadavoy, J. M. C. Yuen, *J. Organometal. Chem.* **1973**, 54, 259-264.
- [11] P. S. Hallman, T. A. Stephenson, G. Wilkinson, *Inorg. Synth.* **1970**, 12, 237-240.
- [12] a) R. A. Schunn, E. R. Wonchoba, *Inorg. Synth.* **1971**, 13, 131-134 ; b) R. A. Schunn, E. R. Wonchoba, G. Wilkinson, *Inorg. Synth.* **2007**, 13, 131-134 (online publication); c) P. S. Hallman, B. R. McGarvey, G. Wilkinson, *J. Chem. Soc. A* **1968**, 3143-3150.
- [13] G. R. Fulmer, A. J. M. Miller, N. H. Sherden, H. E. Gottlieb, A. Nudelman, B. M. Stoltz, J. E. Bercaw, K. I. Goldberg, *Organometallics* **2010**, 29, 2176-2179.



# Chapter 6

## Intermolecular alkylation of carbonyl compounds via coinage metal catalysed C-H bond activation

Ketones, in particular 3-pentanone and 2-butanone, have been investigated as potential substrates in the formation of methyl methacrylate (MMA).  $\alpha$ -Hydoxymethylenation followed by dehydration and Baeyer-Villager oxidation, possibly catalysed by enzymes to reverse the normal selectivity could be a new route to acrylate esters. The catalytic reaction is enabled by a gold carbene hydroxide complex that can act as a catalyst or catalyst precursor in such a way that a substrate undergoes C-H activation and the subsequent metal alkyl can act as a nucleophile towards an electrophilic substrate, in this case formaldehyde.

---

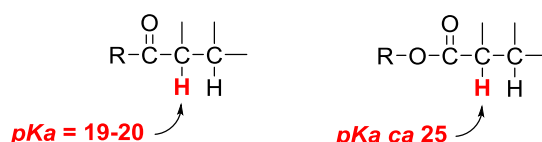
**Keywords:** C-H activation · paraformaldehyde · gold · alkylation · ketones

## 6.1 Introduction

The production of methyl methacrylate (MMA) from a variety of substrates involving more environmental friendly processes has been widely developed and the Lucite Alpha Plant is the result of nearly two decades of R&D studies.<sup>[1]</sup> Although the simple base-catalysed condensation of methyl propanoate (MeP) with formaldehyde has been extensively investigated, the commercialized second stage still suffers of low efficiency with a maximum conversion of 27 % achieved with multiple steps, as already reported in Chapter 1.<sup>[2]</sup>

In Chapter 3 we provided an innovative study concerning the possibility of performing the  $\alpha$ -methylenation of MeP using methanol as *in situ* source of anhydrous formaldehyde. The base-catalysed condensation process of the new formed formaldehyde with MeP affords an intermediate, which spontaneously dehydrates to MMA. Despite the preliminary encouraging results, the achieved yields of MMA and MiBu respectively were still not competitive with those obtained with the current commercialised second stage. The main reason is the extensive formation of sodium propanoate from an unusual reaction of MeP with the base (see Chapter 3). The poor improvements in this field led our attention to a completely different approach for MMA production which involved the investigation of ketones as substrates to accomplish our target. In particular 3-pentanone (DEK) and 2-butanone (MEK) that, once alkylated, could be oxidised to the corresponding esters via a Baeyer-Villiger (BV) reaction and provide MMA as final product (we return to the description of this reaction later on) were seen as possible substrates.

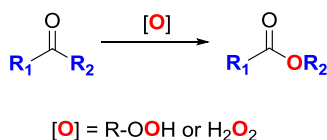
The advantages of ketones, compared to MeP and related esters, are twofold: they do not have a hydrolysable bond and the  $\alpha$ -protons are more acidic (typical  $pK_a$  of  $\alpha$ -protons is 19-20<sup>[3]</sup> while *ca* 25<sup>[4]</sup> for esters; scheme 6.1.1).



**Scheme 6.1.1**  $pK_a$  values of  $\alpha$ -protons of different carbonyl compounds.<sup>[3-4]</sup>

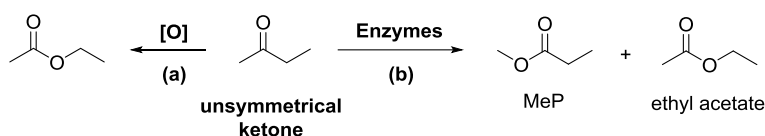
The above cited Baeyer-Villiger oxidation is a very popular organic reaction for the conversion of ketones to esters (Scheme 6.1.2) and cyclic ketones to lactones, discovered for the first time almost 100 years ago.<sup>[5]</sup> In general, in the case of unsymmetrical substrates, the more highly

substituted group migrates via oxidative cleavage of a C-C bond adjacent to a carbonyl, because of the greater ability of the more electron rich group to stabilise a positive charge in the transition state.



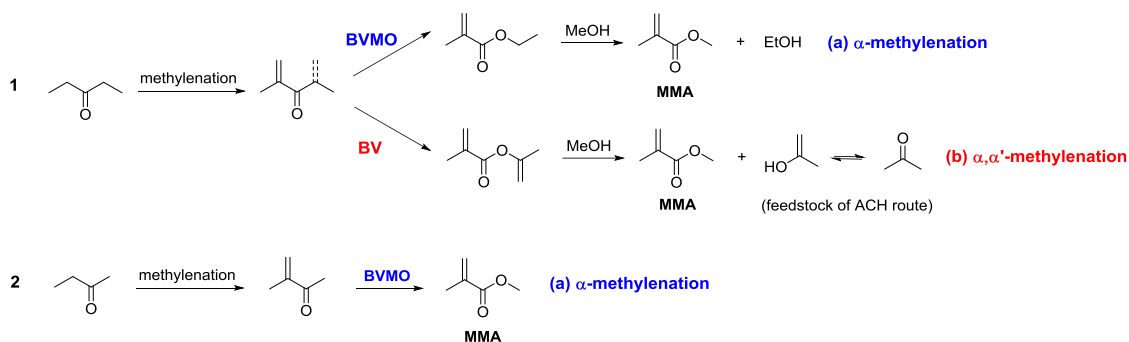
**Scheme 6.1.2** Reaction stoichiometry for a general Bayer-Villiger oxidation.

The most common reagents used to carry out this rearrangement, are hydrogen peroxide and peracids such as *meta*-chloroperoxybenzoic acid (*m*CPBA), peroxybenzoic acid and trifluoroperoxyacetic acid (TFPAA).<sup>[6]</sup> To avoid the use of peracids “green” methods have been developed involving the use of metal catalysts,<sup>[7]</sup> organometallic compounds<sup>[8]</sup> and recently also compressed CO<sub>2</sub> as an alternative reaction medium.<sup>[9]</sup> However a bio-catalytic Baeyer-Villiger oxidation is a more appealing environmental benign process.<sup>[10]</sup> The biological Baeyer-Villiger reaction has already been used by Lucite Int. to produce MeP, together with ethyl acetate (Scheme 6.1.3) from MEK with approximately 27 % yield with oxidation of the less substituted group.<sup>[11]</sup>



**Scheme 6.1.3** Products obtained by classical BV oxidation (a) and enzymatic BV (b) starting from unsymmetrical substrate.

Ideally, the employment of MEK or DEK as substrates, followed by methylenation and subsequent oxidation to the corresponding ester via classical or enzymatic BV reaction (Scheme 6.1.4), would allow us to by-pass problems so far depicted concerning the use of MeP as a substrate for formylation reactions.



**Scheme 6.1.4** Reaction idea for MMA synthesis from DEK (1) or MEK (2) via  $\alpha$ -methylenation and subsequent oxidation using Baeyer-Villager monooxygenase (BVMO) (a) or  $\alpha, \alpha'$ -methylenation and subsequent BV oxidation (b).

In this chapter we will discuss the possibility of performing transition metal catalysed C-C bond formation using formaldehyde as a one carbon alkylating agent involving C(sp<sup>3</sup>)-H bond activation.

Selective C-H bond activation and functionalisation processes catalysed by transition metal complexes have become a topic of great interest over the last 30 years as evidenced by the huge number of works published.<sup>[12]</sup> One of the reasons, for example, is represented by the fact that hydrocarbons, important feedstocks in several industrial processes, are inefficiently used due to the general unreactive nature of  $\sigma$ -bonds. Selective C-H activation also allows the introduction of functional groups into a molecule, thus reducing the number of steps in the total synthesis methods commonly used in drug discovery.<sup>[13]</sup>

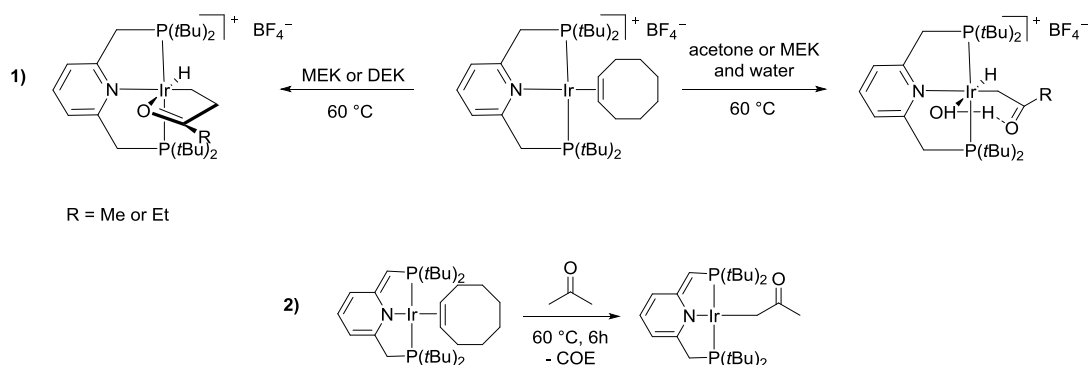
As described by Shilov and Shul'pin in one of the very first reviews<sup>[12a]</sup> on the subject, the "activation" is a process where the strong and inert  $\sigma$ -bond such as C-H bond is replaced with a more reactive one in order to increase its reactivity towards a reagent. In the limited case of C-H activation promoted by metal complexes, the activation could be considered as a process involving the cleavage of the C-H bond and binding of the substrate to a metal centre which results in the formation of organometallic compounds. Based on this mechanism, Shilov and Shul'pin proposed three classes of C-H bond cleavage. The first type, so called "true" activation, involves the direct participation of a transition metal ion in the formation of a  $\sigma$ -organyl derivative, containing the M-C bond, as an intermediate or final product. The C-H bond cleavage can occur via oxidative addition or an electrophilic substitution mechanism. In the second type there is no direct contact between the metal centre and the C-H bond, the metal complex promotes the C-H bond cleavage through the ligand without generating a  $\sigma$ -M-C bond

at any stage. The third type always according to Shilov and Shul'pin excludes any direct contact between the metal complex and the molecule containing the C-H bond, the metal complex only promotes the formation of a reactive species which then cleaves the C-H bond.<sup>[12a]</sup> More recently Labinger and Bercaw re-defined five different classes of activation reaction mechanisms: (i) oxidative addition, (ii)  $\sigma$ -bond metathesis, (iii) metalloradical activation, (iv) 1,2-addition and (v) electrophilic activation. The first four pathways lead to the formation of stable organometallic species while in the fifth one the organometallic species is described as a reaction intermediate.<sup>[14]</sup>

Once selectively activated, the C-H bond can be functionalised via a catalytic process.

Pincer-type complexes have been among the most attractive and studied systems for promoting both stoichiometric and catalytic C-H activations.<sup>[15]</sup> In particular, iridium pincer variants have been described as exceptionally active catalysts.<sup>[15a, 16]</sup>

Among this class of pincer-type complexes we report  $[\text{Ir}(\text{PNP})(\text{COE})][\text{BF}_4]$  (PNP = 2,6-bis((*di*tertbutylphosphino)methyl)pyridine). In a recent paper Milstein and co-workers reported the effect of water on the regioselectivity of  $sp^3$  C-H activation of ketones. In the absence of water the Ir complex selectively promotes the C-H activation of the  $\beta$ -protons despite the greater acidity of the  $\alpha$ -protons, while<sup>[17]</sup> addition of water modulates the regioselectivity of the reaction favouring activation in the  $\alpha$ -position instead (Scheme 6.1.5, reaction 1) and in a subsequent paper they also reported the synthesis of a stable Ir(I) acetylonyl PNP complex involving a reversible ligand dearomatisation mechanism (Scheme 6.1.5, reaction 2).<sup>[16a]</sup>



**Scheme 6.1.5** Milstein's *et al.* work: **1**) effect of water on the regioselectivity of  $sp^3$  C-H activation of ketones; **2**) synthesis of an Ir(I) acetylonyl PNP complex.

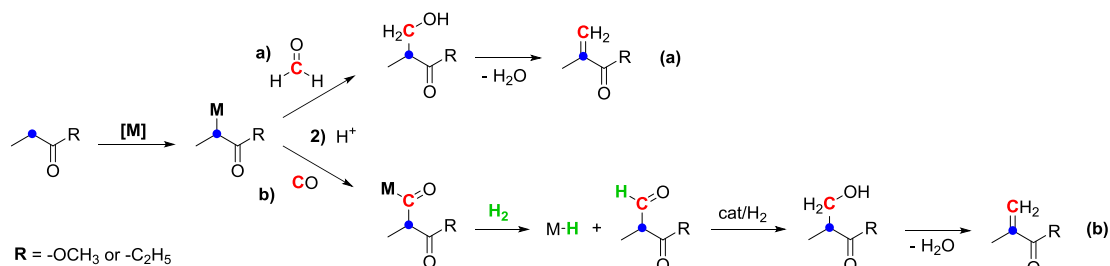
Inspired by Milstein's work, some members of our group recently published a similar approach for the  $\alpha$ -C-H bond activation of MeP. Unlike Milstein's work, in the presence of water, methyl propanoate does not undergo  $\alpha$ -C-H activation, instead the expected hydrolysis of the ester bond occurs leading to the formation of propanoic acid and methanol which respectively generate an Ir(I) propanoate and a carbonyl derivative (the latter via an alcohol decarbonylation mechanism). Reactions of MeP with [Ir(PNP)(COE)][BF<sub>4</sub>] in the absence of added water on the other hand led to selective C-H activation of the methoxy group to give [Ir(H)(PNP){CH<sub>2</sub>OC(O)CH<sub>2</sub>CH<sub>3</sub>}] [BF<sub>4</sub>].<sup>[18]</sup>

Nolan and co-workers have recently reported a series of late-transition metal (LTM) hydroxides and their employment in catalysis, bond activation reactions and synthesis.<sup>[19]</sup> When the M-OH bond is stabilized by coordination of the metal centre to electron-rich NHC ligands these complexes show an interesting reactivity due to the hard base/soft acid behaviour of respectively the hydroxide moiety and the low oxidation state metal centre.<sup>[19b]</sup>

At this stage of our study these well defined NHC-bearing M(I)-hydroxide complexes, where the hydroxide moiety can act as an intramolecular base, were considered promising catalysts for promoting the reaction between ketones and formaldehyde.

## 6.2 Results and Discussion

Since our intention is to study the methylenation of ketones using formaldehyde (first step of reactions 1 and 2 in Figure 6.1.4), we anticipated that, upon coordination to a metal centre, the more reactive C-H bond would then react with formaldehyde (condensation process) or could be functionalised via CO insertion. The first process (Figure 6.2.1-a) produces an alkylated intermediate which in turn dehydrates (spontaneously or assisted) to the desired methylenated derivative, while the second (Figure 6.2.1-b) generates an aldehyde as the final product, which could be hydrogenated to the desired alcohol for dehydration in a subsequent step. The two potential functionalisation pathways may depend on the nature of the transition metal complex involved as well as the reagent (CO or formaldehyde).



**Scheme 6.2.1** Reaction concept for C(sp<sup>3</sup>)-H functionalisation of carbonyl compounds using paraformaldehyde (a) or CO (b) as one carbon alkylating agent.

We started our investigation with three different M(I)-hydroxide complexes provided by the Nolan and Cazin group: [[Ir(cod)(IiPr)(OH)]]<sup>[19b]</sup> (**1**) (cod = 1,5-cycloocatadiene; IiPr = 1,3-(diisopropyl)imidazol-2-ylidene), [Cu(IPr)(OH)]<sup>[19g, 19h]</sup> (**2**) and [Au(IPr)(OH)] (**3**) (IPr = 1,3-bis(2,6-diisopropylphenyl)imidazol-2-ylidene) (for ref. *vide infra*) (see Figure 6.2.1).<sup>†</sup>

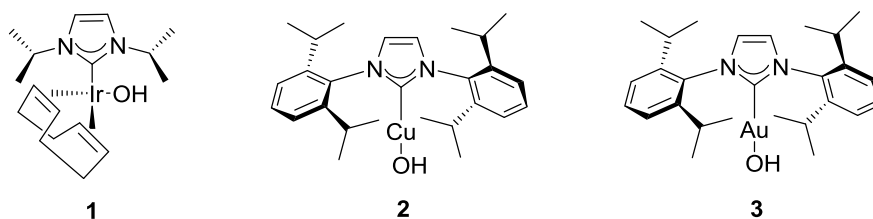


**Figure 6.2.1** LTM-OH investigated in the present study.

The four-coordinate Ir(I) complex **1** is a 16e<sup>-</sup> species with a ligand (cod) that can be easily displaced by another ligand and at the same time a vacant site on the metal centre, therefore once the M-C bond is formed it can be functionalised with CO through pre-coordination (substitution of cod or oxidative addition mechanism) and further CO insertion into the M-C bond. The Au(I) and Cu(I) species are 14e<sup>-</sup> which prefer two-coordinate linear geometry, so typically they are not involved in extra coordination processes, which is the reason why only reactivity towards formaldehyde would be explored in the present study.

A few attempts of  $\alpha$ -activation of DEK with **1** did not provide the expected results. The complicated NMR spectrum of the recovered solid did not allow us to fully identify the Ir species present in the mixture. However, an analysis of 1D and 2D (<sup>1</sup>H, <sup>1</sup>H) spectra did not

<sup>†</sup>Numbering code for cited compounds: metal complexes are listed in numerical order, while organic products in numerical order using **P** as prefix; abbreviations are used for organic substrates.

show evidence of C-H bond activation. Despite these results, one attempt of C-H functionalisation with CO was performed, giving as expected no evidence of CO insertion products. Based on these preliminary results and due to the nature of complex **1** (expensive, and air and nitrogen sensitive) we decided not to test its reactivity towards MeP (as mentioned in § 6.1 the  $\alpha$ -protons are less acidic).

Several examples of X-H activation performed by complex **2**, for which the reactivity is expected to be similar to that of the Au(I) congener, have been already reported, including its employment as a synthon for Cu-alkyl bond formation under mild conditions (RT and without addition of any other reagents). However, in the case of M-C bond formation, an important requirement concerns the acidity of the C-H bond to be activated, for which the  $pK_a$  must be less than 27-30 units; a condition fully satisfied by ketones but borderline for MeP.<sup>[19h]</sup>

Unlike those reported in the literature, C-H bond activation performed by complex **2** was not straightforward. After stirring a mixture of **2** in DEK at room temperature for 16 hours the recovered solid gave evidence of the starting complex as the major species and another Cu complex, possibly the desired Cu(I)-ketonyl complex with low conversion (further investigation is required). In an attempt to push the reaction to completion or at least to obtain the potential ketonyl complex as the major species and isolate it by crystallisation, the reaction was performed at 120 °C without any success, unfortunately. It would be probably worthwhile in the future to explore different reaction conditions that may lead to higher yields of the desired product.

Complex **3** is also a very well defined complex, for which the reactivity towards several substrates has been extensively investigated.<sup>[19g, 19i, 20]</sup> To our delight, Au-C bond formation was performed this time at room temperature without additional reagents affording the Au-ketonyl complex  $[\text{Au}(\text{IPr})\{\text{CH}(\text{CH}_3)\text{C}(\text{O})\text{C}_2\text{H}_5\}]$  (**4**) in ca 80 % isolated yield. One of the advantages of this reaction, compared to those involving complexes **1** and **2**, is that it can be conducted in air using technical grade solvents.

Hashmi and colleagues observed the direct auration of acetone while attempting to crystallise a  $[(\text{Mes}_3\text{P})\text{AuX}]$  ( $\text{Mes}_3\text{P} = (2,4,6\text{-Me}_3\text{C}_6\text{H}_3)_3\text{P}$ ) catalyst from acetone, as proof that C-H activation by gold, when assisted by proper coordinating groups, may occur under very mild conditions.<sup>[21]</sup>



Spectroscopic data were collected for complex **4** and are presented in detail in the experimental section. The methylene protons give rise to an AB pattern because they are diastereotopic.

The structure of **4** was also confirmed by crystallographic analysis (Figure 6.2.2). The C1-Au1-C32 angle was measured to be  $175.8(3)^\circ$  as expected for a linear complex and the 3-pentanone had been activated through the expected  $\alpha$ -C-H bond.

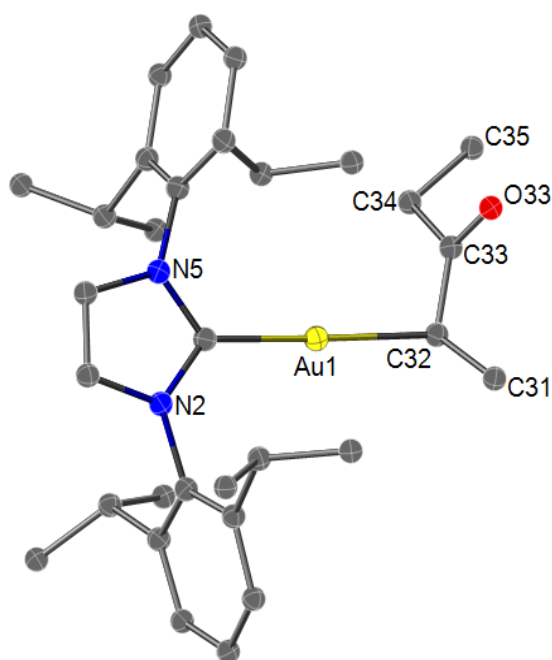


**Figure 6.2.2** Molecular representation of **4** showing 50 % thermal ellipsoids probability. Hydrogen atoms are omitted for clarity. Selected bond lengths [ $\text{\AA}$ ] and bond angles [ $^\circ$ ]: Au1-C1 2.011(7), Au1-C32 2.116(8), C1-Au1-C32  $175.8(3)$ .

Unfortunately, preliminary attempts to perform methylene activation of MeP with complex **4** were unsuccessful, but instead resulted in hydrolysis of the ester bond to provide a propanoate complex  $[\text{Au}(\text{IPr})\{\text{OC}(\text{O})\text{CH}_2\text{CH}_3\}]$  (**5**) (identified by NMR spectroscopy). Although suitable single crystals for X-ray analysis were not obtained, NMR assignments were easily confirmed by preparing complex **5** from a reaction of **3** with propanoic acid. Spectroscopic data collected for the product were in good agreement with those collected for the complex generated with MeP. Once again, metal-catalysed  $\alpha$ -C-H bond activation of MeP was not accomplished. The complex was subsequently crystallographically characterised from a reaction in air with propanal as substrate (see later).

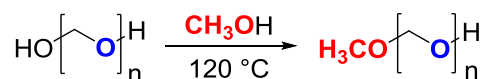
Encouraged by the results achieved with DEK we attempted to functionalise the activated Au-ketonyl bond with paraformaldehyde.

Formaldehyde is one of the most used C<sub>1</sub> electrophiles in organic synthesis and its applications in industrial processes. Examples reported in the literature concerning  $\alpha$ -methylenation/alkylation of simple esters and ketones have been already described in Chapter 3. As mentioned in the introduction to this chapter we also proposed a reaction system where formaldehyde can be produced from methanol by dehydrogenating catalysts so that we could overcome some of the disadvantages of using gaseous formaldehyde. Formaldehyde in fact easily undergoes polymerisation resulting in a not very practical large scale production, transport, storage and subsequent employment as a raw material in chemical synthesis. In the current study we, therefore, used paraformaldehyde as formaldehyde source.

Commercially available paraformaldehyde is a mixture of different chain length polymers of formaldehyde of high molecular weight.<sup>[22]</sup> Gaseous formaldehyde can be generated from paraformaldehyde by dry heating using an inert gas while formaldehyde solutions can be produced by heating solid paraformaldehyde with water to around 55-60 °C in the presence of a base, usually NaOH.<sup>‡</sup> Depolymerisation of polyformaldehyde to monomeric formaldehyde can also be performed in the presence of an acid like phosphoric acid in order to significantly reduce the formation of undesirable solids which are responsible for plugging of lines and affect the operation of pumps during continuous processes.<sup>[23]</sup> Depolymerisation processes which are acid or base catalysed, however, would not be ideal for our purposes, in fact if the substrate involved is an ester and water is produced during the C-H bond activation step, hydrolysis of the ester bond would occur as the main reaction. Furthermore in an attempt to develop a more generic procedure that can be used in the presence of a great variety of transition metals, the employment of formalin may be a limiting factor, since a wide range of metal complexes could be water sensitive. Therefore we propose a system where paraformaldehyde can be successfully depolymerised upon heating a suspension of paraformaldehyde in methanol, in a closed system without addition of a base (Scheme 6.2.2).

---

<sup>‡</sup> From Sigma-Aldrich Product Information; **Cas Number:** 30525-89-4

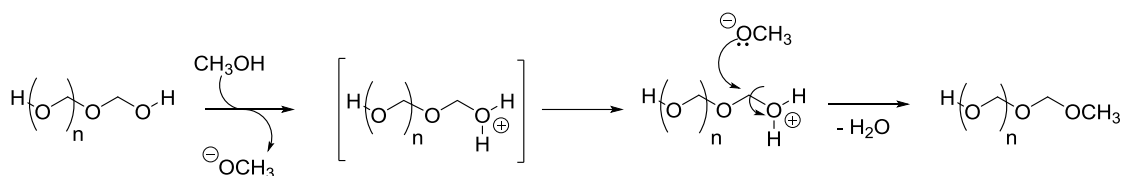


**Scheme 6.2.2** Solubilisation of paraformaldehyde by formation of different chain length oligomers of methoxymethanol.

A mixture of different chain length oligomers of methoxymethanol (alcoform\*)<sup>§</sup> are produced following the mechanism shown in Scheme 6.2.3.

The name alcoform conventionally refers to a solution of formaldehyde in an organic solvent, for example methanol, ethanol, propanol, butanol or iso-butanol or a mixture thereof. Formaldehyde may be added as solid paraformaldehyde and depolymerised in the presence of a base. Dry methyl alcoform, for example, is produced by Lucite Int. by initial addition of sodium hydroxide to paraformaldehyde in water/methanol to produce a methyl alcoform solution containing 50 wt% formaldehyde, 40% methanol and 10% water. The water is then removed by the use of molecular sieves.<sup>[24]</sup>

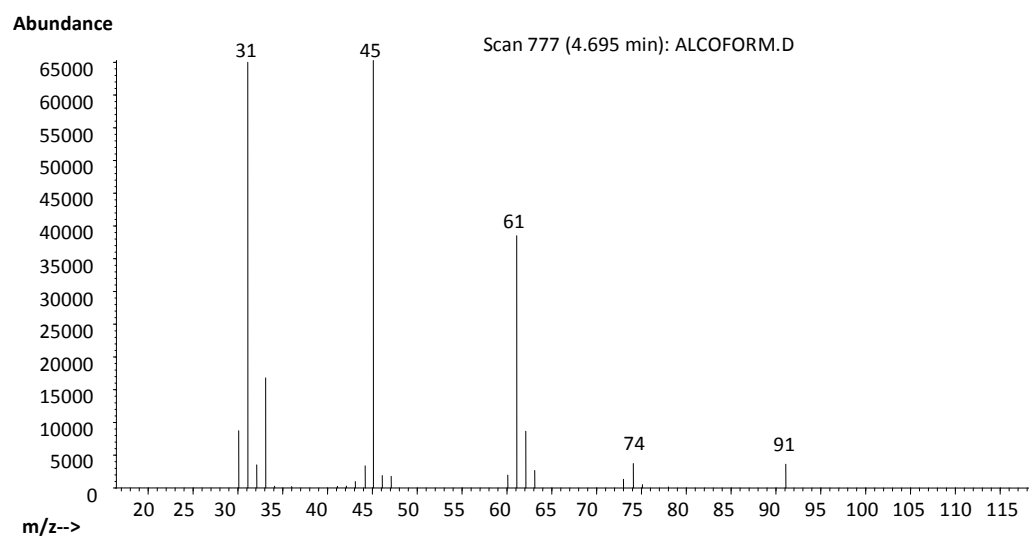
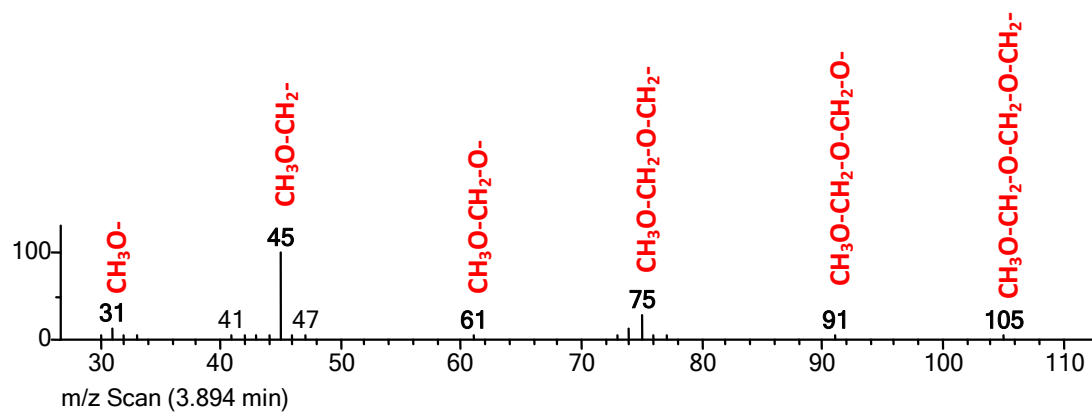
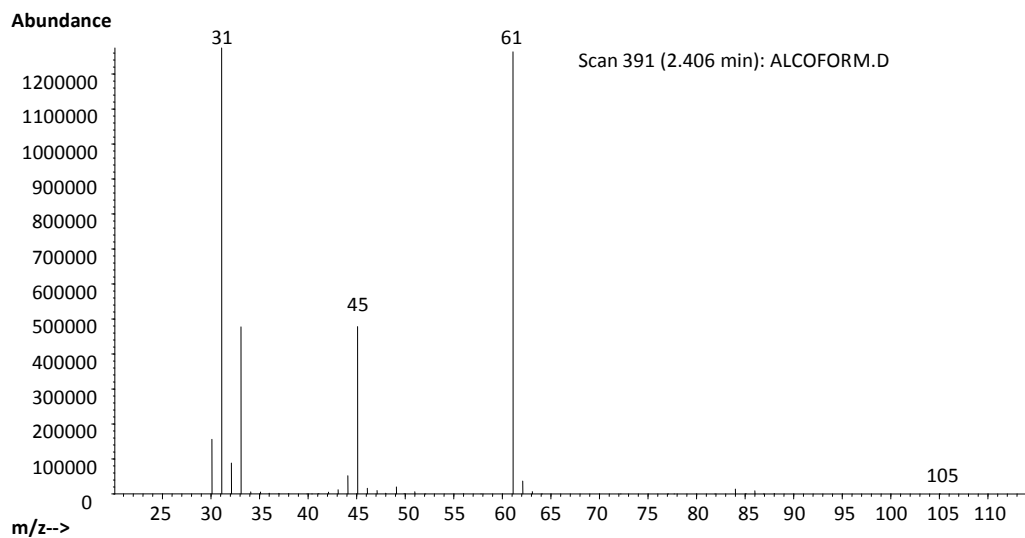
A possible mechanism involves the protonation of oxygen by methanol and formation *in situ* of methoxide ion which generates different chain length oligomers of the form  $\text{CH}_3\text{O}(\text{CH}_2\text{O})_n\text{H}$  by nucleophilic attack of methylenes with water acting as leaving group.



**Scheme 6.2.3** Plausible mechanism for paraformaldehyde depolymerisation in the presence of methanol.

The fragmentation patterns of four peaks present in the GC-MS spectrum of the alcoform\* in DCM (Figure 6.2.3) suggest the presence of formaldehyde (possibly formed during the analysis), methanol and several oligomers of the form  $\text{CH}_3\text{O}(\text{CH}_2\text{O})_n\text{H}$  ( $n < 5$ ) as the main species in the final mixture.

<sup>§</sup> Alcoform\* refers to a formaldehyde solution in methanol obtained without addition of a base.



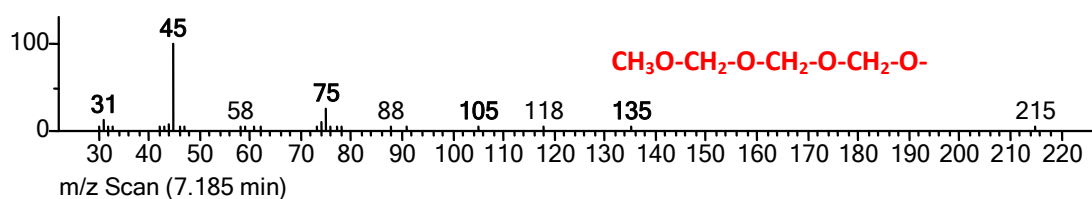


**Figure 6.2.3** GC-MS of the alcoform\* in DCM: fragmentation patterns of four peaks suggesting the presence of formaldehyde (possible formed during the analysis), methanol and several oligomers of the form  $\text{CH}_3\text{O}(\text{CH}_2\text{O})_n\text{H}$  ( $n < 5$ ) as the main species in the final mixture.

A set of preliminary experiments was conducted in the presence of complex **4** (formed *in situ* from **3**) and DEK. DEK, methanol and a stoichiometric amount of paraformaldehyde (relative to DEK) were added and heated at 140 °C for 3/3.5 hours. When the mixture was simply refluxed in an open system no desired products were detected through GC analysis, probably as a consequence of losing formaldehyde by condensation all along the reaction set-up. On the other hand when the reaction was performed in a Fisher-Porter vessel, solubilisation of paraformaldehyde occurred around 100 °C providing in the end a clear solution containing  $\text{MeCH}(\text{CH}_2\text{OH})\text{C}(\text{O})\text{Et}$  (**P1**) as main product and several other by-products (GC yields and conversions will not be reported for these preliminary experiments conducted at 140 °C due to the appearance of coloured solutions). Compound **P1** can be successfully synthesised through a hydroxymethylation reaction of silyl enol ethers with commercial formaldehyde solutions activated by Lanthanide trifluoromethanesulfonates (triflates), especially ytterbium triflate ( $\text{Yb}(\text{OTf})_3$ ), which were found to be stable Lewis acids in water<sup>[25]</sup> or by simple base-catalysed condensation of DEK with formaldehyde used as formalin solutions<sup>[26]</sup> but a metal-catalysed process using paraformaldehyde as formaldehyde source for the synthesis has never been reported before.

Unlike the results we have reported for the ester derivative (refer to Chapter 3), dehydration of the alcohol **P1** did not spontaneously occur under these conditions (only minor amounts of the  $\alpha$ -methylenated product **P2** were detected) along with other species probably as a result of bis-functionalisation: mass spectrometric analysis suggested that  $\text{MeCH}(\text{CH}_2\text{OH})\text{C}(\text{O})\text{C}(\text{CH}_2)\text{Me}$  (**P3**) and  $(\text{MeCH}(\text{CH}_2\text{OH}))_2\text{C}=\text{O}$  (**P4**) were produced (unfortunately these species were not isolated and characterised however the fragmentation pattern matched with the predicted species and they might be expected given the evidence that C-H activation occurs under these conditions).

In order to confirm that the peak at ca 8.8 min in the depicted GC-MS chromatogram (Figure 6.2.4) corresponds to compound **P1**, it was synthesised on larger scale using a base-catalysed procedure and isolated through preliminary distillation and further column chromatography. NMR data of compound **P1** were in good agreement with those previously reported for the (*S*) enantiomer.<sup>[27]</sup>

However, in our case, after purification through silica column chromatography, the <sup>1</sup>H NMR spectrum revealed the presence of two sets of signals with the same multiplicity but a different chemical shift and intensity (Figure 6.2.4). Since GC-MS analysis of the isolated product gave rise to a unique peak we can exclude the presence of an isomer of **P1**, since isomers usually show different retention times and fragmentation patterns. This second species was suggested to be a different conformer of the molecule stabilised by a hydrogen bond between the H of the hydroxyl group and the oxygen of the carbonyl (Figure 6.2.4), which becomes responsible for all the resonances shifting. On the other hand upon heating the mixture of the two species during GC-MS analysis, the hydrogen bond is cleaved resulting in only one peak in the collected chromatogram.

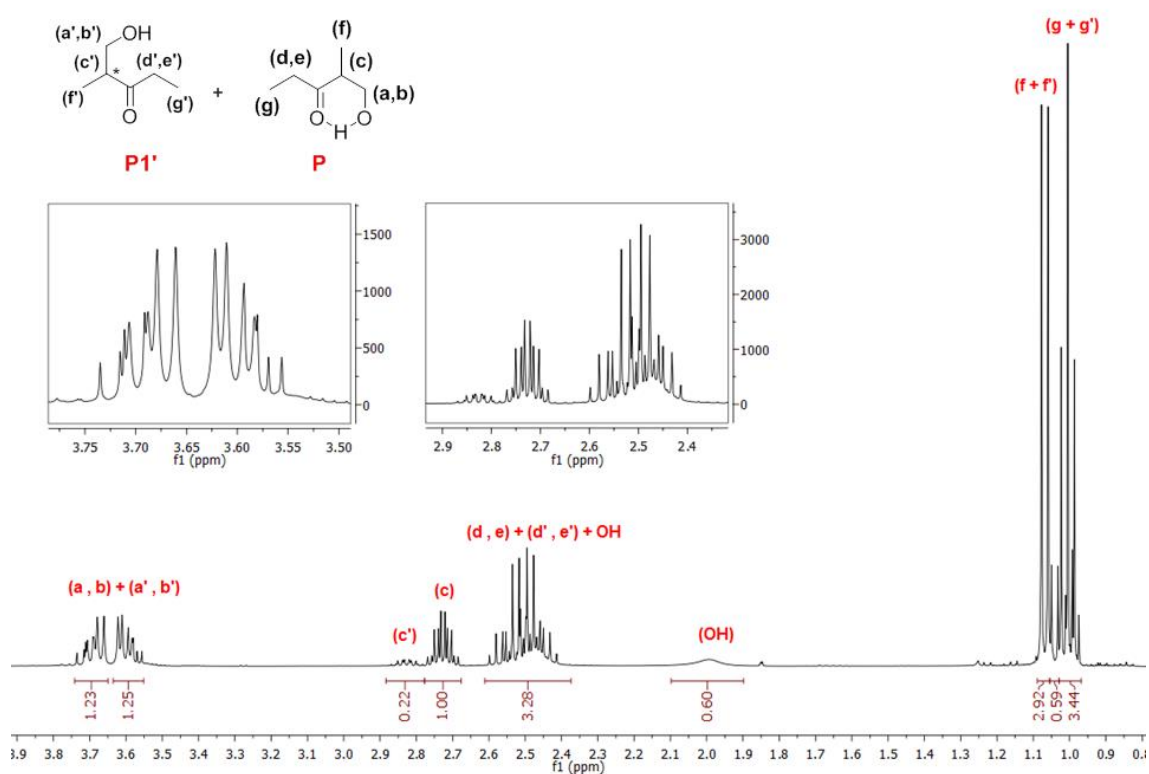


**Figure 6.2.4** <sup>1</sup>H NMR spectrum (400 MHz; CD<sub>2</sub>Cl<sub>2</sub>) of compound **P1** and respectively assignments and integrals.

The resonances corresponding to protons *c* of respectively compound **P1** and its conformer generates two signals at 2.8 and 2.7 ppm with a good separation therefore they could be used for integral calibration, which allowed us to estimate that the two species are in the ratio of 0.2 : 1. In order to establish which is the major species we could use the OH resonances since the proton involved in an intramolecular H bond would be the more deshielded one. The integral of the OH at 2 ppm is 0.6 while if we consider the integral of the signal at ca 2.5 ppm, it is 3.28. The latter integral corresponds to the sum of the integrals of protons *d* and *e* (from compound **P1** and its conformer) and the second OH. By recalling the ratio of 0.2 : 1, the total integral of protons *d* and *e* (both organic species) is 2.4 (0.4 + 2), therefore the difference of 0.88 corresponds to the OH integral. Based on the evidence that the more deshielded OH is the one found in larger amount, we could state that the major species is the conformer with an intramolecular H bond. The formation of this inner hydrogen bond is probably the reason why dehydration of **P1** only occurs to a very small extent at our reaction temperatures. The integral of the free OH at 2.0 is 0.6 rather than 0.2 probably due to exchange with H<sub>2</sub>O in the solvent.

The response factor of the purified organic product **P1** was calculated using decane as internal standard (IS). In order to improve the catalyst activity we varied the reaction parameters. Unfortunately longer reaction time at 140 °C gave evidence of gold decomposition, probably to gold nanoparticles, providing coloured solutions (from pink to red/purple depending on the reaction time and initial concentration of the gold(I) species). The formation of these coloured solutions was easily avoided by reducing the temperature to 120 °C.

Because of gold decomposition we could not increase the reaction temperature in an attempt to *in situ* dehydrate the alkylated product, therefore we decided to target compound **P1** as final product. Hypothetically, once obtained in higher yield it could be isolated and separately dehydrated to the corresponding EtC(O)C(CH<sub>2</sub>)Me (**P2**) derivative. The last reaction could be achieved for example in the presence of hydroquinone, H<sub>3</sub>PO<sub>4</sub> and Cu powder<sup>[28]</sup> or with iodine<sup>[29]</sup>.

Preliminary catalytic experiments were performed starting from catalyst **3**, due to its more readily availability in our laboratories, at 120 °C for 1, 6 and 12 hours (Table 6.2.1, Entries 2, 3 and 6 respectively). Based on the evidence that increasing the reaction time from 6 to 12 hours did not significantly affect the yield of compound **P1** (Table 6.2.1, Entries 3 and 6), an additional experiment was performed under the same reaction conditions (120 °C for 6 h)

(Table 6.2.1, Entry 4) by replacing the metal catalyst with a simple strong base like KOH. The base-catalysed functionalisation of DEK gave rather similar results in terms of conversion and selectivity to **P1**.

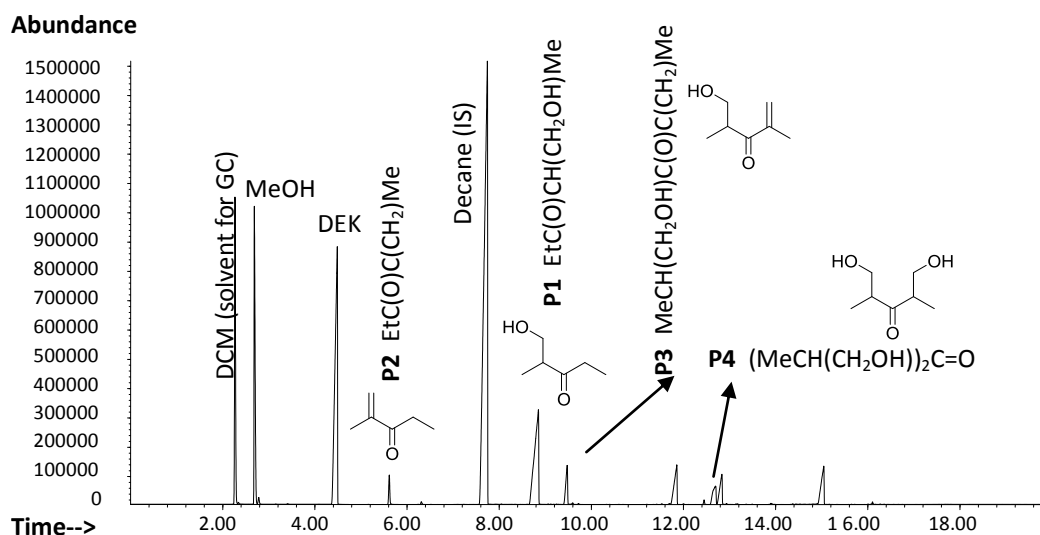


Figure 6.2.5 GC-FID of Table 6.2.1/Entry 3

The temperature required for paraformaldehyde solubilisation was observed to be around 100 °C, but the reaction temperature could not be higher than 140 °C due to significant gold decomposition, therefore additional experiments using catalyst **3** were performed at 100, 110 and 135 °C (Table 6.2.1, Entries 5, 7, 8 and 9) in order to optimise the reaction temperature. The catalytic experiment at 135 °C for 6 h did not exhibit any improvements in terms of **P1** yield (Table 6.2.1, Entry 5), while the catalytic activity of **3** was significantly slowed down when the reaction was performed at 100 °C for 24 hrs (Table 6.2.1, Entry 7). Further experiments were therefore conducted at 110 °C for 24 and 48 h respectively, without any significant increase in product **P1** yield (Table 6.2.1, Entries 8 and 9), while a significant decrease in catalyst **3** selectivity towards compound **P1** was observed after the longer reaction time (Table 6.2.1, Entry 9).

By increasing the concentration of paraformaldehyde (twice the amount of DEK) along with the amount of methanol in the presence of catalyst **3** no improvement was achieved. A general decrease in the catalyst activity was observed to the detriment of compound **P1** (Table 6.2.1, Entry 10).



All the previous reactions were performed at a very low catalyst loading, providing a remarkable catalyst activity (Table 6.2.1, Entries 3, 5, 6, 8 and 9) and in certain cases also selectivity towards the desired product (Table 6.2.1, Entries 2, 5, 7 and 8), hence we decided to investigate how the substrate conversion was affected by higher catalyst loading. However, increasing the catalyst concentration gave rise to a dark purple solution (this entry is not included in Table 6.2.1 because GC yields and conversions were not calculated due to the appearance of the intense colour). The higher concentration of the gold(I) species probably favoured gold aggregation resulting in the formation of coloured solutions, therefore we increased the catalyst loading but we kept the same concentration by doubling the amount of MeOH used. Despite a colourless solution being obtained this time, there was no significant improvement in terms of **P1** yield (Table 6.2.1, Entry 11).

To confirm that the reaction proceeds via C-H activation rather than by a simple base mechanism complex **4** was synthesised, purified and used as a catalyst (0.15 mmol % cat. loading) in the presence of DEK, methanol and paraformaldehyde (stoichiometric amount relative to DEK) at 120 °C for 6 and 12 h providing compound **P1** always as a major product and few side products, mono- and bis-functionalised compounds. The DEK conversion increased with longer reaction time but unfortunately not in favour of compound **P1**; the 1 % decrease in the yield of **P1** from 6 to 12 hours could be due to minor dehydration of **P1** (Table 6.2.1, Entries 12 and 13). However, we proved that complex **4** is an active species in the process of DEK alkylation with formaldehyde, confirming that the alkylation process proceeds *via* C-H activation. As expected, the results of 6 and 12 h experiments were comparable and the yield of compound **P1** was similar to that reported for catalyst **3** (Table 6.2.1, Entries 3, 6, 12 and 13) with formation of a slight pink solution after 12 hours. Surprisingly, by comparing the two 6 h experiments (Table 6.2.1, Entries 3 and 12) we observed a significant increase in catalyst **4** selectivity towards compound **P1**, making **4** a better catalyst for our desired reaction.

Starting from isolated catalyst **4** (in this way the activation step had already taken place and the water formed had been removed) we performed one attempt of DEK alkylation at RT for 12 h using a preformed alcoform\* (120 °C for 3 h in a Fisher-Porter vessel; further reaction details are reported in Table 6.2.1, Entry 14). The recovered reaction mixture showed the presence of only starting materials, no alkylation was observed under these conditions (Table 6.2.1, Entry 14).

**Table 6.2.1** shows preliminary optimisation of the condition for DEK conversion [%] to compound **P1** (Calibrated GC yield).

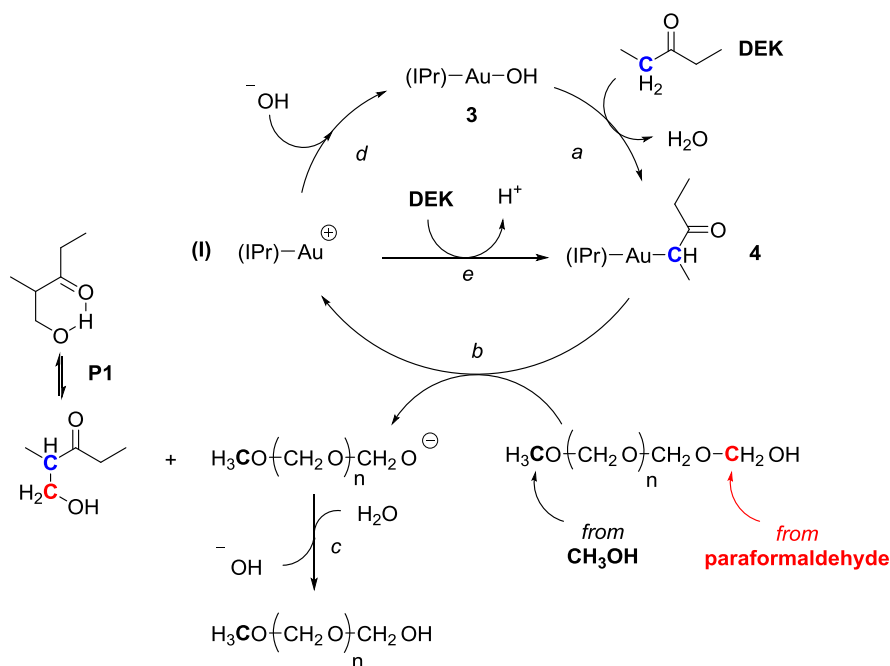
Entry	Cat.	Time [h]	Temp. [°C]	P1 yield [%]	TON	DEK conv. [%]	selectivity [%]
1	blank	6	120	0.2	-	12.0	-
2	(3) <sup>a</sup>	1	120	4.8	32	6.7	71.6
3	(3) <sup>a</sup>	6	120	25.7	171	53.2	48.3
4	KOH <sup>a*</sup>	6	120	25.7	171	61.2	45.7
5	(3) <sup>a</sup>	6	135	24.5	163	30.4	80.7
6	(3) <sup>a</sup>	12	120	27.2	181	54.3	50.1
7	(3) <sup>a</sup>	24	100	8.6	57	11.5	74.8
8	(3) <sup>a</sup>	24	110	26.3	175	33.4	78.7
9	(3) <sup>a</sup>	48	110	28.0	187	61.2	45.7
10	(3) <sup>b</sup>	6	120	20.0	133	32.2	62.1
11	(3) <sup>c</sup>	6	120	28.4	95	53.2	53.4
12	(4) <sup>d</sup>	6	120	28.3	188	29.6	95.6
13	(4) <sup>d</sup>	12	120	27.1	180	38.3	70.7
14	(4) <sup>e</sup>	12	RT	-	-	-	-

<sup>a</sup> DEK (1.2 mL, 11.33 mmol), paraformaldehyde (0.34 g, 11.33 mmol), MeOH (0.6 mL, 14.8 mmol), **3** (10 mg, 0.017 mmol); in a closed Fischer Porter vessel under air; <sup>a\*</sup> DEK (2.4 mL, 22.66 mmol), paraformaldehyde (0.68 g, 22.66 mmol), MeOH (1.2 mL, 29.6 mmol), **KOH** (2 mg, 0.034 mmol) (the reaction was scaled up); <sup>b</sup> paraformaldehyde (0.68 g, 22.66 mmol), MeOH (1.2 mL, 29.6 mmol); <sup>c</sup> **3** (20.0 mg, 0.034 mmol), MeOH (1.2 mL, 29.6 mmol); <sup>d</sup> DEK (0.6 mL, 5.66 mmol), paraformaldehyde (0.17 g, 5.66 mmol), methanol (0.3 mL, 7.4 mmol), **4** (5.7 mg, 0.0085 mmol); <sup>e</sup> paraformaldehyde (0.34 g, 11.33 mmol) was depolymerised in the presence of MeOH (0.6 mL, 14.8 mmol) separately (120 °C; 3 h; Fisher-Porter vessel), then reacted with DEK (1.2 mL, 11.33 mmol) in the presence of **4** (11.4 mg, 0.017 mmol). Yields and conversions were determined by GC-FID analysis using decane as internal standard (IS).

A plausible mechanism for the alkylation of DEK using paraformaldehyde as a one carbon alkylating agent catalysed by **3** was proposed based on some experimental evidence. Irreversible  $\alpha$ -C-H bond activation of DEK (*step a*, Scheme 6.2.4) occurs in the presence of an excess of DEK affording a stable Au-ketonyl complex that was isolated and fully characterised. The more reactive bond can undergo condensation (*step b*) with formaldehyde probably via nucleophilic attack of the activated  $\alpha$ -carbon on the terminal methylene of one of the oligomers of methoxymethanol (proposed mechanism depicted in Scheme 6.2.3). This furnishes the desired product **P1** along with the formation of a gold cationic intermediate and the corresponding anion of the oligomer (n-1) of methoxymethanol, which could be in turn

protonated by H<sub>2</sub>O (*step c*, Scheme 6.2.4) and generate the hydroxyl ion. The hydroxide-bearing species **3** is finally regenerated (*step d*, Scheme 6.2.4). When starting from **4**, water may be taken from the atmosphere or the unstable [Au(IPr)]<sup>+</sup>[19] might react directly with DEK (*step e*), in which case *step c* would be a simple protonation.

Theoretically, the protonation step could involve the participation of MeOH as protonating agent with the formation of the methoxide ion which in turn would generate the corresponding Au(I)-methoxide species. The catalytic cycle could proceed as well via the Au(I)-methoxide species, which is also more basic. The latter option was not depicted in the proposed mechanistic scheme since previous studies conducted with the Au(I)-methoxide by Nolan and co-workers showed that, unlike the Au(I)-OH species, it is very unstable and air sensitive.<sup>[30]</sup>



**Scheme 6.2.4** Proposed mechanism for Au(I)-catalysed C-C bond formation using paraformaldehyde as alkylating agent.

Some mechanistic studies have been conducted to confirm that the C-C bond formation step proceeds according to *step b* depicted in Scheme 6.2.4.

A stoichiometric formation of compound **P1** (relative to complex **4**) was performed in an NMR tube containing complex **4** and 16  $\mu$ L of alcoform\* in CD<sub>2</sub>Cl<sub>2</sub> and monitored over time at room temperature (see Figure 6.2.6). Daily collection of NMR spectra gave evidence of progressive

formation of the organic product **P1** together with conversion of the starting complex **4** into a final different species. Crystals of the  $[\text{Au}(\text{IPr})(\text{Cl})]$  (**6**) were isolated by slow crystallisation from DCM, probably due to the presence of a chlorinated solvent<sup>[19f]</sup> (It is known that **3** can reconvert to **6** on standing in  $\text{CH}_2\text{Cl}_2$ ; the synthesis of **3** from **6** appears in the ESI of the cited paper).

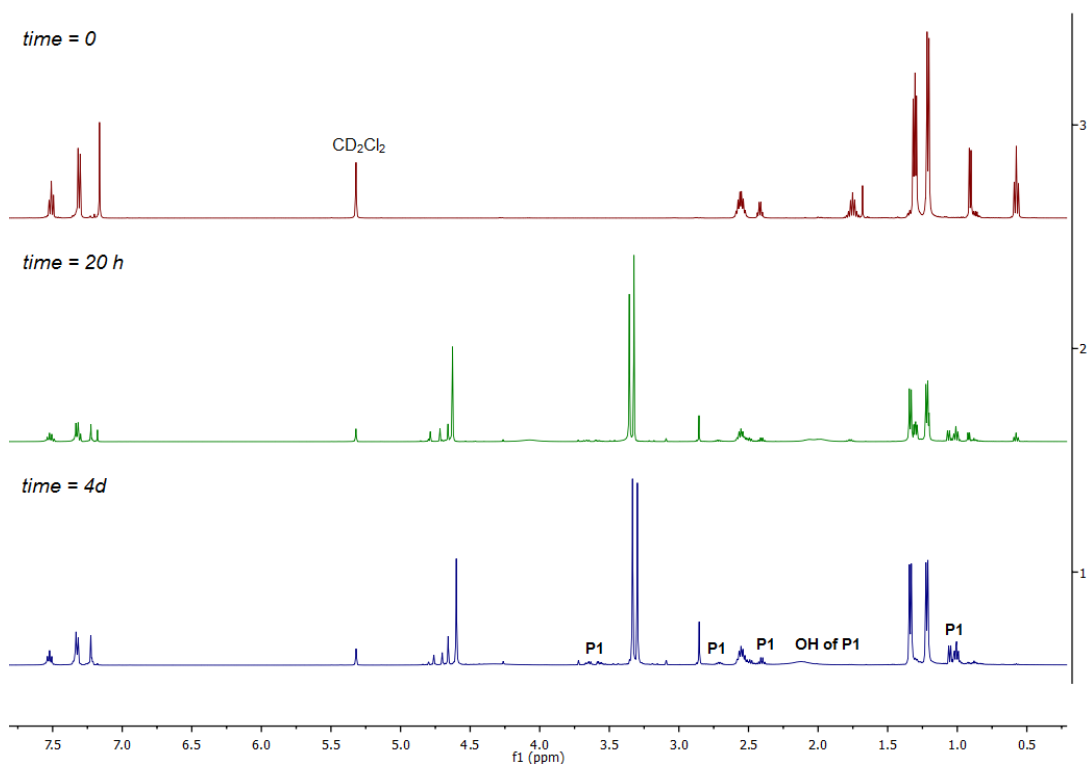


**Figure 6.2.6**  $^1\text{H}$  NMR spectrum ( $\text{CD}_2\text{Cl}_2$ ) of complex **4** upon addition of 16  $\mu\text{L}$  of alcoform\* over selected periods: time 0, ca 20 h, 4 days (from the top) highlighting the progressive formation of **P1**.

In the event that the reaction only proceeds via nucleophilic attack of the activated  $\alpha$ -carbon of **3** on the methylene carbons of the alcoform\*, in the presence of a  $^{13}\text{C}$  labelled alcoform\* where  $^{13}\text{CH}_3\text{OH}$  is the only source of  $^{13}\text{C}$ , we should not observe any  $^{13}\text{C}$  incorporation into the final compound **P1** in the C1 position. Another NMR experiment was hence conducted in the presence of a  $^{13}\text{C}$  labelled alcoform\* (paraformaldehyde was separately depolymerised in the presence of  $^{13}\text{CH}_3\text{OH}$ ) and the recorded  $^{13}\text{C}\{^1\text{H}\}$  UDEFT spectra showed that the integrals ratio of C1/C4 is always 1 in both labelled and unlabelled experiments (Figure 6.2.7), confirming that no  $^{13}\text{C}$  is incorporated into compound **P1**. The final Au(I) species (from NMR tube in  $\text{CD}_2\text{Cl}_2$ ) was crystallised from THF and “the collected structure appears to be some sort of disordered

Cl/OH mixture where the disorder could not be readily refined<sup>\*\*</sup>, however, it provides some experimental evidence that the catalytic cycle was closed.

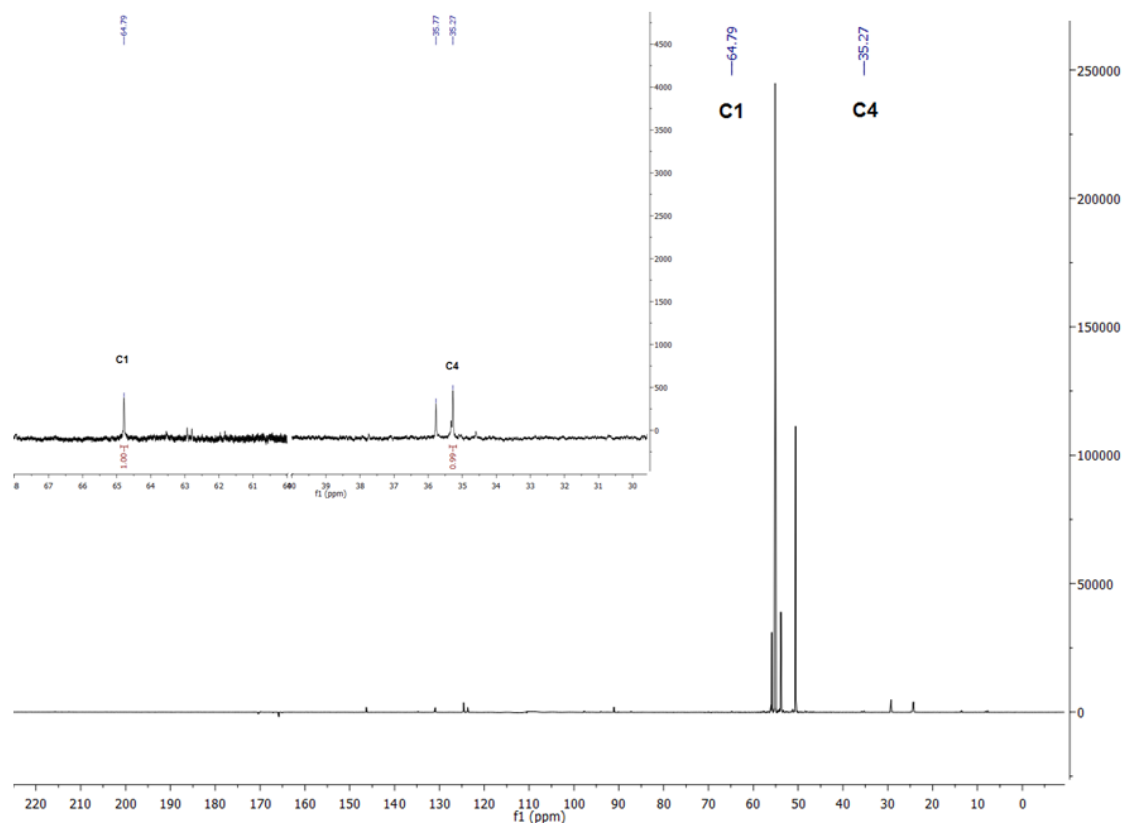


**Figure 6.2.7**  $^{13}\text{C}\{^1\text{H}\}$  UDEFT spectrum (400 MHz;  $\text{CD}_2\text{Cl}_2$ ) of the NMR experiment with  $^{13}\text{C}$  labelled alcoform\* after 4 days showing with the integrals of C1 at 64.79 ppm (1.00) and C4 at 35.27 ppm (0.99).

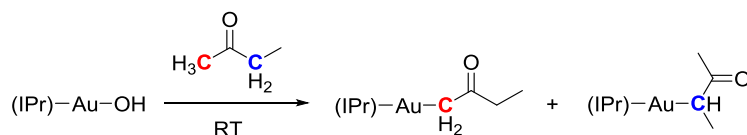
During the blank experiment (performed only by adding few drops of MeOH to a solution of **4** in  $\text{CD}_2\text{Cl}_2$ , no formation of compound **P1** was observed, instead complex **4** slowly frees the ketone giving rise to a new Au species.

Although the catalytic functionalisation of DEK with paraformaldehyde as the source of formaldehyde provided some encouraging results it still requires optimisation and deep understanding of the catalytic cycle. It is still unclear why we did not observe any increase in yield at higher catalyst loading. One of our first assumptions was that the gold species undergoes slow decomposition at high temperature (phenomenon that becomes more evident at 140 °C and higher concentration of the catalyst with the formation of intense coloured

<sup>\*\*</sup> Dr. David Cordes' conclusion after attempting to solve the structure by single-crystal X-Ray Diffraction.

solutions). Although we are aware that the solubilisation of paraformaldehyde in methanol does not take place under 100 °C, we did not fully investigate what temperature is required for the alkylation step.

As part of investigations of a small number of other substrates, the reactivity of **3** towards an unsymmetrical substrate, was explored. Under similar reaction conditions C-H activation of 2-butanone (MEK) occurred on both  $\alpha$ -methyl and  $\alpha$ -methylene positions (Scheme 6.2.5) affording two Au species  $[\text{Au}(\text{IPr})\{\text{CH}(\text{CH}_3)\text{C}(\text{O})\text{CH}_3\}]$  (**7**) and  $[\text{Au}(\text{IPr})\{\text{CH}_2\text{C}(\text{O})\text{CH}_2\text{CH}_3\}]$  (**8**) in a 1 : 1 mixture (integration of the  $^1\text{H}$  NMR spectrum). In principle, the methyl group is expected to be more acidic by *ca.* 0.5  $pK_a$  units,<sup>[3]</sup> less sterically crowded and statistically favoured as it contains 3xH atoms rather than 2 on the  $\alpha$ -methylene carbon atom. DFT calculations (§ 6.4.6) also suggest that the product of C-H abstraction from the  $\alpha$ -methyl group should be slightly more stable than that obtained from abstraction of an  $\alpha$ -methylene by about 7.5  $\text{kJ mol}^{-1}$ . The methyl and methylene deprotonation occurs to the same extent probably as a consequence of the similar  $pK_a$  of the two  $\alpha$  positions. Figure 6.2.8 shows the upfield region of a  $^1\text{H}$  NMR spectrum of the final mixture in  $\text{CD}_2\text{Cl}_2$  which includes the distinctive resonances of the alkyl moiety with corresponding integrals (resonance at 1.66 ppm corresponds to water present in  $\text{CD}_2\text{Cl}_2$ ; all signals will be presented in detail in the experimental section of this chapter).



**Scheme 6.2.5** Au-ketonyl species arising from C-H activation of MEK on  $\alpha$ -methyl and  $\alpha$ -methylene positions.

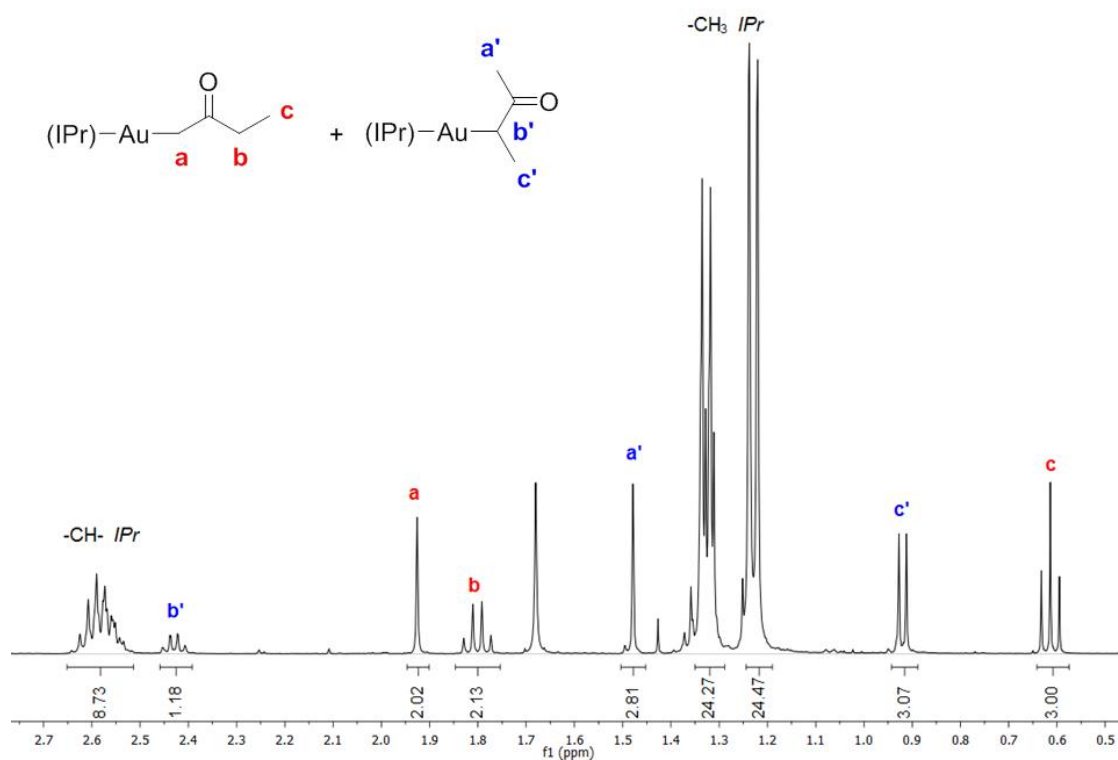


**Figure 6.2.8**  $^1\text{H}$  NMR spectrum (400 MHz;  $\text{CD}_2\text{Cl}_2$ ) of complex complexes **6** and **7** in a 1 : 1 mixture: upfield region showing signals belonging to the aliphatic moiety and respectively assignments and integrals.

Suitable single crystals for X-Ray Diffraction (XRD) were grown starting from a 1 : 1 mixture of **7** and **8**, however, only the structure of **7** was found in the end by crystallographic analysis (Figure 6.2.9).

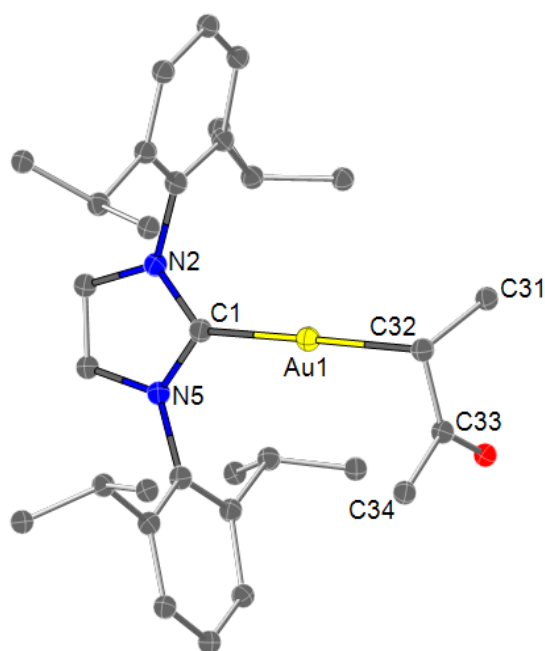


**Figure 6.2.9** Molecular representation of **7** showing 50 % thermal ellipsoids probability. Hydrogen atoms are omitted for clarity. Selected bond lengths [Å] and bond angles [°]: Au1-C1 2.010(5), Au1-C32 2.090(6), C1-Au1-C32 176.3(3).

Based on the evidence that  $\alpha$ -C-H and  $\alpha'$ -C-H bond activation of MEK occurs, we further attempted functionalisation with paraformaldehyde under the same reaction conditions described for DEK. The GC-MS spectrum of the crude product gave evidence for two main species and several minor by-products not all identified. One of the main species was confirmed to be the expected methylene alkylated compound MeC(O)CH(CH<sub>2</sub>OH)Me (**P5**) along with minor amounts of the methylenated derivative MeC(O)C(CH<sub>2</sub>)Me (**P6**) arising by spontaneous dehydration of **P5** (they are known and commercially available compounds) (see Figure 6.2.10). GC-FID yield of **P5** under these condition was estimated to be around 23 % based on simple GC integrals and assuming that all the other species present in the chromatogram arise from MEK conversion. The structure of all other species was not confirmed by simple library matching, although a combined analysis of the fragmentation pattern and the previous evidence of C-H activation on  $\alpha$ -methyl and  $\alpha$ -methylene positions, suggested that we might observe the formation of compound **P5** isomer EtC(O)CH<sub>2</sub>CH<sub>2</sub>OH (**P7**), bis-functionalised products CH<sub>2</sub>=CHC(O)CH(CH<sub>2</sub>OH)Me and MeC(CH<sub>2</sub>)C(O)C<sub>2</sub>H<sub>4</sub>OH and a wide numbers of by-products. The present work requires further investigation and unfortunately



these preliminary catalytic experiments only exhibited poor selectivity towards the desired products.

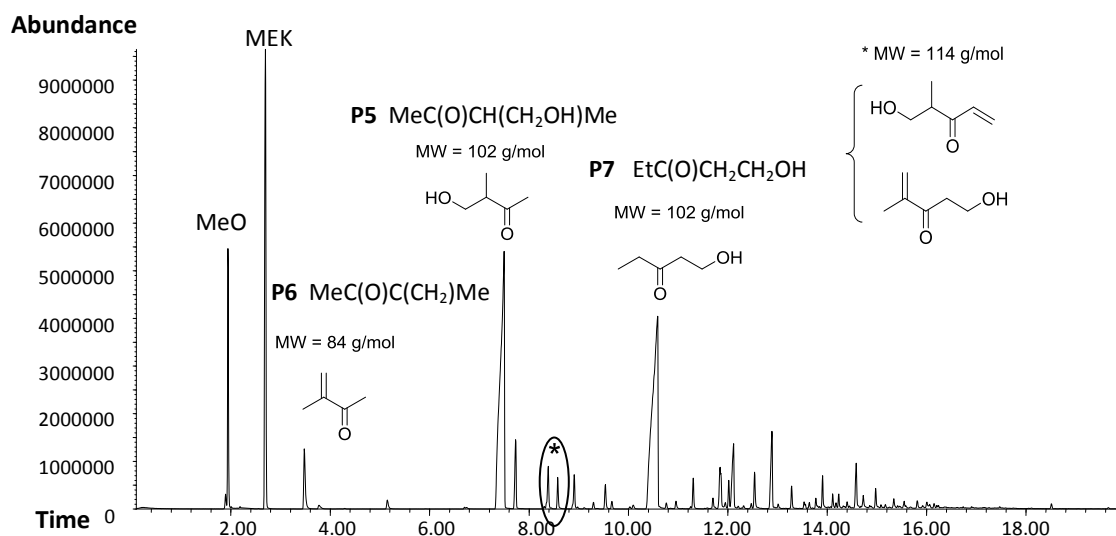


**Figure 6.2.10** GC-MS spectrum of the crude product corresponding to the functionalisation of MEK catalysed by complex **3** giving evidence for two main species and several minor by-products not all identified.

A further preliminary substrate scope was also performed involving two symmetrical substrates and one aldehyde, propanal. Among symmetrical ketones our interest was extended to acetone and 2,4-dimethyl-3-pentanone.

Since the Au(I)-acetyl complex has been already successfully synthesised in the Nolan group,<sup>[19]</sup> we only attempted functionalisation with paraformaldehyde. Attempts of acetone alkylation however, not only generate the expected products, but also large amounts of by-products probably as result of an aldol-condensation reaction. However, the formation of minor amounts of the mono-alkylated and mono-methylenated compounds, MeC(O)CH<sub>2</sub>CH<sub>2</sub>OH (**P8**) and MeC(O)CH=CH<sub>2</sub> (**P9**) respectively, was observed. Due to the large number of peaks in the GC-MS spectrum the species were not all identified.

The employment of 2,4-dimethyl-3-pentanone allowed us to investigate whether or not C-H bond activation occurs in the presence of a more sterically hindered  $\alpha$ -position. The latter substrate, in the presence of **3**, provided potential evidence of  $\beta$ -C-H bond activation (doublet at 0.55 probably attributable to  $\beta$ -CH<sub>2</sub>-Au moiety), however, the desired product was never obtained as the major species, precluding the possibility of confirming the structure by crystallographic analysis. The catalytic experiments showed the presence of only one product

which was always obtained in minor amounts. It was suggested to be the  $\beta$ -methylated product **P10** only based on the GC fragmentation pattern but it was never isolated and fully characterised (Figure 6.2.11).

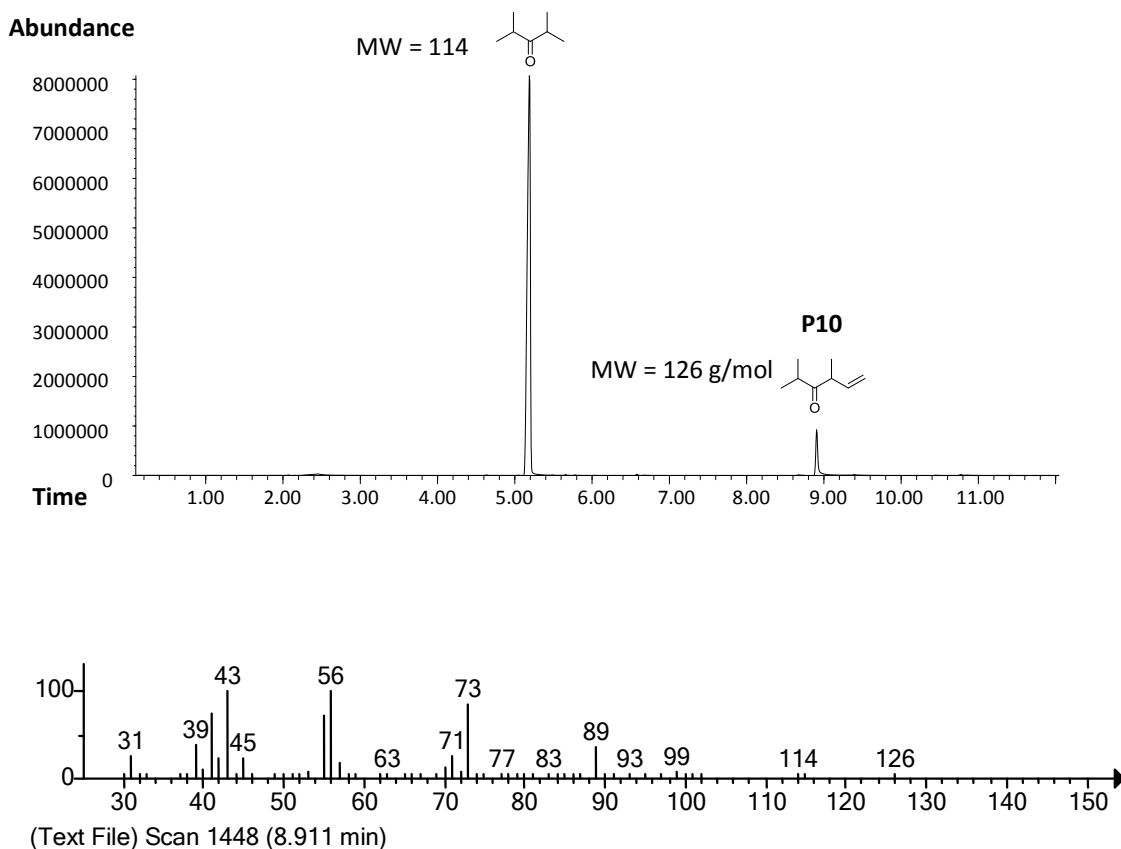


**Figure 6.2.11** GC-MS spectrum of the potential  $\beta$ -C-H bond activation of 2,4-dimethyl-3-pentanone with GC fragmentation pattern of the peak at 8.911 min.

Reaction of **3** with propanal in air only generated the Au(I)-propanoate derivative **5**, for which the structure was successfully confirmed by crystallographic analysis. Carrying out the reaction under argon, but recrystallising the product in air also gave the propanoate complex (Figure 6.2.12).

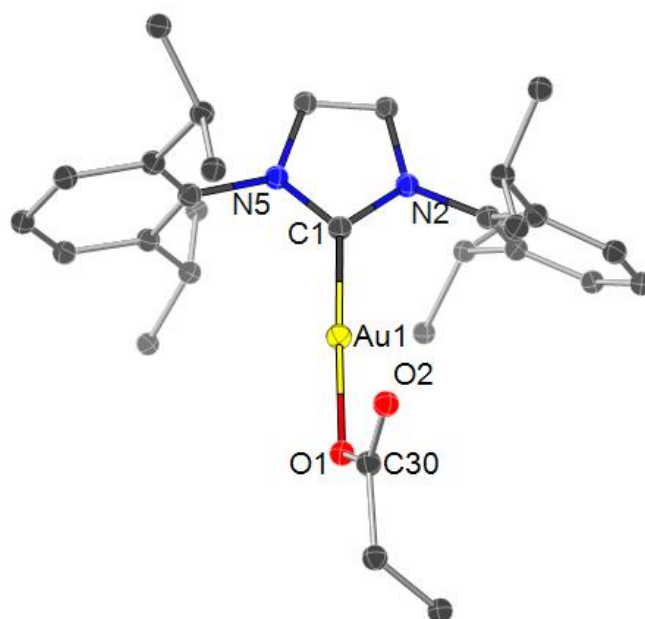


**Figure 6.2.12** Molecular representation of **5** showing 50 % thermal ellipsoids probability. Hydrogen atoms are omitted for clarity. Selected bond lengths [Å] and bond angles [°]: Au1-O1 2.028(6), Au1-C1 1.949(7), O1-Au1-C1 178.3(3).

Formation of the Au(I) propanoate complex is possibly a result of reaction of **3** with propanoic acid, present as an impurity in the propanal batch (GC-MS of the starting material exhibited traces of propanoic acid), rather than oxidation of the aldehyde itself. However, the collected structure by crystallographic analysis allowed us to confirm that the Au(I) species obtained in the presence of MeP is the propanoate derivative ( $^1\text{H}$  NMR spectra of the final species synthesised by reaction with propanal and MeP respectively were perfectly overlapping; Figure 6.2.13).

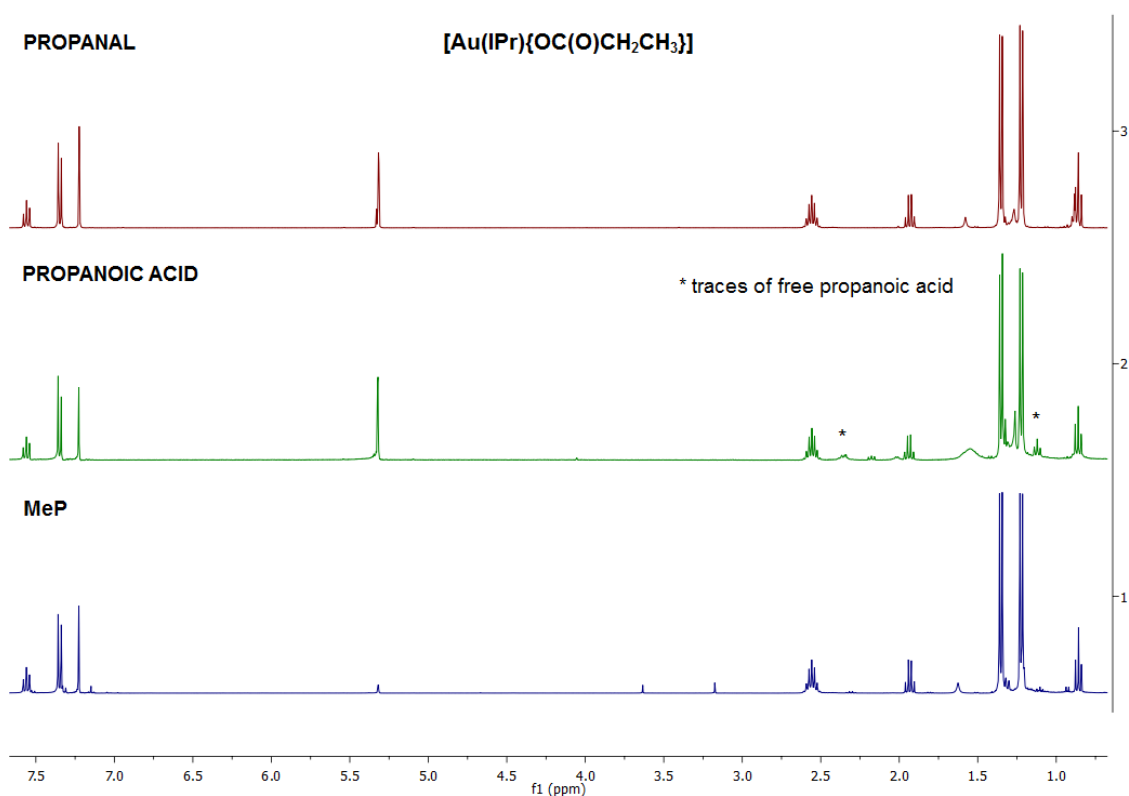


**Figure 6.2.13** <sup>1</sup>H NMR (400 MHz; CD<sub>2</sub>Cl<sub>2</sub>) spectra of [Au(IPr){OC(O)CH<sub>2</sub>CH<sub>3</sub>}] (**5**) obtained by reaction of complex **3** with propanal, propanoic acid and MeP respectively.

Although the stoichiometric reactions between **3** and propanal did not give evidence for C-H activation, we decided to try few catalytic experiments under the same reaction conditions used for DEK and other ketones. In the GC-MS spectrum of the crude product, minor amounts of the α-methylenated propanal (methacrolein **P11**) were detected along with other species, including propanoic acid. However, when the reaction was performed under inert atmosphere only traces of propanoic acid were detected. We still need to define whether propanoic acid formation occurs by spontaneous oxidation of propanal when the reaction is performed without excluding air, or catalyst **3** acts as a mild oxidating agent.

### 6.3 Conclusions and Future Work

The preliminary results reported in this chapter show that [Au(IPr)(OH)] can act as a catalyst or catalyst precursor in the  $\alpha$ -hydroxymethylenation of ketones. In particular 3-pentanone (DEK) and 2-butanone (MEK) were targeted as possible substrates. Both ketones, in fact, once alkylated, could be oxidised to the corresponding esters via a Baeyer-Villiger (BV) reaction and provide MMA as final product, as an alternative route that would overcome several drawbacks related to the employment of an ester (MeP) as substrate. The  $\alpha$ -hydroxymethylenation reaction presented in the current work proceeds via a preliminary C-H activation of the substrate followed by nucleophilic attack of the new formed metal alkyl adduct towards the electrophilic substrate. The encouraging results achieved, however, require further investigation with the development of a more efficient system. Finally, attempts of C-H activation with two other M(I)-hydroxide complexes, [Ir(cod)(IiPr)(OH)] and [Cu(IPr)(OH)] were largely unsuccessful, pointing out something peculiar about the gold(I) hydroxide catalyst.

### 6.4 Experimental Section

#### 6.4.1 General materials and methods

*Au chemistry:* all manipulations and reactions were carried out in air and using technical grade solvents, unless otherwise stated.

*Ir and Cu chemistry:* manipulations and reactions were conducted under Ar gas (dried through a Cr(II)/silica packed glass column) using different techniques including a standard Schlenk, vacuum line and a glove box. Solvents were dried and degassed prior to use.

Methyl propanoate was supplied by Lucite Int.; 3-pentanone, 2-butanone, 2,4-dimethyl-3-pentanone, propanal, paraformaldehyde 95 %, decane (IS), methanol,  $^{13}\text{C}_3\text{OH}$  were purchased from Aldrich; DCM, acetone and hexane from Fisher Scientific.

$\text{CD}_2\text{Cl}_2$  was purchased from Cambridge Isotope Laboratories and filtered over basic  $\text{Al}_2\text{O}_3$  prior to use.

The metal complexes [[Ir(cod)(IiPr)(OH)]<sup>[19b]</sup> (**1**), [Cu(IPr)(OH)]<sup>[19h]</sup> (**2**) and [Au(IPr)(OH)]<sup>[31]</sup> (**3**) were synthesised by known procedures and supplied by members of the group of Steve Nolan.

## 6.4.2 General instruments

NMR spectra were recorded on Bruker Avance II 500 and 400 MHz Spectrometers ( $^1\text{H}$  NMR at 500 MHz and  $^{13}\text{C}$  NMR at 125 MHz or  $^1\text{H}$  NMR at 400 MHz and  $^{13}\text{C}$  NMR at 100 MHz respectively) at RT.  $^1\text{H}$  and  $^{13}\text{C}\{^1\text{H}\}$  spectra are referenced to TMS and the residual proton signal of the solvent was used as internal standard.

$^1\text{H}$  NMR solvent residual signals:  $\text{CD}_2\text{Cl}_2$  set at 5.32 ppm.  $^{13}\text{C}\{^1\text{H}\}$  NMR solvent signals:  $\text{CD}_2\text{Cl}_2$  set at 53.84 ppm.<sup>[32]</sup>

GC analysis were performed using a Hewlett Packard 6890 series GC system equipped with an Agilent J&W HP-1 column capillary (30.0 m x 248  $\mu\text{m}$  x 0.25  $\mu\text{m}$  nominal). Method: flow rate 0.8 mL  $\text{min}^{-1}$  (He carrier gas), split ratio 100:1, starting temperature 50  $^\circ\text{C}$  (4 min) ramp rate 20  $^\circ\text{C min}^{-1}$  to 130  $^\circ\text{C}$  (2 min), ramp rate 20  $^\circ\text{C min}^{-1}$  to 280  $^\circ\text{C}$  (15.50 min). Quantitative analysis, using decane as an internal standard were performed using a flame ionization detector (GC-FID) and qualitative analysis using an HP5973 mass selective detector (GC-MS).

GC-FID integration method details: Initial Area Reject 0; Initial Peak Width 0.038; Shoulder Detection OFF; Initial Threshold 19.

Elemental analyses were performed at London Metropolitan University.

X-ray crystal and molecular structures were obtained by Prof. Alexandra Slawin or Dr. David Cordes. Tables containing full crystal data collection and refinement parameters of compounds **4**<sup>[33]</sup>, **5**<sup>[34]</sup> and **7**<sup>[35]</sup> can be found in the ESI for the thesis. All measurements were made on a Rigaku SCX mini diffractometer using graphite monochromated Mo-K $\alpha$  radiation. Data were collected and processed using CrystalClear (Rigaku). The data were corrected for Lorentz and polarization effects. The structure was solved by heavy-atom Patterson methods<sup>[36]</sup> and expanded using Fourier techniques. The non-hydrogen atoms were refined anisotropically. Hydrogen atoms were refined using the riding model. All calculations were performed using the CrystalStructure crystallographic software package<sup>††</sup> except for refinement, which was performed using SHELX-2013<sup>[37]</sup>.

Figures were generated with CrystalMaker for Windows 50 % thermal probability ellipsoids.

---

<sup>††</sup> CrystalStructure 4.1: Crystal Structure Analysis Package, Rigaku Corporation (2000-2014). Tokyo 196-8666, Japan.

### 6.4.3 Synthetic procedures

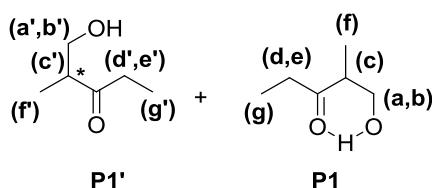
#### 6.4.3.1 1-hydroxy-2-methyl-3-pentanone (P1)

To produce it on larger scale it was synthesised using a base-catalysed procedure.

A Hastelloy® autoclave was charged with **1** (20 mL, 0.189 mol), methanol (9.6 mL, 0.237 mol), KOH (10.6 mg, 0.189 mmol) and paraformaldehyde (5.67 g, 0.189 mol) and heated at 80 °C with stirring for 24 h. The autoclave was then cooled to room temperature and vented to atmosphere to provide a dark yellow mixture.

Compound **P1** was purified through preliminary distillation (to remove alcoform\* components) and subsequent column chromatography on silica gel with gradient elution from 10 to 60 % of EtOAc-hexane. The purified material was used for GC-FID calibrations.

In this experimental section the two conformers will be called: **P1** (major species) and **P1'** (minor species) and they are present in the ratio of 1 : 0.2 (see § 6.2 for detailed explanation); <sup>1</sup>H NMR resonances will be listed as they appear in the spectrum.



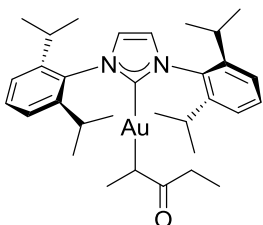
<sup>1</sup>H NMR (400 MHz; CD<sub>2</sub>Cl<sub>2</sub>): δ 3.8-3.5 (m, 2xAB parts of ABX spin systems, 2.4 H,  $J_{HaHb} = 10.9$ ,  $J_{HaHc} = 7.3$ ,  $J_{Ha'Hb'} = 9.5$ ,  $J_{Ha'Hc'} = 7.8$ ,  $J_{HbHc} = 4.5$ ,  $J_{Hb'Hc'} = 5.2$  Hz,  $H_{a,a',b,b'}$ ); 2.83 (ddq, 0.2 H,  $J = 5.2$ , 7.2, 7.3 Hz,  $H_c$ ); 2.73 (tq, 1H,  $J_{HcHf} = 7.2$ ,  $J_{HcHa} = J_{HcHb} = 4.5$  Hz,  $H_c$ ); 2.51 (m, 2xAB signals from ABX<sub>3</sub> spin system and br s (OH from **P1**) overlapping, 3.3 H,  $J_{HdHg} = J_{HeHg} = 7.25$  Hz,  $H_{d,d',e,e'}$ ); 2.0 (br s, 0.88 H, OH from **P1'**); 1.07 (d, 3 H,  $J_{HcHf} = 7.2$  Hz,  $H_f$ ), 1.04 (d, 0.6 H,  $J_{Hc'Hf'} = 7.2$  Hz,  $H_f$ ), 1.0 (t, 3H,  $J_{HgHd} = J_{HeHd} = 7.2$  Hz,  $H_g$ ), 0.99 (t, 0.6 H,  $J_{Hd'Hg'} = J_{He'Hg'} = 7.2$  Hz,  $H_g$ ) ppm.

<sup>13</sup>C{<sup>1</sup>H} NMR (100 MHz; CD<sub>2</sub>Cl<sub>2</sub>): **species P1**: δ = 215.6 (C3 carbonyl), 64.77 (C1), 48.22 (C2), 35.15 (C4), 13.4 (C6), 7.66 (C5) ppm; **species P1'**: δ = 214.1 (C3 carbonyl), 70.0 (C1), 46.5 (C2), 35.2 (C4), 13.7 (C6), 7.66 (C5) ppm.

The peaks at δ = 4.68 ppm in the <sup>1</sup>H NMR spectrum and 90.16 ppm in the <sup>13</sup>C{<sup>1</sup>H} NMR spectrum may be attributable to dimethoxymethane present as an impurity in the final product.

6.4.3.2 [Au(IPr){CH(CH<sub>3</sub>)C(O)CH<sub>2</sub>CH<sub>3</sub>}] (4)

## (1,3-bis(2,6-diisopropylphenyl)-2,3-dihydro-1H-imidazol-2-yl)(3-oxopentan-2-yl)gold



Compound **3** (106 mg, 0.176 mmol) was dissolved in DEK (2 mL, 18.88 mmol) and the solution stirred at RT for 36 h. Evaporation of DEK furnished a colourless oil which was triturated under a mixture of Et<sub>2</sub>O (0.2 mL) and hexane (ca 2 mL). The collected white solid was further washed with hexane (2 x 2 mL) and dried *in vacuo* to furnish the product **4** as a fine white powder (94.5 mg, 0.141 mmol; 80 % yield).

Suitable colourless prisms for single crystal X-Ray diffraction (XRD) were grown by slow vapour diffusion at RT of hexane into a saturated solution of **4** in DCM.

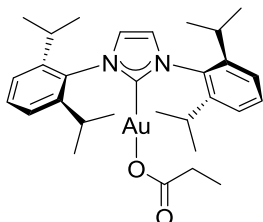
<sup>1</sup>H NMR (500 MHz; CD<sub>2</sub>Cl<sub>2</sub>): δ = 7.51 (t, 2H, *J* = 7.50 Hz, *phen*), 7.31 (d, 4H, *J* = 7.50 Hz, *phen*), 7.16 (s, 2H, *N*-CH), 2.56 and 2.55 (virtual m, two sept, 4H, *J* = 6.85 Hz, -CH- *IPr*), 2.42 (q, 1H, *J* = 6.10 Hz, *Au*-CH-), 1.75 (apparent nonet (q of AB patterns), 2H, *J*<sub>H-H</sub> = 14 Hz, *J*<sub>H-CH<sub>3</sub></sub> = 7 Hz, -CH<sub>2</sub>-), 1.31 and 1.30 (two d, 12H, *J* = 6.86 Hz, -CH<sub>3</sub> *IPr*), 1.21 (d, 12H, *J* = 6.86 Hz, -CH<sub>3</sub> *IPr*), 0.90 (d, 3H, *J* = 6.11 Hz, *Au*-C<sub>α</sub>-CH<sub>3</sub>) 0.57 (t, 3H, *J* = 7.54 Hz, -CH<sub>3</sub> *Et*) ppm.

<sup>13</sup>C{<sup>1</sup>H} NMR (125 MHz; CD<sub>2</sub>Cl<sub>2</sub>): δ = 212.56 (*carbonyl*), 192.81 (*Au*-C<sub>carbene</sub>), 146.23, 146.20 and 134.82 (C *Ar*), 130.55, 124.30, 124.26 and 123.26 (CH *Ar*), 47.70 (*Au*-CH), 35.09 (CH<sub>2</sub>), 29.08 (CH *IPr*), 24.47, 24.45 and 24.06 (CH<sub>3</sub> *IPr*), 14.54 (CH<sub>3</sub> C<sub>α</sub>CH<sub>3</sub>), 10.72 (CH<sub>3</sub>) ppm.

Elemental Anal. Calcd (%) for C<sub>32</sub>H<sub>45</sub>AuN<sub>2</sub>O (670.69): C 57.31; H 6.76; N 4.18. Found: C 57.15; H 6.62; N 4.16.

6.4.3.3 [Au(IPr){OC(O)CH<sub>2</sub>CH<sub>3</sub>}] (5)

## (1,3-bis(2,6-diisopropylphenyl)-2,3-dihydro-1H-imidazol-2-yl)(propionyloxy)gold



a) Compound **3** (5.5 mg, 0.009 mmol) was dissolved in toluene (0.6 mL) and stirred at RT for 4 h in the presence of a large excess of propanoic acid (20 times the amount of [Au]) (0.01



mL, 0.18 mmol). The crude product was reduced to dryness and analysed through NMR spectroscopy.

- b) Compound **3** (15 mg, 0.025 mmol) was suspended in a large excess of MeP (1 mL, 10.38 mmol) and heated at 120 °C under reflux for 3 h with stirring. At the end of this period the reaction mixture was reduced to dryness using a vacuum line and the solid analysed through NMR spectroscopy (all manipulations were performed under an inert atmosphere; MeP was dried and degassed prior to use).
- c) Compound **3** (10 mg, 0.0166 mmol) was dissolved in propanal (1 mL, 13.95 mmol) and stirred at RT for 16 h (under air or inert atmosphere). Evaporation of the aldehyde furnished a white solid which was washed with hexane (ca 1 mL) and dried under vacuum. The resulting white solid was analysed via NMR spectroscopy.

Suitable colourless prisms for single X-Ray diffraction (XRD) were grown by slow vapour diffusion at RT of hexane into a saturated solution of **5** in DCM.

#### NMR of the crystals:

<sup>1</sup>H NMR (400 MHz; CD<sub>2</sub>Cl<sub>2</sub>): δ = 7.56 (t, 2H, *J* = 7.8 Hz, phen), 7.35 (d, 4H, *J* = 7.8 Hz, phen), 7.23 (s, 2H, *N*-CH), 2.56 (sept, 4H, *J* = 6.9 Hz, -CH- *IPr*), 1.93 (q, 2H, *J* = 7.5 Hz, -CH<sub>2</sub>-), 1.35 (d, 12H, *J* = 6.9 Hz, -CH<sub>3</sub> *IPr*), 1.22 (d, 12H, *J* = 6.9 Hz, -CH<sub>3</sub> *IPr*), 0.86 (t, 3H, *J* = 7.5 Hz, -CH<sub>3</sub>) ppm. (the signal at 0.86 ppm is overlapping with another minor signal arising from pentane as a contaminant).

<sup>13</sup>C{<sup>1</sup>H} NMR (100 MHz; CD<sub>2</sub>Cl<sub>2</sub>): δ = 178.78 (CO), 168.9 (Au-C<sub>carbene</sub>), 145.26 and 134.58 (C *Ar*), 131.0, 124.6 and 123.8 (CH *Ar*), 30.4 (CH<sub>2</sub>), 29.26 (CH *IPr*), 24.49 and 24.17 (CH<sub>3</sub> *IPr*), 10.58 (CH<sub>3</sub>) ppm.

Due to the presence of minor amounts of pentane as a contaminant all <sup>13</sup>C resonances were identified with the help of GHSQC and HMBC NMR experiments (for quaternary carbons).

#### 6.4.3.4 [Au(IPr){CH(CH<sub>3</sub>)C(O)CH<sub>3</sub>}] (**7**) and [Au(IPr){CH<sub>2</sub>C(O)CH<sub>2</sub>CH<sub>3</sub>}] (**8**) in a 1 : 1 mixture

Compound **3** (20 mg, 0.033 mmol) was dissolved in MEK (1 mL, 11.16 mmol) and the solution stirred at RT for 16 hours. Evaporation of DEK furnished a colourless oil which was triturated under hexane (ca 1 mL). The collected white solid was further washed with hexane (2 x 2 mL) and dried *in vacuo* to furnish the products **7** and **8** in a 1 : 1 mixture.

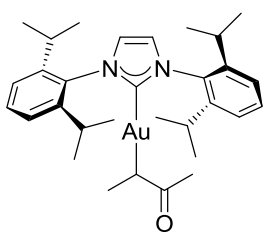
NMR resonances of both species will be listed as they appear in the spectrum, since NMR spectra of the single isolated species have never been recorded.

NMR resonances of both species will be listed as they appear in the spectrum of the mixture:

$^1\text{H}$  NMR (400 MHz;  $\text{CD}_2\text{Cl}_2$ ):  $\delta$  = 7.52 (t, 4H,  $J$  = 7.8 Hz, *phen*), 7.31 (d, 8H,  $J$  = 7.8 Hz, *phen*), 7.16 (s, 4H, *N-CH*), 2.6-2.5 (2 overlapping sept, 8H,  $J$  = 6.8 Hz, -CH- *IPr*), 2.41 (q, 1H,  $J$  = 6.2 Hz, *Au-CH-* complex **7**), 1.91 (s, 2H, *Au-CH<sub>2</sub>-* complex **8**), 1.78 (q, 2H,  $J$  = 7.5 Hz, -CH<sub>2</sub>- *Et* complex **8**), 1.46 (s, 3H, *C(O)CH<sub>3</sub>* complex **7**), 1.33-1.28 (d, 24H,  $J$  = 6.8 Hz, -CH<sub>3</sub> *IPr*), 1.21 (d, 24H,  $J$  = 6.8 Hz, -CH<sub>3</sub> *IPr*), 0.9 (d, 3H,  $J$  = 6.2 Hz, *Au-C $\alpha$ -(CH<sub>3</sub>)* complex **7**), 0.59 (t, 3H, -CH<sub>3</sub> *Et* complex **8**,  $J$  = 7.5 Hz) ppm.

$^{13}\text{C}\{^1\text{H}\}$  NMR (100 MHz;  $\text{CD}_2\text{Cl}_2$ ):  $\delta$  = 214.23 (*carbonyl*), 146.24, 134.84, 134.79, 130.63, 130.58, 124.36, 124.32, 124.29, 123.32 and 123.27 (*aromatic*), 49.01 (*Au-CH* complex **7**), 38.37 (*Au-CH<sub>2</sub>* complex **8**), 35.35 (*CH<sub>2</sub>* complex **8**), 29.10 (*CH<sub>3</sub>* complex **7** and *CH IPr*), 24.49, 24.07 and 24.06 (*CH<sub>3</sub> IPr*), 14.58 (*CH<sub>3</sub> C $\alpha$ CH<sub>3</sub>* complex **7**), 10.10 (*CH<sub>3</sub>* complex **8**) ppm.

All assignments in the aliphatic region were carried out with the help of 2D COSY ( $^1\text{H}, ^1\text{H}$ ) and GHSQC NMR experiments.



Colourless prisms of **7** suitable for single X-Ray diffraction (XRD) were grown by slow vapour diffusion at RT of hexane into a saturated solution of **7** and **8** in DCM.

$^1\text{H}$  NMR of the mixture after crystallisation again exhibited complexes **7** and **8** in a 1 : 1 mixture.

**[Au(IPr){CH(CH<sub>3</sub>)C(O)CH<sub>3</sub>} (1,3-bis(2,6-diisopropylphenyl)-2,3-dihydro-1H-imidazol-2-yl)(3-oxobutan-2-yl)gold (7)**

#### 6.4.3.5 Attempted $\alpha$ -activation of DEK with complexes (1) and (2)

Compound **1** (5 mg, 0.0105 mmol) was solubilised in a large excess of DEK (1 mL, 9.4 mmol) (DEK was dried and distilled under Ar from  $\text{Na}_2\text{SO}_4$  prior to use). The mixture was stirred at RT for 15 h. At the end of the reaction DEK was evaporated under vacuum furnishing an orange/yellow solid which was analysed through NMR spectroscopy in  $\text{C}_6\text{D}_6$ .

Compound **2** (11 mg, 0.023 mmol) was solubilised in a large excess of DEK (2 mL, 18.8 mmol) (DEK was dried and distilled under Ar from  $\text{Na}_2\text{SO}_4$  prior to use). The mixture was stirred at RT or 120 °C (in a Fisher-Porter vessel) for 15 and 14 h respectively. At the end of the reaction DEK was evaporated under vacuum furnishing a yellow oil, which was triturated under hexane

(dried and degassed using a Braun Solvent Purification System) to give a yellow solid and analysed by NMR spectroscopy in  $C_6D_6$ .

Neither experiment provided evidence of C-H activation.

#### 6.4.3.6 Attempted $\alpha$ -activation of MeP with complex **3**

The experiment and manipulations were performed under an inert atmosphere. Complex **3** (15.0 mg, 0.025 mmol) was suspended in a large excess of MeP (1 mL, 10.38 mmol) and stirred for 16 h at RT or heated at 120 °C under reflux for 3 h (MeP was dried, purified and degassed prior to use, following a standard procedure: pre-treatment with  $Na_2CO_3$  and further distillation from  $P_2O_5$ ).

At the end of this period the reaction mixture was reduced to dryness using a vacuum line and the solid analysed through NMR spectroscopy. The reaction at RT gave evidence of two Au species: the starting complex and  $[Au(IPr)\{OC(O)CH_2CH_3\}]$  (**5**) as major species. Suitable single crystals for X-Ray analysis were never obtained but the structure was confirmed by comparing the  $^1H$  NMR signals with those obtained by reacting complex **3** with propanoic acid (see above); while reaction at 120 °C furnishes only compound **5**.

The  $^1H$  NMR spectrum showed that the major product was the same as that obtained from propanal (Figure 6.2.13 and Section 6.4.3/complex **5**).

### 6.4.4 Catalytic experiments

#### 6.4.4.1 Reaction conditions for catalytic experiments using DEK as substrate

The experimental conditions are collected in Table 6.4.4.1 where the numbering scheme is the same as in Table 6.2.1. A Fisher-Porter vessel was charged with the catalyst **3** or **4** or KOH (base-catalysed experiment) (with the exception of **Entry 1** which is the *control experiment*), paraformaldehyde, methanol and DEK in the amounts shown in Table 6.4.4.1 and the mixture heated with stirring to the given temperature for the time shown. At the end of this period the vessel was cooled to room temperature and decane (1 mL, IS) was added to the mixture. Upon addition of decane the formation of two immiscible phases was observed, hence DCM was added to obtain one phase. The resulting solution was analysed by GC-FID.

**6.4.4.2 Reaction procedure for Entry 14 of Table 6.4.4.1**

Paraformaldehyde (0.34 g, 11.33 mmol) was suspended in MeOH (0.6 mL, 14.8 mmol) and the mixture heated to 120 °C for 3 h in a Fisher-Porter vessel. The resulting homogeneous viscous solution was transferred into a round bottomed flask charged with **1** (1.2 mL, 11.33 mmol) and catalyst **4** (11.4 mg, 0.017 mmol) and the mixture was stirred at RT for 12 h. GC-MS analysis of the crude product revealed the presence of only starting materials.

**Table 6.4.4.2.1** Conditions for alkylation of DEK. The results are in Table 6.2.1.

Entry	paraformaldehyde	MeOH	Cat.	t [h]	T [°C]
<b>1</b>	0.34 g, 11.33 mmol	0.6 mL, 14.8 mmol	-	6	120
<b>2</b>	0.34 g, 11.33 mmol	0.6 mL, 14.8 mmol	<b>3</b> (10.0 mg, 0.017mmol)	1	120
<b>3</b>	0.34 g, 11.33 mmol	0.6 mL, 14.8 mmol	<b>3</b> (10.0 mg, 0.017mmol)	6	120
<b>4</b>	0.68 g, 22.66 mmol	1.2 mL, 29.6 mmol	<b>KOH</b> (2 mg, 0.034 mmol)	6	120
<b>5</b>	0.34 g, 11.33 mmol	0.6 mL, 14.8 mmol	<b>3</b> (10.0 mg, 0.017mmol)	6	135
<b>6</b>	0.34 g, 11.33 mmol	0.6 mL, 14.8 mmol	<b>3</b> (10.0 mg, 0.017mmol)	12	120
<b>7</b>	0.34 g, 11.33 mmol	0.6 mL, 14.8 mmol	<b>3</b> (10.0 mg, 0.017mmol)	24	100
<b>8</b>	0.34 g, 11.33 mmol	0.6 mL, 14.8 mmol	<b>3</b> (10.0 mg, 0.017mmol)	24	110
<b>9</b>	0.34 g, 11.33 mmol	0.6 mL, 14.8 mmol	<b>3</b> (10.0 mg, 0.017mmol)	48	110
<b>10</b>	0.68 mg, 22.66 mmol	1.2 mL, 29.6 mmol	<b>3</b> (10.0 mg, 0.017mmol)	6	120
<b>11</b>	0.34 g, 11.33 mmol	1.2 mL, 29.6 mmol	<b>3</b> (20.0 mg, 0.034 mmol)	6	120
<b>12</b>	0.17 g, 5.66 mmol	0.3 mL, 7.4 mmol	<b>4</b> (5.7 mg, 0.008 mmol)	6	120
<b>13</b>	0.17 g, 5.66 mmol	0.3 mL, 7.4 mmol	<b>4</b> (5.7 mg, 0.008 mmol)	12	120
<b>14</b>	0.34 g, 11.33 mmol	0.6 mL, 14.8 mmol	<b>4</b> (11.4 mg, 0.017 mmol)	12	RT

DEK (1.2 mL, 11.33 mmol), except for Entries 4 (2.4 mL, 22.66 mmol), 12 and 13 (0.6 mL, 5.66 mmol).

### 6.4.4.3 Reaction conditions for *preliminary* catalytic experiments using 2-butanone (MEK), acetone and 2,4-dimethyl-3-pentanone as substrates

These reactions were carried out analogously to those reported in Table 6.4.4.1/Entry 6 except where indicated.

Entry	Substrate		T [°C]
1	MEK	1.01 mL, 11.33 mmol	120
2	acetone	0.8 mL, 11.33 mmol	138
3	2,4-dimethyl-3-pentanone	1.6 mL, 11.33 mmol	120

**Table 6.4.4.3.1** *General reaction conditions*: catalyst **3** (10.0 mg, 0.017 mmol), paraformaldehyde (0.34 g, 11.33 mmol), MeOH (0.6 mL, 14.8 mmol); in a Fisher-Porter vessel under stirring for 13h.

## 6.4.5 Mechanistic studies

### 6.4.5.1 Stoichiometric functionalisation of DEK with alcoform\*: NMR experiment

An NMR tube was charged with **4** (20 mg, 0.03 mmol) and preformed alcoform\* (15  $\mu$ L) in  $CD_2Cl_2$ . The alcoform\* was prepared using the same amounts and following the same procedure reported in § 6.4.4 (Table 6.4.4.1, Entry 14).

$^1H$  and 2D ( $^1H, ^1H$ ) NMR spectra were regularly recorded at 3, 5, 20, 24, 48, 72 and 96 h, observing the formation of the organic product **P1** and conversion of complex **3** into a final gold(I) species. After the reaction reached completion (4 days under these conditions) a full NMR characterisation of the sample was performed:  $^{13}C\{^1H\}$  UDEFT, GHSQC and GHMBC NMR spectra as additional experiments. NMR resonances of the new Au(I) species are listed below (resonances of compound **P1** are not listed in this paragraph).

$^1H$  NMR (500 MHz;  $CD_2Cl_2$ ):  $\delta$  = 7.52 (t, 2H,  $J$  = 7.8 Hz, *phen*), 7.32 (d, 4H,  $J$  = 7.8 Hz, *phen*), 7.22 (s, 2H, *N-CH*), 2.55 (sept, 4H,  $J$  = 6.8 Hz, -CH- *IPr*), 1.34 (d, 12H,  $J$  = 6.8 Hz, -CH<sub>3</sub> *IPr*), 1.22 (d, 12H,  $J$  = 6.8 Hz, -CH<sub>3</sub> *IPr*) ppm.

$^{13}C\{^1H\}$  NMR (125 MHz;  $CD_2Cl_2$ ):  $\delta$  = 146.26, 130.86, 124.5, 123.6, 29.19, 24.33, 24.2 ppm

#### 6.4.5.2 Stoichiometric functionalisation of DEK with $^{13}\text{C}$ labelled alcoform\*: NMR experiment

$^{13}\text{C}$  labelled alcoform\* was pre-prepared in a Fisher-Porter vessel by heating a suspension of paraformaldehyde (0.11 g, 3.66 mmol) in  $^{13}\text{CH}_3\text{OH}$  (0.2 mL, 4.93 mmol) at 120 °C with stirring for 5 h. An NMR tube was charged with **4** (20 mg, 0.03 mmol) and of  $^{13}\text{C}$  labelled alcoform\* (16  $\mu\text{L}$ ) in  $\text{CD}_2\text{Cl}_2$  (1 mL).  $^1\text{H}$ ; 2D ( $^1\text{H}, ^1\text{H}$ ),  $^{13}\text{C}\{^1\text{H}\}$  UDEFT, GHSQC and GHMBC NMR spectra were recorded after 1, 2 and 3 days.

$^1\text{H}$  NMR resonances of the organic product **P1** and the new Au(I) species were comparable with those reported for the unlabelled NMR experiment, while all peaks belonging to the alcoform\* exhibited the additional coupling with  $^{13}\text{C}$ . ( $J_{\text{H-C}} = 140.6$  and 6.4 Hz). Only methyl groups arising from methanol gave enhanced  $^{13}\text{C}$  signals.

#### 6.4.5.3 Blank experiment with (**4**) and methanol

A few drops of methanol were added to a solution of **4** (20 mg, 0.03 mmol) in  $\text{CD}_2\text{Cl}_2$  (1 mL) in an NMR tube.

NMR spectra were collected approximately after few hours and then after 3, 6 and 12 days.

Formation of the free ketone was observed in the NMR spectrum together with the conversion of the initial Au(I) species, however the reaction never reached completion under these conditions and a final Au(I) species was never isolated.

### 6.4.6 DFT calculations

#### 6.4.6.1 Computational details

The methodology employed has been validated and performs well for gold complexes.<sup>[38]</sup>

Complex **7** geometries are based on an XRD structure.

Geometries were fully optimized at the PBE0/ECP1 level of theory, i.e. using the PBE0 hybrid functional,<sup>[39]</sup> the Stuttgart-Dresden effective core potential (together with its associated valence basis) on Au,<sup>[40]</sup> and 6-31G\* basis on all other atoms.<sup>[41]</sup> Refined energies were obtained through single-point calculations at the PBE0-D3/ECP2 level, i.e. including Grimme's D3 dispersion correction,<sup>[42]</sup> the same SDD core potential and valence basis on Au and the 6-311+G\*\* basis on all other atoms, in conjunction with the polarisable continuum model (PCM)

by Tomasi *et al.* employing the parameters of dichloromethane and acetone (acetone has a similar dielectric constant to that of 3-butanone) and the default settings in Gaussian03.<sup>[43]</sup> Acquisition of atomic charges was achieved by natural population analysis of the PBE0/ECP2/PCM wavefunctions. All calculations were performed with the Gaussian03 software.

#### 6.4.6.2 GAS and PCM Energies

E [kJ mol <sup>-1</sup> ]	Complex 7	Complex 8
E (PBE0/ECP2)	9.5	0.0
E (PBE0/ECP2/PCM-DCM)	7.6	0.0
E (PBE0/ECP2/PCM-Acetone)	7.4	0.0

**Table 6.4.6.2.1** Relative GAS phase and PCM Energies (DCM and Acetone) in kJ/mol (PBE0/ECP2) with that of the lowest stereoisomer set to 0.0 in each case.

*PBE0/ECP1 coordinates in Å (xyz format) of optimised complexes including total SCF Energy in a.u. are reported in Appendix 2.*

## 6.5 References

- [1] a) M. M. Green, H. A. Wittcoff, in *Organic Chemistry Principles and Industrial Practice*, Wiley-VCH, Weinheim, **2003**, pp. 137-156; b) K. Nagai, *Appl. Catal., A* **2001**, *221*, 367-377; c) G. R. Eastham, R. P. Tooze, X. L. Wang, K. Whiston, World Patent 96/19434, **1996**; d) W. Clegg, M. R. J. Elsegood, G. R. Eastham, R. P. Tooze, X. L. Wang, K. Whiston, *Chem. Commun. (Cambridge)* **1999**, 1877-1878.
- [2] B. Harris, *Ingenia* **2010**, 19-23.
- [3] M. B. Smith, *Organic Chemistry: An Acid - Base Approach*, CRC Press, Boca Raton, FL, **2010**.
- [4] J. McMurry, *Organic Chemistry, 5th Ed.*, Brooks Cole, , Pacific Grove, CA, **2000**.
- [5] A. von Baeyer, V. Villiger, *Ber.* **1899**, *32*, 3625-3633.
- [6] a) G. R. Krow, *Organic Reactions (New York)* **1993**, *43*, 251-798; b) M. Renz, B. Meunier, *Eur. J. Org. Chem.* **1999**, 737-750.
- [7] G. Strukul, *Angew. Chem. Int. Ed.* **1998**, *37*, 1199-1209.
- [8] a) C. Mazzini, J. Lebreton, R. Furstoss, *J. Org. Chem.* **1996**, *61*, 8-9; b) S.-I. Murahashi, S. Ono, Y. Imada, *Angew. Chem. Int. Ed.* **2002**, *41*, 2366-2368; c) O. Fukuda, S. Sakaguchi, Y. Ishii, *Tetrahedron Lett.* **2001**, *42*, 3479-3481.
- [9] C. Bolm, C. Palazzi, G. Francio, W. Leitner, *Chem. Commun. (Cambridge, U. K.)* **2002**, 1588-1589.
- [10] N. M. Kamerbeek, D. B. Janssen, W. J. H. van Berkel, M. W. Fraaije, *Adv. Synth. Catal.* **2003**, *345*, 667-678.
- [11] G. R. Eastham, *Private communication*.
- [12] a) A. E. Shilov, G. B. Shul'pin, *Chem. Rev. (Washington, D. C.)* **1997**, *97*, 2879-2932; b) R. H. Crabtree, *J. Chem. Soc., Dalton Trans.* **2001**, 2437-2450; c) J. Wencel-Delord, T. Droege, F. Liu, F. Glorius, *Chem. Soc. Rev.* **2011**, *40*, 4740-4761; d) R. Jazzar, J. Hitce, A. Renaudat, J. Sofack-Kreutzer, O. Baudoin, *Chem. Eur. J.* **2010**, *16*, 2654-2672; e) Y. Guari, S. Sabo-Etienne, B. Chaudret, *Eur. J. Inorg. Chem.* **1999**, 1047-1055; f) T. C. Boorman, I. Larrosa, *Chem. Soc. Rev.* **2011**, *40*, 1910-1925; g) T. de Haro, C. Nevado, *Synthesis* **2011**, 2530-2539.
- [13] R. G. Bergman, *Nature (London, U. K.)* **2007**, *446*, 391-393.
- [14] J. A. Labinger, J. E. Bercaw, *Nature (London, U. K.)* **2002**, *417*, 507-514.
- [15] a) P. E. Romero, M. T. Whited, R. H. Grubbs, *Organometallics* **2008**, *27*, 3422-3429; b) W. H. Bernskoetter, S. K. Hanson, S. K. Buzak, Z. Davis, P. S. White, R. Swartz, K. I. Goldberg, M. Brookhart, *J. Am. Chem. Soc.* **2009**, *131*, 8603-8613; c) R. B. Bedford, M. Betham, M. E. Blake, S. J. Coles, S. M. Draper, M. B. Hursthouse, P. N. Scully, *Inorg. Chim. Acta* **2006**, *359*, 1870-1878.
- [16] a) L. Schwartsburd, M. A. Iron, L. Konstantinovski, Y. Diskin-Posner, G. Leitus, L. J. W. Shimon, D. Milstein, *Organometallics* **2010**, *29*, 3817-3827; b) J. Meiners, A. Friedrich, E. Herdtweck, S. Schneider, *Organometallics* **2009**, *28*, 6331-6338; c) M. T. Whited, Y. Zhu, S. D. Timpa, C.-H. Chen, B. M. Foxman, O. V. Ozerov, R. H. Grubbs, *Organometallics* **2009**, *28*, 4560-4570.
- [17] M. Feller, A. Karton, G. Leitus, J. M. L. Martin, D. Milstein, *J. Am. Chem. Soc.* **2006**, *128*, 12400-12401.
- [18] J. Coetzee, G. R. Eastham, A. M. Z. Slawin, D. J. Cole-Hamilton, *Dalton Trans.* **2015**, *44*, 1585-1591.
- [19] a) B. J. Truscott, D. J. Nelson, A. M. Z. Slawin, S. P. Nolan, *Chem. Commun. (Cambridge, U. K.)* **2014**, *50*, 286-288; b) B. J. Truscott, D. J. Nelson, C. Lujan, A. M. Z. Slawin, S. P. Nolan, *Chem. Eur. J.* **2013**, *19*, 7904-7916; c) D. J. Nelson, J. A. Fernandez-Salas, B. J.



- Truscott, S. P. Nolan, *Organic & Biomolecular Chemistry* **2014**, *12*, 6672-6676; d) B. J. Truscott, G. C. Fortman, A. M. Z. Slawin, S. P. Nolan, *Organic & Biomolecular Chemistry* **2011**, *9*, 7038-7041; e) B. J. Truscott, A. M. Z. Slawin, S. P. Nolan, *Dalton Trans.* **2013**, *42*, 270-276; f) S. Gaillard, A. M. Z. Slawin, S. P. Nolan, *Chem. Commun. (Cambridge, U. K.)* **2010**, *46*, 2742-2744; g) S. Gaillard, C. S. J. Cazin, S. P. Nolan, *Acc. Chem. Res.* **2012**, *45*, 778-787; h) G. C. Fortman, A. M. Z. Slawin, S. P. Nolan, *Organometallics* **2010**, *29*, 3966-3972; i) P. Nun, G. C. Fortman, A. M. Z. Slawin, S. P. Nolan, *Organometallics* **2011**, *30*, 6347-6350; j) J. D. Egbert, A. Chartoire, A. M. Z. Slawin, S. P. Nolan, *Organometallics* **2011**, *30*, 4494-4496; k) I. I. F. Boogaerts, S. P. Nolan, *J. Am. Chem. Soc.* **2010**, *132*, 8858-8859; l) D. Gasperini, A. Collado, A. Gomez-Suarez, D. B. Cordes, A. M. Z. Slawin, S. P. Nolan, *Chem. Eur. J.* **2015**, *21*, 5403-5412.
- [20] a) S. Gaillard, A. M. Z. Slawin, S. P. Nolan, *Chem. Commun. (Cambridge, U. K.)* **2010**, *46*, 2742-2744; b) G. C. Fortman, A. Poater, J. W. Levell, S. Gaillard, A. M. Z. Slawin, I. D. W. Samuel, L. Cavallo, S. P. Nolan, *Dalton Trans.* **2010**, *39*, 10382-10390; c) S. Gaillard, P. Nun, A. M. Z. Slawin, S. P. Nolan, *Organometallics* **2010**, *29*, 5402-5408; d) A. S. K. Hashmi, A. M. Schuster, S. Gaillard, L. Cavallo, A. Poater, S. P. Nolan, *Organometallics* **2011**, *30*, 6328-6337; e) D. Konkolewicz, S. Gaillard, A. G. West, Y. Y. Cheng, A. Gray-Weale, T. W. Schmidt, S. P. Nolan, S. Perrier, *Organometallics* **2011**, *30*, 1315-1318; f) P. Nun, S. Dupuy, S. Gaillard, A. Poater, L. Cavallo, S. P. Nolan, *Catal. Sci. Technol.* **2011**, *1*, 58-61; g) P. Nun, R. S. Ramon, S. Gaillard, S. P. Nolan, *J. Organomet. Chem.* **2010**, *696*, 7-11; h) S. Dupuy, F. Lazreg, A. M. Z. Slawin, C. S. J. Cazin, S. P. Nolan, *Chem. Commun. (Cambridge, U. K.)* **2011**, *47*, 5455-5457; i) S. Dupuy, A. M. Z. Slawin, S. P. Nolan, *Chem. Eur. J.* **2012**, *18*, 14923-14928, S14923/14921-S14923/14931; j) E. Brule, S. Gaillard, M.-N. Rager, T. Roisnel, V. Guerineau, S. P. Nolan, C. M. Thomas, *Organometallics* **2011**, *30*, 2650-2653.
- [21] A. S. K. Hashmi, S. Schaefer, M. Woelfe, C. Diez Gil, P. Fischer, A. Laguna, M. C. Blanco, M. C. Gimeno, *Angew. Chem. Int. Ed.* **2007**, *46*, 6184-6187, S6184/6181-S6184/6188.
- [22] A. Galat, US2775619, **1956**
- [23] E. N. Wheeler, L. S. Richardson, US3000960 **1961**
- [24] M. Waugh, *Private Communication*.
- [25] S. Kobayashi, I. Hachiya, *J. Org. Chem.* **1994**, *59*, 3590-3596.
- [26] a) J. T. Hays, G. F. Hager, H. M. Engelmann, H. M. Spurlin, *J. Am. Chem. Soc.* **1951**, *73*, 5369-5373; b) G. T. Morgan, E. L. Holmes, *J. Chem. Soc.* **1932**, 2667-2673.
- [27] G. P. Luke, J. Morris, *J. Org. Chem.* **1995**, *60*, 3013-3019.
- [28] J. S. Rommel, J. T. Traxler, R. R. Boettcher, US5703248 A, **1997**
- [29] J. Decombe, *Compt. rend.* **1936**, *202*, 1685-1687.
- [30] A. Collado, *Private Communication*.
- [31] F. Nahra, S. R. Patrick, A. Collado, S. P. Nolan, *Polyhedron* **2014**, Ahead of Print.
- [32] G. R. Fulmer, A. J. M. Miller, N. H. Sherden, H. E. Gottlieb, A. Nudelman, B. M. Stoltz, J. E. Bercaw, K. I. Goldberg, *Organometallics* **2010**, *29*, 2176-2179.
- [33] CCDC 1059500 contains the supplementary crystallographic data for this thesis. These data can be obtained free of charge from The Cambridge Crystallographic Data Centre (CCDC) via [http://www.ccdc.cam.ac.uk/data\\_request/cif](http://www.ccdc.cam.ac.uk/data_request/cif)
- [34] CCDC 1059502 contain the supplementary crystallographic data for this thesis. These data can be obtained free of charge from The Cambridge Crystallographic Data Centre (CCDC) via [http://www.ccdc.cam.ac.uk/data\\_request/cif](http://www.ccdc.cam.ac.uk/data_request/cif)
- [35] CCDC 1059501 contain the supplementary crystallographic data for this thesis. These data can be obtained free of charge from The Cambridge Crystallographic Data Centre (CCDC) via [http://www.ccdc.cam.ac.uk/data\\_request/cif](http://www.ccdc.cam.ac.uk/data_request/cif)

- [36] M. C. Burla, R. Caliendo, M. Camalli, B. Carrozzini, G. L. Cascarano, C. Giacobozzo, M. Mallamo, A. Mazzone, G. Polidori, R. Spagna, *J. Appl. Crystallogr.* **2012**, *45*, 357-361.
- [37] G. M. Sheldrick, *Acta Cryst.* **2008**, *A64*, 112-122.
- [38] a) S. Dupuy, L. Crawford, M. Buehl, A. M. Z. Slawin, S. P. Nolan, *Adv. Synth. Catal.* **2012**, *354*, 2380-2386, S2380/2381-S2380/2342; b) S. Dupuy, L. Crawford, M. Buehl, S. P. Nolan, *Chem. Eur. J.* **2015**, *21*, 3399-3408.
- [39] a) J. P. Perdew, K. Burke, M. Ernzerhof, *Phys. Rev. Lett.* **1996**, *77*, 3865-3868; b) C. Adamo, V. Barone, *J. Chem. Phys.* **1999**, *110*, 6158-6170.
- [40] M. Dolg, U. Wedig, H. Stoll, H. Preuss, *J. Chem. Phys.* **1987**, *86*, 866-872.
- [41] a) W. J. Hehre, R. Ditchfield, J. A. Pople, *J. Chem. Phys.* **1972**, *56*, 2257-2261; b) P. C. Hariharan, J. A. Pople, *Theor. Chim. Acta* **1973**, *28*, 213-222.
- [42] S. Grimme, J. Antony, S. Ehrlich, H. Krieg, *J. Chem. Phys.* **2010**, *132*, 154104/154101-154104/154119.
- [43] Gaussian 03, Revision C.02, M. J. Frisch, G. W. Trucks, H. B. Schlegel, G. E. Scuseria, M. A. Robb, J. R. Cheeseman, J. A. Montgomery, Jr., T. Vreven, K. N. Kudin, J. C. Burant, J. M. Millam, S. S. Iyengar, J. Tomasi, V. Barone, B. Mennucci, M. Cossi, G. Scalmani, N. Rega, G. A. Petersson, H. Nakatsuji, M. Hada, M. Ehara, K. Toyota, R. Fukuda, J. Hasegawa, M. Ishida, T. Nakajima, Y. Honda, O. Kitao, H. Nakai, M. Klene, X. Li, J. E. Knox, H. P. Hratchian, J. B. Cross, V. Bakken, C. Adamo, J. Jaramillo, R. Gomperts, R. E. Stratmann, O. Yazyev, A. J. Austin, R. Cammi, C. Pomelli, J. W. Ochterski, P. Y. Ayala, K. Morokuma, G. A. Voth, P. Salvador, J. J. Dannenberg, V. G. Zakrzewski, S. Dapprich, A. D. Daniels, M. C. Strain, O. Farkas, D. K. Malick, A. D. Rabuck, K. Raghavachari, J. B. Foresman, J. V. Ortiz, Q. Cui, A. G. Baboul, S. Clifford, J. Cioslowski, B. B. Stefanov, G. Liu, A. Liashenko, P. Piskorz, I. Komaromi, R. L. Martin, D. J. Fox, T. Keith, M. A. Al-Laham, C. Y. Peng, A. Nanayakkara, M. Challacombe, P. M. W. Gill, B. Johnson, W. Chen, M. W. Wong, C. Gonzalez, and J. A. Pople, Gaussian, Inc., Wallingford CT, 2004.

## General Conclusions

The main aim of this thesis was to investigate catalytic systems for the alkylation of carbonyl compounds with formaldehyde in an attempt of making acrylate esters.

In this research work we reported a novel approach for the  $\alpha$ -methylenation of methyl propanoate (MeP), an intermediate of the Lucite ALPHA plant, with formaldehyde arising from Ru-catalysed dehydrogenation of methanol. In the proposed catalytic system four main reactions occur: *methanol dehydrogenation*, providing *in situ* production of anhydrous formaldehyde, *MeP deprotonation* and *condensation* with the nascent formaldehyde and partial *hydrogenation* of methyl methacrylate (MMA) to methyl isobutyrate (MiBu). Overall the yields of the two desired products, MMA and MiBu, are modest but not very much lower than that obtained in a commercial high temperature condensation of anhydrous formaldehyde with MeP (17 % per pass). Among the catalysts screened  $[\text{RuH}_2(\text{CO})(\text{PPh}_3)_3]$  was found to be the most active species in the presence of strong bases such as  $\text{NaOCH}_3$  and *t*-BuONa under an atmosphere of ethene, proved to be a more effective hydrogen acceptor under moderate pressures (6 bar). The high reaction temperature required (170 °C) and the low boiling points of methanol and MeP meant that the reaction could not be carried out in an open system to allow for  $\text{H}_2$  venting. The main problem with the reaction is the formation of dimethyl ether and sodium propanoate apparently from the nucleophilic attack of methoxide on MeP with the propanoate anion acting as a leaving group. Attempts to inhibit this kind of reaction using *tert*-butyl propanoate (*t*-BuP) and *t*-BuONa improved the yield of the desired products but were frustrated by transesterification of the ester with methanol, inevitably present for the formation of formaldehyde. Labelling studies showed that the added methylene (MMA) or methyl group (MiBu) arose predominantly from methanol.

The mechanism proposed for the dehydrogenation of methanol catalysed by  $[\text{RuH}_2(\text{CO})(\text{PPh}_3)_3]$  involves an anionic cycle originated by displacement of a phosphine ligand with the methoxide ion arising from deprotonation of methanol. The resulting anionic methoxy intermediate undergoes loss of  $\text{PPh}_3$  followed by  $\beta$ -hydrogen abstraction with subsequent formation of the formaldehyde product which remains coordinated to the metal centre. Nucleophilic attack of deprotonated MeP occurs to the coordinated formaldehyde which electrophilicity is enhanced by coordination to Ru but it could also occur onto free formaldehyde. Subsequent protonation

and decoordination of the condensation adduct produces an anionic trihydrido carbonyl complex which could regenerate the methoxide ion and afford molecular hydrogen by abstracting a proton from a new molecule of methanol. The catalyst is finally regenerated by liberation of H<sub>2</sub> from a molecular hydrogen complex.

A density functional study (DFT) was undertaken to elucidate the proposed mechanism. Two plausible reaction pathways in which all designed intermediates retain the carbonyl ligand were designed. The rate-determining step was found to be the partial decoordination of the formaldehyde product. In order to gain more information about the nature of the transition state involved in the rate-determining step, the <sup>1</sup>H/<sup>2</sup>H kinetic isotope effect was determined experimentally and computationally. The experimental value of 1.3 was in good agreement with the computed 1.6, confirming that the C-H bond under study does not undergo cleavage in the rate-determining step. The overall reaction, however, exhibited a relatively high activation barrier thus is possible only at high temperature.

This kind of homogeneous catalytic systems is affected by the occurrence of side reactions besides H<sub>2</sub> production such as alcohol decarbonylation which was investigated computationally and experimentally. Unexpected reaction intermediates have come to light from additional experiments leading to the design of new multiple and sometimes cross-linked reaction channels with evidences of intramolecular exchange of <sup>2</sup>H and incorporation into the *ortho* positions of the phenyl rings of phosphine ligands.

As an alternative approach to the synthesis of acrylate esters, ketones were investigated as potential substrates in order to overcome some of the problems related to competing reactions that occur at the ester group. Hydroxymethylenation, followed by dehydration and Baeyer-Villiger oxidation, possibly catalysed by enzymes to reverse the normal selectivity, leads to the formation of these acrylate esters. The catalytic reaction is enabled by a gold carbene hydroxide complex [Au(IPr)(OH)], acting as a catalyst or catalyst precursor, in such a way that the substrate undergoes C-H activation and the nascent metal alkyl acts as a nucleophile towards the electrophilic formaldehyde, supplied in the form of alcoform\*, a solution of paraformaldehyde in methanol containing oligomers of the form CH<sub>3</sub>O(CH<sub>2</sub>O)<sub>n</sub>H (n<5) as the main species. Labelling experiments allowed to confirm that methanol was not the source of formaldehyde in this catalytic system. Encouraging results were obtained at very low catalyst loading when using 3-pentanone as substrate at 110 °C for 48 h (TON of 187). The  $\alpha$ -hydroxymethylenated product MeCH(CH<sub>2</sub>OH)C(O)Et was found to exist in two forms that we

assigned as the ring opened and a hydrogen bonded closed form. The major species appeared to be the one stabilised by this intramolecular hydrogen bond and may explain why the final product is stable towards dehydration even at higher temperatures. Similar yields were achieved with a simple base-catalysed condensation reaction in the presence of KOH, however when the Au ketonyl complex  $[\text{Au}(\text{IPr})\{\text{CH}(\text{Me})\text{C}(\text{O})\text{Et}\}]$  was isolated and used directly in catalysis, it exhibited higher selectivity towards the desired product (95.6 %). Attempts to activate methyl propanoate, by this method either catalytically or stoichiometrically were unsuccessful because of the formation of the propanoate complex,  $[\text{Au}(\text{IPr})\{\text{OC}(\text{O})\text{Et}\}]$ , which can also be formed from propanoic acid or from propanal, in air. Ir and Cu hydroxide complexes were broadly unsuccessful suggesting that there seems to be a peculiar reactivity with the gold hydroxide. Based on this preliminary study, the next step deals with the development of less expensive, more efficient and versatile catalytic systems for the alkylation of carbonyl compounds with formaldehyde.

## Appendix 1

**BP86/ECP1 coordinates in Å (xyz format) of optimised complexes reported in Chapter 4 including total SCF Energy in a.u.**

### [RuH<sub>2</sub>(CO)(PPh<sub>3</sub>)<sub>3</sub>] (1)

SCF Done: -3307.40469936

Ru	-0.01763100	0.44698900	-0.38972500	C	-3.71835200	3.00905000	1.49586300
P	-2.21803400	1.11292300	-0.00659100	C	-3.50700900	0.02662400	0.79516700
P	2.22550900	0.99716600	-0.01456700	C	-4.81229200	-0.15051300	0.28329500
P	-0.02506000	-1.93327800	-0.07501100	C	-5.73704100	-0.96547400	0.96093300
C	-2.41798600	2.59339800	1.11526300	H	-3.12956300	-0.32621400	-2.38716800
C	-5.37308500	-1.61037100	2.15433400	H	-4.22630300	0.36619400	-4.50713200
C	-4.07741200	-1.43653700	2.67291300	H	-4.78317900	2.77543500	-4.91175700
C	-3.15194700	-0.62450500	1.99936000	H	-4.24739200	4.48378100	-3.16089500
C	-3.10497100	1.68102100	-1.53839000	H	-3.19805000	3.78601000	-1.01208000
C	-3.39657900	0.72450900	-2.54210500	H	-2.94606200	-2.48050500	0.18256300
C	-4.00650900	1.11807300	-3.74266300	H	-4.62075200	-3.51940400	-1.31915000
C	-4.31596300	2.47031400	-3.97017800	H	-3.91842000	-4.47010700	-3.53411100
C	-4.01477100	3.42779200	-2.98915100	H	-1.50702300	-4.37416900	-4.21011400
C	-3.41722500	3.03728300	-1.77798800	H	0.17840800	-3.36111900	-2.69196000
C	2.56165400	2.81403000	0.33635300	H	1.26233200	-4.49337700	0.91279900
C	-1.30731600	3.31631700	1.59647600	H	3.28370500	-5.74816800	0.18996800
C	1.88604800	3.80324200	-0.41419700	H	4.70998800	-4.87521600	-1.67579600
C	2.20068900	5.16331500	-0.26009600	H	4.08723900	-2.72075900	-2.80749400
C	3.19239100	5.56201500	0.65050400	H	2.07502400	-1.46704500	-2.07310300
C	3.87660200	4.58906900	1.39654200	H	-2.13953000	-0.50654700	2.39678100
C	3.57365800	3.22693000	1.23492100	H	-3.77598800	-1.94448500	3.59385100
C	3.56299300	0.84871300	-1.31630600	H	-6.09338500	-2.24749300	2.67716700
C	3.19113500	0.84342600	-2.67833300	H	-6.74491100	-1.09366000	0.55230100
C	4.16851700	0.83510200	-3.68900900	H	-5.09854800	0.33739300	-0.65240600
C	5.53142900	0.83226700	-3.35286700	H	-4.58962800	2.44632300	1.14812000
C	5.91319800	0.85077200	-2.00009000	H	-0.30257000	2.99457400	1.31261100
C	-1.49002500	4.43350600	2.43132200	H	-0.61431400	4.98298300	2.79150300
C	4.93959300	0.86678400	-0.98960000	H	-2.92180300	5.70922400	3.44928500
C	2.99600600	0.19132600	1.47291500	H	-4.90785800	4.43096500	2.61281700
C	2.63691900	0.64849200	2.76623800	H	4.11724000	2.48240200	1.82259400
C	3.13716400	0.01274200	3.91289500	H	4.65487400	4.88771700	2.10655400
C	3.97958500	-1.10676900	3.79118200	H	3.43226700	6.62256200	0.77584400
C	4.31227900	-1.58836600	2.51622500	H	1.66351700	5.91101900	-0.85257800
C	3.82717600	-0.94636500	1.36282800	H	1.10159800	3.50115000	-1.11571500
C	-1.25906200	-2.83773900	-1.14689000	H	2.13128100	0.84843000	-2.94801200
C	-0.87343800	-3.38176100	-2.39368100	H	5.25014300	0.89326200	0.05846300
C	-1.82677000	-3.95972800	-3.24851400	H	6.97392900	0.85999400	-1.72905900

C	-2.78137500	4.84087600	2.79764500	H	3.85857300	0.83344600	-4.73911500
C	-3.17768500	-4.01449900	-2.86940700	H	6.29307600	0.82429000	-4.13889100
C	-3.57191200	-3.48373900	-1.62964100	H	4.08734300	-1.34031900	0.37687800
C	-2.62414700	-2.89601100	-0.77513800	H	1.96332500	1.50572500	2.86775800
C	-0.34806900	-2.66273200	1.60717800	H	2.86483900	0.39139800	4.90366800
C	-0.99400100	-3.90748800	1.79729000	H	4.36563700	-1.60460500	4.68603800
C	-1.16345000	-4.43280200	3.08978600	H	4.94891900	-2.47213500	2.40976500
C	-0.68194900	-3.73085100	4.20802500	H	-1.37723000	-4.45527800	0.93169100
C	-0.02668000	-2.50103800	4.02769500	H	0.64490900	-1.00902900	2.59978000
C	0.13694600	-1.96838700	2.73839700	H	0.36464700	-1.95183300	4.88986900
C	1.51252000	-2.89562700	-0.53888100	H	-0.81258300	-4.14342600	5.21364600
C	-3.89650000	4.12440400	2.32713700	H	-1.67186000	-5.39356900	3.22096700
C	1.87327600	-4.10784100	0.09204800	H	-0.07072200	2.05484200	-0.56600800
C	3.01721800	-4.81368100	-0.31477300	H	0.04179600	0.72054600	1.25919600
C	3.81741100	-4.32477400	-1.36168400	C	-0.15595500	0.25992500	-2.28260200
C	3.46856600	-3.12318100	-1.99942200	O	-0.25956000	0.17843800	-3.45536300
C	2.32634900	-2.41359800	-1.58855400				

**Complex 2a**

SCF Done: -2274.7915006

Ru	-0.11494500	-1.38446200	-0.55199700	C	-2.85666100	1.70550400	1.90275400
P	-2.02249700	-0.03053500	-0.20833000	C	-3.02452700	2.95992100	2.51278100
P	1.77409300	0.04718500	-0.28328200	H	-0.17329700	-0.22928500	2.07318300
C	-3.64057400	-0.29958300	-1.05853800	H	0.47033700	-2.15469200	3.50291000
C	-2.59254200	4.12572200	1.85746200	H	-1.01553700	-4.15761800	3.65636300
C	-1.98266900	4.03652500	0.59401600	H	-3.09821500	-4.28384900	2.27193300
C	-1.80856400	2.78517400	-0.01955300	H	-3.63599200	-2.47692000	0.64641500
C	-1.89261500	-1.26558900	1.14909800	H	0.41268700	2.02739300	1.38912000
C	-0.72501200	-1.16847500	1.98058500	H	0.78803900	2.90940200	3.67942400
C	-0.42041100	-2.23594200	2.87133800	H	2.80413700	2.19675800	4.99243100
C	-1.25664000	-3.34455200	2.96500200	H	4.43904800	0.59517400	3.97797400
C	-2.43663600	-3.41680100	2.17957800	H	4.06269800	-0.29847600	1.68332800
C	-2.74568600	-2.40493200	1.27862400	H	3.99952400	0.91631300	-2.13750300
C	-3.68372400	-1.12165800	-2.20839500	H	6.15885500	-0.13625500	-2.77727500
C	-4.90225500	-1.35624100	-2.86630700	H	6.83280000	-2.33484300	-1.78407500
C	2.20702900	0.78933400	1.37459600	H	5.30553800	-3.48140600	-0.16201500
C	3.34129600	0.39744200	2.12106300	H	3.12620600	-2.45902400	0.43909200
C	3.55115000	0.90335700	3.41604200	H	-1.31331000	2.71700900	-0.99372400
C	-6.08630300	-0.76990900	-2.38995000	H	-1.63351400	4.94120400	0.08682100
C	2.63657600	1.80465400	3.98443500	H	-2.72448500	5.10245500	2.33352400
C	1.50605100	2.20354800	3.25016900	H	-3.49178500	3.02563100	3.50059600
C	1.28883400	1.69881300	1.95875500	H	-3.17705300	0.79447700	2.41814200
C	1.72694000	1.58130600	-1.34177900	H	-4.80986500	0.96129500	0.27525700
C	2.51431300	2.71871900	-1.04178600	H	-2.75533900	-1.57541500	-2.57150300
C	2.48251000	3.84785900	-1.87619600	H	-4.92312600	-1.99559500	-3.75450700
C	1.67033600	3.85706300	-3.02365400	H	-7.03467500	-0.95247300	-2.90510300
C	0.88820200	2.73171700	-3.33329000	H	-6.96999200	0.52485400	-0.88580200

C	0.91417200	1.60129200	-2.49793500	H	3.14511300	2.71578900	-0.14800300
C	3.41128600	-0.68270500	-0.78910000	H	0.30372600	0.72098500	-2.72484700
C	-6.05068300	0.05997200	-1.25574900	H	0.25683600	2.72971400	-4.22802900
C	4.28079300	-0.04614000	-1.70286200	H	1.64893500	4.73739800	-3.67399400
C	5.50293000	-0.64081600	-2.06048900	H	3.09518900	4.72115100	-1.63005700
C	5.88124200	-1.87242400	-1.50395200	H	-1.24932900	-2.28720000	-1.28315700
C	5.02639200	-2.51471000	-0.59261700	H	0.28219400	-1.30714000	-2.08539300
C	3.79819200	-1.93140800	-0.24350900	C	0.69889900	-3.04158300	-0.43362800
C	-4.83618500	0.29917800	-0.59511300	O	1.10807200	-4.14296800	-0.33099600
C	-2.25333300	1.60695600	0.62619000				

**Complex 2b**

SCF Done: -2274.79340369

Ru	0.00120400	-0.34045600	-0.29785700	C	-4.03242900	-0.80494800	2.03958300
P	-2.28707700	0.00891600	-0.11924100	C	-4.35373800	-0.94893600	3.39959100
P	2.28682000	-0.02551300	-0.16289300	H	-2.76692200	-2.86812900	0.06359800
C	-2.96742200	1.69093300	-0.51629500	H	-4.21897500	-4.45826800	-1.18400900
C	-3.45918900	-0.51060400	4.39018000	H	-5.71986500	-3.62640500	-3.00841700
C	-2.23711000	0.07452500	4.01835700	H	-5.76483500	-1.18596300	-3.56326000
C	-1.91265100	0.22521800	2.66095400	H	-4.34189300	0.41488900	-2.29044200
C	-3.46345500	-1.11110700	-1.01669500	H	-0.96006100	0.68304700	2.36820400
C	-3.43575400	-2.49583600	-0.71907200	H	-1.53019600	0.41020100	4.78372000
C	-4.25028300	-3.39134700	-1.42637400	H	-3.71122100	-0.63016200	5.44857100
C	-5.09177100	-2.92415500	-2.45154800	H	-5.30474800	-1.41026800	3.68510100
C	-5.11616900	-1.55594800	-2.76274700	H	-4.72104900	-1.17361700	1.27360300
C	-4.31031900	-0.65120800	-2.04964500	H	-4.92233400	1.32461500	0.36848100
C	3.00837400	1.50678300	-0.92048800	H	-1.12470900	2.37260200	-1.41373500
C	-2.15842900	2.63973000	-1.17582300	H	-2.02741100	4.63912300	-2.00114200
C	2.42318000	2.05700000	-2.08197500	H	-4.37662000	5.24451900	-1.38125000
C	2.97269000	3.20246400	-2.68081700	H	-5.81738900	3.58119500	-0.18848100
C	4.10772500	3.81501200	-2.12381400	H	4.60635400	1.71637900	0.53781700
C	4.69582800	3.27735400	-0.96641000	H	5.57745000	3.75353400	-0.52572500
C	4.15263200	2.12876300	-0.36848800	H	4.53077900	4.71146800	-2.58796900
C	3.49829000	-1.33091800	-0.70439300	H	2.50931800	3.61887500	-3.58098200
C	3.19261900	-2.68632400	-0.43599000	H	1.52875100	1.58459300	-2.50110300
C	4.08129200	-3.70596500	-0.81106400	H	2.24505400	-2.93904800	0.04955000
C	5.27916500	-3.38964200	-1.47388600	H	4.95100300	0.01778100	-1.59337200
C	5.58590000	-2.04901800	-1.75732300	H	6.51310400	-1.79645700	-2.28169200
C	-2.66663300	3.91174700	-1.49051500	H	3.82821100	-4.74937100	-0.59857100
C	4.70521700	-1.02426700	-1.37261500	H	5.96563200	-4.18652400	-1.77662300
C	2.72748500	0.18533900	1.63676700	H	3.93597100	-1.61170000	1.81080700
C	2.19021000	1.29453100	2.33871900	H	1.57840600	2.02314300	1.79652000
C	2.44230200	1.45774500	3.70905300	H	2.03155100	2.32526100	4.23590600
C	3.21906700	0.51253200	4.40283900	H	3.41096700	0.63939700	5.47295200
C	3.75017700	-0.59189600	3.71787700	H	4.35989300	-1.32815000	4.25151100
C	3.51138000	-0.75532800	2.34232400	H	-0.00476900	0.14362400	-1.77916900
C	-3.98315100	4.25160100	-1.14143100	H	0.08875000	1.28261300	0.11095000



C	-4.79404000	3.31665400	-0.47315000	C	-0.08742100	-2.11026700	-0.99288500
C	-4.29199800	2.04407400	-0.16275500	O	-0.14216100	-3.16931000	-1.50893500
C	-2.80824600	-0.21084200	1.65459500				

---

**Complex 3a**

SCF Done: -2389.9749312

Ru	-0.00160300	-1.12029600	-1.06757500	H	0.83206600	1.63581900	1.90345600
P	1.94253800	-0.15024200	-0.15957400	H	0.80679800	4.09256600	2.22664100
P	-1.86602800	0.00762700	-0.16067500	H	1.97581400	5.59928900	0.58975600
C	3.44879200	-0.37003500	-1.26569500	H	3.17021100	4.59788100	-1.37322700
C	3.68715500	-1.81832800	3.86414000	H	3.21648000	2.12525800	-1.68223000
C	2.78147600	-2.56094000	3.08799000	H	1.46265300	-2.54168000	1.32799700
C	2.25781700	-2.02709900	1.89648800	H	2.46578700	-3.55813400	3.41521500
C	2.03435500	1.70144200	0.08892300	H	4.09416400	-2.23969600	4.79046100
C	1.35650800	2.27958200	1.19096200	H	4.74007900	0.07199100	4.07709400
C	1.34246400	3.67108300	1.36970300	H	3.79420900	1.04235300	1.98032200
C	1.99319600	4.51298100	0.45045500	H	4.93166400	-0.21850800	0.31398200
C	2.65975800	3.95132400	-0.65050700	H	2.23917400	-0.63334000	-3.03203300
C	2.68445100	2.55696800	-0.82966600	H	4.20223100	-0.83149600	-4.58692600
C	-2.58079800	1.52877000	-0.99301800	H	6.53617200	-0.74171700	-3.67211100
C	3.26432300	-0.55923500	-2.65434200	H	6.88700600	-0.44166500	-1.20798900
C	-1.71630800	2.30649700	-1.79673200	H	-4.61335100	1.33231500	-0.25254400
C	-2.18200600	3.47195400	-2.42855000	H	-5.44120600	3.40088200	-1.37827400
C	-3.52000100	3.87252000	-2.27770800	H	-3.88401400	4.77734500	-2.77702600
C	-4.39337100	3.10088700	-1.49156800	H	-1.49664200	4.06233000	-3.04631300
C	-3.92807000	1.93885900	-0.85310300	H	-0.68271300	1.96659500	-1.92906600
C	-1.71799900	0.62061300	1.59771000	H	-0.79768900	-1.26010700	2.15425500
C	-1.10333900	-0.26557600	2.51984600	H	-2.57826400	2.59589900	1.32964600
C	-0.88169300	0.13792400	3.84603100	H	-2.18199600	3.30697700	3.69107300
C	-1.26587800	1.42412700	4.27207000	H	-0.38890700	-0.54941000	4.54199700
C	-1.88018500	2.30463700	3.36621800	H	-1.08127300	1.73938900	5.30514600
C	4.36887600	-0.68222700	-3.51439100	H	-4.00431100	-0.19808600	1.96254100
C	-2.10742500	1.90563400	2.03536400	H	-3.16302800	-2.02313900	-1.86792100
C	-3.44102800	-0.99826900	0.02448200	H	-5.29125700	-3.30174600	-1.73090400
C	-3.82075300	-1.88925800	-1.00572100	H	-6.79535600	-3.03967400	0.25851500
C	-5.02122400	-2.61391700	-0.92232500	H	-6.13641100	-1.48197000	2.10872800
C	-5.86268600	-2.46883200	0.19276800	H	0.36468700	0.03438300	-2.16787000
C	-5.49348100	-1.59475300	1.22857000	H	1.17809200	-2.15256300	-1.53533600
C	-4.29454700	-0.86569800	1.14609500	C	-0.81547800	-1.87014200	-2.54703000
C	5.67614000	-0.63433100	-3.00187900	O	-1.17952500	-2.28117300	-3.60387000
C	5.87245500	-0.46339100	-1.62134600	O	-0.40413400	-2.52233500	0.58868400
C	4.76906500	-0.32819100	-0.76182900	C	-0.76285300	-3.81592300	0.20837700
C	2.64888900	-0.73567500	1.46753400	H	-0.93670400	-4.46046700	1.10774700
C	3.53300000	0.02078600	2.27525100	H	-1.70804600	-3.85782600	-0.38973500
C	4.05370200	-0.52128600	3.46232500	H	0.01621900	-4.33063000	-0.41188300

---

**Complex 3b**

SCF Done: -2389.97256598

Ru	0.03192300	-0.19768300	-0.14935100	H	2.71784100	-2.09901900	-1.88879200
P	2.30820900	0.00586200	0.06817400	H	3.95645000	-4.26355900	-1.90109900
P	-2.26057900	-0.02018300	0.07248700	H	5.23607700	-4.99284200	0.12737500
C	2.95843900	0.88491500	1.59259100	H	5.27129700	-3.53051800	2.16157100
C	4.58181200	2.52632900	-3.17722700	H	4.06803600	-1.34671900	2.15396400
C	3.30412800	2.89361500	-2.72069800	H	1.63650000	2.37097700	-1.42112400
C	2.64255200	2.11160800	-1.76004100	H	2.80912200	3.78279100	-3.12547000
C	3.32131300	-1.56259400	0.12803800	H	5.09248800	3.13441900	-3.93222700
C	3.29636000	-2.40529100	-1.01111800	H	6.18748000	1.06948800	-3.03023600
C	3.98890700	-3.62475800	-1.01212600	H	5.00870200	-0.33036000	-1.33511000
C	4.70438000	-4.03525200	0.12726600	H	4.98862300	1.10816900	0.84988700
C	4.72269900	-3.21594200	1.26672600	H	1.04145300	0.86498900	2.57141500
C	4.04024700	-1.98609100	1.26742700	H	1.87861100	2.00850300	4.65377300
C	-3.04827100	-0.71440000	1.62902200	H	4.28581400	2.69062100	4.81930800
C	2.09159800	1.15904300	2.67178800	H	5.83724000	2.23540700	2.90487700
C	-2.41820500	-1.79807900	2.28159600	H	-4.74652300	0.63788500	1.67726700
C	-2.99970000	-2.38357100	3.41801100	H	-5.77548300	-0.39870300	3.70128800
C	-4.21119000	-1.88858600	3.93037100	H	-4.65860100	-2.34183300	4.82174900
C	-4.83835700	-0.80105600	3.30057000	H	-2.49591200	-3.22266200	3.90980300
C	-4.26332000	-0.21878600	2.15708100	H	-1.45304300	-2.14620300	1.90130100
C	-3.26635400	-0.89611900	-1.23212500	H	-1.67282000	-0.55017900	-2.67049900
C	-2.68722600	-0.96854000	-2.52327700	H	-4.97006500	-1.45796000	-0.00313700
C	-3.38310100	-1.60026700	-3.56817500	H	-6.20055400	-2.56890600	-1.87206500
C	-4.64849800	-2.16850000	-3.34012000	H	-2.92481800	-1.65647800	-4.56173600
C	-5.22162300	-2.11281400	-2.05812200	H	-5.18319200	-2.66605000	-4.15722200
C	2.56801700	1.80248900	3.82765700	H	-4.87981000	1.07124800	-0.98697000
C	-4.53336900	-1.48159200	-1.00691600	H	-1.38198200	2.58173000	1.04263100
C	-3.07446600	1.66833400	0.06187600	H	-2.45377400	4.84706200	1.21040500
C	-2.39853200	2.75081900	0.66949300	H	-4.73684200	5.22377400	0.24494000
C	-2.99628800	4.01945100	0.74019800	H	-5.94081400	3.32737700	-0.86531400
C	-4.27438300	4.23187600	0.19604100	H	0.06524300	-0.56313700	1.43643800
C	-4.95032900	3.16751700	-0.42484300	H	0.11169400	1.40299800	0.38442900
C	-4.35705600	1.89494800	-0.49135800	C	-0.01141500	-2.03074800	-0.61269300
C	3.91579400	2.18606700	3.91991300	O	-0.03814200	-3.19596000	-0.83684600
C	4.78699400	1.92870200	2.84663200	O	0.00624600	0.54318300	-2.23442000
C	4.31266100	1.28518600	1.69207500	C	-0.64806200	1.73727300	-2.50545200
C	3.25924100	0.95435100	-1.23086300	H	-0.39817100	2.10377600	-3.53355500
C	4.53737800	0.58409700	-1.70792000	H	-1.77144500	1.66470100	-2.47136200
C	5.19559400	1.36802400	-2.67244700	H	-0.40292500	2.57434400	-1.79794600

**Complex 4a**

SCF Done: -1357.36927938

Ru	-2.11016600	-0.51312000	-0.14588100	H	3.73897600	-4.40531800	-1.68129800
----	-------------	-------------	-------------	---	------------	-------------	-------------

P	0.22052000	-0.09383800	-0.04804600	H	4.41245100	-2.92265100	0.22291400
C	0.86790500	0.31625000	1.66098800	H	2.90504100	-1.07645100	0.96475500
C	2.01395200	3.51834900	-2.45221000	H	-0.84673500	2.42711500	-0.85826700
C	0.70444300	3.54749600	-1.93927900	H	0.07159900	4.42771300	-2.09974600
C	0.19160100	2.44699800	-1.23275800	H	2.40725100	4.37794600	-3.00687200
C	1.37130300	-1.49430500	-0.51419900	H	3.82907200	2.34410900	-2.67438200
C	0.99611800	-2.34842800	-1.57644900	H	2.92804700	0.38064700	-1.41715400
C	1.84639500	-3.38294900	-1.99770200	H	2.50755100	1.60238600	1.04675500
C	3.08057700	-3.59181600	-1.35717600	H	-0.71666300	-0.82998000	2.57733400
C	3.45855500	-2.75961800	-0.29112500	H	0.06927500	-0.39300100	4.92782500
C	2.61258900	-1.71594200	0.12609400	H	2.07074600	1.06405000	5.32448200
C	0.17996200	-0.22844500	2.77103200	H	3.28237900	2.06559600	3.37510100
C	0.61652800	0.03317800	4.07984900	H	-1.75035400	-1.75244900	-1.08928700
C	1.73744600	0.85247000	4.30237600	H	-1.71230300	-1.75711700	0.79347500
C	2.41796200	1.41285000	3.20875100	O	-2.52062000	1.50853500	-0.19676000
C	1.98741700	1.14803800	1.89612900	C	-3.79158600	2.09542100	-0.22149300
C	0.99929000	1.30108700	-1.02144200	H	-4.62568100	1.36100100	-0.16059200
C	2.30982200	1.27386300	-1.55333100	H	-3.92898000	2.81151500	0.62686600
C	2.81323900	2.37807900	-2.26416400	H	-3.95345800	2.68884900	-1.15632100
H	0.01314600	-2.20203600	-2.03711900	C	-3.78355700	-1.28303200	-0.13904400
H	1.53662400	-4.03622400	-2.82070200	O	-4.78915900	-1.92204800	-0.13166100

**Complex 4b**

SCF Done: -1357.38030580

Ru	-2.16316900	-0.73084800	-0.25843400	H	4.09557300	-3.22972100	-2.69047100
P	0.06845400	0.00902600	-0.05326400	H	4.69699300	-1.99714800	-0.59457900
C	0.80069100	0.13624300	1.67383800	H	2.98129500	-0.61616300	0.58129800
C	1.09835700	4.30134200	-1.66819700	H	-1.46495100	2.40720300	-0.34359600
C	-0.17808800	3.98617300	-1.17029200	H	-0.96470600	4.74914900	-1.15337500
C	-0.46105600	2.69091900	-0.70420300	H	1.31264900	5.31127100	-2.03622800
C	1.40277000	-1.03964900	-0.84981300	H	3.09036300	3.54852400	-2.10375300
C	1.07241000	-1.75300700	-2.02467600	H	2.59804700	1.24460900	-1.27466500
C	2.03767000	-2.53009300	-2.68526700	H	1.85961100	2.01485700	1.43254200
C	3.34592700	-2.61591800	-2.17903800	H	-0.18064100	-1.70927000	2.25109100
C	3.68316600	-1.92335400	-1.00410100	H	0.68646200	-1.67214600	4.59759000
C	2.71997000	-1.14059400	-0.34337400	H	2.11739700	0.23373300	5.37633600
C	0.47129500	-0.89506800	2.58794900	H	2.69277000	2.08211900	3.78679000
C	0.95065800	-0.86436000	3.90624000	H	-2.03030300	-0.99553700	-1.80617000
C	1.75333500	0.20504500	4.34343800	H	-3.70749500	-1.21371300	-0.52974400
C	2.07503600	1.24107400	3.45156900	O	-2.90995400	1.12015800	0.18508300
C	1.60663300	1.20670600	2.12543400	C	-4.24627500	1.51454000	0.01473100
C	0.54496600	1.69330400	-0.72156900	H	-4.96454800	0.66794500	0.07396400
C	1.82307400	2.01668600	-1.23428600	H	-4.53937100	2.25925600	0.79418600
C	2.09703000	3.31303300	-1.70473900	H	-4.41313500	2.01091900	-0.97250000
H	0.03913200	-1.70679200	-2.38529800	C	-1.78631200	-2.50817400	-0.07463000
H	1.76102300	-3.08147500	-3.59049100	O	-1.63768300	-3.68200900	0.10529700

**TS<sub>4-5</sub> (a)****SCF Done:** -1357.35406699

Ru	-2.13697900	0.39223500	-0.17596000	H	3.45739200	4.78779100	-1.05265900
P	0.19873700	0.09659700	-0.07909200	H	1.15206600	4.60299300	-2.01852700
C	1.27020000	1.60323400	-0.34983200	H	-0.25499300	2.57999600	-1.52147500
C	0.77031000	2.65814200	-1.14500400	H	2.95222900	-0.14723900	-1.44567600
C	1.55685800	3.79292400	-1.40219500	H	-0.79051200	-2.32398900	-1.18627900
C	2.84837400	3.89814700	-0.85777200	H	0.21316500	-4.16724400	-2.60232500
C	3.34872900	2.86494900	-0.04776700	H	3.92809700	-1.94803000	-2.87372100
C	2.56569600	1.72503000	0.20578400	H	2.56792400	-3.97194800	-3.44117000
C	1.04413600	-1.15592900	-1.17612400	H	-0.60966700	0.83680800	2.58459900
C	2.36149500	-1.03910600	-1.67842300	H	2.34186600	-1.83935500	0.90971500
C	2.90700400	-2.05016200	-2.48860400	H	3.07640400	-2.48577900	3.21092400
C	2.14115800	-3.18474800	-2.80886700	H	1.97904100	-1.45807500	5.21333900
C	0.82318200	-3.29782700	-2.33214900	H	0.13549400	0.21138000	4.90085300
C	0.26734400	-2.29127400	-1.52355100	H	-1.87478000	1.22683100	-1.47666000
C	0.83577300	-0.43740900	1.59765700	H	-1.74868400	1.80768000	0.53776300
C	1.86923300	-1.38332700	1.78519700	O	-2.51962400	-1.69832900	-0.63580100
C	2.27794800	-1.74654500	3.08110500	C	-3.00153900	-2.17776800	0.58148000
C	1.66220100	-1.17086900	4.20470900	H	-2.24283500	-2.75223600	1.17810300
C	0.62849000	-0.23308700	4.02925900	H	-3.36493200	-1.36540800	1.28046200
C	0.21400600	0.12830500	2.73800700	H	-3.88429900	-2.85986100	0.46150000
H	2.94591000	0.93398000	0.86042300	C	-3.81870300	1.15060500	-0.26664900
H	4.34682100	2.94865100	0.39658600	O	-4.81925500	1.79283700	-0.34728700

**TS<sub>4-5</sub> (b)****SCF Done:** -1357.35684736

Ru	2.17876000	0.68629800	-0.37704500	H	-4.30164900	3.99499300	-0.73687300
P	-0.08111900	0.08152300	-0.00584800	H	-2.02881100	4.69258100	0.05936200
C	-1.45897300	1.32147000	-0.27049000	H	-0.22119500	3.00311200	0.32640800
C	-1.21740200	2.68703500	0.00531900	H	-2.66015600	0.08421400	1.68788300
C	-2.23775500	3.63929500	-0.15655700	H	1.36141800	-1.52509000	1.85112300
C	-3.51077200	3.24854700	-0.60457700	H	0.80473300	-2.63993600	4.04919100
C	-3.76028300	1.89627700	-0.89282000	H	-3.20237500	-0.99400400	3.87476900
C	-2.74397900	0.93975800	-0.72640700	H	-1.47691500	-2.37218400	5.05449400
C	-0.62781100	-0.68348200	1.61488500	H	0.29761600	-0.24672800	-2.85408000
C	-1.90630900	-0.52290900	2.19912500	H	-1.65944100	-2.52095700	0.25752600
C	-2.20896800	-1.12883000	3.43139700	H	-2.32807300	-4.25005600	-1.41615600
C	-1.23937400	-1.90112400	4.09369200	H	-1.70011500	-3.97626000	-3.82535600
C	0.03883200	-2.05528600	3.52713400	H	-0.38835000	-1.96439300	-4.54483100
C	0.35232700	-1.44924500	2.29880400	H	1.79025300	1.36016300	-1.78849700
C	-0.65342700	-1.25509100	-1.18901600	H	3.74005400	1.00755400	-0.76897400
C	-1.38881900	-2.39684600	-0.79515500	O	2.90447000	-1.00634100	0.75162600
C	-1.76218700	-3.36930300	-1.74005500	C	3.43928600	-1.71074300	-0.32574900
C	-1.41054800	-3.21638600	-3.09130200	H	3.16739700	-2.79721500	-0.29956400

C	-0.67594500	-2.08716500	-3.49484900	H	3.06197600	-1.37410700	-1.34470300
C	-0.29668500	-1.11750300	-2.55374000	H	4.55613700	-1.64485200	-0.40558200
H	-2.93708100	-0.11087600	-0.96492800	C	2.16721600	2.37469700	0.17921800
H	-4.74688200	1.58333600	-1.25273100	O	2.19955900	3.50531200	0.58163400

**Complex 5a****SCF Done:** -1357.3588536

Ru	2.20658000	-0.18857400	-0.00376100	H	-2.82995900	-1.63247000	4.87768600
P	-0.14578600	-0.03898200	-0.01494200	H	-3.95745900	-2.02566100	2.67586800
C	-1.03977600	-1.09853300	-1.27343300	H	-2.81109300	-1.39053100	0.55129500
C	-2.17566800	4.13954200	-0.75812300	H	0.77427300	2.39727300	-1.19750900
C	-0.86354400	3.86678600	-1.17937300	H	-0.27756400	4.63930800	-1.69008000
C	-0.28218900	2.60871400	-0.93645100	H	-2.62334200	5.12160400	-0.94944700
C	-1.03735200	-0.61034600	1.53279700	H	-3.92494000	3.36965800	0.27897900
C	-0.40297400	-0.41758100	2.78161800	H	-2.89644800	1.14117900	0.73663400
C	-1.04632900	-0.77644200	3.97677200	H	-2.55405600	0.34765100	-1.84602900
C	-2.33073600	-1.34688200	3.94524400	H	0.35237000	-2.72247400	-0.96175700
C	-2.96395600	-1.56451500	2.71036800	H	-0.80485900	-4.27991500	-2.55310000
C	-2.32301900	-1.20055700	1.51263700	H	-2.82573900	-3.50205600	-3.81766600
C	-0.55342200	-2.40971300	-1.49259000	H	-3.68640600	-1.17545400	-3.46714700
C	-1.19733600	-3.26931900	-2.39499200	H	1.97201900	-1.18050000	-1.23357600
C	-2.32970500	-2.83255900	-3.10631100	H	1.85068000	-1.40635400	1.00516900
C	-2.81270400	-1.52931400	-2.90821800	O	2.61551300	1.82102400	-0.87387500
C	-2.17577200	-0.66808500	-1.99549200	C	2.78280900	2.11831900	0.44353400
C	-1.02371600	1.60172500	-0.26893900	H	2.10912900	2.92652900	0.83600300
C	-2.33491600	1.89671800	0.17700200	H	2.49509400	1.23408900	1.23296200
C	-2.90852200	3.15523100	-0.07076800	H	3.83245000	2.34407100	0.75859900
H	0.61714600	-0.01819900	2.78912700	C	3.86461400	-0.99445900	0.01289600
H	-0.53626100	-0.62224800	4.93398300	O	4.85292600	-1.65801300	0.02144300

**Complex 5b****SCF Done:** -1357.3622698

Ru	2.23021100	-0.12731500	0.68047500	H	-1.93121700	-4.15643000	-3.46352700
P	-0.04709400	0.00951400	0.09878500	H	-2.24514000	-1.75517000	-4.10811100
C	-0.72569300	1.55495000	-0.73307000	H	-1.47811100	0.06217100	-2.58018200
C	-3.19230200	-0.30055100	3.60011800	H	0.05582300	0.60141500	2.94378900
C	-1.89857500	0.20169400	3.82441900	H	-1.60413900	0.53379900	4.82619400
C	-0.97178300	0.26268200	2.77090200	H	-3.91230700	-0.35650800	4.42400000
C	-0.71286400	-1.28977900	-1.06591200	H	-4.55239800	-1.15592300	2.13859700
C	-0.53573800	-2.65188000	-0.71617500	H	-2.90422100	-1.04165600	0.26501000
C	-0.97624800	-3.67292300	-1.57091000	H	-2.78629800	1.43924900	-0.05303400
C	-1.59458900	-3.35740000	-2.79407000	H	1.26993200	2.00798500	-1.46993800
C	-1.76894600	-2.01146400	-3.15493900	H	0.52070400	4.05244800	-2.73919200
C	-1.33557300	-0.98448200	-2.29790500	H	-1.87248700	4.79315800	-2.63691100

C	0.20658300	2.31446900	-1.48487700	H	-3.52063000	3.48701100	-1.27637500
C	-0.21181100	3.47174600	-2.16721600	H	3.75068200	-0.27202200	1.26948300
C	-1.55120900	3.89047600	-2.10458400	H	1.86101600	-0.86184200	2.06844600
C	-2.47747700	3.15668800	-1.34151700	O	2.97289700	1.57190800	-0.55759500
C	-2.06729200	1.99956900	-0.65867900	C	2.75587500	2.22623100	0.60766600
C	-1.32660500	-0.16039200	1.47023600	H	1.96297400	3.01892200	0.57349600
C	-2.62728700	-0.67754700	1.25965100	H	2.32812600	1.54392000	1.53624700
C	-3.55149500	-0.74670200	2.31714400	H	3.66474700	2.63371400	1.11637300
H	-0.03310200	-2.89856000	0.22398100	C	2.57642400	-1.76900200	-0.00467500
H	-0.82341100	-4.71927200	-1.28538000	O	2.87037600	-2.85135300	-0.40856700

**TS<sub>5-6</sub> (a)****SCF Done:** -1357.3573495

Ru	-2.19908600	0.19398200	0.00852900	H	2.95099000	5.03328500	-1.10469200
P	0.14863600	0.06922100	-0.02736400	H	0.63377100	4.65198400	-1.98310300
C	1.06742300	1.67373400	-0.32700000	H	-0.57185500	2.50994200	-1.45137700
C	0.45220000	2.68247900	-1.10242800	H	2.79512200	0.12185500	-1.60093100
C	1.12943700	3.88022900	-1.38408700	H	-0.74267800	-2.35333000	-1.24394100
C	2.42722000	4.09532000	-0.88941600	H	0.27838200	-4.01601200	-2.84163400
C	3.04402600	3.10681200	-0.10495100	H	3.79362400	-1.50553100	-3.21100500
C	2.36974500	1.90515900	0.17535600	H	2.54458700	-3.58700600	-3.82532800
C	0.98629300	-1.04056700	-1.27899100	H	-0.44064500	0.50051400	2.76047000
C	2.25434200	-0.79535200	-1.85612500	H	2.62627900	-1.62248500	0.58296300
C	2.81255100	-1.70948100	-2.76701000	H	3.70721600	-2.29185000	2.73484200
C	2.10948600	-2.87658500	-3.11309800	H	2.73193200	-1.53905900	4.91599400
C	0.84143400	-3.11996800	-2.55758300	H	0.65755600	-0.13180400	4.92841400
C	0.27530300	-2.20852200	-1.64974000	H	-1.96241300	0.94960500	-1.43984800
C	1.03774800	-0.48778300	1.52975000	H	-1.86738400	1.61748600	0.70141800
C	2.20331400	-1.28842000	1.53560400	O	-2.56428400	-1.95617000	-0.52580200
C	2.80845000	-1.66495600	2.74841300	C	-2.67295200	-1.85574900	0.80371600
C	2.26129400	-1.24419000	3.97163600	H	-1.92367200	-2.42221300	1.41061400
C	1.09795200	-0.45354500	3.97818100	H	-2.36861100	-0.57783700	1.53897500
C	0.48719300	-0.08371500	2.76982700	H	-3.69446700	-1.97473100	1.23561800
H	2.84519400	1.14738800	0.80573300	C	-3.90421200	0.89925700	-0.09058000
H	4.04944100	3.27179100	0.29841200	O	-4.94091600	1.47611600	-0.16485500

**TS<sub>5-6</sub> (b)****SCF Done:** -1357.3569849

Ru	2.18799500	-0.05388200	-0.78605100	H	-3.08456700	4.86564400	-1.14141000
P	-0.04081500	0.02736200	-0.08634100	H	-0.61963000	4.96414000	-0.68948000
C	-1.06234100	1.56446700	-0.44986600	H	0.66310700	2.86144900	-0.28319600
C	-0.41663800	2.82227200	-0.45120500	H	-2.29248000	0.98431100	1.80137100
C	-1.14146300	4.00094300	-0.69157000	H	1.34745500	-1.35379000	1.99593100
C	-2.52251600	3.94566900	-0.94643700	H	0.91308200	-1.80622800	4.43347900

---

C	-3.17460300	2.70183700	-0.96210100	H	-2.70819600	0.56754600	4.23052100
C	-2.45202200	1.52085400	-0.71566100	H	-1.11275500	-0.84019000	5.55042100
C	-0.46999900	-0.19545500	1.73090100	H	-0.22966800	-1.07177300	-2.74766100
C	-1.60123300	0.35874600	2.37518600	H	-2.35068000	-1.69832400	0.96372400
C	-1.83111800	0.12670000	3.74272700	H	-3.82151300	-3.38085100	-0.14956300
C	-0.93430200	-0.66219400	4.48380700	H	-3.52414200	-3.89613200	-2.58316100
C	0.19990900	-1.20685900	3.85645800	H	-1.72926100	-2.72739000	-3.88716100
C	0.43914500	-0.97198100	2.49146200	H	3.64748200	-0.13791000	-1.52145500
C	-1.20183100	-1.25422900	-0.82354800	H	1.78886700	0.71262600	-2.14148400
C	-2.21700400	-1.92184300	-0.09918300	O	2.90145700	-1.68138800	0.64206100
C	-3.04523900	-2.86863200	-0.72941400	C	2.46002700	-2.28380800	-0.43604100
C	-2.87900400	-3.15843800	-2.09340900	H	1.48575800	-2.82392700	-0.38166100
C	-1.87231500	-2.50189400	-2.82449000	H	2.00190400	-1.38710200	-1.80146700
C	-1.03861200	-1.56409000	-2.19621900	H	3.19902900	-2.79935000	-1.08909800
H	-2.96271700	0.55338800	-0.74545300	C	2.81662700	1.58494300	-0.14586900
H	-4.24878400	2.64666200	-1.17241700	O	3.30421100	2.61957900	0.17636200

---

**Complex 6a**

SCF Done: -1357.37333045

Ru	2.21689800	0.27830800	-0.08211100	H	-3.06043800	5.08307500	-0.33785700
P	-0.15333300	0.07748300	-0.01697800	H	-0.89481400	4.92262200	0.91494800
C	-1.11609600	1.67259300	-0.17803500	H	0.35711200	2.74981400	0.98091500
C	-0.60612000	2.82539200	0.46532300	H	-2.77347700	0.56646400	1.47299900
C	-1.30673600	4.04043400	0.41286900	H	0.77528400	-1.87960600	1.86563600
C	-2.52030600	4.13105000	-0.29123600	H	-0.23377800	-2.99304900	3.89565800
C	-3.03046600	2.99721800	-0.94334000	H	-3.76581700	-0.51087000	3.49668600
C	-2.33590900	1.77517400	-0.88485700	H	-2.50413100	-2.30422600	4.70609300
C	-0.95653400	-0.62582000	1.51657000	H	0.58433800	-0.63891200	-2.71965800
C	-2.22762500	-0.22779900	1.99236800	H	-2.74248500	-1.54100600	-0.12044200
C	-2.78222100	-0.83126200	3.13485800	H	-3.83180700	-2.85135000	-1.94363700
C	-2.07200000	-1.83563000	3.81456100	H	-2.72611000	-3.04749700	-4.18279200
C	-0.80089900	-2.22552300	3.35732200	H	-0.51238000	-1.93714800	-4.57468700
C	-0.23909800	-1.62450200	2.21816000	H	2.00678100	1.09967400	1.36841100
C	-1.02397400	-0.96438400	-1.31801400	H	1.91368900	1.77385100	-0.59925500
C	-2.26462200	-1.61027000	-1.10270600	O	2.52606600	-1.65931000	0.92149600
C	-2.87343000	-2.35342400	-2.12918100	C	2.55443700	-1.82871500	-0.39747800
C	-2.25249200	-2.46525600	-3.38466200	H	1.69762200	-2.34485700	-0.88631300
C	-1.01299800	-1.84053200	-3.60498900	H	2.18423200	0.25273100	-1.73123500
C	-0.40074300	-1.10173000	-2.57921600	H	3.53112800	-2.05117200	-0.87807400
H	-2.73477200	0.89582000	-1.39934100	C	3.99236900	0.78652900	-0.11592900
H	-3.97010300	3.06000300	-1.50349900	O	5.11258400	1.17513800	-0.15291300

---

**Complex 6b**

SCF Done: -1357.36370778

Ru	2.13712700	-0.15583100	-0.88207700	H	-3.19078200	4.49724500	-2.12534100
P	-0.07318900	0.02379900	-0.12269700	H	-0.69365500	4.63597300	-1.94844000
C	-1.12828200	1.43158400	-0.78385300	H	0.61447600	2.65845800	-1.12987100
C	-0.47864600	2.62411100	-1.17573800	H	-2.09259700	1.58821100	1.61360000
C	-1.21700400	3.72168100	-1.64767300	H	1.28178400	-1.06885700	2.14329400
C	-2.61662400	3.64348600	-1.74870000	H	0.98342800	-0.93769200	4.63798700
C	-3.27417200	2.45904900	-1.37631700	H	-2.37426500	1.74765600	4.08855100
C	-2.53710400	1.36187700	-0.89664900	H	-0.84472400	0.47657700	5.61051300
C	-0.40470900	0.22304900	1.71570500	H	-0.30056200	-1.78939200	-2.36309000
C	-1.42615100	1.02541800	2.27495900	H	-2.38283000	-1.30262600	1.38849000
C	-1.58263100	1.11535400	3.67018000	H	-3.90026500	-3.19793700	0.80636100
C	-0.72389400	0.40331100	4.52379100	H	-3.64454700	-4.38630100	-1.38364400
C	0.30008500	-0.39170000	3.97807100	H	-1.84525600	-3.67385300	-2.97831900
C	0.46647000	-0.47857300	2.58635200	H	3.53077900	-0.34600800	-1.70478700
C	-1.25830300	-1.39840700	-0.46710700	H	1.84012100	0.93683600	-2.01944700
C	-2.27195400	-1.81559700	0.42806300	O	2.67201000	-1.74231600	0.63935300
C	-3.12447700	-2.88478800	0.09829800	C	2.42789100	-2.30821000	-0.51139900
C	-2.98144900	-3.55196400	-1.12953800	H	1.46798500	-2.85097400	-0.65696100
C	-1.97332500	-3.15099600	-2.02395000	H	1.65920100	-0.88626000	-2.27581500
C	-1.11579200	-2.08968000	-1.69335100	H	3.27317400	-2.68396100	-1.12427800
H	-3.05113500	0.43480800	-0.62324000	C	3.11471700	1.24640500	-0.03871700
H	-4.36401600	2.38449700	-1.46461200	O	3.81925000	2.13615500	0.29393700

**TS<sub>6-7</sub> (a)**

SCF Done: -1357.3269569

Ru	2.12413200	-0.54063600	0.04862800	H	-1.66125600	5.17287700	-1.81628400
P	-0.18178100	-0.12259000	0.03752000	H	0.15293800	3.85302500	-2.93656600
C	-0.72549300	1.58877200	-0.50339900	H	0.76644600	1.57888100	-2.07021200
C	-0.04469600	2.15425100	-1.61023100	H	0.54453100	-0.17487500	2.82963500
C	-0.38582600	3.43135700	-2.08089200	H	-3.14477600	-0.59901500	0.63556900
C	-1.40071900	4.17353100	-1.45017600	H	-4.42261800	-0.75978400	2.77138800
C	-2.06998300	3.63105700	-0.34148900	H	-0.73541800	-0.30653300	5.00250100
C	-1.73627900	2.34791200	0.12925000	H	-3.22493800	-0.60446000	4.96634600
C	-1.21718800	-0.31704500	1.60046100	H	0.02288200	-2.87806800	-0.88816100
C	-0.55166900	-0.25569100	2.84392900	H	-2.64460300	0.43093700	-1.64186700
C	-1.27076600	-0.35170000	4.04738600	H	-4.04424700	-1.01607700	-3.11803900
C	-2.66527200	-0.52275300	4.02775300	H	-3.42956200	-3.41952500	-3.46807500
C	-3.33763600	-0.60681700	2.79616600	H	-1.39071600	-4.35328600	-2.34645600
C	-2.62002100	-0.50669300	1.59175600	H	2.13553200	-0.78712500	1.72863800
C	-1.24098100	-1.14422900	-1.12741900	H	1.92025100	-0.59375500	-1.62977200
C	-2.38354600	-0.62320600	-1.77884900	O	2.64590800	1.62209500	-0.17948500
C	-3.16665800	-1.43857500	-2.61560300	C	3.55908400	1.96253700	0.61162600
C	-2.82095700	-2.78513000	-2.81413400	H	3.63893600	1.51632700	1.62285000
C	-1.67982900	-3.30941900	-2.18174500	H	4.34324800	2.68264100	0.28028200
C	-0.89351600	-2.49579700	-1.35101500	H	1.74713700	-2.08826800	-0.09512900
H	-2.26336500	1.92843000	0.99115500	C	3.85159600	-1.19579600	-0.03983900
H	-2.85590700	4.20560500	0.16199400	O	4.93066100	-1.69465900	-0.09594800



**TS<sub>6-7</sub> (b)****SCF Done:** -1357.3299006

Ru	2.10998800	0.10120200	-0.96079200	H	-2.46875400	-5.25474500	0.34203300
P	-0.06383800	0.02767200	-0.15344600	H	-2.83214400	-3.57313800	2.16419600
C	-1.42558400	0.88195400	-1.13521900	H	-1.84484800	-1.29103400	1.97799800
C	-0.88556500	1.76478200	4.15936500	H	-2.52904900	1.31805100	1.18442500
C	-1.92620100	1.79292700	3.21540800	H	-2.90054100	2.21739300	3.48417300
C	-1.71957600	1.28487300	1.92077800	H	-1.04499800	2.16548000	5.16678600
C	-0.89721900	-1.65570600	0.05920600	H	1.18894200	1.22680200	4.52185200
C	-0.69358400	-2.62192500	-0.95814600	H	1.55790300	0.36441300	2.19240900
C	-1.26010200	-3.90237700	-0.85953900	H	-3.03482700	-0.50342500	-0.67765800
C	-2.03341800	-4.25233800	0.26221700	H	-0.04054600	2.38622100	-1.82886000
C	-2.23610700	-3.30958700	1.28266100	H	-1.77419300	3.67937900	-3.10275300
C	-1.67765500	-2.02199400	1.18124700	H	-4.14004000	2.85229700	-3.18595000
C	-1.08682300	2.06074800	-1.83848800	H	-4.76045500	0.74825200	-1.97575500
C	-2.05836100	2.76882100	-2.56341800	H	1.74162400	-1.11732100	-2.09715300
C	-3.38437300	2.30420800	-2.61196000	H	3.47476200	0.04926300	-1.86641600
C	-3.73202600	1.12530500	-1.93211300	O	3.25864100	-1.38266900	0.36877100
C	-2.76146900	0.42062600	-1.19739500	C	2.92446500	-2.52170300	-0.00434500
C	-0.46687300	0.74424400	1.54645100	H	1.86712700	-2.79984400	-0.18646500
C	0.57450400	0.73738100	2.50279100	H	3.70196100	-3.30803200	-0.17099600
C	0.36579600	1.23632400	3.79877900	H	1.72493600	0.94697600	-2.24441700
H	-0.05679400	-2.34657100	-1.80873900	C	2.73483800	1.68292700	-0.17120100
H	-1.09080300	-4.63185700	-1.65980200	O	3.14771200	2.74348600	0.18187300

**Complex 7a****SCF Done:** -1357.33467306

Ru	-2.11112800	-0.55164400	0.14988300	C	3.16037900	-1.72581200	-2.45813900
P	0.19208800	-0.12768300	0.04930700	C	1.30626600	0.11010700	4.04810200
H	-1.93795400	-0.85664100	-1.50855200	H	-0.67748600	1.23758500	-2.31955800
H	-2.12262500	-0.64944900	1.83544800	H	2.15156900	2.10833300	0.82842900
O	-2.58919900	1.50855800	0.09906500	H	3.17463400	-0.48004700	0.67487100
H	-1.66993200	-2.09726000	0.30451800	H	-0.51543100	0.12256800	2.82655100
C	1.23483100	-1.26935700	-1.01078600	H	2.66427800	0.23183100	-1.66184100
C	0.71854200	1.51307000	-0.68911900	H	-0.05987900	-2.95080600	-0.62373900
C	1.24490900	-0.13195800	1.61324200	C	2.70337700	-0.03846800	4.04018700
C	-3.63500100	2.20163400	0.09981800	C	1.33358200	3.99398700	-1.91499300
C	2.65075200	-0.29432700	1.61765100	C	2.79289200	-3.07901900	-2.53718400
C	0.07997700	1.90458800	-1.89238300	H	-0.11293300	3.41528000	-3.43105500
C	1.65759700	2.39262300	-0.10515900	H	2.69043700	4.29501200	-0.24639400
C	0.86527000	-2.62933500	-1.11489300	H	4.46118100	-0.38157700	2.80918900
C	2.38784400	-0.82663600	-1.70154800	H	0.77352000	0.25416500	4.99478300
C	0.58176500	0.05804300	2.84514600	H	1.33519700	-4.57578100	-1.93884000

H	-4.64152900	1.73546000	0.06574500	H	4.04617200	-1.36407000	-2.99255000
H	-3.56330500	3.30722300	0.14959500	H	1.57071200	4.95342700	-2.38802600
C	3.37352500	-0.24703400	2.82206500	H	3.26773100	-0.00519100	4.97896600
C	0.39117800	3.12961900	-2.50110500	H	3.39312000	-3.77879800	-3.12929000
C	1.96104600	3.62420200	-0.71465400	C	-3.83041100	-1.23195900	0.10271100
C	1.64121700	-3.52627000	-1.86620900	O	-4.90285000	-1.74604200	0.06853500

**Complex 7b**

SCF Done: -1357.33912014

Ru	-1.99178000	-0.14563200	-1.10422600	C	3.94014000	-0.11904100	-1.94152500
P	0.12547400	-0.04641800	-0.15600700	C	-0.16564700	-2.32599100	3.31068900
H	-1.31663800	0.86688700	-2.27024300	H	-0.28735300	2.62305300	-1.13402700
H	-3.16855500	-0.10870100	-2.24143200	H	1.71201500	0.92410500	2.29838800
O	-2.83437200	1.58887100	-0.14533800	H	2.73765500	-1.27015800	0.92856300
H	-1.47700000	-1.25005500	-2.14561500	H	-1.46242900	-1.25482700	1.92134700
C	1.60325800	-0.41660000	-1.26129100	H	2.97769200	0.99295100	-0.34402300
C	0.69068400	1.61962700	0.51239900	H	0.46797200	-1.83333200	-2.42490800
C	0.60538000	-1.12972400	1.31617900	C	1.14994700	-2.73255200	3.59192600
C	-3.83587800	1.75153100	0.57660600	C	1.41376200	4.21759300	1.39377400
C	1.92446000	-1.55362600	1.60390700	C	3.78597000	-1.09654200	-2.93846700
C	0.31360000	2.76780100	-0.22801000	H	0.37844600	4.92636600	-0.38146800
C	1.42341500	1.79981700	1.70906300	H	2.34507400	3.20916400	3.07703800
C	1.45755000	-1.38592900	-2.27901800	H	3.21969700	-2.67562800	2.93445800
C	2.85823100	0.21872900	-1.10865200	H	-0.98908400	-2.63687900	3.96317400
C	-0.43549300	-1.53789600	2.18005100	H	2.40521400	-2.47725400	-3.89223500
H	-4.43307100	0.88711200	0.93883600	H	4.90298100	0.38882300	-1.81360300
H	-4.15660100	2.77669400	0.86114100	H	1.69216700	5.22108700	1.73466100
C	2.19307100	-2.34941900	2.73177100	H	1.35936100	-3.35637100	4.46804100
C	0.67855800	4.05129500	0.20593500	H	4.62803300	-1.35734100	-3.58932800
C	1.77958400	3.08918600	2.14563800	C	-2.96973000	-1.53120200	-0.28954700
C	2.54027000	-1.72643600	-3.10563500	O	-3.60140000	-2.48329200	0.05565600

**Complex 8a**

SCF Done: -1242.8072294

Ru	2.34656700	0.25008900	0.11474900	H	-2.80533100	0.49303100	-1.12316900
P	0.03392600	0.06920100	-0.02590600	H	-4.16240200	2.55194700	-1.49646700
C	-1.06086900	1.56082300	-0.38594800	H	-3.18617000	4.80564600	-1.00626300
C	-0.51386400	2.83848900	-0.13348200	H	-0.83516600	4.98130500	-0.15041700
C	-1.27737500	3.99839300	-0.34827700	H	0.53184500	2.88310200	0.20528800
C	-2.59365400	3.90060700	-0.83050700	H	-2.34417300	0.91099100	1.71462500
C	-3.14251700	2.63553500	-1.10385100	H	0.71998200	-2.13652400	1.68166900
C	-2.38235500	1.47361300	-0.88450300	H	-0.18143400	-3.06806300	3.83301400
C	-0.76295600	-0.56388300	1.54739200	H	-3.23260700	0.00902100	3.86977300
C	-1.87355900	0.03959000	2.17957400	H	-2.15969900	-1.98875800	4.93250900

C	-2.37200600	-0.47228400	3.39140900	H	1.00014900	-0.92938900	-2.56514100
C	-1.77067600	-1.59273300	3.98798100	H	-2.44689600	-1.68171800	-0.08080400
C	-0.66157500	-2.19871200	3.37029500	H	-3.34909100	-3.26860400	-1.78498900
C	-0.15775800	-1.68883100	2.16399700	H	-2.09108600	-3.67140600	-3.91310800
C	-0.69157600	-1.15219600	-1.24611200	H	0.08586600	-2.49442700	-4.31073500
C	-1.90795100	-1.83716000	-1.02129700	H	2.29633300	1.92780500	0.40848300
C	-2.40973000	-2.73809200	-1.97767000	H	2.37731700	0.52799600	-1.42570600
C	-1.70258400	-2.96666800	-3.16954600	H	2.33638600	-1.43591700	-0.13161500
C	-0.48336000	-2.30268000	-3.39451500	C	4.19303100	0.29651200	-0.01931500
C	0.02350400	-1.40935300	-2.43731400	O	5.37191800	0.32702900	-0.18089500

**Complex 8b****SCF Done:** -1242.8171538

Ru	2.00569400	-1.35803800	-0.52143600	H	-1.98261300	2.10452400	-0.25135700
P	0.09558500	-0.15311500	-0.09448800	H	-1.86512600	4.53469300	0.29644600
C	0.08797200	1.70106900	0.27359800	H	0.28068000	5.53722000	1.11360800
C	1.29518900	2.28402300	0.71861400	H	2.31050300	4.08510000	1.36478400
C	1.36230800	3.65345400	1.02564300	H	2.18386500	1.64792200	0.79004800
C	0.22614900	4.46760200	0.88227800	H	-1.24765600	1.14860700	2.35317300
C	-0.97777100	3.90413300	0.42507300	H	-0.64263700	-2.81041200	0.72574300
C	-1.04762100	2.53307200	0.12309900	H	-1.82640500	-3.80441400	2.70377800
C	-0.88090700	-0.76443100	1.39435200	H	-2.38960100	0.16700600	4.34266000
C	-1.37227500	0.06440800	2.43019100	H	-2.69317100	-2.31295700	4.52453000
C	-2.01840300	-0.49182200	3.54908000	H	0.14529600	-0.16515600	-2.99045400
C	-2.19023600	-1.88204200	3.65175900	H	-2.95252600	-0.27356300	0.01376600
C	-1.70393200	-2.71792900	2.62975200	H	-4.70084900	-0.25129600	-1.77053000
C	-1.05057900	-2.16841600	1.51634300	H	-4.03124600	-0.15740700	-4.18255300
C	-1.28429900	-0.17417400	-1.37188900	H	-1.60073900	-0.10842500	-4.79375200
C	-2.65799200	-0.21777600	-1.03916200	H	3.04728500	-2.53037200	-1.02029500
C	-3.64064700	-0.21121100	-2.04583900	H	2.08758400	-0.90521900	-2.01510900
C	-3.26594200	-0.16018400	-3.39848700	H	0.95536900	-2.57293700	-1.06628900
C	-1.90220200	-0.12923500	-3.74052000	C	3.49188800	-0.26187100	-0.18459600
C	-0.92039500	-0.14305400	-2.73741000	O	4.49198100	0.37547700	-0.04862300

**Complex 9a****SCF Done:** -2275.43439374

Ru	0.00479000	-1.40430200	0.71839100	C	-4.21097500	1.09774600	1.41981000
P	-1.94041000	-0.24634600	0.16938300	C	-4.82010100	1.83818900	2.44698300
P	1.87045800	-0.17780100	0.09073900	H	-2.74732000	-3.01108700	0.77965200
C	-1.99383800	0.98042200	-1.25203700	H	-4.70963200	-4.44218100	0.15108100
C	-4.08142700	2.20934700	3.58430300	H	-6.43431900	-3.57269400	-1.44926400
C	-2.73559500	1.82324000	3.69388300	H	-6.17948200	-1.26933300	-2.40604400
C	-2.12564000	1.08216900	2.66683300	H	-4.23874700	0.14643900	-1.75612400
C	-3.38204300	-1.32110500	-0.40043100	H	-1.09067200	0.72161100	2.75213000

C	-3.52758800	-2.62930000	0.11223600	H	-2.15824000	2.08494400	4.58769000
C	-4.62091700	-3.42926800	-0.25722700	H	-4.55917900	2.78182000	4.38720100
C	-5.58597500	-2.94426600	-1.15636700	H	-5.87710800	2.11530200	2.36365100
C	-5.44433300	-1.65328100	-1.68966600	H	-4.80131400	0.78144500	0.55433600
C	-4.35262900	-0.84903000	-1.31680800	H	-3.13153400	2.55788400	-0.28830400
C	2.98904800	-0.87140500	-1.26666400	H	-0.82313600	-0.37123300	-2.46871400
C	-1.34801400	0.59091300	-2.45057400	H	-0.85852300	1.10759800	-4.49500600
C	2.39957100	-1.75275300	-2.20114900	H	-2.01637200	3.32946000	-4.40271100
C	3.15762300	-2.29945800	-3.25047500	H	-3.13545600	4.05499900	-2.28261900
C	4.52115700	-1.98638400	-3.37711700	H	4.85051500	0.06494200	-0.65257200
C	5.12607900	-1.12959600	-2.44130900	H	6.19411200	-0.89636100	-2.51978600
C	4.36767100	-0.57849400	-1.39418100	H	5.11425800	-2.42017400	-4.18996000
C	3.18921700	0.08214500	1.41844800	H	2.68255000	-2.98613100	-3.96007800
C	3.30665400	-0.86107000	2.46425100	H	1.34490400	-2.02199600	-2.05674500
C	4.30330500	-0.72538100	3.44489700	H	2.58326500	-1.68019000	2.51168000
C	5.19167600	0.36314500	3.41033900	H	3.97468100	1.94753700	0.62737000
C	5.07150100	1.32152600	2.39081000	H	5.74520000	2.18563900	2.36541000
C	-1.36464300	1.42612600	-3.57707900	H	4.37578400	-1.46964400	4.24572000
C	4.07865300	1.18374200	1.40455500	H	5.96331500	0.47080900	4.18071300
C	1.76755100	1.61505400	-0.45974400	H	0.41605900	2.07104000	1.17245800
C	2.44798800	2.14863300	-1.57756400	H	3.06736300	1.49053200	-2.19390800
C	2.34307800	3.51525300	-1.89527800	H	2.87497900	3.90983100	-2.76861000
C	1.56455600	4.37069000	-1.10017300	H	1.48410000	5.43454000	-1.34846400
C	0.87636700	3.84867400	0.00959400	H	0.25249300	4.50353500	0.62760200
C	0.97011500	2.48476200	0.32257700	H	0.18713900	-0.70528600	2.23671500
C	-2.01230100	2.67364300	-3.52525200	H	-1.15683900	-2.20838300	1.54803400
C	-2.63944100	3.07922800	-2.33699100	H	-0.39836900	-2.08641700	-0.77854100
C	-2.63314400	2.23910000	-1.20833500	C	0.90649300	-2.98909700	1.06138900
C	-2.84825600	0.72421400	1.50817800	O	1.36692200	-4.06696800	1.25837500

**Complex 9b**

SCF Done: -2275.44213115

Ru	-0.00588700	-0.39677600	0.06194400	C	4.40350400	0.76688200	1.84937600
P	2.24638400	-0.02741500	0.04995600	C	5.07229200	0.75637900	3.08627300
P	-2.25696900	-0.02507100	0.01594700	H	1.10491300	2.65547900	-0.19208600
C	3.31810600	-1.24572900	-0.89120800	H	1.92540900	4.83729800	-1.12994900
C	4.55069100	0.02270700	4.16532500	H	4.15828400	4.94766000	-2.26889000
C	3.35002400	-0.68983900	4.00489200	H	5.55620200	2.87580800	-2.45134400
C	2.67524600	-0.67197600	2.77300100	H	4.73958100	0.72658800	-1.49126300
C	2.87997300	1.55976900	-0.73385200	H	1.70708600	-1.17202900	2.64176900
C	2.09498500	2.73155400	-0.65642600	H	2.92650300	-1.25104200	4.84533800
C	2.55441500	3.94279400	-1.19792800	H	5.07135300	0.01699200	5.12944100
C	3.80373000	4.00423900	-1.83913200	H	5.99902600	1.32878300	3.20711000
C	4.58797400	2.84353500	-1.93901100	H	4.80591300	1.35423000	1.01788400
C	4.13147200	1.63102900	-1.39169200	H	4.95870800	-1.36729400	0.52616300
C	-2.90556300	1.36496000	-1.08391200	H	1.83783300	-1.38041100	-2.46012100
C	2.82711000	-1.71900300	-2.13159500	H	3.17717300	-2.98165600	-3.85427700

C	-2.16040700	1.73259500	-2.22577000	H	5.40379400	-3.79396200	-3.03530500
C	-2.61968000	2.74012400	-3.09064400	H	6.28216500	-2.98770200	-0.83212900
C	-3.82741700	3.40652600	-2.82422500	H	-4.69214700	1.80006200	0.07495000
C	-4.57228900	3.06075000	-1.68386700	H	-5.50888200	3.58340400	-1.45889200
C	-4.11647200	2.04872600	-0.82147400	H	-4.18175700	4.19771300	-3.49443700
C	-3.10468400	0.46295000	1.62148200	H	-2.02233000	3.01118700	-3.96830000
C	-2.35600800	1.16866500	2.58996000	H	-1.20210800	1.22350700	-2.39140500
C	-2.95254800	1.58439500	3.79126400	H	-1.29414900	1.34689900	2.38824700
C	-4.30186300	1.28876500	4.05365300	H	-5.04212000	-0.41382700	1.17314500
C	-5.05148800	0.57035000	3.10790500	H	-6.09915600	0.32079200	3.31067500
C	3.57686800	-2.62257800	-2.89967700	H	-2.35536800	2.12927100	4.53082200
C	-4.45879300	0.16036200	1.89989600	H	-4.76282600	1.60587400	4.99569700
C	-3.41318500	-1.40600100	-0.50093400	H	-2.51595400	-2.75693400	0.93862500
C	-4.37162100	-1.28840300	-1.53230300	H	-4.48779800	-0.33226600	-2.05024300
C	-5.17350300	-2.38709800	-1.89257600	H	-5.90768000	-2.27964800	-2.69906400
C	-5.03549400	-3.61408400	-1.22490600	H	-5.65836900	-4.46953800	-1.50817200
C	-4.08430300	-3.74204200	-0.19630100	H	-3.95923300	-4.69884300	0.32191800
C	-3.27740500	-2.65175900	0.15918100	H	-0.08603500	-0.55961800	1.72965500
C	4.82445400	-3.08022800	-2.43936900	H	-0.08622700	1.24281200	0.45188500
C	5.31631700	-2.62803500	-1.20461100	H	0.09695100	0.05681200	-1.56408000
C	4.57102600	-1.71521800	-0.43593800	C	0.04104600	-2.26389400	-0.20748100
C	3.19874700	0.04551400	1.67463800	O	0.06968500	-3.44712800	-0.31744000

### Complex 10a

SCF Done: -2275.99128072

Ru	0.01205800	-1.43062700	-0.82873400	C	1.14792700	2.26784200	-1.41043300
P	-1.94251000	-0.23853100	-0.15594800	H	3.63476000	-2.48389500	0.16452100
P	1.87824100	-0.12214300	-0.05948300	H	5.66655600	-3.23199000	-1.05430500
C	-3.36558400	-1.34006300	0.33686900	H	6.67019500	-1.78889500	-2.83932100
C	-3.14014100	-2.65939200	0.78575000	H	5.62459900	0.42129600	-3.38081800
C	-4.21495700	-3.46367300	1.20294400	H	3.60040100	1.18340000	-2.15113700
C	-5.52675800	-2.96481900	1.16779400	H	3.26818400	2.20281700	1.27692600
C	-5.76290800	-1.65435100	0.71724500	H	3.32483200	4.64287700	0.78730200
C	-4.69140400	-0.84531400	0.30883200	H	1.98953300	5.57729500	-1.11500400
C	-2.77004800	0.79139500	-1.47394800	H	0.58244900	4.04489400	-2.51376500
C	-2.89410000	0.23154600	-2.76865200	H	0.50545300	1.60705000	-2.00218900
C	-3.52110300	0.94660800	-3.79975300	H	-4.88237500	0.17183300	-0.04581800
C	-4.03231600	2.23380900	-3.55823700	H	-6.78374100	-1.26083800	0.68013300
C	-3.92043500	2.79681100	-2.27724500	H	-6.36386200	-3.59552600	1.48349500
C	-3.29812600	2.08123400	-1.23875000	H	-4.02297000	-4.48562700	1.54539100
C	-1.92472400	0.92494200	1.29947900	H	-2.11902500	-3.05119300	0.78750200
C	-2.60622900	0.62176200	2.50069100	H	-2.50235100	-0.77371700	-2.95920000
C	-2.53415500	1.49259700	3.60159000	H	-3.20928000	2.52900900	-0.24503200
C	-1.79108000	2.68045600	3.51723000	H	-4.31981000	3.79698400	-2.07981800
C	-1.10895000	2.99187900	2.32867500	H	-3.61107300	0.49666700	-4.79381800
C	-1.16718800	2.12009700	1.23030100	H	-4.51771200	2.79249400	-4.36460600
C	3.46503500	-0.59814400	-0.91348400	H	-0.61284200	2.36197200	0.31962000

C	4.04350100	0.21200000	-1.91531300	H	-3.20280800	-0.29146100	2.56786900
C	5.18968800	-0.21836600	-2.60611500	H	-3.06902400	1.24195400	4.52340000
C	5.77758500	-1.45563600	-2.30098500	H	-1.73941300	3.35941600	4.37410800
C	5.21485800	-2.26553300	-1.29924100	H	-0.51714500	3.90922500	2.25399400
C	4.06648800	-1.84474900	-0.61199400	H	4.51928900	0.01731100	1.37462000
C	2.38726500	-0.23592000	1.72489800	H	0.35203700	-0.54804900	2.40541000
C	3.73833500	-0.10687400	2.13036900	H	0.96258100	-0.64503500	4.82148800
C	4.08242300	-0.17154300	3.49041100	H	3.35708600	-0.41649200	5.52192500
C	3.08626800	-0.36291100	4.46269200	H	5.13158600	-0.07916500	3.78914400
C	1.74406500	-0.49251200	4.07063700	H	0.35284800	-0.53738100	-2.32310400
C	1.39566700	-0.43323200	2.71130500	H	-0.28626500	-1.11765600	-2.52341700
C	1.90946000	1.72575500	-0.34903900	H	-1.18114600	-2.47107300	-1.19623500
C	2.69124800	2.60162900	0.43786100	H	-0.13595300	-2.06568100	0.65383400
C	2.71681600	3.97898400	0.16428900	C	1.04372800	-2.94897000	-1.20794100
C	1.96693500	4.50381800	-0.90247300	O	1.56230200	-3.98430300	-1.40637700
C	1.18116100	3.64538600	-1.68898300				

**Complex 10b**

SCF Done: -2275.99602209

Ru	0.00399400	0.31763300	0.18402000	C	-4.50892900	-1.32313100	3.33530700
P	-2.29966700	-0.00742400	0.03295600	H	-1.06039700	-2.59313100	-0.74000500
P	2.31027300	0.00299500	0.01891400	H	-1.93414700	-4.63981800	-1.88574000
C	-3.27360200	1.31553400	-0.83848000	H	-4.31260700	-4.71489500	-2.67129000
C	-4.36584000	-0.25425900	4.23319500	H	-5.80376200	-2.73659500	-2.30325900
C	-3.63451500	0.88527600	3.85166800	H	-4.92597200	-0.70300700	-1.16988600
C	-3.04294200	0.94947600	2.58182200	H	-2.46374400	1.83258300	2.29137100
C	-2.93361900	-1.52061900	-0.85423900	H	-3.51992300	1.72349000	4.54636000
C	-2.10164400	-2.63865300	-1.07412400	H	-4.81971800	-0.30667800	5.22773100
C	-2.59641400	-3.78359700	-1.72211100	H	-5.07650500	-2.21296200	3.62599200
C	-3.92850500	-3.82521400	-2.16222900	H	-4.05033400	-2.09006400	1.35764400
C	-4.76615300	-2.71519800	-1.95504700	H	-4.92090100	1.39202500	0.57804900
C	-4.27459900	-1.57077300	-1.30874400	H	-1.78608200	1.50064800	-2.40709300
C	2.90804400	-1.27761800	-1.19339100	H	-3.05888200	3.23053100	-3.68069000
C	-2.75801100	1.84854200	-2.04241300	H	-5.26233600	4.05348500	-2.82004000
C	2.09944300	-1.67770600	-2.27863200	H	-6.18713200	3.12815300	-0.68617800
C	2.56476700	-2.62828000	-3.20316800	H	4.82261700	-1.57073100	-0.20125000
C	3.84039200	-3.19478700	-3.05198300	H	5.64573900	-3.25099600	-1.84401000
C	4.65294600	-2.80794800	-1.97185300	H	4.20005900	-3.93918800	-3.76947200
C	4.19230700	-1.85662200	-1.04879700	H	1.92395500	-2.92831700	-4.03852100
C	3.13423000	-0.60344000	1.57604000	H	1.10049400	-1.24321700	-2.37940200
C	2.50931700	-1.64632900	2.30042800	H	1.55853100	-2.05150000	1.93862400
C	3.09467100	-2.15263000	3.47035600	H	4.84620400	0.73248800	1.50718000
C	4.30930100	-1.62201400	3.93925000	H	5.88208900	-0.16706500	3.59082100
C	4.93692200	-0.58566100	3.23012300	H	2.59871900	-2.96005500	4.01843600
C	-3.47349800	2.82407000	-2.75288800	H	4.76217400	-2.01354500	4.85549300
C	4.35758600	-0.07952400	2.05304800	H	2.61908400	2.63157700	1.25451100
C	3.36843700	1.46603600	-0.42299200	H	4.29048000	0.59363100	-2.18540600

C	4.21192300	1.48368200	-1.55542300	H	5.59528700	2.63765400	-2.75870900
C	4.95127500	2.63654300	-1.87346400	H	5.44269600	4.67463500	-1.31178500
C	4.86635700	3.77836000	-1.06219100	H	3.95526900	4.65930100	0.70349600
C	4.03229300	3.77010700	0.06995400	H	0.11899600	0.69193400	1.94358800
C	3.28300700	2.62695900	0.38377400	H	-0.07071200	-0.14204200	1.90420900
C	-4.70942800	3.28644500	-2.26891500	H	0.09646800	-1.33992100	0.15145800
C	-5.22775500	2.76796200	-1.07140400	H	-0.01778700	0.15940100	-1.42144000
C	-4.51779800	1.78580400	-0.35934000	C	-0.05775600	2.22056000	-0.05380700
C	-3.18542900	-0.12211700	1.66576200	O	-0.08764800	3.38098300	-0.22816500
C	-3.92704400	-1.25842200	2.05650500				

**TS<sub>10-2</sub> (a)****SCF Done:** -2275.96390761

Ru	0.01732400	-1.52588800	-0.31827000	C	-1.78708000	-0.06321000	2.71524300
P	1.95958400	-0.16962700	-0.13176500	H	-3.01783200	-1.75094600	-2.21764500
P	-1.88677900	-0.11960900	-0.09252900	H	-5.17420200	-2.95674300	-2.53084900
C	3.31188200	-0.56823100	-1.33730800	H	-6.91939400	-2.89987500	-0.73499300
C	3.00439300	-1.18757600	-2.56795900	H	-6.49319500	-1.61529500	1.37058700
C	4.02336200	-1.48368000	-3.48902100	H	-4.34443400	-0.39530700	1.68066600
C	5.35956700	-1.17492200	-3.18711500	H	-2.70446600	2.66697400	0.85740500
C	5.67799400	-0.56837400	-1.95939200	H	-2.85968900	3.66413100	3.14121300
C	4.66191700	-0.26445000	-1.03982700	H	-2.33471900	2.27702600	5.15709700
C	2.77273300	-0.57949700	1.49676300	H	-1.64981400	-0.11655600	4.87640900
C	3.08910600	-1.93514200	1.76524300	H	-1.47423700	-1.10705100	2.59537600
C	3.66997600	-2.30135300	2.98861200	H	4.91232400	0.19498200	-0.07858700
C	3.93877000	-1.32585300	3.96430900	H	6.71939500	-0.33732700	-1.71397400
C	3.63055500	0.01984500	3.70795300	H	6.15334900	-1.41465000	-3.90162600
C	3.05279400	0.39401000	2.48259600	H	3.77108600	-1.96828500	-4.43756200
C	1.99684700	1.69286800	-0.11194400	H	1.96576900	-1.46031800	-2.77919900
C	2.87638000	2.45982900	-0.90893300	H	2.87485900	-2.69554100	1.00725500
C	2.83781000	3.86429700	-0.86322300	H	2.81674600	1.44395200	2.28927700
C	1.93033500	4.52137200	-0.01761200	H	3.84232700	0.78583600	4.46097700
C	1.04683900	3.76777500	0.77420600	H	3.91055100	-3.35216800	3.17917600
C	1.06883700	2.36585100	0.71993800	H	4.38877600	-1.61423900	4.91951100
C	-3.53086300	-0.98511700	-0.24730300	H	0.35074100	1.79062100	1.31287100
C	-4.52233500	-0.95385800	0.75765900	H	3.59384600	1.95620600	-1.56218100
C	-5.73548900	-1.64389800	0.58079100	H	3.52355900	4.44366200	-1.48998800
C	-5.97540900	-2.36266600	-0.60012700	H	1.90400300	5.61491400	0.01842000
C	-4.99613000	-2.39444400	-1.60878700	H	0.32304900	4.26736500	1.42527300
C	-3.78192800	-1.71544600	-1.43386000	H	-4.29192900	1.51042500	-0.82728300
C	-2.17960400	1.27313000	-1.29393400	H	-0.14464100	1.24137300	-2.02924500
C	-3.45430600	1.87666700	-1.42898100	H	-0.49650800	3.09280400	-3.66977100
C	-3.65346000	2.91710200	-2.34954000	H	-2.74948400	4.16824900	-3.87715000
C	-2.58956000	3.36106300	-3.15523000	H	-4.64364600	3.37385800	-2.44698600
C	-1.32714000	2.75857400	-3.04025600	H	-0.09725700	-3.40733100	2.01383100
C	-1.12341100	1.71978200	-2.11583000	H	-0.14691600	-3.49787200	2.76077300
C	-2.08566800	0.71077700	1.56629700	H	1.28260600	-2.53638400	-0.56790400

C	-2.47189200	2.05947400	1.73660700	H	-0.03116200	-1.32840200	-1.86275400
C	-2.55818100	2.61797500	3.02410700	C	-0.92785900	-3.10402900	-0.63732500
C	-2.26597000	1.83935600	4.15626100	O	-1.40310100	-4.14815700	-0.90308200
C	-1.88198000	0.49613100	3.99934600				

---

**Complex 11**
**SCF Done:** -3194.01836339

Ru	-0.03814300	0.36602100	-0.13237300	C	-2.50510000	-2.84641800	0.44956800
P	2.12421100	1.15934900	-0.11294100	C	3.85866900	3.03719900	-1.39974000
P	-2.27520800	0.87887200	-0.12868700	C	3.77576800	0.27397900	-0.12406300
P	0.13855400	-1.98069400	-0.09592100	C	4.73970100	0.42963800	0.89983200
C	2.54171500	2.52290800	-1.31504200	C	5.97086600	-0.24630900	0.82842500
C	6.25909400	-1.08000600	-0.26439000	H	1.96207100	0.12635400	2.62105400
C	5.30961300	-1.23722100	-1.28894900	H	1.77569000	1.19661200	4.85961900
C	4.07823900	-0.56710800	-1.22153800	H	1.87097300	3.69170000	5.07642200
C	2.17580300	2.01119700	1.54243000	H	2.17235200	5.10582000	3.03262000
C	2.00612900	1.21851400	2.70698300	H	2.36174600	4.03802000	0.78742900
C	1.90206200	1.82313900	3.97068000	H	2.85915800	-1.83231500	1.05744900
C	1.95764600	3.22192200	4.09167500	H	3.84382000	-2.46996300	3.24210400
C	2.12423800	4.01548900	2.94387300	H	2.43424200	-3.60741900	4.98146900
C	2.23313300	3.41655000	1.67810900	H	0.03389800	-4.12145100	4.48163500
C	-2.69289100	2.60822400	-0.72145000	H	-0.94545000	-3.51611000	2.27444200
C	1.54254400	3.06898700	-2.15237600	H	-0.30927200	-4.67940500	-1.43063000
C	-2.07172300	3.71120800	-0.08653500	H	-2.23971300	-6.24709100	-1.43863000
C	-2.35404300	5.02278700	-0.49401700	H	-4.34533200	-5.66050500	-0.21449200
C	-3.24984900	5.25778100	-1.55349400	H	-4.50981100	-3.46497600	0.98162400
C	-3.86708700	4.17331600	-2.19320900	H	-2.59264500	-1.87881700	0.95124100
C	-3.59845500	2.85573300	-1.77571900	H	3.33941600	-0.71104000	-2.01548100
C	-3.07590300	0.95013700	1.55740400	H	5.51857800	-1.89138500	-2.14077900
C	-2.46714000	0.25913900	2.63023300	H	7.21768100	-1.60586700	-0.31741800
C	-3.02408600	0.30256800	3.91988900	H	6.70786900	-0.11398000	1.62764800
C	-4.19549300	1.03992800	4.15485200	H	4.51958100	1.07634600	1.75377600
C	-4.80201800	1.74453900	3.09997200	H	4.64670400	2.61023400	-0.77232200
C	1.85355900	4.10718800	-3.04760900	H	0.52352500	2.67592600	-2.08616500
C	-4.24419200	1.70846800	1.81209300	H	1.06769200	4.51702200	-3.69038300
C	-3.50349100	-0.08570200	-1.14806200	H	3.39958800	5.42467900	-3.81450100
C	-3.07476200	-0.53076100	-2.42100600	H	5.18433100	4.46824600	-2.34026500
C	-3.94960300	-1.23343700	-3.26413100	H	-4.09076800	2.01794300	-2.27600700
C	-5.26141500	-1.51291000	-2.84470900	H	-4.56523700	4.34552800	-3.01901600
C	-5.69405000	-1.08466500	-1.57897300	H	-3.46239900	6.28198200	-1.87644300
C	-4.82364900	-0.37158900	-0.73680700	H	-1.86853500	5.86330700	0.01266600
C	0.87779100	-2.61419000	1.50970400	H	-1.35677000	3.53306800	0.72387500
C	0.09703200	-3.26630700	2.49247700	H	-1.54586900	-0.30800200	2.44986900
C	0.65425200	-3.61300900	3.73585200	H	-4.69730900	2.28844000	1.00229700
C	3.16012700	4.61571300	-3.11674900	H	-5.70623600	2.33402300	3.28337900
C	2.00049800	-3.32825900	4.01597700	H	-2.53566000	-0.23420200	4.73969400
C	2.79007400	-2.69075100	3.04329000	H	-4.62945800	1.07662500	5.15915700



C	2.23441700	-2.32766200	1.80576400	H	-5.16772000	-0.04162700	0.24783000
C	1.26236500	-2.75943200	-1.36788700	H	-2.04175900	-0.33627200	-2.73061100
C	2.05985100	-3.89595400	-1.10234300	H	-3.60176000	-1.57382100	-4.24485200
C	2.85557200	-4.46250000	-2.11326600	H	-5.94027100	-2.06964400	-3.49839700
C	2.85652500	-3.91189800	-3.40589700	H	-6.71289700	-1.30523700	-1.24368300
C	2.06048300	-2.78681000	-3.68423100	H	2.06218000	-4.32769900	-0.09721400
C	1.27310100	-2.21282400	-2.67253800	H	0.67046200	-1.32133700	-2.87663200
C	-1.30466700	-3.17261500	-0.22113100	H	2.05539700	-2.35163300	-4.68913900
C	4.16223600	4.07910400	-2.28932100	H	3.47294100	-4.35779000	-4.19311700
C	-1.22724600	-4.40922300	-0.90228800	H	3.47320900	-5.33836300	-1.88917000
C	-2.31712400	-5.29549200	-0.90224000	H	-0.05125300	1.99001100	-0.20873500
C	-3.49772300	-4.96777800	-0.21575500	H	-0.08983600	0.38898000	-1.69291400
C	-3.58843000	-3.73998000	0.45927200				

## Complex 12

SCF Done: -2276.59492901

Ru	-0.00630600	-0.15029000	-0.02744700	C	-5.23195200	-1.13439200	-2.78843100
P	-2.28513700	0.05536300	-0.01638800	H	-1.48268500	2.38376800	-1.55658000
P	2.23570800	0.07147200	-0.01449700	H	-2.44521800	4.67431200	-1.92742400
C	-3.14132400	-0.50537900	1.55602700	H	-4.51661500	5.37284900	-0.69994600
C	-4.75817400	-2.39954100	-3.17284000	H	-5.62889200	3.76471300	0.86660500
C	-3.56446600	-2.89732100	-2.61783500	H	-4.68644000	1.47770500	1.19067600
C	-2.84458300	-2.13777700	-1.68135200	H	-1.89092500	-2.48840200	-1.25165900
C	-3.03165700	1.76900700	-0.18515300	H	-3.18515900	-3.87920300	-2.92326400
C	-2.40830600	2.69082400	-1.05751800	H	-5.31280800	-2.99279100	-3.90883800
C	-2.94366300	3.97475000	-1.24722600	H	-6.15540500	-0.73657200	-3.22497600
C	-4.10504100	4.36731300	-0.55873600	H	-4.88853900	0.61687100	-1.54978500
C	-4.72858300	3.46529800	0.31819500	H	-4.98108500	-1.23547000	0.66355700
C	-4.19970200	2.17425300	0.50104200	H	-1.40902800	0.05584800	2.71273200
C	2.98395700	1.76535400	0.31282700	H	-2.42861200	-0.61422900	4.91815600
C	-2.42711300	-0.34911000	2.76742200	H	-4.72053400	-1.62860100	4.97274500
C	2.24631900	2.91596600	-0.04773700	H	-5.98927800	-1.94533000	2.83767200
C	2.78500300	4.19931200	0.14041100	H	4.83273700	1.05673500	1.20438000
C	4.06543300	4.35848000	0.69806700	H	5.79426900	3.33746800	1.52782800
C	4.80221500	3.22384300	1.07609200	H	4.48130200	5.36100900	0.84837600
C	4.26589800	1.93761100	0.88709200	H	2.19500500	5.07937300	-0.13921900
C	3.12237300	-0.35010400	-1.61784600	H	1.23566300	2.77349200	-0.44471900
C	4.36269400	0.19483900	-2.02361900	H	4.85712300	0.93857300	-1.38993900
C	4.94451500	-0.18424600	-3.24762600	H	1.48089800	-1.64069100	-2.17612000
C	4.29526800	-1.11029000	-4.08114400	H	2.53417900	-2.35733600	-4.34628600
C	3.05525500	-1.64837600	-3.69330200	H	5.90238500	0.25243700	-3.55299100
C	-2.99614600	-0.74129100	3.98957600	H	4.74700500	-1.40096000	-5.03625900
C	2.46907700	-1.26727900	-2.47492000	H	1.72384700	-0.65611300	2.69714100
C	3.27098700	-0.91592800	1.21015600	H	4.95410300	-1.40571400	-0.07054000
C	4.52337900	-1.50886500	0.93075700	H	6.17474300	-2.69667600	1.68663800
C	5.20782100	-2.23686000	1.92127100	H	5.18749300	-2.94852200	3.97435900
C	4.65437000	-2.37927900	3.20488400	H	2.95974400	-1.91888100	4.48579400

---

C	3.40538800	-1.79945300	3.49177800	H	0.04160400	1.17135100	-0.93555900
C	2.71739400	-1.07995300	2.50291000	H	-0.03380300	1.10628300	0.97027200
C	-4.28113200	-1.31187900	4.02024900	O	-0.19605200	-2.22704900	-0.15505200
C	-4.99319200	-1.48839800	2.82216800	C	0.76636300	-3.22256500	0.03540500
C	-4.42937700	-1.08667900	1.59736500	H	1.80846700	-2.91109600	-0.22089900
C	-3.32424100	-0.86662000	-1.27648200	H	0.80205600	-3.57871700	1.09240200
C	-4.52113000	-0.37140700	-1.84384000	H	0.54614700	-4.12403400	-0.59150000

## Appendix 2

**PBE0/ECP1 coordinates of optimised complexes in Å (xyz format) including total SCF Energy in a.u.**

**[Au(IPr){CH(CH<sub>3</sub>)C(O)CH<sub>3</sub>}] (7)**

SCF Done: -1526.04213434

Au	0.08982900	-0.72953400	-1.00482700	H	-5.15932600	1.46840600	-1.46771400
O	2.01536200	-3.67497900	-1.51642900	H	-1.57417200	-1.02977800	2.44192400
N	-1.40681500	0.94004100	1.11207800	H	-2.75934400	-2.24471300	4.22343700
N	0.71416600	1.18524400	1.29040300	H	-4.27712600	-2.16951800	3.31971100
C	-0.23408300	0.57221600	0.53719200	H	-3.54307100	-0.67950000	3.93091700
C	-1.19549500	1.76306300	2.20301400	H	-3.08472600	-3.45346400	1.34385100
C	0.14597400	1.91740900	2.31588500	H	-1.61167700	-3.48881000	2.32643100
C	-2.70146000	0.52174800	0.65367800	H	-1.57259300	-2.79213800	0.69395000
C	-3.24799900	-0.66023700	1.17698500	H	-1.82397400	2.78552900	-0.33487000
C	-4.50865100	-1.04284500	0.71373400	H	-4.59946000	3.67170800	-1.27730700
C	-5.18893200	-0.28113800	-0.22735700	H	-3.16866700	4.69015800	-1.08845800
C	-4.62106800	0.88436800	-0.72614500	H	-3.92822000	3.95379600	0.33619200
C	-3.36407500	1.31453100	-0.29678100	H	-1.88714900	3.25027900	-2.75660200
C	-2.52054700	-1.52185200	2.19154900	H	-3.26253300	2.15019000	-2.95882000
C	-3.32282700	-1.65787800	3.48923100	H	-1.68696000	1.50913300	-2.45752200
C	-2.17806900	-2.89331200	1.60107900	H	4.60695500	2.72781200	-0.57158800
C	-2.75007900	2.57264000	-0.88081000	H	5.91277300	0.87980200	0.41161100
C	-3.66619000	3.78808300	-0.71462300	H	4.79822900	-0.84370300	1.77952500
C	-2.37385200	2.35571100	-2.35028000	H	0.92347500	3.18735300	0.01821800
C	2.12683300	1.09251300	1.04580600	H	3.52941600	4.70254900	-0.51668000
C	2.73126700	2.08410400	0.25691800	H	2.60723500	4.75669900	0.99319100
C	4.10692900	1.98315600	0.04164700	H	1.89418400	5.36819300	-0.51238000
C	4.84275400	0.94099000	0.59107700	H	1.35769500	2.00268500	-2.11490600
C	4.21425600	-0.02854200	1.36220300	H	2.81330000	2.98070300	-2.37774900
C	2.83960700	0.01954500	1.60452800	H	1.21917200	3.75760800	-2.36734100
C	1.93957800	3.20419900	-0.39213000	H	1.09415600	-0.93985500	2.35103700
C	2.52885600	4.58322300	-0.08574300	H	3.60146900	-0.91566300	4.10850800
C	1.82509300	2.97061000	-1.90250500	H	2.02265800	-1.57973500	4.56212500
C	2.17908000	-1.04439600	2.46076300	H	2.20938400	0.16358200	4.28719200
C	2.52162600	-0.82807400	3.93966200	H	1.97977200	-3.19242000	2.60520600
C	2.54257900	-2.46229700	2.01222200	H	3.60728500	-2.67484100	2.16474400
C	-0.60875000	-3.27009600	-2.52149900	H	2.31050500	-2.63417800	0.95599700
C	0.44502900	-2.16892300	-2.50103400	H	-0.61909600	-3.81950600	-1.57530500
C	1.80121100	-2.64296100	-2.14598200	H	-0.40181300	-4.00569900	-3.31258900
C	2.98291900	-1.77489800	-2.56340800	H	-1.61144100	-2.86350400	-2.69381400
H	-2.01274700	2.15590600	2.78759900	H	0.47329600	-1.61587300	-3.45008800
H	0.74523800	2.47489600	3.01883300	H	3.65074700	-2.37204700	-3.19526600

H	-4.95970500	-1.95643400	1.09159400	H	3.55213800	-1.47928900	-1.67552600
H	-6.16723400	-0.59960500	-0.57717000	H	2.68199100	-0.87470800	-3.10797600

**[Au(IPr){CH<sub>2</sub>C(O)CH<sub>2</sub>CH<sub>3</sub>}] (8)**

SCF Done : -1526.04689241

Au	0.11465600	-0.66054700	-1.05873400	H	-4.30764000	-2.88378500	2.84659400
O	2.26144700	-3.38924200	-1.51037700	H	-3.82191300	-1.35528700	3.59598800
N	-1.69417800	0.69028000	1.03106200	H	-2.83221100	-3.86209200	0.88760900
N	0.36718300	1.14946400	1.39031700	H	-1.44530600	-3.79291700	1.98733200
C	-0.44895600	0.48764300	0.53102400	H	-1.36577600	-2.98423000	0.41007600
C	-1.65664900	1.46086700	2.17850200	H	-2.21810700	2.55140200	-0.35920200
C	-0.35269700	1.75022000	2.40600300	H	-5.01549600	3.18284600	-1.43335500
C	-2.89692600	0.15574200	0.45790100	H	-3.72204900	4.33940600	-1.10186800
C	-3.33567200	-1.10845900	0.88162700	H	-4.47604300	3.44444800	0.23225700
C	-4.51250200	-1.60100400	0.31376100	H	-2.19036600	3.14531300	-2.75306900
C	-5.21560900	-0.86600100	-0.63186900	H	-3.41874900	1.91486100	-3.09963100
C	-4.75420600	0.38174600	-1.03171200	H	-1.81343700	1.42215000	-2.52860400
C	-3.58395600	0.92278700	-0.49573300	H	4.20353400	3.21365900	-0.03146200
C	-2.57750300	-1.94292200	1.89673900	H	5.62239500	1.45592600	0.96232800
C	-3.44377700	-2.26593100	3.11786100	H	4.59759000	-0.46148100	2.12712200
C	-2.02348600	-3.21869000	1.25412700	H	0.45232000	3.21882100	0.22227100
C	-3.08113400	2.27163700	-0.97390900	H	2.89195100	5.06663800	0.12995200
C	-4.13592200	3.36858200	-0.80648900	H	1.80166500	4.87863900	1.51151100
C	-2.59656100	2.18118200	-2.42479700	H	1.19686900	5.54097200	-0.01959700
C	1.79619600	1.22097500	1.26280900	H	1.26557100	2.29610500	-1.92989100
C	2.34982800	2.32020000	0.58785900	H	2.59841100	3.46594200	-1.94279100
C	3.74130800	2.38102200	0.49196700	H	0.92375100	4.03635600	-2.05776400
C	4.54099100	1.39051700	1.04734100	H	0.89145800	-0.98721200	2.36368700
C	3.96264700	0.31155200	1.70379000	H	3.24554700	-0.84506100	4.31696600
C	2.57584800	0.19591500	1.82262900	H	1.71103600	-1.68548800	4.59518100
C	1.49618600	3.39325700	-0.06184500	H	1.74334200	0.08312200	4.44897000
C	1.87031900	4.79702000	0.42104400	H	1.99410800	-3.15029900	2.54469200
C	1.57572200	3.28979300	-1.58869700	H	3.58295300	-2.43821700	2.26140000
C	1.97063500	-0.98818600	2.55295700	H	2.37358900	-2.44584600	0.96404600
C	2.17815900	-0.84722400	4.06544100	C	3.25549500	-1.63668900	-2.79278400
C	2.51432700	-2.32586000	2.04339300	C	4.54602100	-1.87415100	-2.02703800
C	2.06709700	-2.41772900	-2.23283000	H	2.99804400	-0.57016800	-2.82759800
H	-2.55334500	1.72594400	2.71668400	H	3.36945700	-1.94945300	-3.84230400
H	0.12768200	2.32341500	3.18366100	H	5.39893600	-1.40388700	-2.52899900
H	-4.87837800	-2.57956900	0.61298400	H	4.47693200	-1.46163800	-1.01413700
H	-6.12748700	-1.27007600	-1.06341200	H	4.73735000	-2.94648000	-1.93141400
H	-5.30805900	0.94405400	-1.77876400	C	0.72124900	-1.92830500	-2.60415600
H	-1.72087400	-1.35758200	2.24909000	H	0.00763300	-2.75868800	-2.65015100
H	-2.85992300	-2.82321500	3.85917100	H	0.72376800	-1.37545300	-3.55169300